Plasma Amino Acid and Metabolite Changes in Pigs During Endotoxemia

Kathryn Leigh Price

Dissertation submitted to the faculty of the Virginia Polytechnic Institute and State University in partial fulfillment of the requirements for the degree of

Doctor of Philosophy
In

Animal and Poultry Sciences

Jeffery E. Escobar, Committee Chair
Mark D. Hanigan
Allen F. Harper
Kevin D. Pelzer

November 15, 2011
Blacksburg, Virginia

Keywords: amino acids, blood metabolites, pigs, endotoxemia, *Salmonella*, NτMH

Plasma Amino Acid and Metabolite Changes in Pigs During Endotoxemia

Kathryn Leigh Price

ABSTRACT

The nutritional status, especially circulating amino acid (AA) levels, can drastically change during a non-infectious (i.e., LPS) or infectious (e.g., *Salmonella*) challenge. Thus, study 1 examined the effect of LPS treatment (N = 9, 26.9 ± 1.07 kg BW) on plasma AA and metabolite levels in pigs. Data were used to generate prediction equations establishing mathematical relationships between plasma AA levels and numerous blood metabolites (e.g., total lipid, LDL, HDL, blood urea nitrogen, etc). These equations have the potential to improve the nutritional treatment and recovery of acute and chronically ill patients.

Study 2 (19.1 ± 0.37 kg) was a continuation of study 1 except the sampling time was increased from 12 to 24 h. One-half of the pigs in study 2 were treated with LPS (N=15) and the other one-half were saline treated control animals (N = 16). This design allows for monitoring changes in plasma AA and their catabolism in response to endotoxemia. Area under the curve (AUC) was calculated for a selected AA to report AA balances. During the induction phase of an acute challenge (t = -2 to 12 h), analyzed AA were in a negative balance indicating heavy AA catabolism. However, during the recovery phase (t = 12 to 24 h) half of the AA were in a positive balance while the other half were still negative. The ability of equations to accurately predict AA concentrations was tested. Results indicate poor performance possibly due to heavy term biases. Thus, it was concluded that equations need to be revisited and non-linear terms need to be evaluated. Nonetheless, routine clinical blood metabolites can be used to estimate plasma AA levels during immune activation.

We successfully established a porcine *Salmonella enterica* serovar Typhimurium model. Pigs infected with *Salmonella* had a febrile response for 4 d and exhibited marked changes in their fecal bacterial populations.

Finally, we investigated plasma changes in N-τ-methyl histidine (NτMH) in healthy and LPS-treated pigs. NτMH is a post-translationally modified AA that has historically been used as an indirect marker of muscle protein breakdown in rodents and humans. However, the major form (i.e., free or acetylated) of NτMH in pig plasma was unknown. Results indicate that only 15% of plasma NτMH is in the free form and the remainder is acetylated. Furthermore, LPS treated pigs had increased acetylated and total NτMH fractions while free NτMH did not change. Therefore, to accurately monitor plasma changes in NτMH as an indicator of muscle proteolysis, plasma samples must be subjected to acid hydrolysis.

Biography

Kathryn Leigh Price was born on February 23, 1983 in High Point, North Carolina. She graduated from McMichael High School in Madison, North Carolina in 2001. Kathryn attended North Carolina State University and completed her Bachelors of Science degrees in Animal and Poultry Science, with concentrations in Feed Mill Management and Agricultural Business Management in December 2005. Kathryn completed her Masters of Science degree in Animal Science at North Carolina State University under the direction of Dr. Jack Odle. For her M.S., she conducted research on improving post-weaning pig performance. She continued her pursuit for higher education by working with Dr. Jeffery Escobar at Virginia Tech. Her dissertation research has also been working with pigs but looking more in depth at the AA metabolism changes a pig experiences during endotoxemia.

Acknowledgements

I would like to thank Dr. Jeffery Escobar for his patience, guidance, and constant support during my Ph.D. During my time in his laboratory I not only gained invaluable experiences but further grew as an individual. I am glad I found such a good "home" in the Escobar lab and would like to thank Dr. Jack Odle for his gentle nudge to work with Dr. Escobar. I would also like to thank my committee members for their guidance Drs. Mark Hanigan, Allen Harper, and Kevin Pelzer.

My labmates, colleagues, and VT friends have provided me with support, love, and many laughs! I especially owe a big thanks to Elizabeth Ramirez, and Chasity Cox, Heather Totty for being great friends and of course Thank you El Rodeo for providing us with many delicious meals! Even though Blacksburg is one of the coldest places during the winter, the summer days spent floating the river, playing together on a dart team, and cutting up in the lab are memories I will cherish and be ever thankful for. Additionally, thank you to my Raleigh friends (even if you have now moved from Raleigh). I owe a special Thank you to my VT mom, Melissa Cromer, for her love, support, and for being a great therapist!!!

My family knows I am forever grateful to them for their love and support; even though they can't understand a word of my dissertation. I love and thank you for believing in me over the past 10 years while I completed my many degrees. I think I am officially done with school, smile Dad!

Table of Contents

List of tables

Chapter 3

Chapter 4

Chapter 5

List of Figures

Chapter 3

Chapter 4

Chapter 5

Chapter 6

Chapter 1

1.1 Introduction

Invading pathogens initiate a proinflammatory, innate immune response that works immediately to fight the pathogen and return the body to homeostasis. The innate immune system is capable of recognizing unique microbial pathogen-associated molecular patterns via pattern recognition receptors (Janssens and Beyaert, 2003; Mogensen, 2009; Kawai and Akira, 2010). Once the host immune system recognizes the pathogen, there is a release of inflammatory cytokines (IL-1, IL-6, and TNF-α) which stimulate a reduction in feed intake, skeletal muscle protein synthesis and stimulate skeletal muscle proteolysis and liver protein synthesis. All of these responses are important to the animals' ability to fight off the pathogen. Increasing liver protein synthesis stimulates the production and release of acute phase proteins (Johnson and Escobar, 2005). All of the changes that occur in response to immune system activation cause changes in amino acid (AA) metabolism. Nutritional requirements of pigs have been developed but for healthy animals only. There is no set of feeding guidelines available for sick pigs.

Developing nutritional requirements of sick animals will require research in the field of nutrition and immunology. Employing every available method for monitoring pig health is essential. Blood urea nitrogen is a commonly measured marker of skeletal muscle proteolysis because as skeletal muscle protein degradation increases so does blood urea nitrogen. Another marker of skeletal muscle protein degradation is N-τ-methyl histidine (NτMH). NτMH is a post-translationally modified AA that is released during skeletal muscle proteolysis, cannot be reused by the body for protein synthesis and travels via the blood to the kidneys where it is filtered for

excretion in the urine. In humans the majority of NτMH is in the free (non-acetylated) form (Munro and Young, 1978) while in rodents it is primarily in the total (acetylated) form (Brenner eta., 1987). Total NτMH can be measured in acid hydrolyzed samples because the acid hydrolysis removes the acetyl group (Kuhl et al., 1996).

To study changes in AA metabolism, animal models of disease must be employed. Rodents are a common model of disease due to their small size and availability of knock-out lines; however, pigs are a much more appropriate model to monitor changes in human health due to their similarity in size, digestive function, and immune system activation and response (Lunney, 2007).

Salmonella is one of the most reported bacterial infections in humans each year (FSIS/USDA, 2006) and is responsible for an estimated $2.4 billion loss to the swine industry each year (ERS/USDA, 2003). The transmission of *Salmonella* is primarily due to fecal-oral transmission. *Salmonella* infections usually occur due to unsanitary conditions. Treatment for a *Salmonella* infection is rest and fluid replacement therapy. However, if the patient becomes septic, the patient may be hospitalized and antibiotics prescribed to help combat the infection. Pigs inoculated with *Salmonella* Typhimurium (most common of *Salmonella* outbreaks) will exhibit clinical signs and have symptoms similar to a human, whereas, a rodent infected with the same bacteria will exhibit a Typhoid fever like response (Balaji et al., 2000).

Lipopolysaccharide (LPS) challenge is a commonly used acute non-infectious model of disease. Lipopolysaccharide is the outer layer of gram negative bacteria and induces a septic shock like syndrome in pigs (Wojnar et al., 1999) resulting in increased inflammatory cytokines,

a reduction in feed intake, and an increase in rectal temperature (Dritz et al., 1996; Webel et al., 2006; Frank et al., 2005; Orellana et al., 2002).

The studies conducted in this dissertation were designed to test and evaluate changes in pig health, AA, and blood metabolites in response to a LPS challenge. This was tested by running 2 trials using LPS as an acute non-infectious challenge to pigs. Results from trial 1 (12 h LPS treatment) were used to generate prediction equations for blood AA concentrations which were tested with the data from trial 2 (24 h LPS treatment). Additionally, a second model of animal health was created using *Salmonella* Typhimurium. Finally, a HPLC method for detecting N-τ-methyl-histidine in pigs was developed.

1.2 Literature cited

Balaji, R., K. J. Wright, C. M. Hill, S. S. Dritz, E. L. Knoppel, and J. E. Minton. 2000. Acute phase responses of pigs challenged orally with *Salmonella typhimurium*. J. Anim. Sci. 78:1885-1891.

Brenner, U., L. Herbertz, P. Thul, M. Walter, M. Meibert., J. M. Muller, and H. Reinauer. 1987. The contribution of small gut to the 3-methylhistidine metabolism in the adult rat. Metabolism. 26:416-418.

Dritz, S. S., K. Q. Owen, R. D. Goodband, J. L. Nelssen, M. D. Tokach, M. M. Chengappa, and F. Blecha. 1996. Influence of lipopolysaccharide-induced immune challenge and diet complexity on growth performance and acute-phase protein production in segregated early-weaned pigs. J. Anim. Sci. 74:1620-1628.

ERS/USDA. 2003. Calculating the cost of Foodborne Illness: A New Tool to Value Food Safety Risks. Economic Research Service. United States Department of Agriculture. http://www.ers.usda.gov. Accessed June 20, 2008.

FSIS/USDA. 2006. Foodborne Illness and Disease: *Salmonella* Questions and Answers. Food Safety and Inspection Service. United States Department of Agriculture. http://www.fsis.usda.gov. Accessed June 20, 2008.

Frank, J. W., M. A. Mellencamp, J. A. Carroll, R. D. Boyd, and G. L. Allee. 2005. Acute feed intake and acute-phase protein responses following a lipopolysaccharide challenge in pigs from two dam lines. Vet. Imm. Immunopath. 107:179-187.

Janssens, S and R. Beyaert. 2003. Role of toll-like receptors in pathogen recognition. Clin. Microbiology Rev. 16:637-646.

Johnson, R. W. and J. Esocbar. 2005 Cytokine regulation of protein accretion in growing animals In. *Biology of metabolism in growing animals*, vol. 3. D. G. Burrin and H. J. Mersman, Eds. Elsevier. Pgs: 83-106.

Kawai. T. and S. Akira. 2010. The role of pattern-recognition receptors in innate immunity: update on toll-like receptors. Nature Immunology. 11:373-384.

Kuhl, D. A., J. T. Methvin, and R. N. Dickerson. 1996. Standardization of acid hydrolysis procedure for urinary 3-methylhistidine determination by high-performance liquid chromatography. J. Chromatography B. 681:390-394.

Lunney, J. K. 2007. Advances in swine biomedical model genomics. Intl. J. Bio. Sci. 3:179-184.

Mogensen. 2009. Pathogen recognition and inflammatory signaling in innate immune defenses. Clin. Microbiology Rev. 22:240-273.

Munro, H. N. and V. R. Young. 1978. Urinary excretion of Nτ-methylhistidine (3-methylhistidine): a tool to study metabolic responses in relation to nutrient and hormonal status in healthy and disease of man. Am. J. Clin. Nutr. 31:1608-1614.

Orellana, R. A., P. M. J. O'Connoer, H. V. Nguyen, J. A. Bush, A. Suryawan, M. C. Thivierge, M. L. Fiorotto, and T. A. Davis. 2002. Endotoxemia reduces skeletal muscle protein synthesis in neonates. Am. J. Physio. Endocrinol. Metab. 283:E909-E916.

Webel, D. M., B. N. Finck, D. H. Baker, and R. W. Jonhson. 1997. Time course of increased plasma cytokines, cortisol, and urea nitrogen in pigs following intraperitoneal injection of lipopolysaccharide. J. Anim. Sci. 75:1514-1520.

Wojnar, M. M., J. Fa, Y. H. Li, and C. H. Lang. 1999. Endotoxin-induced changes in IGF-1 differ in rats provided enteral vs. parenteral nutrition. Am. Phys. Soc. E455-E464.

Chapter 2

Review of Literature

2.1 Introduction

The review articles by Kawai and Akira (2010), Janssens and Beyart (2003), and Mogensen (2009) were used to explain the innate immune response. When pathogens infect animals, a coordinated immune response is initiated to eliminate them and return the body to homeostasis. The innate branch of the immune system is responsible for mounting the initial generic response while the adaptive branch mounts the later and specific response and results in immunological memory against the pathogen. Microorganisms have evolved to contain several closely related molecules that are not present in the host and are thereby recognized by the host immune system. Those unique microbial molecules are called pathogen-associated molecular patterns (PAMP). Cells of the innate immune branch have developed pattern recognition receptors (PRR) capable of detecting PAMP. These receptors are divided into two families. Endocytic PRR are found on the surface of phagocytic cells (e.g., macrophages) and promote attachment of microbes followed by engulfment and destruction. Examples of endocytic PRR include mannose, scavenger, opsonin, and *N*-formyl methionine. Signaling PRR can be found on the outside surface and inside of immune cells, as well as secreted molecules in plasma and tissue fluids. Signaling PRR bind a plethora of microbial molecules and trigger intracellular signaling events that promote the synthesis and release of regulatory molecules such as cytokines. The Toll-like receptor (TLR) family is an example of signaling PRR and TLR4 is the extracellular receptor responsible for recognizing lipopolysaccharide (LPS), an invariant component of the cell wall of Gram-negative bacteria like *Escherichia coli* and *Salmonella enterica*. Toll-like receptors are expressed on macrophages, dendritic cells, and B lymphocytes

among many cells. Thus, a septicemia-like condition can easily be induced experimentally using cell-free supernatants and sterile solutions containing PAMP, which will activate signaling cascades resulting in the release of cytokines (Janssens and Beyaert, 2003; Mogensen, 2009; Kawai and Akira, 2010). These molecules not only coordinate the immune response but also act on disparate physiological systems and tissues and are responsible for important metabolic changes.

There are 21 genetically coded proteins that can be translated into amino acids (AA) but only 9 of those are considered truly essential, meaning they must be consumed in the diet. An essential AA is classified as one that must be continually consumed because it cannot be made either at all or at a rate to support the metabolic needs of the animal. Lysine is an example of an essential AA and is usually the first limiting AA in most swine diets because it is relatively low, compared to the AA requirements of pigs, in grains commonly used to formulate diets, such as corn, barley, and wheat. Therefore, lysine must be supplemented in the diet to maximize growth, and once the diet is formulated to meet the lysine requirement, the requirements for the other essential AA are usually met. Methionine is another essential AA and while it is relatively low in soybean meal it is high in corn; therefore, diets formulated with corn and soybean meal generally contain an appropriate AA balance for the nutritional needs of pigs. A subset of AA (arginine, glutamine, and histidine) are considered conditionally essential meaning that these AA could be synthesized by the body at a rate to meet the needs of the animal; however, during growth, disease, or pregnancy these AA may need to be included in the diet (NRC, 1998). To determine the level of essential AA required for pigs, the ideal protein concept is generally used (Baker et al., 1966a; 1966b, Baker and Allee, 1970, Fuller et al. 1989). This concept expresses

AA requirements as a ratio of the lysine requirement. Thus, mathematical estimates of AA requirements are commonly derived from the experimental quantification of lysine needs as:

$$\text{Ratio}_{\text{maintenance}} = \frac{\text{Mean of maintenance requirements for each AA}}{\text{Maintenance requirement for Lysine}}$$

The majority of research on the nutritional requirements of pigs has been performed in healthy animals; however, when an animal gets sick it is still unclear as to the best way to feed these animals. Research has shown that requirements for some AA may increase while others may decrease. Debate on specific AA requirements in sick animals is further complicated by appetite reduction. Scientists have shown that animals kept in a dirty environment, one that affords a high level of pathogen exposure, consume less feed and grow slower (Stahly et al., 1994).

AA requirements for growth are easily determined by observing lean tissue deposition in growing animals. Precise quantification of protein synthesis and degradation rates during health and disease could be used to estimate AA requirements. Utilization of direct markers to measure protein synthesis or degradation are costly, time consuming, usually invasive and rather tedious. An alternative is to use endogenous indirect markers that can be readily quantified in tissue or fluid samples.

Plasma is one of the most commonly collected and tested samples in human and veterinary medicine as well as in animal and biomedical research. It is relatively simple to collect plasma or urine samples from humans; however, collection from livestock and other animals can be more difficult, especially urine. Thus, finding markers in blood, plasma, serum, or saliva are preferred in animal research compared to other tissues or fluids. Examples of endogenous indirect markers of protein metabolism include blood urea nitrogen (BUN) and N-τ-

methyl histidine (NτMH), a post-translationally modified AA released during muscle proteolysis that cannot be reused for protein synthesis. Consequently, NτMH is released into circulation, filtered by the kidneys, and finally excreted from the body in the urine (Young et al., 1972). Excess levels of AA in blood are catabolized in the liver resulting in increased ureagenesis. As muscle protein is broken down, e.g. during disease, NτMH levels in plasma and urine are increased. Similarly, excesses of certain AA released from muscle during disease-induced catabolism must be eliminated via hepatic deamination and generation of urea. Both BUN (Stipanuk and Watford, 2000) and NτMH (Young et al., 1972) travel, in blood, to the kidneys for excretion, thus circulating levels reflect AA and protein catabolism, respectively.

Animal models allow us to gain knowledge and test procedures and interventions that will be unethical to perform in human subjects. Compared to rodents, pigs offer superior similarities in organ size, digestive physiology, and responses to disease with humans. Pigs infected with *Salmonella enterica* or exposed to LPS exhibit a similar as humans when infected with the same pathogen or PAMP. To the contrary, mice do not exhibit comparable gastroenteritis symptoms after *Salmonella* infection to those of humans or pigs (Balaji et al., 2000).

2.2 Cytokines and tissue protein accretion

Cytokines have the ability to greatly and differentially influence rates of protein synthesis and protein degradation in different organs of humans and animals. Elevated inflammatory cytokine levels generally lead to reductions in appetite (i.e., anorexia) and whole-body protein accretion, the latter reflecting the balance between protein degradation and protein synthesis. However, there are tissue differential effects of inflammatory cytokines. While muscle

undergoes increased degradation and reduced synthesis, cytokines cause hepatic protein synthesis to increase, mainly to produce acute phase proteins (Johnson and Escobar, 2005).

2.2.1 Protein synthesis

Insulin resistance is a major concern for physicians when treating patients with muscle wasting or sepsis. Insulin is a potent stimulator of skeletal muscle protein synthesis; however, in adult pigs, treated with LPS, protein synthesis rates are decreased regardless of insulin level (i.e. insulin resistance). Conversely, in septic neonatal pigs, when insulin levels are maintained then there is an improvement of protein synthesis levels (Orellana et al., 2006). Past research has shown, that the reduction in protein synthesis rates after LPS treatment, in adult rats, is due to a reduction in translation efficiency of the proteins downstream of the mTOR and eIF2B signaling pathways and not due to a reduction in ribosome number (Orellana et al., 2006). Protein synthesis (pathway, stimulators, and inhibitors) has been well described by Orellana et al. (2002; 2006; 2007) and will not be described in this review.

During an immunological insult the amount of protein being synthesized in skeletal muscle is severely decreased while the protein synthesis capability of the liver, heart, and lungs is increased. Inflammatory cytokines [e.g., interleukin (IL)-1, IL-6, and tumor necrosis factor (TNF)-α] are responsible for the increased uptake of hepatic AA and the subsequent induction of acute phase production in the liver (Johnson and Escobar, 2005). While skeletal muscle protein synthesis rates are very low during disease or sepsis, treating muscle with an IL-1 (Vary et al., 1996) or TNF-α (Cooney et al., 1999) receptor antagonist can return the rate of protein synthesis to control levels. Inflammatory cytokines can also decrease skeletal muscle protein synthesis by

reducing the ability of insulin-like growth factor-I (IGF-I), growth hormone (GH), or growth hormone releasing hormone (GHRH) receptors to recognize their respective ligand (French et al., 1996). In IL-6 injected mice, IGF-I levels were reduced and growth was stunted in healthy mice consuming their normal meal. A reduction in GH receptors in the liver occurs with elevated TNF-α and IL-1 levels, which could possibly lead to a reduction in IGF-I synthesis and release (De Benedetti et al., 1997).

2.2.2 Protein degradation

Chronically injecting animals with IL-1, TNF-α, or both leads to an increase in liver weight but a reduction in the weight of the animal (Fong et al., 1989). The release of inflammatory cytokines, due to sepsis, results in the activation of the ATP-dependent-ubiquitin proteolytic pathway in muscle (Llovera et al., 1988a). This proteolytic pathway is thoroughly described elsewhere (Lecker et al., 1999). Briefly, multiple ubiquitin peptide units are attached to the ε-amino group of lysine residues in the target protein. This covalent modification destines the protein for proteosomal degradation culminating with the release of free AA. Ubiquitin is not degraded, instead it is recycled to target more proteins. A bolus injection of TNF-α into the gastrocnemius muscle of rats leads to a rapid increase in ubiquitin mRNA expression (Garcia-Martinez et al., 1995). Increases in muscle ubiquitin protein content have been quantified as soon as 6 h after a bolus injection with TNF-α or IL-1 in rodents and cultured cells (Llovera et al., 1988a). The other major proteolytic pathways (i.e., calcium-dependent and lysosomal) are thought to play important roles in the degradation of sarcomeric proteins, which are not susceptible to ATP-dependent-ubiquitin degradation (Johnson and Escobar, 2005).

2.3 Metabolism of amino acids during disease

The nutritional requirement of healthy animals is well characterized; however, those requirements change drastically during disease. Anorexia (i.e. a reduction or cessation of appetite) is common during disease or stress thus increasing the need for endogenous AA obtained via proteolysis. Anorexia has been proven to be beneficial to sick animals. Mice experimentally inoculated with LD_{50} of *Listeria monocytogenes* were either force-fed to maintain feed intake levels comparable to that of healthy controls or allowed free access to feed. Force-feeding mice increased mortality from 50% mortality to 100% mortality (Murray and Murray, 1979). Furthermore, in animals that had the ability to mobilize endogenous resources, as indicated by reductions in body weight, had a better survival rate. In healthy adult animals, arginine (Arg), glutamine (Gln), and cysteine (Cys) are classified as nonessential AA (i.e., not required in the diet); however, during disease, stress, or injury these three AA may become limiting due to high metabolic demands (Le Floc'h et al., 2004). Sick animals become more selective in their macronutrient intake compared to healthy animals. There is roughly a 50% reduction in total caloric intake in sick animals, and interestingly, sick animals consume less protein during times of inflammatory stress thus reducing proteins available to support the AA needs of the animal. Supplementation of diets with lysine, a limiting AA for healthy growing animals, does not appear to ameliorate the negative protein balance or increase protein accretion during immunological stress in pigs or chicks (Webel et al., 1998).

2.3.1 Changes in amino acid requirements during disease

Arginine is required during an immunological insult due to its role as a precursor for nitric oxide (NO) and urea, as well as its conversion to ornithine for the production of

polyamines to support T-lymphocyte production (Le Floc'h et al., 2004). Production of NO stimulates tissue repair by increasing blood flow as well as being essential to the cytotoxicity activity of phagocytic cells. Increased muscle protein degradation during immune activation increases ureagenesis and hence Arg demands. During sepsis, Cys and to a lesser extent Gln play key roles in stimulating the production of glutathione which is needed to help protect host cells from oxidative damage. The amount of free radicals produced during illness increases significantly mainly to destroy pathogens but they can also damage the cells of the host. Glutathione has a free sulfhydryl group that can readily bind free radicals thus protecting the host's cells (Reeds and Jahoor, 2001; Le Floc'h et al., 2004). Therefore, demands for Cys and Gln are expected to be increased during disease. In addition to being a precursor of glutathione, Gln is also important for the production of intestinal mucosa and immune cells (Reeds and Jahoor, 2001). Glutamine has also been shown to improve nitrogen balance when administered intravenously to sick humans; however, when administered enterally there was no reported improvement in nitrogen balance (Reeds and Jahoor et al., 2001). The lack of enteral effect is probably due to a high intestinal demand for Gln. In healthy pigs, the majority of dietary Gln is taken up by the intestine; however, little dietary Gln enters portal circulation (Wu, 1998).

Furthermore, absorption of AA or nutrients can be greatly impacted during disease due to an alteration in gut motility and transit time of feedstuffs through the gastrointestinal tract (GI). A reduction in gut motility leads to constipation while an increase in gut motility results in diarrhea. Pigs treated, continuously, with *E. coli* derived endotoxin have increased motility, contractions, and transit time of feedstuffs through the GI thus leading to diarrhea (Bruins et al., 2003). In pigs treated once with *E. coli*-LPS, gastric emptying was also increased; however, there is a dose dependent response (Jia-Xian et al., 1996). However, while treating pigs with 10

μg/kg BW LPS results in an acute disease and changes to blood parameters in pigs, it does not result in increased motility or contractions in the GI. From past research, it appears that a dose of at least 25 μg/kg BW of LPS is needed to cause an increase in gastric emptying and consequently an increase in diarrheal episodes. Bouts of diarrhea can negatively impact growth performance or the ability of the host to mount a robust immune response due to a reduction in nutrient and water absorption (Jia-Xian et al., 1996).

2.3.2 Hepatic acute phase proteins

Phenylalanine (Phe) and tryptophan (Trp) are essential AA in healthy animals that may become even more important during disease primarily to support hepatic acute phase protein (APP) production. Reeds et al. (1994), reported that the aromatic AA (Phe, Trp, and tyrosine) makeup a large percentage of the AA profile in hepatic APP. Infection, trauma, and cancer can activate hepatic APP synthesis (Gruys et al., 2005). To support hepatic APP production, increased protein degradation and AA mobilization from skeletal muscle to the liver is thought to occur (Gruys et al., 2005). While skeletal muscle protein synthesis is severely decreased during disease, liver protein synthesis is markedly increased to allow for the production of APP (Orellana et. al., 2002). Inflammatory cytokines like TNF-α, IL-1β and IL-6 are well stimulators of hepatic APP synthesis and release (van Miert et al., 1995). Interestingly, TNF-α was increased in LPS treated pigs (Webel et al., 1997) but not in pigs or calves challenged with *Salmonella* (Balaji et al., 2000). In this later study, IL-1 and IL-6, which are known to be elevated in LPS treated pigs, were not measured. The authors suggested that the lack of response in plasma TNF-α was likely due to localized intestinal increase in the inflammatory cytokines.

Synthesis of hepatic APP precedes the release of specific antibodies and the down regulation of APP is directly proportional to the receding infection (Le Floc'h et al., 2004). Commonly measured hepatic APP include C-reactive protein, serum amyloid-A, haptoglobin, and fibrinogen (Reeds et al., 1994; Heinrich et al., 1990). Hepatic APP activation due to infection can result in a 2- to 100-fold increase in plasma APP (Le Floc'h et al., 2004). During the acute immune response skeletal muscle AA are released in excess of hepatic metabolic needs thus causing increased levels of certain AA in plasma and urea in plasma and urine (Le Floc'h et al., 2004; Reeds et al., 1004).

2.3.3 Muscle degradation

During disease, stress, or trauma, the aromatic AA appear to become limiting and can result in degradation of the host endogenous proteins. Consequently, resulting in a reduced ability to combat pathogenic organisms (Reeds et al., 1994). Also, the increased rate of hepatic deamination leads to an increase in AA-derived carbon skeletons being used for gluconeogenesis (Wannemacher, 1977). The breakdown of muscle protein to meet the increased hepatic AA need during an infection is a large metabolic burden for the body. For example, synthesis of 1 g of hepatic APP requires the breakdown of 1.5 to 2 g of mixed skeletal muscle proteins in order to meet the need for aromatic AA due to their low presence in muscle. Muscle-derived AA in excess of hepatic metabolic needs are degraded, excreted from the body and thus contribute to the negative nitrogen balance commonly quantified in sick humans and animals (Reeds et al., 1994).

2.3.3.1 Muscle fiber type

Inflammatory cytokines affect muscle fiber types differentially. In general terms, muscles containing fast-twitch fibers are subjected to increased protein degradation and reduced protein synthesis whereas slow-twitch muscle fibers are susceptible to increased protein degradation but unaltered protein synthesis. This is particularly important because the increased muscling in pigs (Rahelic and Puac, 1981) and chickens is mainly composed of fast-twitch muscle fibers. This means that modern leaner animals are potentially more susceptible to metabolic alteration during immunological insult (Johnson and Escobar, 2005).

2.3.3.2 Blood urea nitrogen

During catabolism some AA are deaminated yielding the corresponding keto acid, and the α-amino group used to synthesize urea. The carbon skeletons liberated during AA catabolism become intermediates that can readily enter the citric acid cycle for energy production. Amino acids are used as a fuel source for the liver, intestines, immune cells, and other tissues. The catabolism of AA leads to an increase in circulating ammonia, which is toxic at high levels. Therefore, the liver (i.e., the major site of urea production) uses ammonia and other nitrogen sources to create urea, which travels in circulation to the kidneys to be excreted via urine. The liver is the only organ in mammals that contains all the enzymes necessary for urea production. In healthy adult humans and animals, nitrogen loss from the body would be roughly the same as the daily nitrogen intake. However, in sick animals breaking down muscle protein coupled with reduced feed intake results in a nitrogen negative state (Stipanuk and Watford, 2000). Thus, an increase in AA breakdown and nitrogen excretion leads to elevated blood (plasma) urea nitrogen (BUN, PUN) levels. Pigs treated with LPS had increased plasma levels of IL-6 and TNF-α preceding an increase in PUN (Webel et al., 1997). The authors

interpreted this finding as an indicator that skeletal muscle protein was being broken down. In rodents, injections of IL-1, TNF-α, or both but not IL-6 lead to an increase in skeletal muscle protein breakdown and a concomitant increase in nitrogen excretion (i.e., elevated BUN) (Llovera et al., 1998b).

2.3.3.3 N-τ-methyl histidine

The post-translational methylation of histidine occurs in the muscle. Methylated histidine, from S-adenosylmethionine, leads to the production of NτMH and is an important part of the contractile actin and myosin proteins (Kuhl et al., 1996). NτMH is released from skeletal muscle during proteolysis, cannot be reused for protein synthesis, and is therefore excreted from the body in urine (Young et al., 1972). Young et al., (1972) developed a set of criteria for identifying a potential endogenous AA marker for skeletal muscle proteolysis including post-translational modification, absence in other tissues, released during proteolysis at a comparable rate to all other AA, the inability to be reused for protein synthesis, and hence destined for quantitative excretion. NτMH was first discovered in human urine by Tallan et al. (1954) and remarkably met all of the selection criteria. To test its feasibility as an endogenous skeletal muscle proteolysis indicator, human subjects were fed either a control or protein-free diet and the amount of NτMH excreted in urine was determined (Kadowaki et al., 1989). They observed increased urinary excretion of NτMH in humans fed the protein-free diet compared to control which was correlated with nitrogen imbalance and muscle protein breakdown. In humans, NτMH exists mainly in the free form (i.e., non-acetylated) in plasma and urine (Munro and Young, 1978); however, this may not be the case in other animal species. For example, acetylated NτMH represents 80-90% of the total NτMH found in rodents (Brenner et al., 1987),

whereas in humans the acetylated form accounts for less than 5% of excreted NτMH (Kuhl et. al., 1996).

Conventional analysis of AA in physiological fluids only detects the free form of NτMH because the acetylated form apparently interferes with the derivatization reaction needed to quantify AA (Kuhl et al., 1996). Acid hydrolysis removes the acetylation of NτMH, thus allowing it to be readily derivatized and quantified using conventional AA analysis. After acid hydrolysis treatment, NτMH quantification will include both free and acetylated fractions (i.e., total NτMH). Because free NτMH can be quantified without the need of acid hydrolysis, the acetylated fraction is then calculated by subtracting the free fraction from the total fraction. Kuhl et al. (1972) conducted a series of experiments to optimize perchloric acid hydrolysis to de-acetylate NτMH at various temperatures and incubation times no longer than 24 h. They concluded that to accurately quantify NτMH in rodent urine, samples (80-90% acetylated) must be subjected to acid hydrolysis for 1.5-4 h at 100°C or for 8-12 h at 80°C. The release of NτMH from skeletal muscle and its ability to be quantified and measured in plasma, rather than urine, make it an attractive marker for nutritional status of sick livestock and poultry.

However, during the past 30 years there has been a change in the nomenclature when referring to NτMH. The original synonym for NτMH was 3-MH; however, this term is now used to describe π-MH whose original synonym was 1-MH. The current synonym for NτMH is 1-MH and π-MH is 3-MH. Changes in the nomenclature are important to note for scientists wishing to use NτMH as a marker may be using π-MH as a standard, which, has not been validated as an indicator of skeletal muscle proteolysis (Young et al., 1972).

2.4 Alterations in blood metabolites during endotoxemia

Hyperglycemia in non-diabetic hospital patients is a major concern of physicians due to increased organ failure and eventually mortality of these patients (Anderson et al., 2004; Spitzer et al., 1985). Accompanied with hyperglycemia during sepsis is hyperinsulinemia indicating insulin resistance in septic patients. It is believed that hyperglycemia is a result of increased glycogenolysis (breakdown of muscle glycogen to produce glucose); however, muscle glycogen is quickly depleted. Once muscle glycogen is depleted, glucose is supplied by the breakdown of skeletal muscle proteins (gluconeogenesis) (Anderson et al., 2004).

Conversely, in LPS treated young pigs, glucose levels are decreased, hypoglycemia, indicating impairment in glucose synthesis during endotoxemia. In the study by Orellana et al. (2002), all neonatal pigs were continuously infused with glucose, insulin, and BCAA to maintain a fed state, half were continuously infused with LPS while the remaining half received sterile saline. Prior to LPS treatment, insulin and glucose levels were no different between groups. After LPS, insulin levels were elevated while glucose levels were reduced due to LPS treatment. In the neonatal pig model, it is unknown if the reduced glucose level, in the presence of increased insulin levels, is because they do not experience the typical insulin resistance response, seen in adult humans, or if there is impairment in gluconeogenesis (Orellana et al., 2002).

Alanine (Ala) is one of the main AA liberated from skeletal muscle during proteolysis, possibly in excess of demand (Orellana et al., 2007), and is important for the inter-organ shuffling of nitrogen for urea production (Glucose-Alanine cycle). In the Glucose-Alanine cycle, Ala is released from skeletal muscle, travels to the liver, and via alanine aminotransferase (Alt), is transaminated to pyruvate. Glucose is produced, in the liver, from pyruvate by gluconeogenesis (Stipanuk and Watford. 2000). Similarly to the Glucose-Alanine cycle is the

Cori cycle, where lactate is released from skeletal muscle and travels to the liver for glucose production (Spitzer et al., 1985). Reduced glucose levels in response to LPS treatment are not due to reduced lactate levels, as lactate levels are elevated in neonatal pigs treated with LPS (Orellana et al., 2002).

Glucose uptake by cells is generally elevated during endotoxemia; however, glucose metabolism by the cells is altered (Fink, 2003). Additionally, glucose synthesis is reduced even in the presence of precursors such as alanine and lactate (Spitzer et al., 1985). The fact that Ala, Alt, lactate, and lactate dehydrogenase levels are elevated after LPS treatment with no increase in glucose levels, may indicate a reduction in gluconeogenic activity, due to a reduction in pyruvate dehydrogenase (enzyme necessary for conversion of pyruvate to glucose) (Fink, 2003).

2.5 Experimental disease and animal models

Current treatment for a foodborne illness, such as a *Salmonella* infection, is fluid therapy and antibiotics only when necessary. During salmonellosis, the circulating AA profile of a patient is greatly altered. Understanding and being able to better predict changes in circulating AA could help the recovery of patients. The pig is a good animal model to study the effects of diseases on AA metabolism. Thus, induction of experimental sepsis or infections with a foodborne pathogen, such as *Salmonella*, will enable us to gain additional knowledge on the proper nutritional care of animals and humans with enteric foodborne illnesses.

Swine are a better animal model for human research compared to rodents due to the similarity in size and physiology of pigs to humans (Lunney, 2007). Additionally, pigs are a superior animal model compared to rodents when working with *Salmonella*. Rodents challenged with *Salmonella enterica* serotype Typhimurium exhibit clinical symptoms similar to those in

humans infected with *Salmonella* Typhi. Whereas, pigs infected with *Salmonella* Typhimurium exhibit signs and symptoms similar to the response humans experiencing *Salmonella* Typhimurium infection, including decrease in feed intake, increase in rectal temperature, and changes in nutritional requirements (Balaji et al., 2000).

2.5.1 *Salmonella enterica*

Bacterial foodborne pathogens represent 35.8% of all known foodborne illnesses reported annually in the US (Mead et al., 1999). In 2004, *Salmonella* (42%) was the most commonly reported infectious pathogen compared to *Campylobacter* (37%), *Shigella* (15%), and *E. coli* 0157:H7 (2.6%) (FSIS/USDA, 2006). Infections caused by *Salmonella* impact both human health and the animal industry. Activation of the immune system, trauma or change in nutritional status can result in an increase in protein degradation and decrease in protein synthesis thus leading to an increase in acute phase proteins being released to help combat perceived changes in the status of the animal. Ultimately, these metabolic disturbances result in changes of nutrient requirements, especially requirements for AA.

An estimated 13% of all known human illnesses (38.6 million known illnesses each year) in the US each year are thought to be caused by bacterial challenges, and *Salmonella* accounts for 27% of all foodborne bacterial infections (Mead et al., 1999). In 2005, the number of reported *Salmonella* cases in the US was 35,836 (CDC, 2005). However, the estimated number of annual *Salmonella* infections in 1999 was approximately 1.4 million cases (Mead et al., 1999). *Salmonella* Enteritidis and Typhimurium are the two main serotypes that account for approximately 37.9% of all *Salmonella* outbreaks in humans (CDC, 2005). Pork consumption is believed to be responsible for 6 to 9% of all *Salmonella* outbreaks in the US (Frenzen et al.,

1999). A *Salmonella* infection on a swine farm can pose a risk to humans but it can also negatively impact the growth performance of the pigs resulting in an economic loss. Annually in the US, $2.4 billion are lost due to *Salmonella* infections in livestock (ERS/USDA, 2003).

Salmonella is primarily transmitted to humans via contaminated feces and improper handling techniques of foods for human consumption (FSIS/USDA, 2006). Outbreaks of diseases causing diarrhea in developing countries are the most common illnesses afflicting young children (Kosek et al., 2003). The majority of *Salmonella spp.* cases in Mexico are attributed to pork consumption. A survey of meat from Mexico showed that meat from pork (36%) and swine intestine (42%) accounted for the largest percentage of positive *Salmonella* samples. Additionally, cases caused by meats from beef and poultry (30% and 21%, respectively) and from cattle and poultry intestine (21% and 17%, respectively) were much lower than those from pork. In 2008, 12% of children hospitalized for diarrhea in Mexico tested positive for *Salmonella* (Zaidi, et al., 2008). Adult animals seldom exhibit clinical signs of a *Salmonella* inhabitation thus it is common for a *Salmonella* infection to begin at the lairage pens of slaughter plants. The bacteria live in the digestive tract of animals and if the tract is opened during slaughter the carcass could potentially become contaminated (Salyers and Whitt, 2002).

The most common modes of *Salmonella* infection in both developing and developed countries are through the ingestion of contaminated meats, eggs, and produce (Callaway et al., 2008). An infection generally results in fever, abdominal cramps, nausea, and diarrhea and these symptoms are usually observed within the first 12 to 48 h of bacterial contamination. In most cases the infection is self-limiting within 4 d; however, in more severe cases it can persist longer or result in septicemia (i.e. enter the bloodstream). The typical treatment protocol for an infection is a bland diet and fluids (Merck, 2003). Most individuals recover from a *Salmonella*

infection without the need for antibiotics. However, people with a weakened immune system, children, and the elderly are at a greater risk of acquiring a life threatening infection and therefore may require antibiotic and nutritional interventions (FSIS/USDA, 2006; Merck, 2003).

Salmonella are rod shaped, Gram-negative facultative anaerobic bacteria that are commonly present in the digestive tracts of livestock and humans. The two diseases attributed to *Salmonella* are Typhoid fever or gastroenteritis. *Salmonella* Typhi is responsible for causing Typhoid fever and is more life-threatening than *Salmonella* Typhimurium which causes gastroenteritis. The symptoms of *Salmonella* Typhi infection are more severe than those previously described for *Salmonella* Typhimurium. Symptoms of Typhoid fever include high fever, anorexia, convulsions, and delusions. Both organisms can produce asymptomatic carriers and be shed in the feces for a long time after the clinical signs were noticed making the transmission of bacteria very easy from host to host. It is generally agreed that *Salmonella* enter the mucosal cells of the ileum through the M cells where the bacteria multiply. Diarrhea is a common symptom due to the pathogenesis of the disease. Once in the mucosal cells, the bacteria elicit an inflammatory response leading to a host release of prostaglandins, which increase cyclic AMP (c-AMP) levels. An increase in c-AMP results in an uptake of sodium and increased chloride being released from the cell leading to diarrhea (mucosal cells secrete water) (Salyers and Whitt, 2002).

2.5.2 Lipopolysaccharide

Disease and sepsis can greatly impact the animal industry causing a reduction in growth performance, increased veterinary costs, and increased feeding cost all of which lead to a decrease in profits. Lipopolysaccharide has been used as a non-infectious model of disease in

pigs that has been well characterized (Webel et al., 1997; Frank et al., 2005; Orellana et al., 2002) causing a septic-like response (Wojnar et al., 1999). Gram-negative bacteria are surrounded by an outer membrane layer containing LPS that is absent in Gram-positive bacteria. Upon entering the body, LPS is recognized by TLR4, whose activation initiates a series of intracellular cascade events ultimately leading to the nuclear translocation of nuclear factor κB, which is then responsible for increasing the expression of the inflammatory genes (Kawai and Akira, 2010). This in turn leads to the synthesis and release of inflammatory cytokines (Janssens and Beyaert, 2003; Mogensen, 2009; Kawai and Akira, 2010).

Administration of LPS to pigs, results in a reduction in feed intake (Dritz et al., 1996) and increased body temperature, cytokines, and BUN thus making it a reliable and repeatable model to study the intricate relationship between nutrition and disease (Webel, et. al., 1997). Endotoxemia, due to LPS treatment, can also cause an increase in gastric emptying and diarrhea thus leading to a reduction in nutrient and water absorption which could further decrease the ability of the host to mount a strong immune response during sepsis (Jia-Xian et al., 1996). During an immune insult with LPS, circulating cytokines (TNF-α, IL-1, and IL-6) are increased and act on skeletal muscle to reduce protein synthesis and enhance protein degradation and in liver increase the production of acute phase proteins in the liver (Orellana et al., 2002: Webel et al., 1997). Infection or LPS exposure cause a large release of AA from skeletal muscle, which are required for the synthesis of hepatic acute phase proteins (Reeds et al., 1994; Webel et al., 1997) or nitric oxide production (Tracey et al., 1995). While LPS can be used as a model of disease it only causes an acute response and, therefore, a chronic infectious model (i.e. *Salmonella* challenge) is still necessary to fully understand and characterize changes to nutrition requirements and muscle protein.

2.6 General conclusion

Activation of the innate immune response leads to an increase in inflammatory cytokine release resulting in an induction of hepatic acute phase proteins, a reduction in feed intake, increase in body temperature, and major changes in the utilization of several AA, all of which occur to help the host to mount a strong response against an invading pathogen (e.g., *Salmonella* and *E. coli*). Additionally, during immune system activation, skeletal muscle protein synthesis is reduced and protein degradation is increased while liver protein synthesis is elevated. An increase in skeletal muscle proteolysis leads to an increase in circulating AA and ultimately leads to an increase in circulating nitrogen products. This excess nitrogen is reflected by elevated ammonia levels, which must be removed from the body primarily through the production of urea in the liver and subsequent urinary excretion. Blood urea nitrogen and plasma NτMH can be used as indirect markers for skeletal muscle proteolysis as an alternative to invasive, expensive, and unpractical direct markers in human and veterinary medicine. In terms of animal models of disease, pigs make an ideal model due to their similarity in size, digestive capability, and immune response system compared to humans. Current literature begins to paint a picture on how the nutritional requirements of sick animals are altered; however, no AA nutritional interventions have been outlined for sick humans and animals.

2.7 Literature Cited

Anderson, S. K., J. Gjedsted, C. Christiansen, and E. Tonnesen. 2004. The roles of insulin and hyperglycemia in sepsis pathogenesis. J. Leukocyte Bio. 75:413-421.

Baker, H., and G. L. Allee. 1970. Effect of dietary carbohydrate on assessment of the leucine need for maintenance of adult swine. J. Nutr. 100:277–280.

Baker, D. H., D. E. Becker, H. W. Norton, A. H. Jensen, and B. G. Harmon. 1966a. Quantitative evaluation of the threonine, isoleucine, valine and phenylalanine needs of adult swine for maintenance. J. Nutr. 88:391–396.

Baker, D. H., D. E. Becker, H. W. Norton, A. H. Jensen, and B. G. Harmon. 1966b. Quantitative evaluation of the tryptophan, methionine and lysine needs of adult swine for maintenance. J. Nutr. 89:441–447.

Balaji, R., K. J. Wright, C. M. Hill, S. S. Dritz, E. L. Knoppel, and J. E. Minton. 2000. Acute phase responses of pigs challenged orally with *Salmonella typhimurium*. J. Anim. Sci. 78:1885-1891.

Brenner, U., L. Herbertz, P. Thul, M. Walter, M. Meibert., J. M. Muller, and H. Reinauer. 1987. The contribution of small gut to the 3-methylhistidine metabolism in the adult rat. Metabolism. 26:416-418.

Bruins, M. J., Y. C. Luiking, P. B. Soeters, L. M. A. Akkermans, and N. E. P. Deutz. 2003. Effect of prolonged hyperdynamic endotoxemia on jejunal motility in fasted and enterally fed pigs. Annals of Surgery. 237:44-51.

CDC. 2005. Bacterial Foorborne and Diarrheal Disease National Case Surveillance. Annual Report, 2005. Centers for Disease Control and Prevention. Division of Foodborne, Bacterial, and Mycotic Diseases.

Callaway, T. R., T. S. Edrington, R. C. Anderson, J. A. Byrd, and D. J. Nisbet. 2008. Gastrointestinal microbial ecology and the safety of our food supply as related to *Salmonella*. J. Anim. Sci. 86:E163-E172.

Cooney, R., S. R. Kimball, R. Eckman, G. Maish., 3rd, M. Shumate, and T. C. Vary. 1999. TNF-binding protein ameliorates inhibition of skeletal muscle protein synthesis during sepsis. Amer. J. Physiol. 276:E611-E619.

De Benedetti, F., T. Alonzi, A. Moretta, D. Lazzaro, P. Costa, V. Poli, A. Martini, G. Ciliberto, and E. Fattori. 1997. Interleukin 6 causes growth impairment in transgenic mice through a decrease in insulin-like growth factor-I. A model for stunted growth in children with chronic inflammation. J. Clin. Invest. 99:643-650.

Dritz, S. S., K. Q. Owen, R. D. Goodband, J. L. Nelssen, M. D. Tokach, M. M. Chengappa, and F. Blecha. 1996. Influence of lipopolysaccharide-induced immune challenge and diet complexity on growth performance and acute-phase protein production in segregated early-weaned pigs. J. Anim. Sci. 74:1620-1628.

ERS/USDA. 2003. Calculating the cost of Foodborne Illness: A New Tool to Value Food Safety Risks. Economic Research Service. United States Department of Agriculture. http://www.ers.usda.gov. Accessed June 20, 2008.

Fink, M. P. 2003. Cytopathic hypoxia In: The sepsis text. Jean-Louis Vincent, J. Carlet, S. M. Opal, eds. Kluwer Academic Publishers, Norwell MA, 02061, Pgs:271-284.

Frank, J. W., M. A. Mellencamp, J. A. Carroll, R. D. Boyd, and G. L. Allee. 2005. Acute feed intake and acute-phase protein responses following a lipopolysaccharide challenge in pigs from two dam lines. Vet. Imm. Immunopath. 107:179-187.

Frenzen, P.D., J. C. Buzby, and T. Roberts. 1999. An updated estimate of the economic costs of human illness due to foodborne *Salmonella* in the United States. In: Proceedings of the 3rd International Symposium on the Epidemiology and Control of *Salmonella* in Pork. Washington, DC, p. 215-218.

FSIS/USDA. 2006. Foodborne Illness and Disease: *Salmonella* Questions and Answers. Food Safety and Inspection Service. United States Department of Agriculture. http://www.fsis.usda.gov. Accessed June 20, 2008.

Fong, Y., L. L. Moldawer, M. Marano, H. Wei, A. Barber, K. Manogue, K. J. Tracey, G. Kuo, D. A. Fischman, A. Cerami, AND S. F. Lowery. 1989. Chronic cachectin/TNF or IL-1 alpha induces cachexia with redistribution of body proteins. Amer. J. Physiol. 256:R659-R665.

French, R.A., Zachary, J.F., Dantzer, R., Frawley, L.S., Chizzonite, R., Parnet, P., Kelley, K.W. 1996. Dual expression of p80 type I and p68 type II interleukin-I receptors on anterior pituitary cells synthesizing growth hormone. Endocrinology 137:4027-4036.

Garcia-Martinez, C., M. Llovera, N. Agell, F. J. Lopez-Soriano, and J. M. Argiles. 1995. Ubiquitin gene expression in skeletal muscle is increased during sepsis: involvement of TNF-alpha but not IL-1. Biochem. Biophys. Res. Commun. 217:839-844.

Gruys, E., M. J. M. Toussaint, T. A. Niewold, and S. J. Koopmans. 2005. Acute phase reaction and acute phase proteins. J. Zhejiang Univ. 6B:1045-1056.

Heinrich, P. C., T. A. Castell, T. Andus. 1990. Interleukin-6 and the acute phase response. Biochem. J. 265:621-636.

Janssens, S and R. Beyaert. 2003. Role of toll-like receptors in pathogen recognition. Clin. Microbiology Rev. 16:637-646.

Jia-Xian, L., J. R. Oliver, J. B. Philips. 1996. Endotoxin induces biphasic alterations in small intestinal myoelectric activity in fasted newborn piglets. Ped. Res. 40:822-826.

Johnson, R. W. and J. Esocbar. 2005 Cytokine regulation of protein accretion in growing animals In. *Biology of metabolism in growing animals*, vol. 3. D. G. Burrin and H. J. Mersman, Eds. Elsevier. Pgs: 83-106.

Kadowaki, M., N. Harada, S. Takahashi, T. Noguchi, and H. Naito. 1989. Differential regulation of the degradation of myofibrillar and total proteins in skeletal muscle of rats: Effects of streptozotocin-induced diabetes, dietary protein and starvation. J. Nutr. 119:471-477.

Kawai. T. and S. Akira. 2010. The role of pattern-recognition receptors in innate immunity: update on toll-like receptors. Nature Immunology. 11:373-384.

Kosek, M., C Bern, and R. L. Guerrant. 2003. The global burden of diarrhoeal disease, as estimated from studies published between 1992 and 2000. Bull. World Health Organ. 81:197-204.

Kuhl, D. A., J. T. Methvin, and R. N. Dickerson. 1996. Standardization of acid hydrolysis procedure for urinary 3-methylhistidine determination by high-performance liquid chromatography. J. Chromatography B. 681:390-394.

Le Floc'h, N. D. Melchior, and C. Obled. 2004. Modifications of protein and amino acid metabolism during inflammation and immune system activation. Livestock Prod. Sci. 87:37-45.

Lecker, S. H., V. Solomon, S. R. Price, Y. T. Kwon, W. E. Mitch, A. L. Goldberg. 1999. Ubiquitin conjugation by the N-end rule pathway and mRNAs for its components increase in muscles of diabetic rats. J. Clin. Invest. 104:1411-1420.

Llovera, M., N. Carbo, J. Lopez-Soriano, C. Garcia-Martinez, S. Busquets, B. Alvarez, N. Agell, P. Costelli, F. J. Lopez-Soriano, A. Celada, and J. M. Argiles. 1998a. Different cytokines modulate ubiquitin gene expression in rat skeletal muscle. Cancer Lett. 133:83-87.

Llovera, M., C. Garcia-Martinez, J. Lopez-Soriano, N. Carbo, N. Agell, F. J. Lopez-Soriano, and J. M. Argiles, J.M. 1998b. Role of TNF receptor 1 in protein turnover during cancer cachexia using gene knockout mice. Mol. Cell. Endocrinol. 142:183-189.

Lunney, J. K. 2007. Advances in swine biomedical model genomics. Intl. J. Bio. Sci. 3:179-184.

Mead, P.S., L. Slutsker, V. Dietz, L. F. McCraig, J. S. Bresee, C. Shapiro, P. M. Griffin, and R. V. Tauxe. 1999. Food-related illness and death in the United States. Emerg. Infect. Dis. 5:607-625.

Merck & Co., Inc. 2003. Infections: Bacterial *Salmonella* infections. Merck, Whitehouse Station, NJ. http://www.merck.com/mmhe/sec17/ch190/ch190p.html. Accessed August 27, 2008.

Mogensen. 2009. Pathogen recognition and inflammatory signaling in innate immune defenses. Clin. Microbiology Rev. 22:240-273.

Munro, H. N. and V. R. Young. 1978. Urinary excretion of Nτ-methylhistidine (3-methylhistidine): a tool to study metabolic responses in relation to nutrient and hormonal status in healthy and disease of man. Am. J. Clin. Nutr. 31:1608-1614.

Murray, M.J. and A. B. Murray, A.B. 1979. Anorexia of infection as a mechanism of host defense. Amer. J. Clin. Nutr. 32:593-596.

NRC. 1998. Nutrient Requirements of Swine. 10th ed. Natl. Acad. Press, Washington, DC.

Orellana, R. A., A. Jeyapalan, J. Escobar, J. W. Frank, H. V. Nguyen, A. Suryawan, and T. A. Davis. 2007. Amino acids augment muscle protein synthesis in neonatal pigs during acute endotoxemia by stimulating mTOR-dependent translation initiation. Am. J. Physiol. Endocrinol. Metab. 293:E1416-E1425.

Orellana, R. A., S. R. Kimball, A. Suryawan, J. Escobar, H. V. Nguyen, L. S. Jefferson, and T. A. Davis. 2006. Insulin stimulated muscle protein synthesis in neonates during endotoxemia despite repression of translation initiation. Am. J. Physiol. Endocrinol. Metab. 292:E629-E636.

Orellana, R. A., P. M. J. O'Connoer, H. V. Nguyen, J. A. Bush, A. Suryawan, M. C. Thivierge, M. L. Fiorotto, and T. A. Davis. 2002. Endotoxemia reduces skeletal muscle protein synthesis in neonates. Am. J. Physio. Endocrinol. Metab. 283:E909-E916.

Rahelic, S. and S. Puac. 1981. Fiber types in longissimus dorsi from wild and highly selected pig breeds. Meat Sci. 5:439.

Reeds, P. J., C. R. Fjeld, F. Jahoor. 1994. Do the differences between the amino acid compositions of acute-phase and muscle proteins have a bearing on nitrogen loss in traumatic states? J. Nutr. 124:906-910.

Reeds, P. J. and F. Jahoor. 2001. The amino acid requirements of disease. Clin Nutr. Supp. 1:15-22.

Salyers, A. A. and D. D. Whitt. 2002. *Salmonella* subspecies In Bacterial pathogenesis A molecular approach 2nd Ed. ASM Press, Washington, DC. Pgs:381-397.

Spitzer, J. A., K. M. Nelson, and R. E. Fish. 1985. Time course of changes in gluconeogenesis from various precursors in chronically endotoxemic rats. Metabolism 34:842-849.

Stahly, T.S., S.G. Swenson, D.R. Zimmerman, and N.R. Williams. 1994. Impact of porcine plasma proteins on postweaning growth of pigs with a low and high level of antigen exposure. Iowa State University Swine Research Report. Pg 3-5.

Stipanuk, M. H. and M. Watford. 2000. Amino acid metabolism. In: Biochemical and physiological aspects of human nutrition. M. H. Stipanuk, ed. W.B. Saunders Co, Pg 233-286.

Tallan, H. W. H. Stein, and S. Moore. 1954. 3-Methylhistidine, a new amino acid from human urine. J. Biol. Chem. 206:825-834.

Tracey, W. R., J. Tse, and G. Carter. 1995. Lipopolysaccharide-induced changes in plasma nitrite and nitrate concentrations in rats and mice: pharmacological evaluation of nitric oxide synthase inhibitors. J. Pharmacol. Experimental Therapeutics. 272:1011-1015.

van Miert, A. S. J. P. A. M. 1995. Pro-inflammatory cytokines in a ruminant model: pathophysiological, pharmacological, and therapeutic aspects. Vet. Quart. 175:41-50.

Vary, T.C., E. L. Owens, J. K. Beers, K. Verner, and R. N. Cooney. 1996. Sepsis inhibits synthesis of myofibrillar and sarcoplasmic proteins: modulation by interleukin-1 receptor antagonist. Shock 6:13-28.

Wannemacher, R. W. 1977. Key role of various individual amino acids in host response to infection. Amer. J. Clin. Nutr. 30:1269-1280.

Webel, D. M., B. N. Finck, D. H. Baker, and R. W. Jonhson. 1997. Time course of increased plasma cytokines, cortisol, and urea nitrogen in pigs following intraperitoneal injection of lipopolysaccharide. J. Anim. Sci. 75:1514-1520.

Webel, D.M., R. W. Johnson, and D. H. Baker. 1998. Lipopolysaccharide-induced reductions in food intake do not decrease the efficiency of lysine and threonine utilization for protein accretion in chickens. J. Nutr. 128:1760-1766.

Wojnar, M. M., J. Fa, Y. H. Li, and C. H. Lang. 1999. Endotoxin-induced changes in IGF-1 differ in rats provided enteral vs. parenteral nutrition. Am. Phys. Soc. E455-E464.

Wu, G. 1998. Intestinal mucosal amino acid catabolism. J. Nutr. 128:1249-1252.

Young, V. R., S. D. Alexis, B. S. Baliga, and H. N. Munro. 1972. Metabolism of administered 3-Methylhistidine. J. Biol. Chem. 247:3592-3600.

Zaidi, M. B., J. J. Calva, M. T. Estrada-Garcis, V. Leon, G. Vazquez, G. Figuero, E. Lopez, J. Contreras, J. Abbott, S. Zhau, P. McDermott, and L. Tollefson. 2008. Integrated Food chain Surveillance System for *Salmonella spp.* in Mexico. Emerg. Infect. Dis. 14:429-435.

CHAPTER 3

Estimating plasma amino acid levels using blood metabolites during endotoxemia

3.1 Abstract

Immune activation affects amino acid metabolism, protein synthesis, and protein degradation rates. Lipopolysaccharide (LPS) offers a non-infectious and well-characterized model of immune activation. Nine pigs were fitted with indwelling jugular catheters and allowed to recover from the surgery. Pigs were feed-deprived overnight, fed a meal and 2 h later were treated with 10 μg/kg body weight of *E. coli* derived LPS. Blood samples and rectal temperatures were obtained at 2-h intervals from before the meal to 12-h post-LPS treatment. Overall, rectal temperatures were elevated, plasma amino acid levels were decreased, and blood metabolite concentrations varied due to LPS treatment. The main goal of this study was to use blood metabolites to create an array of equations to predict changes in plasma amino acid levels during sickness. Ten equations for each amino acid were created using different blood metabolites. The results of this study show promise for being able to predict amino acid levels using blood metabolites and this could prove useful when planning nutritional interventions for sick patients or animals.

3.2 Introduction

The nutritional requirements of animals or humans are greatly altered during disease. For example, dietary non-essential amino acids (AA), such as arginine, glutamine, and cysteine are in such demand during a disease challenge that they purportedly become dietary essential (Reeds et al., 1994). Arginine is required during sepsis for the production of nitric oxide (NO) and urea,

which are important for mounting an immune response and for the removal of nitrogen, respectively (Stipanuk and Watford, 2000). Nearly all dietary glutamine is taken up by the intestines (Wu, 1998). Glutamine is rapidly taken up in cells that have a high turnover rate, such as intestinal and immune cells. Additionally, glutamine can aid in the metabolism and transport of nitrogen in the body (Stipanuk and Watford, 2000). The majority of available cysteine is used for the production of glutathione which helps protect cells from oxidative damage (Stipanuk and Watford, 2000; Reeds and Jahoor, 2001; Le Floc'h et al., 2004).

Lipopolysaccharide (LPS) is an invariant component of the cell wall of Gram-negative bacteria commonly used to induce an acute and well-characterized immunological insult (Webel et al., 1997; Reeds et al., 1994). During either an infectious or non-infectious challenge there are several classical signs of altered health status such as fever, anorexia, and muscle proteins catabolism leading to elevated blood urea nitrogen (Johnson and Escobar, 2005).

Skeletal muscle proteolysis is increased and skeletal muscle protein synthesis is decreased during an immunological insult. Conversely, liver protein synthesis is increased during disease to favor the synthesis of acute phase proteins that are used to help mount a defense against the invading pathogen. Although not measured during this trial, inflammatory cytokines (TNF-α, IL-1β, and IL-6) have been reported to be elevated during LPS treatment and they help stimulate the production of acute phase proteins, decrease skeletal muscle protein synthesis, and increase skeletal muscle proteolysis (Orellana et al., 2002: Webel et al., 1997; Klasing and Austic, 1984; Argiles and Lopez-Soriano, 1990).

The objective of this study was to develop a set of equations to predict plasma AA levels using blood metabolites (e.g., HDL, LDL, BUN, etc) during endotoxemia. Clinicians and

veterinarians routinely request profiles of blood metabolites; however, they seldom order an AA profile. We feel this is a novel research idea and could possibly help understand changes in AA nutritional requirements during disease. Human and animal health care professionals may use predicted AA levels to tailor nutritional interventions. Due to their similarities with humans in organ size, digestive physiology, and immune responses, pigs were used as the experimental animal.

3.3 Materials and Methods

The Virginia Tech Institutional Animal Care and Use Committee approved all procedures.

3.3.1 Animals, housing, diets, and experimental protocol

A total of 9 crossbred castrated males (26.9 ± 1.07 kg BW) were individually housed in pens located inside an environmentally controlled room. Rooms were separately ventilated with 100% clean air (i.e., no recirculation), and were under negative pressure at all times, and automated systems controlled the temperature and lighting (18 h light: 6 h dark with lights on at 0600) of each individual room. Each pen contained a plastic coated expanded metal floor, a nipple waterer, and self-feeder. All pigs were fed a common corn-soybean meal diet at 90% of their free-choice average daily feed intake to insure complete consumption of each meal bout. Pigs were fed 3 times each d and had continuous free access to water. After an adjustment period of 10 d, indwelling jugular vein catheters were surgically implanted for serial blood collection as previously described (Escobar et al., 2006). All pigs were treated for 3 d post-surgery with i.v. flunixin meglumine twice each d for pain management (4 mg/kg BW, Flunixijet, Butler Animal Health, Dublin, OH) and i.m. ceftiofur-HCl (5 mg/kg BW, once each d

as bacterial prophylaxis, Excenel-RTU, Pfizer, New York, NY). Ten days after surgery, a venous blood sample was collected into Li-heparinized Vacutainers (BD, Franklin Lakes, NJ) and pigs were fed one-third of their normal feed intake every 20 min for the next 1 h. Two h after initial feeding (i.e., t = 0) another blood sample was collected and all pigs were treated intravenously with 10 μg/kg of body weight of LPS from (*E. coli* 055:B5, Sigma-Aldrich, St. Louis, MO) suspended in 0.9% sterile saline (i.e. 1 ml/10 kg BW). Samples were collected from pigs for 12 h post LPS treatment. Blood samples were collected, post-LPS infusion, to determine concentrations of glucose and lactate every 20 min, and hematocrit, AA, and metabolites every 2 h. Blood samples were centrifuged (5810R, Eppendorf, Hamburg, Germany) at 3,000×g for 5 min at 4°C and the resulting plasma was collected, transferred to 2-mL microcentrifuge tubes (Eppendorf, Hamburg, Germany), and stored at -80ºC until analyzed for AA and various metabolites.

3.3.2 Analyses of blood metabolites

Various clinical-grade commercial kits were purchased to determine the concentration of metabolites in plasma according to each manufacturer's instructions (Table 3.1). Haptoglobin, fibrinogen, and C-reactive protein ELISA were purchased from Immunology Consultants Laboratory (Newberg, OR). Serum amyloid A ELISA was purchased from Tridelta Development (Boonton, NJ). A nitrate and nitrite assay kit was purchased from Cayman Chemical (Ann Arbor, MI). Direct low density lipoprotein cholesterol, triglyceride-glycerophosphate oxidase, creatinine, amylase, urea nitrogen, aspartate aminotransferase, direct high density lipoprotein cholesterol, total bilirubin, calcium, γ-glutamyl transferase, lactate dehydrogenase, inorganic phosphorus, total lipid, alanine aminotransferase, alkaline

phosphatase, albumin, creatine kinase, and total protein were purchased from Teco Diagnostics (Anaheim, CA).

3.3.3 Plasma amino acids

Plasma samples (500 μL) were combined with an equal volume of 0.4 mM norleucine (Sigma Aldrich, CAS 327-57-1) as the internal standard, filtered at 10,000×g for 10 min at 4°C using 10k MW cutoff filters (Pall Corp., Port Washington, NY). An aliquot (25 μL) was transferred to a glass Kimble tube, vacuum dried, derivatized with phenyl isothiocyanate (Acros Organics, Geel, Belgium, CAS 103-72-0), and separated using a 2695 Alliance HPLC equipped with a 30-cm Pico-Tag column, 2487 UV/Vis detector, and Empower software (all from Waters Corp., Milford, MA) using previously described conditions (Cohen et al., 1989). All AA concentrations are expressed in μmol/L.

3.3.4 Model development and prediction equations

To determine prediction equations, the PROC REG procedure of SAS (SAS Institute, Cary, NC) was used with a backwards selection method. Each AA was individually regressed against all available blood metabolites regardless of time of collection during the study. Parameter estimates (α), standard errors (SE), probability-values (P-value), coefficient of regression (R^2), mean square error (MSE), MSE/p and the square root of the mean square error (RMSE) were obtained for each SAS-generated equation for each AA using the following general equation:

$$[AA] = \text{intercept} + (\alpha_1 \times [\text{metab}_1]) + (\alpha_2 \times [\text{metab}_2]) + \ldots + (\alpha_n \times [\text{metab}_n])$$

where, [AA] is the plasma concentration of an AA in μmol/L, intercept is the intercept of the multiple-linear regression equation, PE is parameter estimate for a metabolite, and [metabolite] is the plasma concentration of each metabolite in its appropriate concentration units (Table 3.1). For each AA, multiple-linear regression equations including 1 to 10 different metabolite terms are presented (Tables 3.2 to 3.23).

3.3.5 Statistical analysis

Data were checked for normality and outliers were removed using the PROC UNIVARIATE procedure of SAS. The PROC MIXED procedure of SAS was used to examine effects of treatment on AA and metabolite concentrations; least square means (lsmeans) were obtained with the LSMEANS option and Tukey adjustment. Data are expressed as lsmeans ± pooled SE.

3.4 Results and Discussion

3.4.1 Response of AA and blood metabolites to LPS treatment

Lipopolysaccharide is commonly used to induce an acute immune response. Treatment of pigs with 10 μg/kg BW of LPS resulted in elevated (P < 0.0001; Figure 3.1) rectal temperatures from 1-h post-LPS treatment through 7-h post-LPS. At 8-h post-LPS and for the remainder of the sampling period (to t = 12) rectal temperature remained at baseline levels. Rectal temperatures peaked at t = 3 (41.76 ± 0.145), about 1.5°C over baseline.

Immune activation altered AA metabolism as exemplified in the relationship between phenylalanine (Phe) or tyrosine (Tyr) during LPS treatment. In healthy animals, Phe is readily converted to Tyr and can help meet the Tyr requirement (Stipanuk and Watford, 2000).

However, Tyr cannot be converted to Phe. In LPS treated pigs Phe (Figure 3.7A) concentrations began rising over baseline 6 h after LPS treatment ($P < 0.001$) but Tyr (Figure 3.7B) levels remained at or numerically lowered from baseline ($P < 0.001$). Twelve hours after LPS exposure, plasma Phe levels were higher than baseline ($P = 0.004$) and comparable to postprandial levels ($P = 0.98$). Conversely, 12 h after LPS treatment plasma Tyr levels were lower than baseline ($P < 0.0001$). The increase in Phe and Tyr levels, and most other AA, after the meal indicates appropriate digestion of proteins and absorption of AA. The linear increase in plasma Phe levels from 6 to 12 h after LPS treatment was not matched with a similar response in Tyr levels, which remained flat. Thus, a classic nutrition principle establishing the conversion of Phe to Tyr appears to be altered after LPS exposure.

The plasma concentration of the majority of AA increased after meal consumption. Overall, LPS treatment resulted in the reduction ($P = 0.03$) in plasma AA levels (except Alanine was elevated after LPS, explained later in this Discussion) and the concentration of many AA began increasing at 6 or 8 h post-LPS (Figures 3.2-3.10) with the exception of tyrosine, tryptophan, and glutamate. The rise in plasma AA levels is more likely explained by the body's attempt to return to normal and I snot due to digestion activity because the pigs were only fed one time during the trial (t = -2). Twelve hours after LPS treatment, the increase in plasma Phe and Lys to postprandial levels (Figure 3.7A and B) is not likely explained by undigested feed in the intestine because similar increases were not measured for other essential AA like Trp (Figure 3.8A), Arg (Figure 3.10B), Leu (Figure 3.6A), Val, and Ile (Figure 3.6B). Maintenance of plasma Ala (Figure 3.2A) at postprandial levels with elevated plasma ALT (Figure 3.12B) and BUN (Figure 3.14A) after LPS treatment can be jointly interpreted to suggest increased skeletal muscle proteolysis. Some AA catabolism performed in muscle (e.g., BCAA) generates amino

groups that could be transferred to pyruvate to form Ala, which travels to the liver, where ALT will transaminate Ala to pyruvate and glutamate (Glu). Pyruvate can be used for gluconeogenesis in liver and glucose can travel to skeletal muscle thus completing the glucose-Ala cycle. Increased plasma lactate, presumably from anaerobic glycolysis in skeletal muscle origin, can also be converted to glucose in the liver and hence contribute to increased Ala formation in muscle (Stipanuk and Watford, 2000). In the liver, Glu can be readily deaminated to form urea or transaminated in other tissues to form Gln, another well-known shuttle of nitrogen in the body. Furthermore, Glu is an endogenous precursor of Arg, the immediate precursor of ureagenesis in liver (Stipanuk and Watford, 2000). During sepsis, muscle proteolysis, hepatic uptake of AA and liver protein synthesis are elevated thus leading to elevated nitrogen loss from the body (Reeds et al., 1994)).

Urea is produced during the conversion of Arg to ornithine (Orn). Blood urea nitrogen (BUN) is an indicator of skeletal muscle protein breakdown and changes are seen quickly after LPS treatment. Blood urea nitrogen levels increased ($P < 0.0001$, Figure 3.14A) linearly and remained elevated until the final blood sample collection at 12 h post-LPS treatment. A similar linear increase in BUN, during the first 12-h after LPS treatment, was quantified in pigs treated with 5 μg/kg BW of LPS (Webel et al., 1997). In the same study, pigs treated with 0.5 μg/kg BW LPS exhibited no increases in BUN levels over saline treated pigs. Finally, regardless of LPS dose, BUN returned to baseline values 24-h after LPS treatment (Webel et al., 1997). In our study, elevated BUN levels at 12 h after LPS treatment indicates that pigs were still actively breaking down muscle protein to satisfy AA demands of other body tissues and organs such as the liver. As BUN levels were increasing, Arg levels were decreasing and remained low throughout the study ($r = -0.25$, $P = 0.03$).

In addition to monitoring changes in BUN, plasma Alanine (Ala, Figure 3.2A), alanine aminotransferase (ALT, Figure 3.12B), aspartate aminotransferase (AST, Figure 3.12A), lactate (Lac, Figure 3.19A), and lactate dehydrogenase (LDH, Figure 3.19B) can be used as markers of skeletal muscle activity. In the current study, 2 h after LPS treatment, plasma Ala levels were no different ($P = 0.22$) from baseline (pre-fed) levels; however, at t = 4, through the remainder of the trial (t = 12 h), Ala levels were greater ($P = 0.02$) than baseline levels. Additionally, ALT levels were elevated ($P < 0.0211$) over baseline levels with the exception of t = 6 and 8 h post-LPS where ALT levels were no different ($P > 0.97$) from baseline levels. Aspartate aminotransferase levels were elevated ($P = 0.01$) 4-h after LPS treatment and remained elevated for the remainder of the 12-h sampling period. Plasma lactate levels were elevated ($P < 0.01$) after LPS treatment and had returned to baseline at the conclusion of the study ($P = 0.08$ at t = 12). Lactate dehydrogenase (LDH) levels were not different from baseline levels; however, numerically, LDH levels were greater than baseline levels for the entire 12 h after LPS administration. A significant rise in LDH, over baseline levels, could possibly be observed by increasing the number of animals (Chapter 4). Alanine, ALT, AST, Lac, and LDH all increased in response to LPS injection, thus an indicator of increased skeletal muscle activity (i.e. skeletal muscle proteolysis).

In the current study, glucose levels (Figure 3.22A) dropped below baseline (pre-fed) levels ($P < 0.003$) and remained low for the entire 12-h blood sampling period. Blood glucose levels began increasing at 8 h post-LPS; however, at t = 12 h glucose levels were still slightly below baseline levels ($P = 0.07$), an indication of impaired gluconeogenesis and a likely contributor to enhance glucose-Ala and glucose-lactate cycles between skeletal muscle and liver. In another pig study, however, glucose levels were unchanged when pigs were treated with 0.5 or

5 μg/kg BW LPS (Webel et al., 1997) thus indicating a potential role of LPS and hence immune activation of altered body metabolism. Our results are opposite of what occurs in humans in response to LPS treatment. In humans, LPS treatment or sepsis seen in hospitalized patients is accompanied with elevated glucose levels (Agwunobi et al., 2000). In rats, LPS treatment has been shown to increase plasma glucose immediately after LPS with glucose levels returning to normal within 2 h (Lang et al., 1992).

Hematocrit (HCT) levels can be impacted by the health status or level of hydration. A dehydrated animal will experience a drop in HCT levels and vice versa. In 1 study involving pigs, LPS treatment reduced packed cell volume; however, the biological justification for the decline in HCT in response to LPS was unknown (Saedeleer, V. De et al., 1991). In the current study, we observed a numerical ($P > 0.33$) increase in HCT (Figure 3.24A) initially after LPS but at 8 h after LPS HCT levels began falling and were lower ($P = 0.007$) than baseline at 12 h after LPS treatment; however, this effect is possibly confounded by the fact that during the 12-h sampling period 1 L of saline was infused into the animal. Conversely, in rats, HCT levels initially increase in response to LPS with levels returning to baseline quickly (within 2 h) thus indicating an initial loss of plasma water with the body quickly correcting the perceived dehydration (Lambalgen et al., 1988) which is a response that more closely mimicked our results.

Nitric oxide (NO) is produced during direct conversion of Arg to Cit in various tissues and immune cells. It serves as a vasodilator and oxidative radical of phagocytic immune cells to destroy pathogens (Mori, 2007). Both LPS challenge and cytokine stimulation increased NO production (Mori, 2007). As expected, total plasma NO was elevated after LPS treatment ($P = 0.0003$; Figure 3.20C).

3.4.2 Prediction equations

It is unlikely that data for all terms (i.e., metabolites) would be available at all times due to limited testing, which justifies the need for a range of prediction equations capable to accommodate different clinical scenarios. Thus, clinicians may order laboratory analyses for humans or animals based on their clinical training and professional judgment without the need for ordering additional clinical exams just to be able to predict plasma concentrations of AA. For each of the 22 different AA, Tables 3.2 to 3.23 list all the blood metabolites included in each model, parameter estimates, SE, *P*-value of each metabolite within the model, R^2, mean square error (MSE), and MSE/p, where p is the number of terms in the model (Kitchenham et al., 1999), are listed for each generated prediction equation. A standard error (std err) and *P*-value for each metabolite, in each model, are included in the tables (just under the LSMEAN). The *P*-value (for each metabolite in each model) is listed as an indication of the importance (or not) of each term in that particular equation. The MSE/p will tell you when to stop adding or subtracting terms from the model, meaning it will help indicate (better than R^2) the best model to use. Mean square error accounts for the error associated with each model; however you cannot compare 1 MSE with another for any given AA; therefore, dividing MSE by p accounts for the error and the number of terms in the model thus allowing the within AA comparison of error associated with each model. Mean square error divided by the number of parameters in the model increases as the number of terms in the model decreases (Tables 3.2 to 3.23) thus indicating we are justified using any of the equations with 10 or fewer terms in the model. If the MSE/p decreased when going from the 6th term to the 5-term model then that would indicate that the 5th term model would be the best; however, this was not the case in our equations.

3.5 Implications

It is evident from this trial that blood metabolites and AA are impacted during immune activation. A 12-h LPS model may not be long enough to include metabolic recovery. Data used to generate the predicting equations have two main constraints: short-term duration and non-infectious challenge. Our 12-h model focused on the induction and establishment of an acute immune response, where most metabolic alterations take place. The value of including the recovery phase in the animal disease model is debatable because the host metabolism will be returning to, rather than departing from, normal metabolism and the most precarious phase of the disease has already been overcome and critical clinical and nutritional care will be dwindling. With a few exceptions, humans and animals usually succumb to pathogenic disease rather than chemically defined immune activation. However, the underlying metabolic alterations during immune activation are common for infectious and non-infectious acute immune stimulation. Therefore, the use of the prediction equations proposed herein should be applicable to acute immune activation. Nevertheless, the purpose of this study was to establish a biological relationship between circulating AA and metabolite levels that can be further mathematically defined for prediction purposes. Production animals are not kept in sterile environments and are thus exposed to a wide array of pathogens and non-infectious antigens capable of activating immune responses and negatively impacting growth performance. Because nutrient requirements have not been established for sick animals, clearly best feeding practices and nutritional intervention strategies cannot be developed. Nonetheless understanding metabolic changes during illness and their impact on AA needs will contribute to improve the nutritional care of sick humans and animals.

3.6 Tables

Table 3.1. List of all metabolites analyzed

Acronym	Description	Assay	Units	Provider
ALT	Alanine aminotransferase	Colorimetric	IU/L	Teco Diagnostics, A526-120
ALB	Albumin	Colorimetric	g/dL	Teco Diagnostics, A502-480
ALK	Alkaline phosphatase	Colorimetric	IU/L	Teco Diagnostics, A506-120
AMY	Amylase	Enzymatic, kinetic	IU/L	Teco Diagnostics, A533-60
AST	Aspartate aminotransferase	Colorimetric	IU/L	Teco Diagnostics, A561-120
BIL	Bilirubin	Colorimetric	mg/dL	Teco Diagnostics, B576-480
BUN	Blood urea nitrogen	Enzymatic, endpoint	mg/dL	Teco Diagnostics, B551-132
CA	Calcium	Colorimetric	mg/dL	Teco Diagnostics, C503-480
CHOL	Cholesterol	Enzymatic, endpoint	mg/L	Teco Diagnostics, C509-400
CK	Creatine kinase	Enzymatic, kinetic	IU/L	Teco Diagnostics, C512-240
CRTN	Creatinine	Colorimetric	mg/dL	Teco Diagnostics, C513-480
CRP	C-reactive protein	ELISA	ng/dL	Immunology Consultants Lab., e-5crp
FIB	Fibrinogen	ELISA	mg/dL	Immunology Consultants Lab., e-5fib
GGT	Gamma-glutamyl transferase	Enzymatic, kinetic	IU/L	Teco Diagnostics, G571-150
GLC	Glucose	Immobilized membrane	mg/dL	Yellow Springs Instruments
HAPT	Haptoglobin	ELISA	ng/dL	Immunology Consultants Lab., e-5hpt
HCT	Hematocrit	Centrifugation	%	In-house
HDL	High-density lipoprotein	Colorimetric	mg/dL	Teco Diagnostics, H513-100
iP	Inorganic phosphorus	Colorimetric	mg/L	Teco Diagnostics, I515-480
LAC	L-Lactate	In house	mg/dL	YSI
LDH	L-Lactate dehydrogenase	Enzymatic, kinetic	IU/L	Teco Diagnostics, L535-240
LDL	Low-density lipoprotein	Colorimetric	mg/dL	Teco Diagnostics, L530-100
NO_3	Nitrate	Colorimetric	μM	Cayman, 780001
NO_2	Nitrite	Colorimetric	μM	Cayman, 780001
NO_X	Total Nitric Oxide products	Colorimetric	μM	Cayman, 780001
SAA	Serum amyloid A	ELISA	pmol/L	Tridelta Development Ltd, TP-802
TL	Total lipid	Colorimetric	mg/dL	Teco Diagnostics, T526-480
TP	Total protein	Biuret	g/dL	Teco Diagnostics, T528-480
TG	Triglyceride	Enzymatic, endpoint	mg/dL	Teco Diagnostics, T531-400
UA	Uric acid	Enzymatic, end-point	mg/dL	Teco Diagnostics, U580-240

Table 3.2. Alanine prediction equations containing 1 to 10 terms. Equations with more than 10 terms were calculated but are not shown.

	Number of terms in prediction equation									
Item	10	9	8	7	6	5	4	3	2	1
Intercept	1097.136	1466.17	1321.73	1848.61	2119.21	2126.10	1489.86	1126.87	734.28	826.99
Std err*	644.111	564.59	574.32	500.14	390.09	397.29	290.05	252.12	112.90	106.14
p-value	0.1014	0.0155	0.0296	0.0010	<0.0001	<0.0001	<0.0001	<0.0001	<0.0001	<0.0001
TP	134.725									
Std err	115.778									
p-value	0.2560									
CA	-83.229	-72.863								
Std err	45.752	45.193								
p-value	0.0814	0.1195								
BUN	46.076	43.517	37.468							
Std err	21.679	21.719	22.041							
p-value	0.0440	0.0561	0.1011							
HDL	14.755	19.673	14.910	5.430						
Std err	9.441	8.502	8.214	6.238						
p-value	0.1312	0.0292	0.0810	0.3917						
TG	-6.554	-5.494	-6.299	-3.940	-3.625					
Std err	2.916	2.789	2.827	2.548	2.511					
p-value	0.0341	0.0601	0.0347	0.1337	0.1599					
GLC	-11.246	-9.996	-10.903	-9.380	-9.046	-9.649				
Std err	4.321	4.214	4.303	4.354	4.318	4.377				
p-value	0.0156	0.0257	0.0177	0.0403	0.0453	0.0356				
CRTN	-284.875	-275.538	-259.712	-167.121	-174.649	-184.441	-144.878			
Std err	81.046	81.217	83.064	64.870	64.012	64.831	66.184			
p-value	0.0018	0.0023	0.0043	0.0158	0.0109	0.0081	0.0365			
LDL	-7.966	-7.748	-7.729	-7.713	-7.049	-7.491	-6.711	-5.457		
Std err	2.759	2.772	2.856	2.954	2.842	2.878	3.034	3.156		
p-value	0.0081	0.0098	0.0119	0.0146	0.0194	0.0144	0.0347	0.0938		
CK	-0.450	-0.507	-0.445	-0.312	-0.243	-0.238	-0.208	-0.144	-0.137	
Std err	0.138	0.130	0.128	0.104	0.068	0.069	0.072	0.069	0.071	
p-value	0.0033	0.0006	0.0018	0.0059	0.0013	0.0017	0.0069	0.0465	0.0637	
LDH	4.180	4.170	3.743	3.277	2.921	2.927	2.665	2.180	2.439	1.472
Std err	0.784	0.789	0.766	0.740	0.614	0.625	0.652	0.650	0.651	0.430
p-value	<0.0001	<0.0001	<0.0001	0.0001	<0.0001	<0.0001	0.0003	0.0021	0.0007	0.0017
Overall model statistics										
R^2	0.6887	0.6711	0.6369	0.5966	0.5852	0.5544	0.4797	0.3966	0.3384	0.2621
MSE*	39408.0	39966.0	42425.0	45394.0	45001.0	46684.0	52690.0	59135.0	62811.0	67932.0
MSE/p*	3940.80	4440.67	5303.13	6484.86	7500.17	9336.80	13172.50	19711.67	31405.50	67932.00
RMSE*	198.51	199.91	205.97	213.06	212.13	216.06	229.54	243.18	250.62	260.64

*Std err, standard error; MSE, mean standard error; MSE/p, MSE divided by number of terms in model; RMSE, square root of MSE.

Table 3.3. Arginine prediction equations containing 1 to 10 terms. Equations with more than 10 terms were calculated but are not shown.

	Number of terms in prediction equation									
Item	10	9	8	7	6	5	4	3	2	1
Intercept	-342.41	-262.93	-310.84	-347.33	-359.30	-145.70	-97.60	-158.31	295.21	312.40
Std err*	182.37	166.56	166.97	177.91	188.40	167.48	16.87	164.55	34.28	35.66
p-value	0.0726	0.1270	0.0740	0.0613	0.0668	0.3915	0.5595	0.3435	<0.0001	<0.0001
AMY	-0.043									
Std err	0.400									
p-value	0.3008									
CRTN	-19.459	-23.887								
Std err	16.720	16.228								
p-value	0.2557	0.1535								
LDL	-1.827	-1.846	-1.685							
Std err	0.747	0.749	0.758							
p-value	0.0222	0.0210	0.0350							
LAC	-9.942	10.057	12.104	10.371						
Std err	4.762	4.772	4.666	4.926						
p-value	0.0476	0.0453	0.0154	0.0447						
HCT	10.414	10.342	9.491	8.169	7.306					
Std err	3.132	3.138	3.153	3.315	3.486					
p-value	0.0028	0.0029	0.0057	0.0204	0.0452					
TG	-2.729	-3.214	-3.503	-3.125	-1.873	-1.079				
Std err	1.060	0.958	0.989	1.010	0.865	0.822				
p-value	0.0166	0.0025	0.0011	0.0046	0.0391	0.1998				
NO_x	-9.156	-10.215	-9.872	-8.219	-6.698	-5.578	-4.905			
Std err	2.951	2.782	2.834	2.928	3.007	3.127	3.122			
p-value	0.0049	0.0011	0.0018	0.0092	0.0341	0.0849	0.1266			
TP	90.476	73.953	75.067	66.953	79.865	79.821	67.544	71.626		
Std err	27.447	22.620	23.109	24.432	25.058	26.483	25.071	25.520		
p-value	0.0030	0.0031	0.0032	0.0107	0.0035	0.0053	0.0114	0.0086		
LDH	0.526	0.464	0.517	0.578	0.559	0.506	0.502	0.555	0.412	
Std err	0.156	0.144	0.143	0.150	0.159	0.166	0.168	0.168	0.177	
p-value	0.0024	0.0036	0.0013	0.0007	0.0015	0.0048	0.0055	0.0024	0.0263	
ALK	-8.394	-8.423	-9.877	-9.664	-7.620	-7.189	-7.466	-8.716	-9.622	-5.525
Std err	2.307	2.312	2.137	2.286	2.193	2.308	2.325	2.236	2.439	1.800
p-value	0.0013	0.0012	<0.0001	0.0002	0.0017	0.0041	0.0031	0.0005	0.0004	0.0043
Overall model statistics										
R^2	0.7463	0.7345	0.7115	0.6566	0.6002	0.5375	0.5100	0.4697	0.3350	0.2221
MSE*	2799.93	2813.21	2939.44	3369.55	3782.64	4225.28	4326.86	4531.82	5505.77	6244.93
MSE/p*	280.00	312.58	367.43	481.36	630.44	845.06	1081.72	1510.61	2752.89	6244.93
RMSE*	52.91	53.04	54.22	58.05	61.50	65.00	65.78	67.32	74.20	79.02

*Std err, standard error; MSE, mean standard error; MSE/p, MSE divided by number of terms in model; RMSE, square root of MSE.

Table 3.4. Asparagine prediction equations containing 1 to 10 terms. Equations with more than 10 terms were calculated but are not shown.

	Number of terms in prediction equation									
Item	10	9	8	7	6	5	4	3	2	1
Intercept	31.637	19.050	24.274	6.254	41.763	36.008	-1.898	176.019	120.752	83.462
Std err*	63.905	64.244	65.174	66.859	71.810	74.887	78.489	25.959	19.163	14.436
p-value	0.6234	0.7684	0.7115	0.9259	0.5640	0.6331	0.9808	<0.0001	<0.0001	<0.0001
HAPT	0.000004									
Std err	0.000003									
p-value	0.1515									
LAC	3.251	2.547								
Std err	1.729	1.685								
p-value	0.0677	0.1387								
ALK	-2.499	-2.155	-1.667							
Std err	0.901	0.883	0.834							
p-value	0.0085	0.0192	0.0526							
TG	-1.078	-1.198	-0.933	-1.095						
Std err	0.399	0.397	0.361	0.365						
p-value	0.0103	0.0044	0.0136	0.0045						
CRP	-0.0004	-0.0004	-0.0004	-0.0005	-0.0003					
Std err	0.0001	0.0001	0.0001	0.0001	0.0001					
p-value	0.0016	0.0023	0.0013	0.0009	0.0336					
LDL	-1.037	-1.064	-1.041	-1.092	-1.093	-1.005				
Std err	0.313	0.317	0.322	0.332	0.363	0.376				
p-value	0.0020	0.0018	0.0024	0.0021	0.0044	0.0106				
TP	41.167	50.050	52.223	58.325	42.923	33.896	27.160			
Std err	12.816	11.452	11.542	11.530	11.268	10.949	11.373			
p-value	0.0027	<0.0001	<0.0001	<0.0001	0.0004	0.0034	0.0213			
CRTN	-21.980	-28.104	-30.261	-35.464	-31.885	-21.197	-22.098	-23.978		
Std err	9.014	8.100	8.100	7.945	8.572	7.365	7.854	8.212		
p-value	0.0195	0.0013	0.0006	<0.0001	0.0006	0.0062	0.0073	0.0055		
NO_x	-3.443	-3.563	-3.027	-3.681	-3.778	-4.636	-4.002	-4.235	-4.113	
Std err	1.193	1.208	1.173	1.167	1.272	1.264	1.325	1.389	1.497	
p-value	0.0064	0.0053	0.0136	0.0030	0.0049	0.0007	0.0042	0.0038	0.0086	
LDH	0.327	0.309	0.280	0.192	0.217	0.269	0.308	0.226	0.216	0.202
Std err	0.071	0.071	0.070	0.056	0.061	0.058	0.060	0.052	0.056	0.600
p-value	<0.0001	0.0001	0.0003	0.0014	0.0009	<0.0001	<0.0001	<0.0001	0.0003	0.0014
Overall model statistics										
R^2	0.7366	0.7218	0.7055	0.6761	0.6049	0.5595	0.4864	0.4198	0.3099	0.1967
MSE*	704.04	724.66	747.94	802.50	955.65	1040.70	1185.80	1309.73	1523.98	1736.21
MSE/p*	70.40	80.52	93.49	114.64	159.28	208.14	296.45	436.58	761.99	1736.21
RMSE*	26.53	26.92	27.35	28.33	30.91	32.26	34.44	36.19	39.04	41.67

*Std err, standard error; MSE, mean standard error; MSE/p, MSE divided by number of terms in model; RMSE, square root of MSE.

Table 3.5. Aspartate prediction equations containing 1 to 10 terms. Equations with more than 10 terms were calculated but are not shown.

	Number of terms in prediction equation									
Item	10	9	8	7	6	5	4	3	2	1
Intercept	2.050	4.469	17.885	23.491	21.864	19.769	28.597	32.105	28.827	32.538
Std err*	17.042	17.155	9.534	7.305	6.970	7.014	5.519	3.303	2.711	2.726
p-value	0.9052	0.7966	0.0719	0.0034	0.004	0.0086	<0.0001	<0.0001	<0.0001	<0.0001
iP	-0.777									
Std err	0.606									
p-value	0.2116									
CHOL	3.073	1.950								
Std err	2.224	2.071								
p-value	0.1798	0.3554								
HCT	0.593	0.464	0.223							
Std err	0.363	0.353	0.242							
p-value	0.1152	0.2007	0.3667							
TL	-0.022	-0.016	-0.019	-0.011						
Std err	0.017	0.017	0.016	0.014						
p-value	0.2060	0.3452	0.2615	0.4315						
SAA	-0.012	-0.013	-0.010	-0.011	-0.009					
Std err	0.007	0.007	0.006	0.006	0.005					
p-value	0.0955	0.0792	0.1244	0.0902	0.1264					
CK	-0.007	-0.006	-0.005	-0.005	-0.004	-0.003				
Std err	0.003	0.002	0.002	0.002	0.002	0.002				
p-value	0.0071	0.0148	0.0183	0.0184	0.0233	0.0653				
HDL	0.401	0.371	0.283	0.288	0.269	0.210	0.059			
Std err	0.147	0.147	0.114	0.113	0.11	0.106	0.074			
p-value	0.0118	0.0184	0.0194	0.0172	0.0211	0.0572	0.4322			
AMY	-0.005	-0.006	-0.006	-0.006	-0.006	-0.004	-0.003	-0.003		
Std err	0.002	0.002	0.002	0.002	0.002	0.002	0.002	0.002		
p-value	0.0671	0.0146	0.0169	0.0161	0.0106	0.0369	0.0854	0.1085		
LDH	0.062	0.053	0.047	0.045	0.042	0.041	0.020	0.021	0.020	
Std err	0.016	0.015	0.0131	0.013	0.012	0.013	0.007	0.006	0.007	
p-value	0.0007	0.0013	0.0013	0.0017	0.0019	0.0029	0.0046	0.0023	0.0042	
CRTN	-5.59	-4.976	-4.074	-3.880	-3.746	-3.465	-3.321	-3.733	-4.050	-3.723
Std err	1.53	1.476	1.12	1.097	1.077	1.089	1.134	1.002	1.010	1.127
p-value	0.0013	0.0024	0.0012	0.0015	0.0017	0.0035	0.0064	0.0008	.0003	0.0023
Overall model statistics										
R^2	0.637	0.612	0.598	0.585	0.575	0.537	0.479	0.468	0.421	0.249
MSE*	12.662	12.989	12.933	12.858	12.692	13.341	14.528	14.357	15.133	19.040
MSE/p*	1.27	1.44	1.62	1.84	2.12	2.67	3.63	4.79	7.57	19.040
RMSE*	3.56	3.60	3.60	3.59	3.56	3.65	3.81	3.79	3.89	4.36

*Std err, standard error; MSE, mean standard error; MSE/p, MSE divided by number of terms in model; RMSE, square root of MSE.

Table 3.6. Citrulline prediction equations containing 1 to 10 terms. Equations with more than 10 terms were calculated but are not shown.

	Number of terms in prediction equation									
Item	10	9	8	7	6	5	4	3	2	1
Intercept	-201.48	-127.22	-129.17	-89.53	-110.29	-101.58	-51.12	0.204	51.72	36.62
Std err*	79.45	55.24	57.32	50.55	49.04	50.30	41.96	43.199	31.15	28.21
p-value	0.0181	0.0299	0.0329	0.0879	0.0326	0.0528	0.2325	0.9963	0.1066	0.2033
HDL	0.442									
Std err	0.344									
p-value	0.2110									
BIL	27.463	19.259								
Std err	12.696	11.117								
p-value	0.0407	0.0955								
LAC	3.223	2.246	1.740							
Std err	1.442	1.242	1.253							
p-value	0.0350	0.0826	0.1766							
LDL	-0.423	-0.350	-0.295	-0.260						
Std err	0.189	0.183	0.187	0.188						
p-value	0.0347	0.0669	0.1259	0.1785						
TG	-0.921	-0.755	-0.553	-0.324	-0.326					
Std err	0.293	0.267	0.249	0.190	0.193					
p-value	0.0044	0.0090	0.0352	0.0988	0.1025					
GLC	0.976	0.813	0.737	0.568	0.613	0.551				
Std err	0.341	0.321	0.330	0.312	0.315	0.323				
p-value	0.0086	0.0179	0.0343	0.0796	0.0621	0.0988				
LDH	0.093	0.094	0.106	0.098	0.106	0.105	0.122			
Std err	0.037	0.038	0.039	0.039	0.039	0.040	0.040			
p-value	0.0203	0.0197	0.0106	0.0178	0.0110	0.0145	0.0049			
CHOL	29.061	22.061	22.025	18.435	18.468	19.660	18.834	110.406		
Std err	8.041	5.992	6.218	5.682	5.771	5.907	6.072	18.542		
p-value	0.0014	0.0011	0.0015	0.0034	0.0034	0.0024	0.0042	0.1043		
AST	-0.586	-0.519	-0.525	-0.435	-0.411	-0.394	-0.458	-0.157	-0.098	
Std err	0.143	0.134	0.129	0.216	0.126	0.130	0.128	0.092	0.087	
p-value	0.0004	0.0007	0.0009	0.0018	0.0030	0.0051	0.0012	0.0964	0.2694	
HCT	5.644	4.774	5.248	4.682	4.648	4.211	3.639	2.639	1.342	1.599
Std err	1.308	1.133	1.141	1.085	1.102	1.104	1.085	1.162	0.895	0.869
p-value	0.0002	0.0003	<0.0001	<0.0001	0.0002	0.0007	0.0022	0.0308	0.1437	0.0747
Overall model statistics										
R^2	0.6333	0.6081	0.5611	0.5285	0.4952	0.4438	0.3880	0.1998	0.1275	0.0931
MSE*	174.21	178.75	192.51	199.14	205.60	218.72	232.64	294.35	310.91	313.39
MSE/p*	17.42	19.86	24.06	28.45	34.27	43.74	58.16	98.12	155.46	313.39
RMSE*	13.20	13.37	13.87	14.11	14.34	14.79	15.25	17.16	140.57	17.70

*Std err, standard error; MSE, mean standard error; MSE/p, MSE divided by number of terms in model; RMSE, square root of MSE.

Table 3.7. Glycine prediction equations containing 1 to 10 terms. Equations with more than 10 terms were calculated but are not shown.

	Number of terms in prediction equation									
Item	10	9	8	7	6	5	4	3	2	1
Intercept	1125.07	1143.43	837.896	936.324	1372.765	1462.540	1412.372	902.279	1263.83	607.660
Std err*	311.11	310.97	282.864	288.610	239.066	253.859	266.024	203.289	201.03	171.556
p-value	0.0014	0.0011	0.0065	0.0031	<0.0001	<0.0001	<0.0001	0.0001	<0.0001	0.0012
CK	-0.052									
Std err	0.052									
p-value	0.3135									
SAA	-0.444	-0.364								
Std err	0.202	0.186								
p-value	0.0376	0.0622								
TL	-1.370	-1.171	-0.947							
Std err	0.550	0.515	0.529							
p-value	0.0200	0.0318	0.0848							
HCT	21.213	21.112	25.209	17.712						
Std err	8.185	8.194	8.338	7.502						
p-value	0.0160	0.0163	0.0056	0.0257						
AST	2.910	2.768	3.091	3.544	2.660					
Std err	1.064	1.056	1.098	1.112	1.129					
p-value	0.0115	0.0147	0.0092	0.0036	0.0257					
ALK	-21.814	-17.710	-17.106	-18.417	-15.388	-10.778				
Std err	6.122	4.651	4.886	5.024	5.240	5.228				
p-value	0.0016	0.0008	0.0017	0.0011	0.0066	0.0483				
CA	-85.558	-82.971	-86.226	-78.995	-74.483	-100.386	-87.860			
Std err	27.144	27.060	28.431	29.272	31.506	31.759	32.817			
p-value	0.0043	0.0051	0.0054	0.0119	0.0252	0.0037	0.0119			
LDH	1.930	1.355	1.472	1.352	1.319	1.789	1.162	1.063		
Std err	0.672	0.373	0.388	0.397	0.428	0.408	0.285	0.310		
p-value	0.0083	0.0013	0.0008	0.0021	0.0046	0.0001	0.0003	0.0017		
GGT	-10.588	-12.861	-13.839	-14.572	-13.496	-12.038	-14.020	-14.114	-19.209	
Std err	3.713	2.989	3.102	3.198	3.414	3.612	3.665	4.013	4.311	
p-value	0.0088	0.0002	0.0001	0.0001	0.0005	0.0024	0.0006	0.0014	<0.0001	
AMY	0.461	0.455	0.495	0.447	0.505	0.542	0.514	0.438	0.458	0.521
Std err	0.073	0.073	0.074	0.072	0.073	0.077	0.079	0.083	0.094	0.116
p-value	<0.0001	<0.0001	<0.0001	<.0001	<0.0001	<0.0001	<0.0001	<0.0001	<0.0001	<0.0001
Overall model statistics										
R^2	0.8999	0.8954	0.8795	0.8646	0.8367	0.8043	0.7756	0.7220	0.6163	0.3783
MSE*	13955	13989	15501	16770	19509	22572	25017	29994	40098	63011
MSE/p*	1395.50	1554.33	1937.63	2395.71	3251.50	4514.40	6254.25	9998.00	20049.00	63011.00
RMSE*	118.13	118.28	124.50	129.50	139.67	150.24	158.17	173.19	200.24	251.02

*Std err, standard error; MSE, mean standard error; MSE/p, MSE divided by number of terms in model; RMSE, square root of MSE.

Table 3.8. Glutamate prediction equations containing 1 to 10 terms. Equations with more than 10 terms were calculated but are not shown.

	Number of terms in prediction equation									
Item	10	9	8	7	6	5	4	3	2	1
Intercept	-48.316	179.104	434.807	333.945	221.649	246.471	183.906	297.662	371.378	387.393
Std err*	223.646	201.543	122.166	104.717	83.108	82.028	68.229	33.735	24.026	26.086
p-value	0.8308	0.3827	0.0015	0.0036	0.0126	0.0054	0.0114	<0.0001	<0.0001	<0.0001
GGT	2.652									
Std err	1.356									
p-value	0.0622									
HCT	9.258	6.688								
Std err	4.244	4.257								
p-value	0.0392	0.1288								
CA	-20.389	19.710	-16.450							
Std err	10.237	10.794	10.887							
p-value	0.0579	0.0798	0.1429							
TL	-0.597	-0.508	-0.391	-0.381						
Std err	0.221	0.229	0.104	0.227						
p-value	0.0126	0.0356	0.0900	0.1049						
ALT	0.918	0.756	0.712	0.712	0.485					
Std err	0.353	0.361	0.371	0.379	0.366					
p-value	0.0156	0.0468	0.0656	0.0712	0.1954					
NO_2	-12.001	-9.362	-9.728	-10.521	-9.135	-8.018				
Std err	5.472	5.595	5.746	5.860	5.983	6.000				
p-value	0.0382	0.1067	0.1024	0.0836	0.1380	0.1918				
GLC	4.976	3.594	2.715	-2.369	2.320	2.026	2.035			
Std err	1.304	1.156	1.039	1.038	1.070	1.061	1.074			
p-value	0.0008	0.0046	0.0147	0.0305	0.0388	0.0661	0.0678			
LDH	0.550	0.457	0.340	0.370	0.362	0.316	0.310	0.312		
Std err	0.113	0.108	0.104	0.105	0.108	0.071	0.105	0.109		
p-value	<0.0001	0.0003	0.0007	0.0015	0.0023	0.0049	0.0061	0.0076		
SAA	0.341	0.345	0.309	0.303	0.345	0.333	0.337	0.318	0.212	
Std err	0.070	0.0073	0.072	0.073	0.071	0.071	0.072	0.074	0.071	
p-value	<0.0001	<0.0001	0.0002	0.0003	<0.0001	<0.0001	<0.0001	0.0002	<0.0001	
CHOL	-90.051	-96.927	-108.688	-100.553	-82.375	-74.017	-75.215	-74.703	-64.479	-50.006
Std err	18.842	19.529	18.539	18.156	15.035	13.829	13.979	14.548	15.598	16.515
p-value	<0.0001	<0.0001	<0.0001	<0.0001	<0.0001	<0.0001	<0.0001	<0.0001	<0.0001	0.0048
Overall model statistics										
R^2	0.7495	0.7095	0.6808	0.6528	0.6166	0.5925	0.5674	0.5157	0.3883	0.2174
MSE*	2183.85	2430.62	2567.85	2689.86	2864.26	2939.30	3016.28	3268.25	3999.08	4960.81
MSE/p*	218.39	270.07	320.98	384.27	477.38	587.86	754.07	1089.42	1999.54	4960.81
RMSE*	46.73	49.30	50.67	51.86	53.52	54.22	54.92	57.17	63.24	70.43

*Std err, standard error; MSE, mean standard error; MSE/p, MSE divided by number of terms in model; RMSE, square root of MSE.

Table 3.9. Glutamine prediction equations containing 1 to 10 terms. Equations with more than 10 terms were calculated but are not shown.

	Number of terms in prediction equation									
Item	10	9	8	7	6	5	4	3	2	1
Intercept	1032.40	898.36	1121.04	1258.45	1464.93	1654.35	1570.85	1395.87	1179.26	950.49
Std err*	359.35	335.03	300.84	280.62	163.48	143.62	151.59	126.26	104.14	41.62
p-value	0.0082	0.0126	0.0009	0.0001	<0.0001	<0.0001	<0.0001	<0.0001	<0.0001	<0.0001
CA	-25.154									
Std err	24.541									
p-value	0.3152									
CK	0.037	0.031								
Std err	0.023	0.022								
p-value	0.1146	0.1704								
AMY	-0.128	-0.138	-0.106							
Std err	0.090	0.089	0.088							
p-value	0.1665	0.1351	0.2387							
TP	140.085	130.259	98.783	46.929						
Std err	70.076	69.485	66.995	51.758						
p-value	0.0566	0.0721	0.1519	0.3723						
NO_2	28.659	26.507	25.087	24.001	25.988					
Std err	12.558	12.393	12.576	12.645	12.415					
p-value	0.0313	0.0420	0.0563	0.0680	0.0452					
CRP	-0.002	-0.002	-0.002	-0.001	-0.001	-0.001				
Std err	0.0006	0.0006	0.0006	0.0005	0.0004	0.0004				
p-value	0.0049	0.0058	0.0064	0.0094	0.0090	0.0165				
CHOL	-73.745	-65.387	-77.096	-77.559	-82.402	-82.003	-64.753			
Std err	32.068	31.044	30.456	30.698	30.137	31.789	33.673			
p-value	0.0301	0.0450	0.0175	0.0175	0.0105	0.0150	0.0637			
NO_x	-16.956	-15.152	-15.172	-18.093	-18.717	-17.191	-17.700	-15.305		
Std err	5.791	5.22	5.623	5.114	5.052	5.273	5.713	5.806		
p-value	0.0072	0.0109	0.0119	0.0014	0.0009	0.0028	0.0041	0.0128		
LDL	-5.121	-4.981	-5.334	-5.057	-4.722	-4.578	-5.376	-4.845	-3.965	
Std err	1.441	1.435	1.439	1.432	1.379	1.453	1.538	1.576	1.673	
p-value	0.0015	0.0018	0.0010	0.0014	0.0019	0.0037	0.0015	0.0043	0.0238	
TG	-6.525	-6.519	-7.116	-7.780	-7.068	-7.561	-6.128	-4.592	-3.882	-4.347
Std err	1.848	1.851	1.834	1.763	1.573	1.641	1.671	1.528	1.634	1.729
p-value	0.0016	0.0016	0.0006	0.0001	0.0001	<0.0001	0.0009	0.0051	0.0235	0.0168
Overall model statistics										
R^2	0.6892	0.6761	0.6513	0.6326	0.6218	0.5646	0.4711	0.4080	0.2794	0.1568
MSE*	11252	11274	11687	11875	11802	13133	15441	16743	19761	22444
MSE/p*	1125.20	1252.67	1460.88	1696.43	1967.00	2626.60	3860.25	5581.00	9880.50	22444.00
RMSE*	106.08	106.18	108.11	108.97	108.64	114.60	124.26	129.39	140.57	149.81

*Std err, standard error; MSE, mean standard error; MSE/p, MSE divided by number of terms in model; RMSE, square root of MSE.

Table 3.10. Histidine prediction equations containing 1 to 10 terms. Equations with more than 10 terms were calculated but are not shown.

	Number of terms in prediction equation									
Item	10	9	8	7	6	5	4	3	2	1
Intercept	-289.825	-253.500	-199.867	-129.519	7.612	-19.416	47.207	47.522	102.261	84.133
Std err*	139.231	137.700	128.187	122.017	80.429	75.579	62.932	63.609	18.469	10.172
p-value	0.0482	0.0775	0.1311	0.2979	0.9253	0.7991	0.4590	0.4606	<0.0001	<0.0001
TL	-0.131									
Std err	0.105									
p-value	0.2230									
SAA	-0.068	-0.050								
Std err	0.049	0.047								
p-value	0.1770	0.3025								
CRTN	-15.486	-15.226	-12.364							
Std err	8.575	8.669	8.249							
p-value	0.0835	0.0913	0.1460							
CHOL	33.515	32.918	26.845	15.330						
Std err	13.827	13.974	12.755	10.414						
p-value	0.0233	0.0266	0.0451	0.1526						
iP	-6.492	-5.865	-6.398	-5.514	-3.040					
Std err	3.458	3.460	3.430	3.456	3.082					
p-value	0.0727	0.1025	0.0735	0.1223	0.3325					
HCT	7.081	6.045	5.598	3.627	1.665	1.981				
Std err	2.410	2.288	2.253	1.872	1.341	1.302				
p-value	0.0072	0.0140	0.0198	0.0632	0.2248	0.1390				
GGT	-1.475	-1.409	-1.317	-1.252	-1.104	-0.949	-0.797			
Std err	0.615	0.620	0.615	0.627	0.632	0.611	0.616			
p-value	0.0245	0.0317	0.0417	0.0561	0.0914	0.1316	0.2060			
TP	55.087	47.977	36.315	33.142	20.462	19.215	16.354	10.376		
Std err	18.980	18.312	14.613	14.789	12.269	12.198	12.313	11.535		
p-value	0.0078	0.0147	0.0197	0.0334	0.1065	0.1260	0.1942	0.3753		
AMY	-0.054	-0.051	-0.037	-0.040	-0.036	-0.036	-0.027	-0.021	-0.014	
Std err	0.021	0.021	0.016	0.016	0.016	0.016	0.015	0.014	0.012	
p-value	0.0160	0.0218	0.0275	0.0173	0.0330	0.0289	0.0777	0.1503	0.2494	
LDH	0.217	0.203	0.201	0.184	0.151	0.156	0.139	0.144	0.113	0.107
Std err	0.057	0.057	0.057	0.057	0.054	0.053	0.053	0.054	0.041	0.041
p-value	0.0009	0.0015	0.0015	0.0033	0.0086	0.0067	0.0142	0.0118	0.0101	0.0139
Overall model statistics										
R^2	0.4964	0.4635	0.4397	0.3913	0.3425	0.3196	0.2653	0.2244	0.2042	0.1699
MSE*	520.46	532.23	534.45	559.12	582.43	581.87	607.36	620.51	616.81	623.84
MSE/p*	52.05	59.14	66.81	79.87	97.07	116.37	151.84	206.84	308.41	623.84
RMSE*	22.81	23.07	23.12	23.65	24.13	24.12	24.64	24.91	24.84	24.98

*Std err, standard error; MSE, mean standard error; MSE/p, MSE divided by number of terms in model; RMSE, square root of MSE.

Table 3.11. Isoleucine prediction equations containing 1 to 10 terms. Equations with more than 10 terms were calculated but are not shown.

	Number of terms in prediction equation									
Item	10	9	8	7	6	5	4	3	2	1
Intercept	-496.42	-504.01	-505.90	-589.19	-431.31	-370.67	-275.90	-230.40	-189.21	-22.06
Std err*	94.87	97.94	101.79	100.04	73.61	70.53	66.23	67.92	65.10	37.48
p-value	<0.0001	<0.0001	<0.0001	<0.0001	<0.0001	<0.0001	0.0001	0.0015	0.0057	0.5590
HAPT	0.000005									
Std err	0.000003									
p-value	0.0665									
LDL	-0.778	-0.724								
Std err	0.346	0.357								
p-value	0.0307	0.0493								
ALK	-2.065	-1.902	-1.762							
Std err	0.723	0.742	0.768							
p-value	0.0070	0.0144	0.0272							
ALB	53.493	43.580	38.575	36.506						
Std err	15.683	15.273	15.666	16.453						
p-value	0.0016	0.0070	0.0183	0.0322						
LAC	6.611	5.884	5.934	4.850	4.035					
Std err	1.748	1.762	1.831	1.861	1.910					
p-value	0.0005	0.0019	0.0024	0.0128	0.0408					
CK	0.027	0.027	0.029	0.025	0.018	0.016				
Std err	0.006	0.006	0.006	0.006	0.006	0.006				
p-value	<0.0001	<0.0001	<0.0001	0.0003	0.0027	0.0084				
AMY	-0.107	-0.108	-0.102	-0.113	-0.090	-0.071	-0.054			
Std err	0.021	0.022	0.022	0.023	0.022	0.020	0.021			
p-value	<0.0001	<0.0001	<0.0001	<0.0001	0.0001	0.0011	0.0128			
CRP	-0.0005	-0.0004	-0.0004	-0.0004	-0.0004	-0.0004	-0.0004	-0.0002		
Std err	0.0001	0.0001	0.0001	0.0001	0.0001	0.0001	0.0001	0.0001		
p-value	<0.0001	0.0004	0.0012	0.0017	0.0007	0.0008	0.0041	0.0882		
TP	77.643	87.681	78.4447	92.937	89.673	87.668	65.942	44.061	32.562	
Std err	15.613	15.173	15.045	14.365	14.958	15.531	14.394	14.394	10.751	
p-value	<0.0001	<0.0001	<0.0001	<0.0001	<0.0001	<0.0001	<0.0001	0.0009	0.0041	
GLC	2.365	2.520	2.794	2.932	3.011	2.364	2.629	2.335	2.443	2.739
Std err	0.552	0.564	0.569	0.595	0.622	0.563	0.597	0.623	0.634	0.679
p-value	0.0001	<0.0001	<0.0001	<0.0001	<0.0001	0.0001	<0.0001	0.0005	0.0004	0.0002
Overall model statistics										
R^2	0.7557	0.7321	0.7030	0.6629	0.6214	0.5802	0.5038	0.4259	0.3862	0.2611
MSE*	769.79	821.43	887.27	981.90	1075.86	1164.58	1344.51	1520.21	1589.165	1871.51
MSE/p*	76.98	91.27	110.91	140.27	179.31	232.92	336.13	506.74	794.58	1871.51
RMSE*	27.75	28.66	29.79	31.34	32.80	34.13	36.67	38.99	39.86	43.26

*Std err, standard error; MSE, mean standard error; MSE/p, MSE divided by number of terms in model; RMSE, square root of MSE.

Table 3.12. Leucine prediction equations containing 1 to 10 terms. Equations with more than 10 terms were calculated but are not shown.

	Number of terms in prediction equation									
Item	10	9	8	7	6	5	4	3	2	1
Intercept	-368.40	-261.76	-305.55	-279.14	-97.63	-69.51	-8.57	122.08	84.41	-2.40
Std err*	153.64	116.81	114.65	118.15	112.01	119.03	124.88	86.01	87.11	78.51
p-value	0.0246	0.0342	0.0131	0.0256	0.3909	0.5637	0.9458	0.1658	0.3398	0.9758
ALB	28.697									
Std err	26.955									
p-value	0.2976									
LDL	-1.070	-0.959								
Std err	0.689	0.683								
p-value	0.0088	0.1726								
LAC	5.775	6.025	5.738							
Std err	3.176	3.176	3.228							
p-value	0.0815	0.0694	0.0871							
HDL	4.588	4.708	3.971	4.528						
Std err	1.608	1.609	1.549	1.576						
p-value	0.0088	0.0072	0.0165	0.0078						
CRP	-0.0006	-0.0007	-0.0007	-0.0008	-0.0005					
Std err	0.0002	0.0002	0.0002	0.0002	0.0003					
p-value	0.0175	0.0032	0.0052	0.0026	0.0312					
CK	-0.105	-0.111	-0.099	-0.110	-0.057	-0.055				
Std err	0.028	0.027	0.027	0.268	0.022	0.023				
p-value	0.0010	0.0005	0.0010	0.0003	0.0141	0.0245				
GGT	5.382	5.235	5.251	5.634	6.372	4.349	2.443			
Std err	1.630	1.628	1.658	1.709	1.896	1.788	1.717			
p-value	0.0030	0.0036	0.0039	0.0027	0.0023	0.0214	0.1651			
LDH	1.233	1.236	1.198	1.260	1.702	1.050	0.409	0.324		
Std err	0.265	0.266	0.270	0.278	0.297	0.317	0.177	0.170		
p-value	0.0001	<0.0001	0.0001	0.0001	0.0019	0.0025	0.0283	0.0654		
ALK	-12.796	-12.897	-12.350	-11.808	-11.609	-10.747	-6.989	-6.639	-3.220	
Std err	2.204	2.208	2.213	2.278	2.555	2.702	2.352	2.377	1.627	
p-value	<0.0001	<0.0001	<0.0001	<0.0001	<0.0001	0.0004	0.0058	0.0089	0.0565	
GLC	3.856	4.235	4.479	4.165	4.743	3.974	4.349	3.506	4.376	4.880
Std err	1.233	1.184	1.193	1.226	1.357	1.405	1.500	1.400	1.378	1.413
p-value	0.0046	0.0015	0.0009	0.0021	0.0016	0.0084	0.0069	0.0178	0.0033	0.0015
Overall model statistics										
R^2	0.7655	0.7545	0.7351	0.7029	0.6121	0.5407	0.4515	0.4145	0.3456	0.2656
MSE*	2355.19	2367.76	2456.20	2652.75	3339.97	3817.81	4407.17	4552.77	4929.71	5365.07
MSE/p*	235.52	263.08	307.03	378.96	556.66	763.56	1101.79	1517.59	2464.86	5365.07
RMSE*	48.53	48.66	49.56	51.50	57.79	61.79	66.39	67.47	70.21	73.25

*Std err, standard error; MSE, mean standard error; MSE/p, MSE divided by number of terms in model; RMSE, square root of MSE.

Table 3.13. Lysine prediction equations containing 1 to 10 terms. Equations with more than 10 terms were calculated but are not shown.

	Number of terms in predicting equation									
Item	10	9	8	7	6	5	4	3	2	1
Intercept	-626.657	-623.577	61.489	295.985	364.116	237.555	307.022	262.519	225.916	275.743
Std err*	228.763	257.934	146.932	88.984	78.887	50.290	42.732	39.890	42.257	22.407
p-value	0.0114	0.0232	0.6790	0.0025	<0.0001	<0.0001	<0.0001	<0.0001	<0.0001	<0.0001
Nox	-9.776									
Std err	3.504									
p-value	0.0102									
HCT	17.096	14.442								
Std err	4.295	4.723								
p-value	0.0006	0.0053								
HDL	7.507	6.846	4.048							
Std err	1.809	2.022	2.073							
p-value	0.0004	0.0023	0.0617							
CHOL	99.003	98.809	43.853	28.597						
Std err	21.874	24.664	19.416	18.678						
p-value	0.0001	0.0005	0.0325	0.1374						
LDL	-3.211	-2.559	-2.115	-1.683	-1.884					
Std err	0.747	0.800	0.905	0.922	0.934					
p-value	0.0002	0.0037	0.0273	0.0789	0.0533					
LAC	23.184	19.617	16.192	15.985	15.149	13.544				
Std err	4.418	4.768	5.327	5.597	5.702	5.938				
p-value	<0.0001	0.0004	0.0053	0.0082	0.0129	0.0301				
TG	-4.823	-3.886	-3.121	-3.205	-3.751	-3.684	-2.050			
Std err	0.809	0.952	1.056	1.109	1.075	1.130	0.933			
p-value	<0.0001	0.0004	0.0066	0.0075	0.0016	0.0028	0.0358			
ALK	-13.176	-16.631	-14.151	-13.735	-13.590	-12.755	-9.700	-9.168		
Std err	2.554	2.519	2.741	2.871	2.938	3.059	2.936	3.102		
p-value	<0.0001	<0.0001	<0.0001	<0.0001	<0.0001	0.0003	0.0025	0.0059		
LDH	1.353	1.763	1.463	1.163	1.181	1.222	1.123	1.069	0.337	
Std err	0.291	0.282	0.304	0.276	0.282	0.296	0.313	0.330	0.244	
p-value	<0.0001	<0.0001	<0.0001	0.0003	0.0003	0.0003	0.0012	0.0029	0.1761	
CK	-0.158	-0.189	-0.157	-0.105	-0.109	-0.104	-0.101	-0.093	-0.057	-0.028
Std err	0.030	0.032	0.035	0.023	0.023	0.024	0.026	0.027	0.027	0.017
p-value	<0.0001	<0.0001	0.0001	<0.0001	<0.0001	0.0002	0.0004	0.0016	0.0406	0.1072
Overall model statistics										
R^2	0.8089	0.7470	0.6523	0.6013	0.5667	0.5037	0.4147	0.3204	0.1288	0.0767
MSE*	2573.34	3271.56	4322.35	4772.80	5001.92	5531.36	6306.30	7085.85	8799.34	9043.08
MSE/p*	257.33	363.51	540.29	681.83	833.65	1106.27	1576.58	2361.95	4399.67	9043.08
RMSE*	50.73	57.20	65.74	69.09	70.72	74.37	79.41	84.18	93.80	95.10

*Std err, standard error; MSE, mean standard error; MSE/p, MSE divided by number of terms in model; RMSE, square root of MSE.

Table 3.14. Methionine prediction equations containing 1 to 10 terms. Equations with more than 10 terms were calculated but are not shown.

	Number of terms in prediction equation									
Item	10	9	8	7	6	5	4	3	2	1
Intercept	-148.13	-120.94	-121.90	-120.93	-74.05	-66.97	-57.71	-31.97	-40.82	21.72
Std err*	45.47	45.90	45.78	46.67	38.00	38.58	38.28	37.51	38.87	32.06
p-value	0.0033	0.0142	0.0131	0.0152	0.0614	0.0932	0.1421	0.4005	0.3011	0.5016
HDL	1.248									
Std err	0.625									
p-value	0.0574									
CK	-0.021	-0.004								
Std err	0.009	0.005								
p-value	0.0357	0.3592								
CRTN	-12.846	-9.117	-6.944							
Std err	5.402	5.362	4.819							
p-value	0.0257	0.1015	0.1615							
BUN	4.538	2.867	2.713	1.636						
Std err	1.444	1.245	1.231	0.997						
p-value	0.0044	0.0299	0.0366	0.1125						
TG	-0.673	-0.551	-0.529	-0.452	-0.343					
Std err	0.227	0.232	0.230	0.228	0.225					
p-value	0.0068	0.0252	0.0296	0.0576	0.1374					
SAA	-0.062	-0.052	-0.050	-0.045	-0.040	-0.031				
Std err	0.023	0.024	0.024	0.024	0.024	0.024				
p-value	0.0129	0.0370	0.0432	0.0711	0.1117	0.2120				
AMY	-0.027	-0.028	-0.029	-0.030	-0.024	-0.028	-0.018			
Std err	0.012	0.012	0.012	0.012	0.012	0.012	0.009			
p-value	0.0270	0.0302	0.0225	0.0220	0.0561	0.0280	0.0611			
GGT	-1.042	-1062	-1.191	-1.210	-1.233	-1.059	-0.963	-0.729		
Std err	0.373	0.395	0.369	0.376	0.387	0.379	0.375	0.371		
p-value	0.0101	0.0125	0.0034	0.0034	0.0035	0.0090	0.0154	0.0581		
LDH	0.156	0.101	0.071	0.077	0.075	0.086	0.090	0.065	0.079	
Std err	0.051	0.012	0.031	0.031	0.032	0.032	0.009	0.031	0.032	
p-value	0.0051	0.0335	0.0310	0.0208	0.0269	0.0126	0.0093	0.0450	0.0175	
TP	36.977	44.848	45.730	44.135	36.889	33.861	27.981	18.723	15.932	7.985
Std err	9.838	9.535	9.465	9.586	8.761	8.729	7.491	6.040	6.129	5.649
p-value	0.0010	<0.0001	<0.0001	<0.0001	0.0002	0.0006	0.0008	0.0041	0.0140	0.1669
Overall model statistics										
R^2	0.6206	0.5576	0.5421	0.5056	0.4563	0.4109	0.3778	0.2993	0.2118	0.0571
MSE*	191.35	191.80	190.86	198.46	210.75	220.16	224.77	244.98	266.96	309.67
MSE/p*	19.14	21.31	23.86	28.35	35.13	44.03	56.19	81.66	133.48	309.67
RMSE*	13.83	13.85	13.82	14.09	14.52	14.84	14.99	15.65	16.34	17.60

*Std err, standard error; MSE, mean standard error; MSE/p, MSE divided by number of terms in model; RMSE, square root of MSE.

Table 3.15. Ornithine prediction equations containing 1 to 10 terms. Equations with more than 10 terms were calculated but are not shown.

	Number of terms in prediction equation									
Item	10	9	8	7	6	5	4	3	2	1
Intercept	-3.310	6.556	14.718	-25.453	-47.788	-58.257	-32.075	154.308	164.780	176.221
Std err*	55.958	59.233	62.854	64.331	66.200	70.198	69.117	14.740	16.313	18.106
p-value	0.9533	0.9128	0.8167	0.6955	0.4764	0.4134	0.6459	<0.0001	<0.0001	<0.0001
TL	-0.161									
Std err	0.087									
p-value	<0.0001									
CRP	-0.0003	-0.0002								
Std err	0.0001	0.0001								
p-value	0.0156	0.0462								
AST	-0.667	-0.611	-0.453							
Std err	0.197	0.207	0.205							
p-value	0.0024	0.0068	0.0363							
LDL	-0.699	-0.826	-0.726	-0.640						
Std err	0.289	0.300	0.315	0.334						
p-value	0.0237	0.0109	0.0296	0.0664						
LAC	7.476	7.064	6.180	5.070	4.690					
Std err	1.817	1.919	1.991	2.059	2.145					
p-value	0.0004	0.0011	0.0046	0.0205	0.0373					
TG	-1.776	-1.847	-1.323	-1.053	-1.011	-0.508				
Std err	0.411	0.435	0.379	0.384	0.401	0.349				
p-value	0.0002	0.0003	0.0017	0.0106	0.0176	0.1559				
TP	42.011	36.790	27.837	33.289	29.748	35.436	29.537			
Std err	10.229	10.527	10.234	10.620	10.943	11.300	10.746			
p-value	0.0004	0.0018	0.0115	0.0041	0.0111	0.0039	0.0100			
CK	-0.026	-0.025	-0.029	-0.034	-0.033	-0.031	-0.030	-0.032		
Std err	0.007	0.008	0.008	0.008	0.008	0.009	0.009	0.010		
p-value	0.0017	0.0034	0.0011	0.0003	0.0006	0.0015	0.0025	0.0032		
LDH	0.615	0.601	0.659	0.662	0.671	0.646	0.625	0.585	0.274	
Std err	0.087	0.092	0.094	0.100	0.105	0.111	0.112	0.122	0.084	
p-value	<0.0001	<0.0001	<0.0001	<0.0001	<0.0001	<0.0001	<0.0001	<0.0001	0.0026	
ALK	-6.512	-6.856	-0.453	-8.052	-7.853	-6.720	-6.683	-7.158	-5.501	-2.774
Std err	0.978	1.023	0.205	1.060	1.104	1.037	1.056	1.146	1.160	0.914
p-value	<0.0001	<0.0001	0.0363	<0.0001	<0.0001	<0.0001	<0.0001	<0.0001	<0.0001	0.0047
Overall model statistics										
R^2	0.8495	0.8231	0.7919	0.7529	0.7194	0.6715	0.6475	0.5587	0.4131	0.2182
MSE*	426.10	480.98	543.92	621.93	681.02	769.79	798.60	967.47	1246.49	1610.09
MSE/p*	42.61	53.44	67.99	88.85	113.50	153.96	199.65	322.49	623.25	1610.09
RMSE*	20.64	21.93	23.32	24.94	26.10	27.75	28.26	31.10	35.31	40.13

*Std err, standard error; MSE, mean standard error; MSE/p, MSE divided by number of terms in model; RMSE, square root of MSE.

Table 3.16. Phenylalanine prediction equations containing 1 to 10 terms. Equations with more than 10 terms were calculated but not shown.

	Number of terms in prediction equation									
Item	10	9	8	7	6	5	4	3	2	1
Intercept	-217.610	-264.020	-242.886	-69.764	63.025	122.736	145.159	194.83	171.391	194.304
Std err*	96.575	95.606	101.988	66.504	53.847	32.400	28.768	24.646	16.826	16.181
p-value	0.0341	0.0109	0.0252	0.3038	0.2521	0.0007	<0.0001	<0.0001	<0.0001	<0.0001
CRTN	-16.161									
Std err	9.815									
p-value	0.1132									
LDL	0.371	-0.833								
Std err	0.097	0.383								
p-value	0.0009	0.0394								
ALB	48.074	49.344	37.878							
Std err	16.725	17.292	17.662							
p-value	0.0086	0.0088	0.0419							
CK	-0.044	-0.035	-0.032	-0.043						
Std err	0.015	0.014	0.015	0.015						
p-value	0.0063	0.0199	0.0414	0.0080						
HDL	3.442	3.464	3.023	2.986	0.088					
Std err	0.807	0.835	0.869	0.927	0.638					
p-value	0.0003	0.0004	0.0019	0.0034	0.1800					
LDH	0.371	0.358	0.359	0.362	0.127	0.130				
Std err	0.097	0.100	0.108	0.115	0.091	0.092				
p-value	0.0009	0.0016	0.0027	0.0040	0.1728	0.1672				
LAC	9.963	12.086	10.507	7.441	8.918	8.343	7.677			
Std err	2.890	2.677	2.763	2.523	2.781	2.793	2.801			
p-value	0.0022	0.0001	0.0008	0.0066	0.0034	0.0058	0.0104			
TG	-2.188	-2.602	-2.278	-1.469	-1.574	-1.627	-1.599	-0.670		
Std err	0.615	0.581	0.602	0.501	0.563	0.571	0.580	0.519		
p-value	0.0017	0.0002	0.0009	0.0070	0.0094	0.0081	0.0100	0.2069		
CHOL	51.733	53.594	51.827	47.075	44.065	37.727	30.424	23.057	29.010	
Std err	9.575	9.841	10.517	10.969	12.298	11.584	10.556	11.261	10.381	
p-value	<0.0001	<0.0001	<0.0001	0.0002	0.0013	0.0029	0.0074	0.0495	0.0088	
AST	-1.479	-1.784	-1.614	-1.277	-1.439	-1.383	-1.043	-0.747	-0.720	-0.458
Std err	0.345	0.302	0.313	0.289	0.319	0.321	0.217	0.208	0.210	0.206
p-value	0.0003	<0.0001	<0.0001	0.0002	0.0001	0.0002	<0.0001	0.0012	0.0017	0.0333
Overall model statistics										
R^2	0.7826	0.7570	0.7090	0.6555	0.5461	0.5143	0.4794	0.3446	0.3082	0.1339
MSE*	652.08	698.57	803.21	914.40	1159.97	1197.02	1238.75	1507.58	1539.87	1867.57
MSE/p*	65.21	77.62	100.40	130.63	193.33	239.40	309.69	502.53	769.94	1867.57
RMSE*	25.54	26.43	28.34	30.24	34.06	34.60	35.20	38.83	39.24	43.22

*Std err, standard error; MSE, mean standard error; MSE/p, MSE divided by number of terms in model; RMSE, square root of MSE.

Table 3.17. Proline prediction equations containing 1 to 10 terms. Equations with more than 10 terms were calculated but are not shown.

	Number of terms in prediction equation									
Item	10	9	8	7	6	5	4	3	2	1
Intercept	-547.44	-205.52	-261.09	-31.67	169.14	52.87	111.25	284.40	576.00	483.52
Std err*	297.11	251.03	265.29	243.50	143.52	151.30	150.74	142.38	54.61	56.12
p-value	0.0778	<0.0001	0.3341	0.8975	0.2485	0.7293	0.4662	0.0546	<0.0001	<0.0001
ALB	91.134									
Std err	47.257									
p-value	0.0657									
LDL	-2.837	-2.362								
Std err	1.101	1.130								
p-value	0.0166	0.0470								
AMY	-0.188	-0.146	-0.129							
Std err	0.067	0.067	0.071							
p-value	0.0100	0.0389	0.0795							
TP	138.484	132.192	103.902	45.348						
Std err	49.491	51.999	53.357	44.440						
p-value	0.0100	0.0176	0.0624	0.3166						
CRP	-0.002	-0.002	-0.002	-0.001	-0.001					
Std err	0.0004	0.0004	0.0004	0.0004	0.0004					
p-value	0.0014	0.0005	0.0016	0.0074	0.0112					
TG	-5.037	-4.416	-4.252	-4.828	-4.364	-2.517				
Std err	1.467	1.507	1.599	1.634	1.571	1.564				
p-value	0.0022	0.0071	0.0132	0.0064	0.0096	0.1183				
LAC	33.888	30.576	29.486	27.739	29.675	24.527	15.658			
Std err	7.185	7.346	7.787	8.055	7.835	8.396	6.501			
p-value	<0.0001	0.0003	0.0008	0.0019	0.0007	0.0067	0.0224			
GLC	6.657	7.555	7.925	6.932	7.515	6.799	5.979	5.094		
Std err	1.914	1.955	2.069	2.081	2.002	2.192	2.188	2.318		
p-value	0.0019	0.0007	0.0007	0.0025	0.0008	0.0043	0.0104	0.0356		
ALK	-16.055	-15.290	-14.799	-16.211	-16.635	-14.961	-13.501	-10.815	-13.928	
Std err	3.155	3.296	3.494	3.551	3.530	3.839	3.828	3.935	3.885	
p-value	<0.0001	<0.0001	0.0003	<0.0001	<0.0001	0.0005	0.0014	0.0099	0.0011	
LDH	0.862	0.739	0.806	0.776	0.719	0.956	0.964	0.899	1.100	0.373
Std err	0.230	0.232	0.244	0.254	0.248	0.256	0.263	0.281	0.281	0.227
p-value	0.0010	0.0039	0.0028	0.0050	0.0072	0.0008	0.0009	0.0032	0.0005	0.1107
Overall model statistics										
R^2	0.7814	0.7475	0.7034	0.6654	0.6525	0.5609	0.5217	0.4292	0.3403	0.0753
MSE*	6172.1	6843.4	7729.4	8397.0	8409.3	10259.0	10803.0	12476.0	13969.0	18987.0
MSE/p*	617.21	760.38	966.18	1199.57	1401.55	2051.80	2700.75	4158.67	6984.50	18987.00
RMSE*	78.56	82.72	87.92	91.63	91.70	101.29	103.94	111.70	118.19	137.79

*Std err, standard error; MSE, mean standard error; MSE/p, MSE divided by number of terms in model; RMSE, square root of MSE.

Table 3.18. Serine prediction equations containing 1 to 10 terms. Equations with more than 10 terms were calculated but are not shown.

	Number of terms in prediction equation									
Item	10	9	8	7	6	5	4	3	2	1
Intercept	-84.461	-14.633	245.454	255.580	281.012	429.712	513.851	657.650	533.322	410.694
Std err*	253.750	246.444	158.618	160.037	155.081	115.373	107.912	88.132	75.445	60.147
p-value	0.7423	0.9531	0.1343	0.1223	0.0811	0.0009	<0.0001	<0.0001	<0.0001	<0.0001
HAPT	-0.0000093									
Std err	0.0000086									
p-value	0.2878									
HCT	7.627	6.656								
Std err	4.946	4.883								
p-value	0.1367	0.1855								
ALT	-0.817	-0.623	-0.488							
Std err	0.436	0.340	0.394							
p-value	0.0737	0.1319	0.2265							
LAC	8.094	7.078	5.668	2.884						
Std err	4.561	4.481	4.434	3.863						
p-value	0.8920	0.1273	0.2129	0.4621						
TP	56.521	40.072	31.608	31.693	31.334					
Std err	27.234	22.741	22.249	22.478	22.288					
p-value	0.0493	0.0908	0.1678	0.1704	0.1712					
CHOL	105.037	90.940	56.700	48.443	41.945	30.586				
Std err	35.539	33.221	22.110	21.300	19.280	17.808				
p-value	0.0071	0.0115	0.0167	0.0314	0.0385	0.0969				
CA	47.991	42.883	40.482	41.393	38.939	41.304	28.353			
Std err	15.755	15.097	15.249	15.388	14.909	15.070	13.479			
p-value	0.0057	0.0090	0.0136	0.0123	0.0145	0.0106	0.442			
CRTN	-108.152	-83.840	-65.723	-63.489	-60.684	-66.935	-61.877	-49.287		
Std err	33.020	24.410	20.823	10.121	20.449	20.305	20.755	20.977		
p-value	0.0033	0.0022	0.0041	0.0055	0.0062	0.0027	0.0058	0.0256		
GGT	-5.255	-5.718	-5.299	-5.382	-5.214	-4.716	-4.915	-4.318	-3.428	
Std err	1.411	1.351	1.338	1.350	1.320	1.294	1.331	1.373	1.413	
p-value	0.0011	0.0003	0.0005	0.0005	0.0005	0.0011	0.0009	0.0037	0.0212	
iP	-52.367	-46.573	-43.059	-42.823	-39.618	-35.360	-27.788	-25.468	-28.943	-25.749
Std err	11.457	10.184	10.020	10.121	9.090	8.719	7.771	8.120	8.546	9.066
p-value	0.0001	0.0001	0.0002	0.0003	0.0002	0.0004	0.0012	0.0038	0.0019	0.0078
Overall model statistics										
R^2	0.6625	0.6451	0.6176	0.5941	0.5854	0.5551	0.5082	0.4331	0.3288	0.2013
MSE*	2860.68	2882.65	2981.57	3043.24	2993.33	3097.72	3306.01	3683.40	4220.56	4865.33
MSE/p*	286.07	320.29	372.70	434.75	498.89	619.54	826.50	1227.80	2110.28	4865.33
RMSE*	53.49	53.69	54.60	55.17	54.71	55.66	57.50	60.69	64.97	69.75

*Std err, standard error; MSE, mean standard error; MSE/p, MSE divided by number of terms in model; RMSE, square root of MSE.

Table 3.19. Taurine prediction equations containing 1 to 10 terms. Equations with more than 10 terms were calculated but are not shown.

	Number of terms in prediction equation									
Item	10	9	8	7	6	5	4	3	2	1
Intercept	-219.91	-186.44	-191.22	-93.19	-219.06	-62.38	-26.76	142.53	105.74	78.24
Std err*	110.76	109.61	110.93	87.23	83.22	70.63	71.97	35.66	24.59	17.12
p-value	0.0586	0.1014	0.0966	0.2948	0.0136	0.3844	0.7126	0.0004	0.0001	<0.0001
CA	7.293									
Std err	5.439									
p-value	0.1925									
CK	-0.011	-0.010								
Std err	0.008	0.008								
p-value	0.1828	0.2096								
LDH	0.131	0.148	0.080							
Std err	0.077	0.077	0.057							
p-value	0.01007	0.0677	0.1754							
ALB	-36.321	-36.644	-31.370	-38.943						
Std err	14.903	15.137	14.756	13.955						
p-value	0.0226	0.0231	0.0432	0.0095						
CHOL	32.233	30.459	29.918	29.572	24.938					
Std err	7.703	7.708	7.794	7.924	8.636					
p-value	0.0003	0.0006	0.0007	0.0009	0.0074					
SAA	-0.198	-0.200	-0.196	-0.203	-0.181	-0.102				
Std err	0.046	0.047	0.047	0.048	0.052	0.050				
p-value	0.0002	0.0002	0.0003	0.0002	0.0018	0.0504				
TP	106.756	110.406	109.617	99.693	93.281	64.219	44.549			
Std err	18.456	18.543	18.766	17.661	19.518	18.719	16.876			
p-value	<0.0001	<0.0001	<0.0001	<0.0001	<0.0001	0.0018	0.0130			
AMY	-0.112	-0.110	-0.111	-0.099	-0.117	-0.097	-0.063	-0.024		
Std err	0.024	0.024	0.024	0.023	0.025	0.026	0.021	0.017		
p-value	<0.0001	0.0001	<0.0001	0.0002	<0.0001	0.0010	0.0064	0.1698		
GGT	-4.102	-4.125	-4.190	-4.299	-3.890	-3.697	-3.505	-1.522	-1.267	
Std err	0.804	0.817	0.825	0.836	0.917	1.024	1.072	0.835	0.828	
p-value	<0.0001	<0.0001	<0.0001	<0.0001	0.0002	0.0011	0.0027	0.0782	0.1356	
NO_x	6.451	6.081	5.745	5.382	6.445	5.951	6.278	3.119	2.639	1.649
Std err	1.562	1.561	1.559	1.563	1.590	1.882	1.972	1.712	1.702	1.607
p-value	0.0004	0.0006	0.0011	0.0019	0.0007	0.0037	0.0034	0.0780	0.1310	0.3121
Overall model statistics										
R^2	0.7076	0.6857	0.6648	0.6398	0.5359	0.3977	0.3112	0.4080	0.2794	0.1568
MSE*	559.34	577.19	591.81	612.42	760.88	953.40	1054.09	16743.00	19761.00	22444.00
MSE/p*	55.93	64.13	73.98	87.49	126.81	190.68	263.52	5581.00	9880.50	22444.00
RMSE*	23.65	24.02	24.33	24.75	27.58	30.88	32.47	129.39	140.57	149.81

*Std err, standard error; MSE, mean standard error; MSE/p, MSE divided by number of terms in model; RMSE, square root of MSE.

Table 3.20. Threonine prediction equations containing 1 to 10 terms. Equations with more than 10 terms were calculated but are not shown.

	Number of terms in prediction equation									
Item	10	9	8	7	6	5	4	3	2	1
Intercept	39.258	30.204	-28.825	-37.809	-27.460	-1.571	-61.736	-21.428	28.432	142.888
Std err*	97.498	97.615	87.506	89.202	90.595	92.164	94.354	90.690	91.088	14.643
p-value	0.6895	0.7587	0.7436	0.6739	0.7633	0.9865	0.5164	0.8143	0.7564	<0.0001
LDL	-0.510									
Std err	0.441									
p-value	0.2547									
AST	-0.302	-0.335								
Std err	0.255	0.255								
p-value	0.2449	0.1961								
CK	-0.019	-0.018	-0.017							
Std err	0.010	0.010	0.010							
p-value	0.0658	0.0819	0.1067							
TG	-1.113	-1.162	-0.992	-0.838						
Std err	0.536	0.536	0.526	0.528						
p-value	0.0447	0.0366	0.0664	0.1204						
SAA	-0.099	-0.102	-0.106	-0.107	-0.094					
Std err	0.048	0.048	0.049	0.050	0.050					
p-value	0.0479	0.0427	0.0353	0.0386	0.0683					
CRTN	-32.769	-31.026	-36.176	-29.330	-27.212	-26.936				
Std err	11.543	11.495	10.909	10.306	10.406	10.711				
p-value	0.0073	0.0103	0.0020	0.0070	0.0124	0.0158				
CRP	-0.0005	-0.0004	-0.0005	-0.0005	-0.0004	-0.0004	-0.0002			
Std err	0.0002	0.0002	0.0002	0.0002	0.0002	0.0002	0.0002			
p-value	0.0113	0.0186	0.0074	0.0099	0.0274	0.0147	0.1730			
AMY	-0.055	-0.049	-0.069	-0.076	-0.088	-0.067	-0.062	-0.044		
Std err	0.030	0.029	0.025	0.026	0.025	0.023	0.024	0.020		
p-value	0.0724	0.1019	0.0097	0.0052	0.0011	0.0057	0.0137	0.0377		
TP	64.208	57.128	72.430	74.316	68.703	56.557	50.523	35.277	18.207	
Std err	22.488	21.736	18.535	18.894	18.901	18.274	19.204	15.903	14.304	
p-value	0.0070	0.0123	0.0004	0.0003	0.0008	0.0035	0.0118	0.0317	0.2096	
LDH	0.465	0.483	0.441	0.317	0.350	0.354	0.381	0.384	0.314	0.260
Std err	0.108	0.108	0.104	0.073	0.071	0.073	0.077	0.077	0.073	0.060
p-value	0.0001	<0.0001	0.0001	<0.0001	<0.0001	<0.0001	<0.0001	<0.0001	<0.0001	<0.0001
Overall model statistics										
R^2	0.6161	0.6022	0.5840	0.5550	0.5270	0.4865	0.4092	0.3828	0.3184	0.2939
MSE*	1300.29	1311.87	1336.48	1394.150	1445.76	1532.98	1721.66	1757.65	1898.00	1923.59
MSE/p*	130.03	145.76	167.06	199.16	240.96	306.60	430.42	585.88	949.00	1923.59
RMSE*	36.06	36.22	36.56	37.34	38.02	39.15	41.49	41.92	43.57	43.86

*Std err, standard error; MSE, mean standard error; MSE/p, MSE divided by number of terms in model; RMSE, square root of MSE.

Table 3.21. Tryptophan prediction equations containing 1 to 10 terms. Equations with more than 10 terms were calculated but are not shown.

	Number of terms in prediction equation									
Item	10	9	8	7	6	5	4	3	2	1
Intercept	-195.82	-187.60	-134.68	-131.79	-129.83	-139.96	-134.25	-147.56	-198.55	-121.791
Std err*	53.75	53.54	45.30	46.22	45.28	47.26	46.83	46.86	48.73	40.047
p-value	0.0013	0.0017	0.0063	0.0082	0.0078	0.0061	0.0075	0.0036	0.0003	0.0046
CRP	0.0001									
Std err	0.00009									
p-value	0.2709									
BUN	3.795	2.997								
Std err	1.881	1.751								
p-value	0.0549	0.0995								
HDL	1.715	1.726	0.956							
Std err	0.768	0.772	0.650							
p-value	0.0351	0.0346	0.1535							
CK	-0.021	-0.021	-0.014	-0.002						
Std err	0.010	0.010	0.010	0.005						
p-value	0.0467	0.0517	0.1533	0.6866						
LAC	3.863	3.909	2.572	2.627	2.728					
Std err	1.534	1.542	1.378	1.407	1.364					
p-value	0.0189	0.0179	0.0733	0.0728	0.0553					
TG	-0.854	-0.951	-0.522	-0.590	-0.586	-0.230				
Std err	0.384	0.376	0.291	0.293	0.289	0.238				
p-value	0.0359	0.0182	0.0843	0.0544	0.0518	0.3431				
NO_2	-3.871	-3.786	-4.036	-4.260	-4.112	-3.530	-2.987			
Std err	1.960	1.969	2.035	2.073	2.010	2.089	2.010			
p-value	0.0599	0.0660	0.0580	0.0496	0.0503	0.1019	0.1476			
AST	-0.660	-0.661	-0.475	-0.500	-0.506	-0.393	-0.370	-0.387		
Std err	0.170	0.171	0.137	0.139	0.136	0.130	0.128	0.130		
p-value	0.0007	0.0007	0.0018	0.0013	0.0009	0.0052	0.0070	0.0055		
LDH	0.289	0.271	0.242	0.201	0.186	0.184	0.175	0.171	0.097	
Std err	0.064	0.062	0.062	0.056	0.042	0.044	0.043	0.043	0.040	
p-value	0.0001	0.0002	0.0006	0.0013	0.0001	0.0002	0.0003	0.0004	0.0200	
TP	23.295	25.433	27.917	37.188	36.774	40.114	37.635	36.095	43.313	33.574
Std err	9.718	9.582	9.817	7.683	7.801	7.682	7.230	7.293	7.685	7.057
p-value	0.0247	0.0136	0.0086	<0.0001	<0.0001	<0.0001	<0.0001	<0.0001	<0.0001	<0.0001
Overall model statistics										
R^2	0.7610	0.7484	0.7189	0.6955	0.6936	0.6499	0.6387	0.6121	0.5005	0.4069
MSE*	267.73	270.62	290.68	303.18	294.16	324.58	323.81	336.45	419.65	483.23
MSE/p*	26.77	30.07	36.34	43.31	49.03	64.92	80.95	112.15	209.83	483.23
RMSE*	16.36	16.45	17.05	17.41	17.15	18.02	17.99	18.34	20.49	21.98

*Std err, standard error; MSE, mean standard error; MSE/p, MSE divided by number of terms in model; RMSE, square root of MSE.

Table 3.22. Tyrosine prediction equations containing 1 to 10 terms. Equations with more than 10 terms were calculated but are not shown.

	Number of terms in prediction equation									
Item	10	9	8	7	6	5	4	3	2	1
Intercept	-184.33	-194.98	-179.20	-132.88	-131.74	2.241	-2.12	-21.39	177.04	187.65
Std err*	74.37	77.78	79.45	74.42	73.98	58.388	61.04	67.21	20.43	21.36
p-value	0.0206	0.0190	0.0327	0.0854	0.0858	0.9696	0.9726	0.7524	<0.0001	<0.0001
LDL	-0.777									
Std err	0.415									
p-value	0.0735									
BIL	56.831	41.860								
Std err	26.150	26.114								
p-value	0.0399	0.1215								
TG	-1.380	-1.162	-0.763							
Std err	0.550	0.564	0.521							
p-value	0.0192	0.0498	0.1548							
LAC	-5.498	4.805	4.118	1.694						
Std err	2.477	2.569	2.608	2.059						
p-value	0.0361	0.0732	0.1264	0.4179						
HDL	-3.497	2.891	2.378	2.209	2.269					
Std err	0.917	0.900	0.867	0.877	0.869					
p-value	0.0008	0.0036	0.0108	0.0180	0.0143					
CK	-0.065	-0.056	-0.052	-0.049	-0.050	-0.022				
Std err	0.015	0.015	0.015	0.015	0.015	0.011				
p-value	0.0002	0.0009	0.0019	0.0034	0.0022	0.0598				
CRTN	-25.052	-23.042	-23.095	-26.605	-28.632	-34.019	-28.485			
Std err	9.161	9.542	9.826	9.730	9.358	10.002	10.038			
p-value	0.0115	0.0234	0.0266	0.0109	0.0048	0.0020	0.0081			
HCT	5.998	5.928	7.171	6.324	6.691	7.067	7.105	6.052		
Std err	1.764	1.850	1.729	1.664	1.594	1.739	1.820	1.974		
p-value	0.0024	0.0037	0.0003	0.0007	0.0002	0.0003	0.0005	0.0045		
LDH	0.714	0.691	0.694	0.652	0.655	0.487	0.279	0.314	0.254	
Std err	0.130	0.136	0.140	0.140	0.139	0.135	0.087	0.096	0.105	
p-value	<0.0001	<0.0001	<0.0001	<0.0001	<0.0001	0.0012	0.0033	0.0025	0.0217	
ALK	-7.166	-6.912	-7.090	-6.261	-5.908	-5.689	-4.776	-5.921	-5.352	-2.822
Std err	1.263	1.317	1.352	1.253	1.171	1.279	1.247	1.307	1.454	1.078
p-value	<0.0001	<0.0001	<0.0001	<0.0001	<0.0001	0.0001	0.0006	<0.0001	0.0008	0.0133
Overall model statistics										
R^2	0.7854	0.7541	0.7288	0.7064	0.6990	0.6258	0.5762	0.4625	0.2994	0.1718
MSE*	798.70	878.80	931.80	971.40	960.20	1152.80	1261.90	1549.00	1955.80	2241.90
MSE/p*	79.87	97.64	116.48	138.77	160.03	230.56	315.48	516.33	977.90	2241.90
RMSE*	28.26	29.64	30.53	31.17	30.99	33.95	35.52	39.36	44.22	47.35

*Std err, standard error; MSE, mean standard error; MSE/p, MSE divided by number of terms in model; RMSE, square root of MSE.

Table 3.23. Valine prediction equations containing 1 to 10 terms. Equations with more than 10 terms were calculated but are not shown.

	Number of terms in prediction equation									
Item	10	9	8	7	6	5	4	3	2	1
Intercept	-204.83	-157.57	-260.05	-352.62	-239.93	-228.04	-256.72	-55.27	112.81	417.81
Std err*	179.20	175.49	181.84	187.20	171.32	173.20	176.77	129.43	122.06	32.55
p-value	0.2604	0.3749	0.1607	0.0669	0.1689	0.1951	0.1537	0.6715	0.3603	<0.0001
GLC	1.482									
Std err	1.262									
p-value	0.2478									
ALK	-3.736	-3.804								
Std err	1.512	1.518								
p-value	0.0182	0.0166								
CHOL	-44.078	-45.607	-38.709							
Std err	15.722	15.746	16.520							
p-value	0.0080	0.0062	0.0243							
TG	-2.969	-3.010	-2.559	-1.378						
Std err	1.002	1.006	1.006	0.977						
p-value	0.0053	0.0049	0.0200	0.1662						
LAC	15.049	14.036	9.804	7.711	4.483					
Std err	3.994	3.929	3.768	3.861	3.147					
p-value	0.0006	0.0010	0.0130	0.0526	0.1618					
LDL	-1.617	-1.952	-1.761	-1.523	-1.487	-1.427				
Std err	0.759	0.707	0.749	0.783	0.792	0.800				
p-value	0.0399	0.0088	0.0239	0.0587	0.0675	0.0818				
ALB	90.738	99.147	79.151	64.855	46.010	49.928	46.874			
Std err	29.607	28.871	29.565	30.510	27.756	27.957	28.603			
p-value	0.0041	0.0015	0.0108	0.0397	0.1050	0.0813	0.1086			
CK	0.036	0.040	0.030	0.034	0.031	0.030	0.036	0.032		
Std err	0.011	0.011	0.011	0.012	0.012	0.012	0.012	0.012		
p-value	0.0032	0.0010	0.0098	0.0061	0.0101	0.0146	0.0036	0.0087		
TP	49.500	57.461	82.561	95.068	88.017	88.476	77.857	79.632	52.279	
Std err	23.027	22.116	21.011	21.432	21.090	21.345	21.011	21.381	20.249	
p-value	0.0382	0.0133	0.0003	<0.0001	0.0002	0.0002	0.0006	0.0006	0.0132	
NO_x	-11.849	-13.484	-13.774	-12.624	-11.327	-10.283	-9.527	-10.171	-8.671	-9.779
Std err	2.991	2.661	2.833	2.943	2.829	2.765	2.801	2.826	2.968	3.112
p-value	0.0003	<0.0001	<0.0001	0.0001	0.0003	0.0006	0.0015	0.0008	0.0054	0.0029
Overall model statistics										
R^2	0.6474	0.6343	0.5739	0.5139	0.4897	0.4644	0.4239	0.3879	0.2830	0.1767
MSE*	3380.45	3414.16	3876.40	4311.59	4415.585	4523.89	4753.28	4935.37	5653.07	6349.33
MSE/p*	338.05	379.35	484.55	615.94	735.93	904.78	1188.32	1645.12	2826.54	6349.33
RMSE*	58.14	58.43	62.26	65.66	66.45	67.26	68.94	70.25	75.19	79.68

*Std err, standard error; MSE, mean square error; RMSE, square root MSE.

3.7 Figures

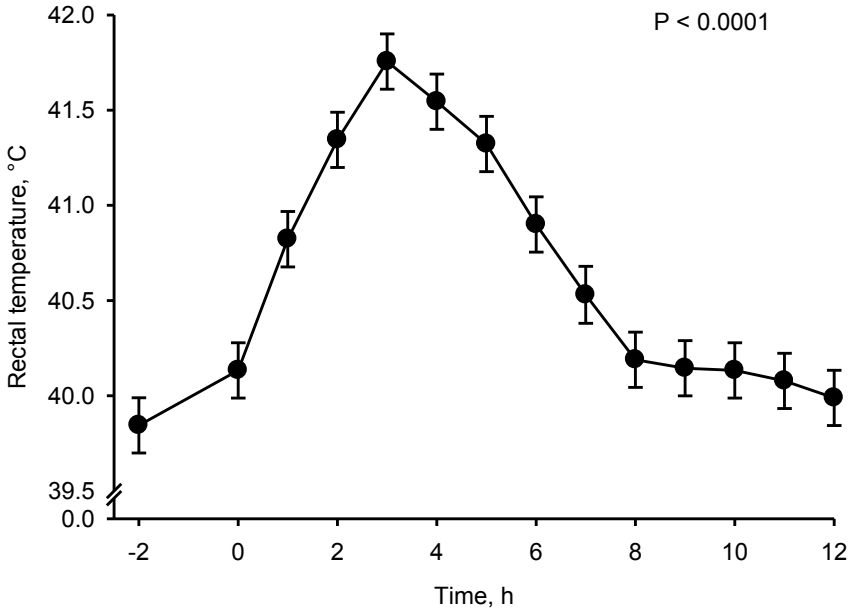

Figure 3.1. Changes in rectal temperature in lipopolysaccharide (LPS, 10 µg/kg BW) treated pigs. Pigs were food-deprived overnight, fed at t = -2 and treated with LPS at t = 0. Values are LSMEANS ± SEM (n = 9).

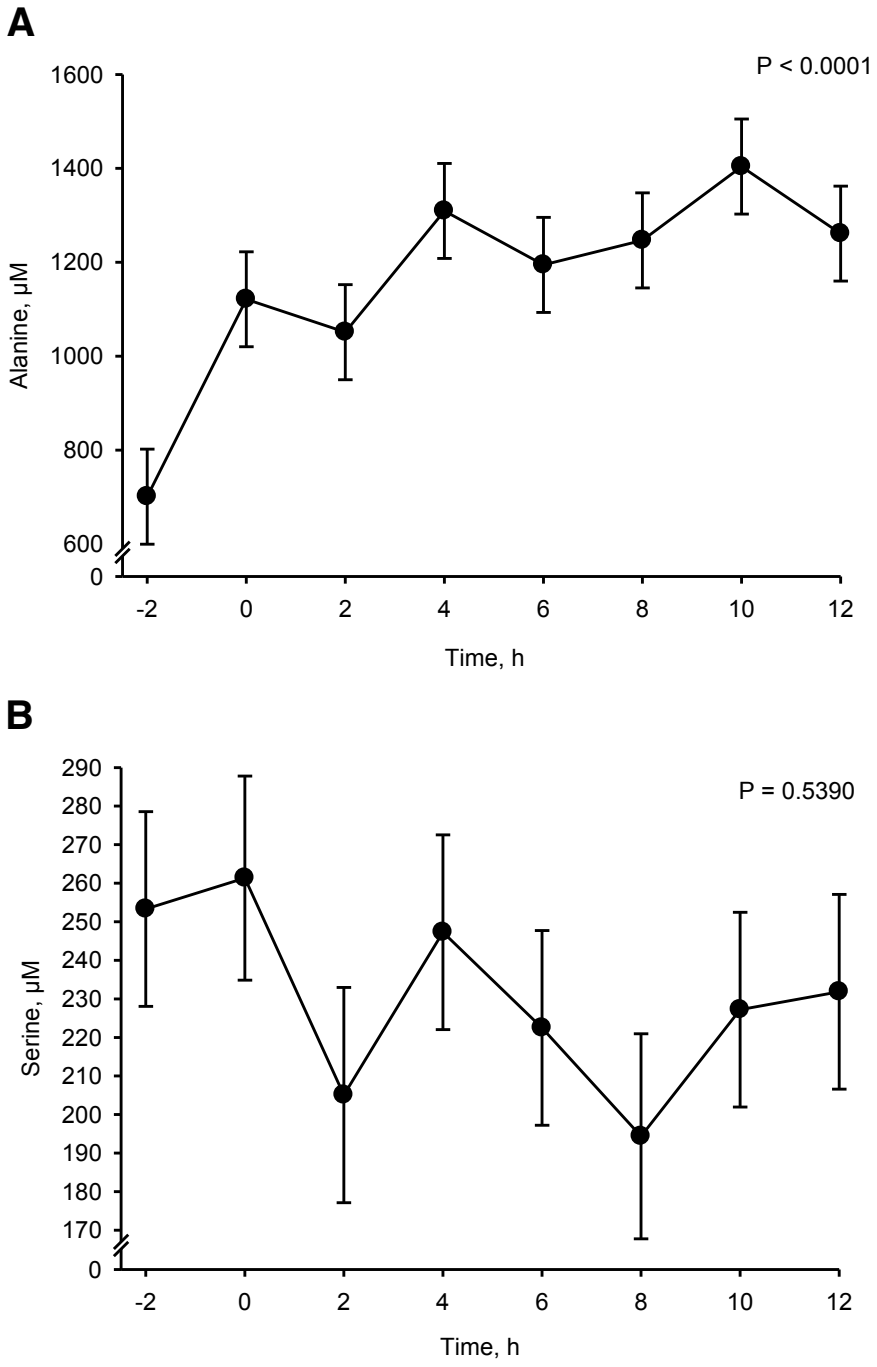

Figure 3.2. Changes in plasma alanine (A) and serine (B) levels in lipopolysaccharide (LPS, 10 µg/kg BW) treated pigs. Pigs were food-deprived overnight, fed at t = -2 and treated with LPS at t = 0. Values are LSMEANS ± SEM (n = 9).

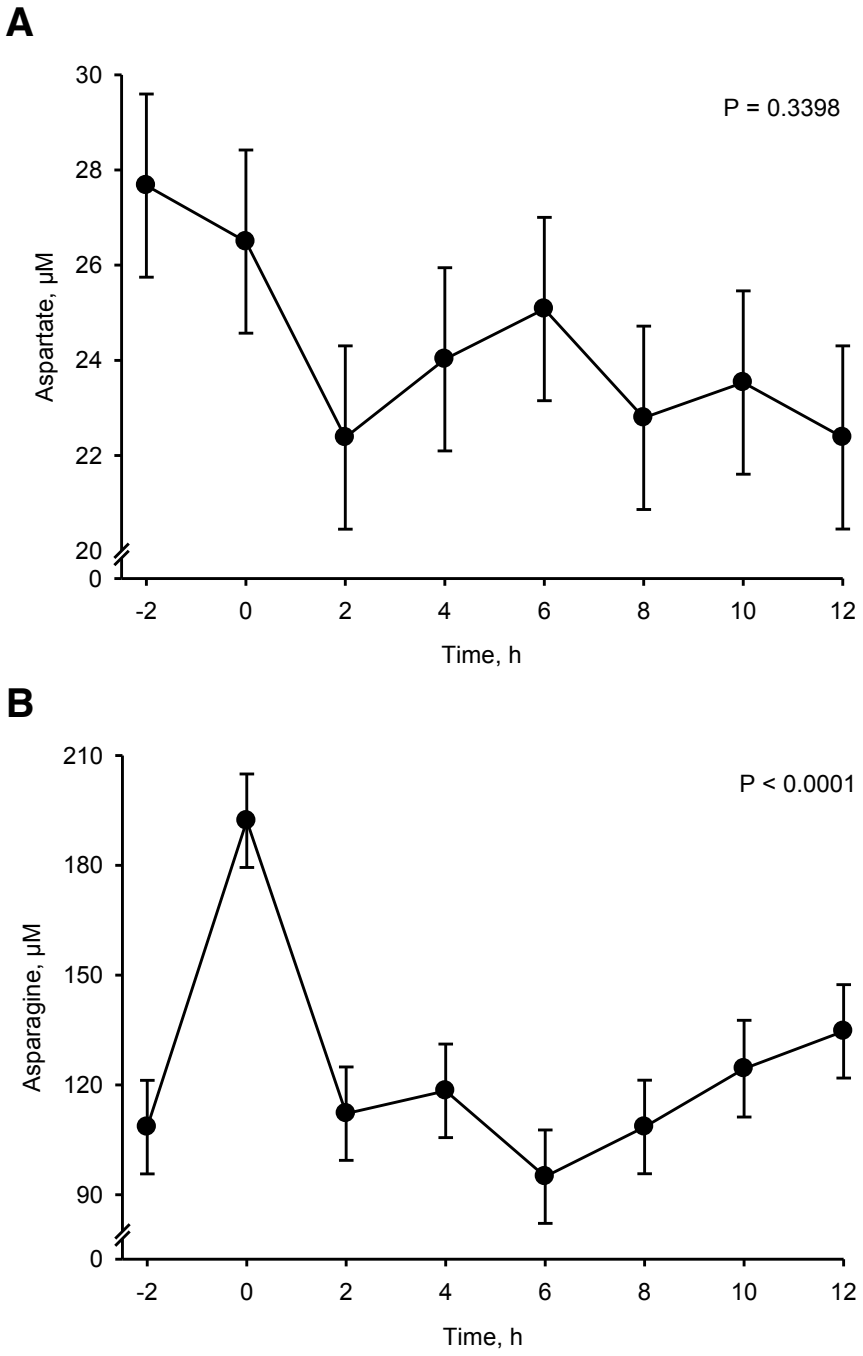

Figure 3.3. Changes in plasma aspartate (A) and asparagine (B) levels in lipopolysaccharide (LPS, 10 µg/kg BW) treated pigs. Pigs were food-deprived overnight, fed at t = -2 and treated with LPS at t = 0. Values are LSMEANS ± SEM (n = 9).

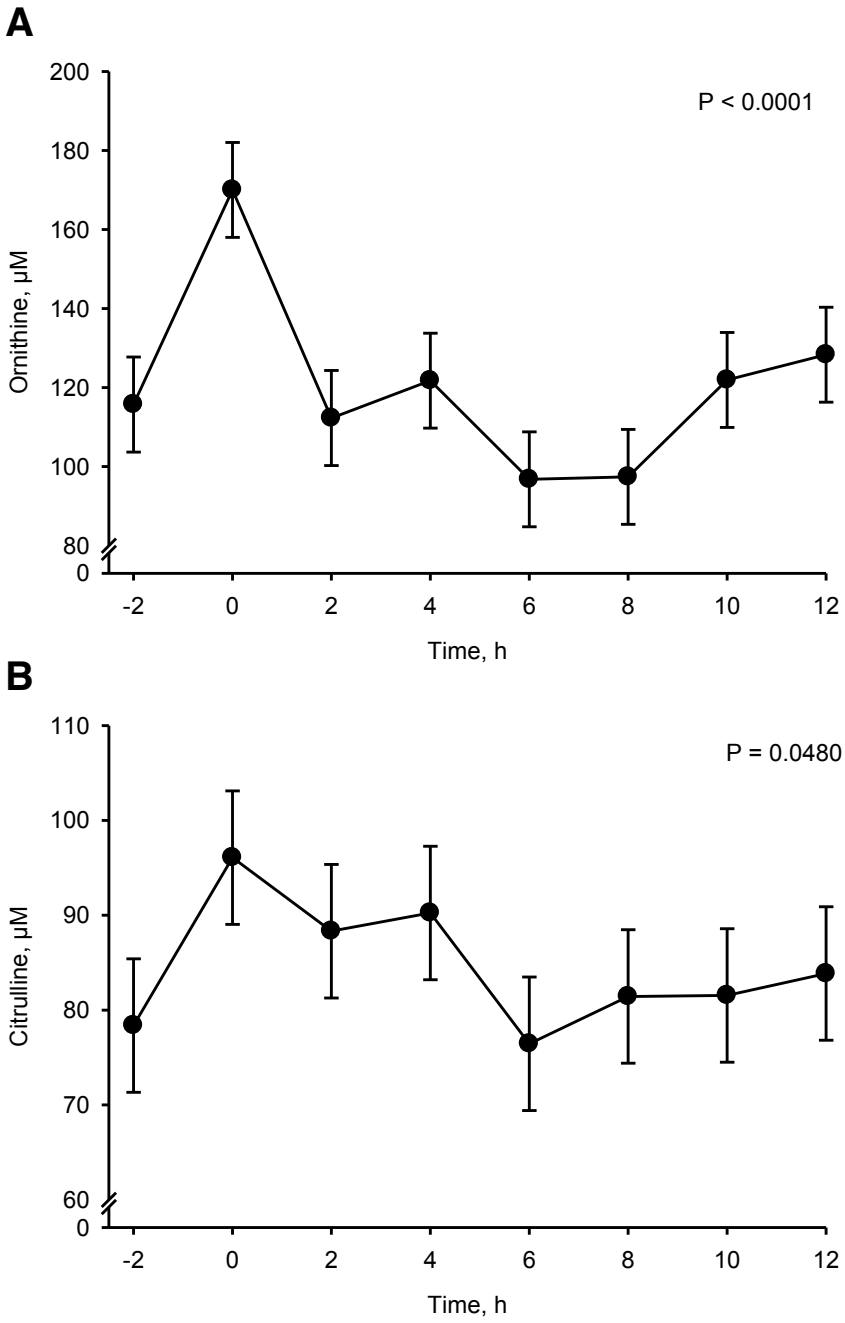

Figure 3.4. Changes in plasma ornithine (A) and citrulline (B) levels in lipopolysaccharide (LPS, 10 µg/kg BW) treated pigs. Pigs were food-deprived overnight, fed at t = -2 and treated with LPS at t = 0. Values are LSMEANS ± SEM (n = 9).

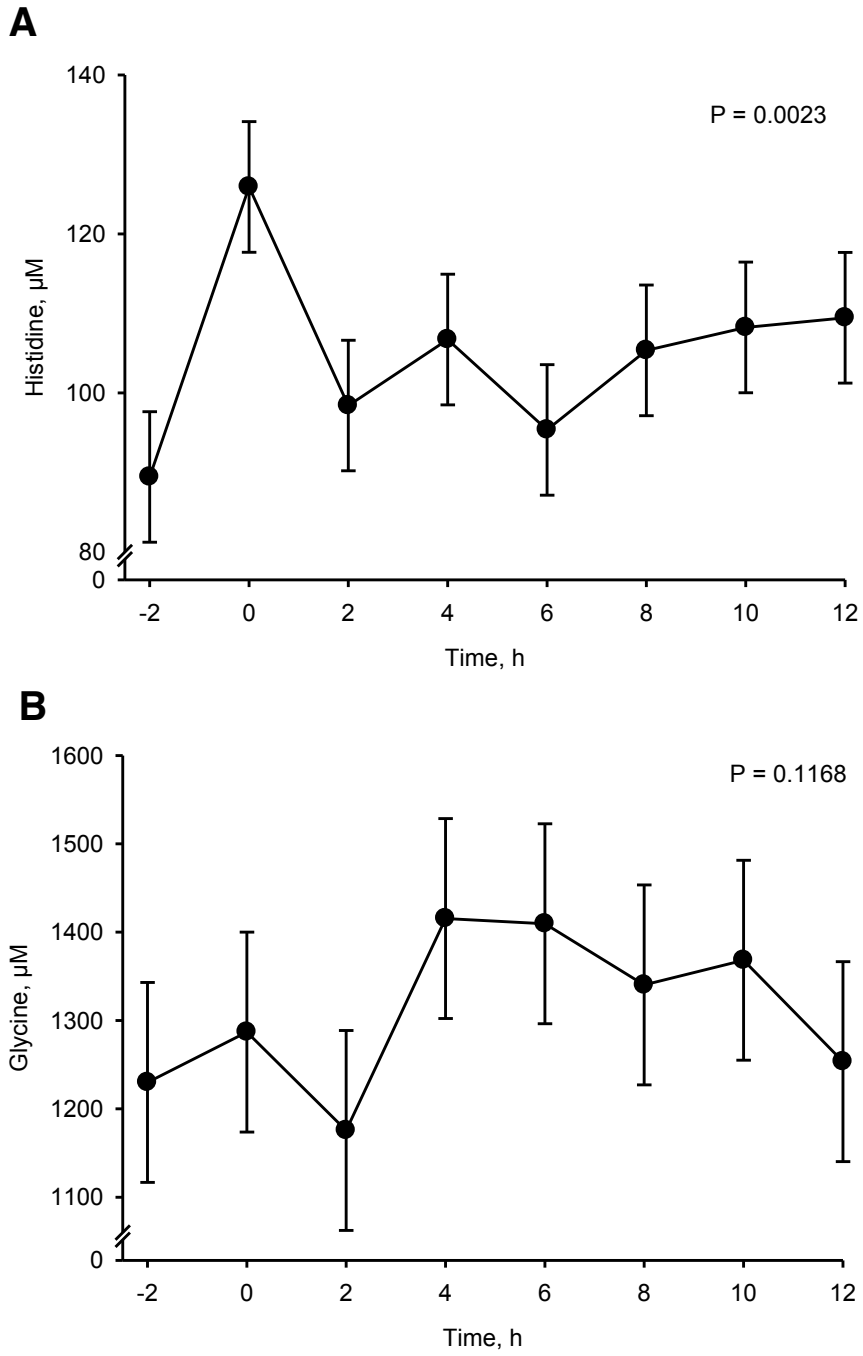

Figure 3.5. Changes in plasma histidine (A) and glycine (B) levels in lipopolysaccharide (LPS, 10 µg/kg BW) treated pigs. Pigs were food-deprived overnight, fed at t = -2 and treated with LPS at t = 0. Values are LSMEANS ± SEM (n = 9).

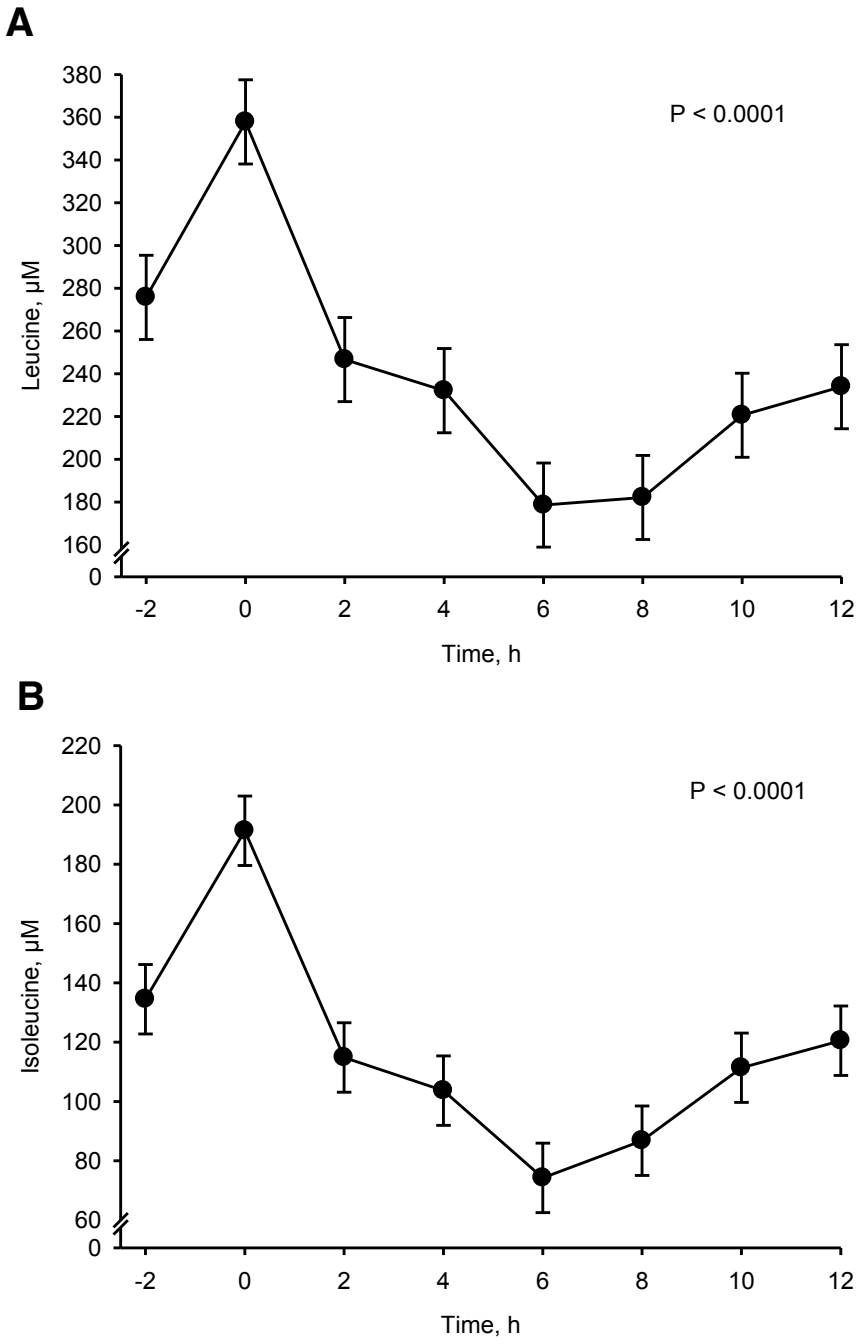

Figure 3.6. Changes in plasma leucine (A) and isoleucine (B) levels in lipopolysaccharide (LPS, 10 µg/kg BW) treated pigs. Pigs were food-deprived overnight, fed at t = -2 and treated with LPS at t = 0. Values are LSMEANS ± SEM (n = 9).

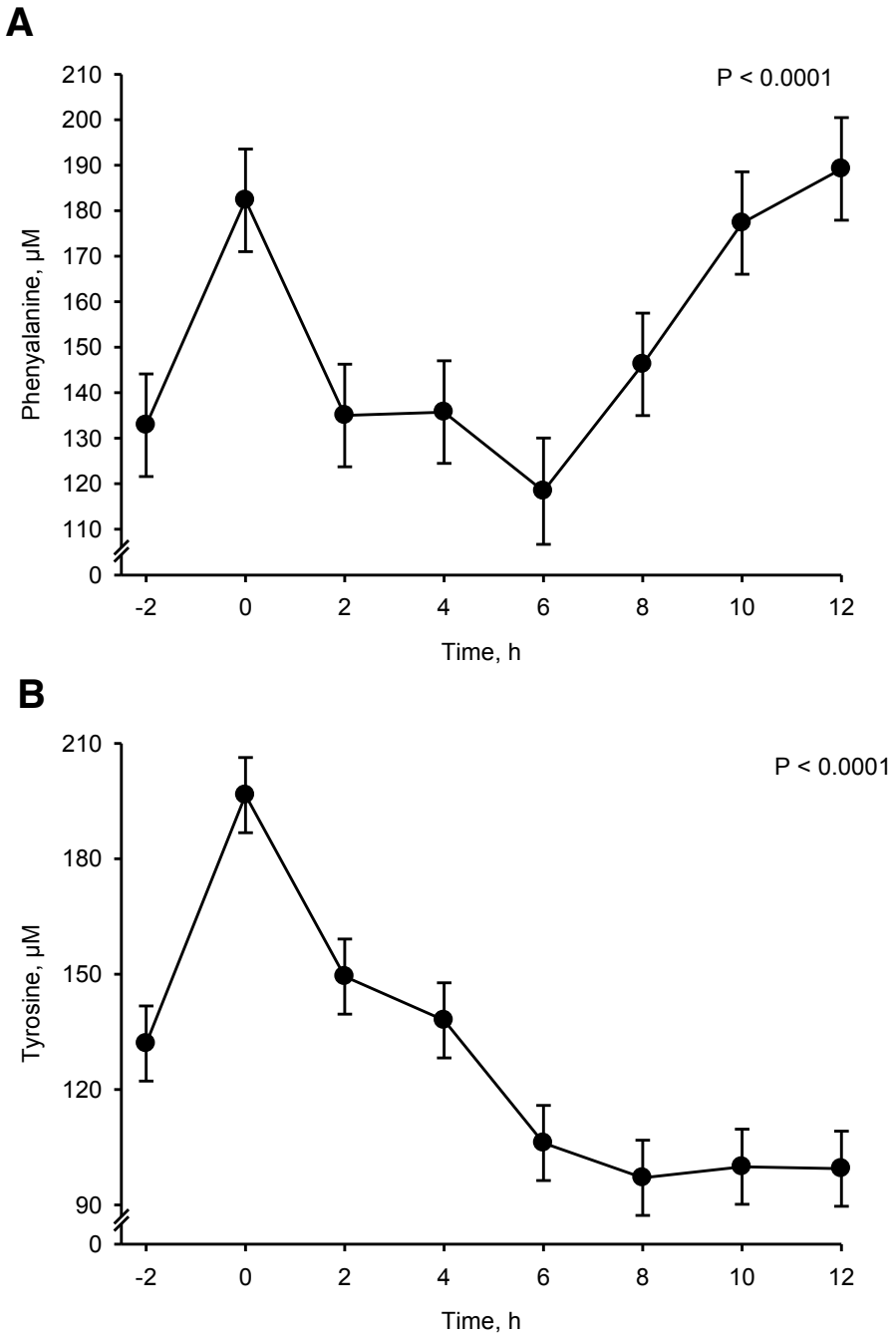

Figure 3.7. Changes in plasma phenylalanine (A) and tyrosine (B) levels in lipopolysaccharide (LPS, 10 µg/kg BW) treated pigs. Pigs were food-deprived overnight, fed at t = -2 and treated with LPS at t = 0. Values are LSMEANS ± SEM (n = 9).

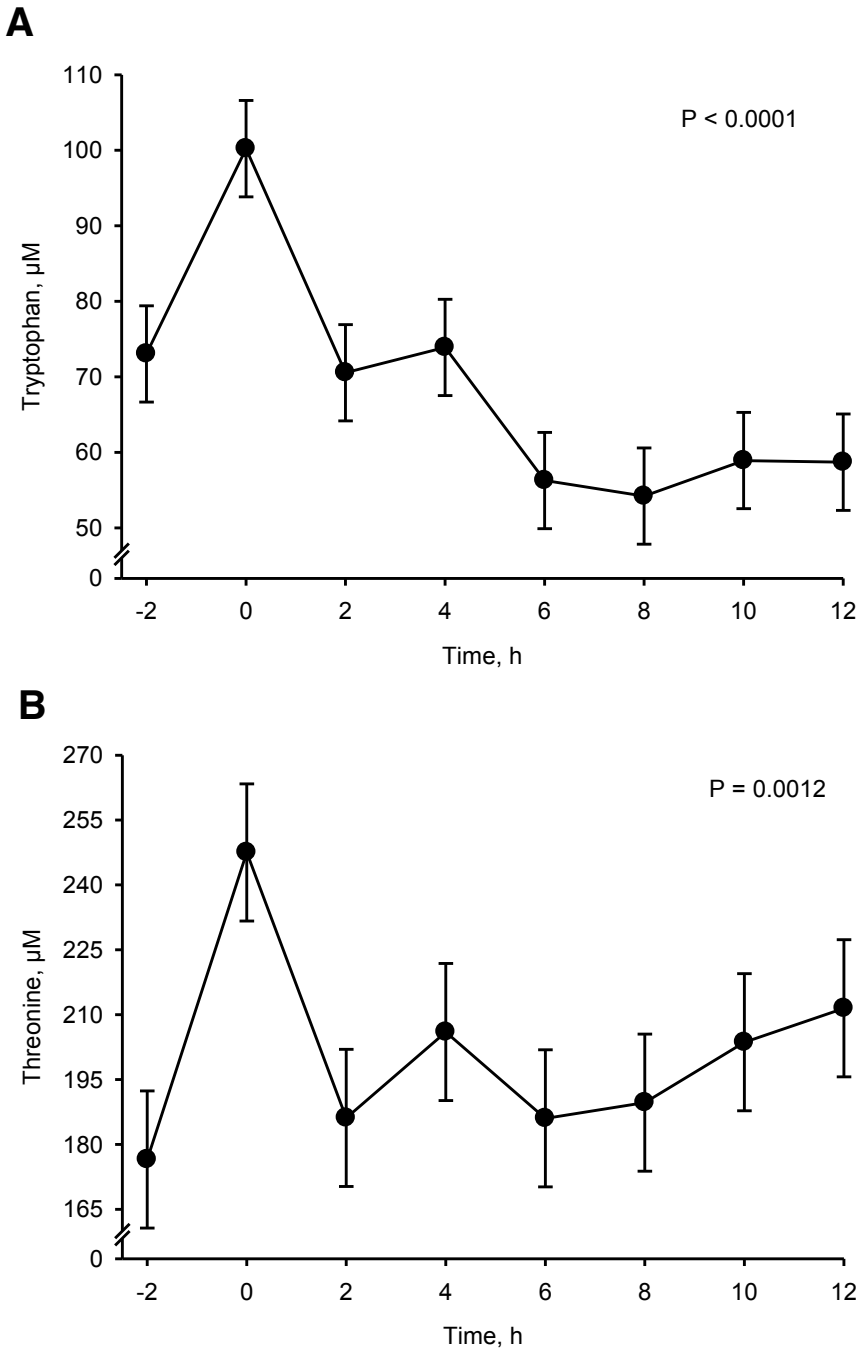

Figure 3.8. Changes in plasma tryptophan (A) and threonine (B) levels in lipopolysaccharide (LPS, 10 µg/kg BW) treated pigs. Pigs were food-deprived overnight, fed at t = -2 and treated with LPS at t = 0. Values are LSMEANS ± SEM (n = 9).

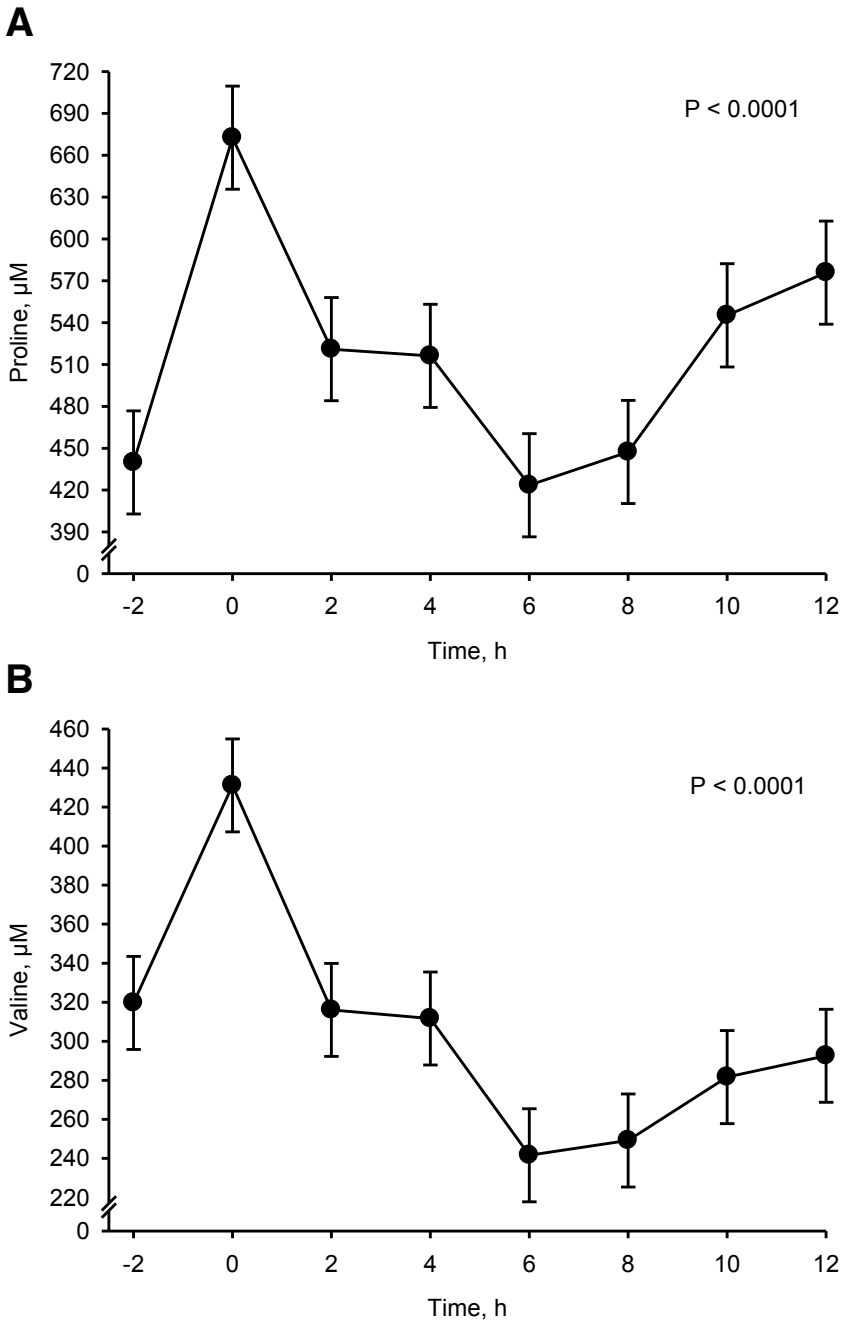

Figure 3.9. Changes in plasma proline (A) and valine (B) levels in lipopolysaccharide (LPS, 10 µg/kg BW) treated pigs. Pigs were food-deprived overnight, fed at t = -2 and treated with LPS at t = 0. Values are LSMEANS ± SEM (n = 9).

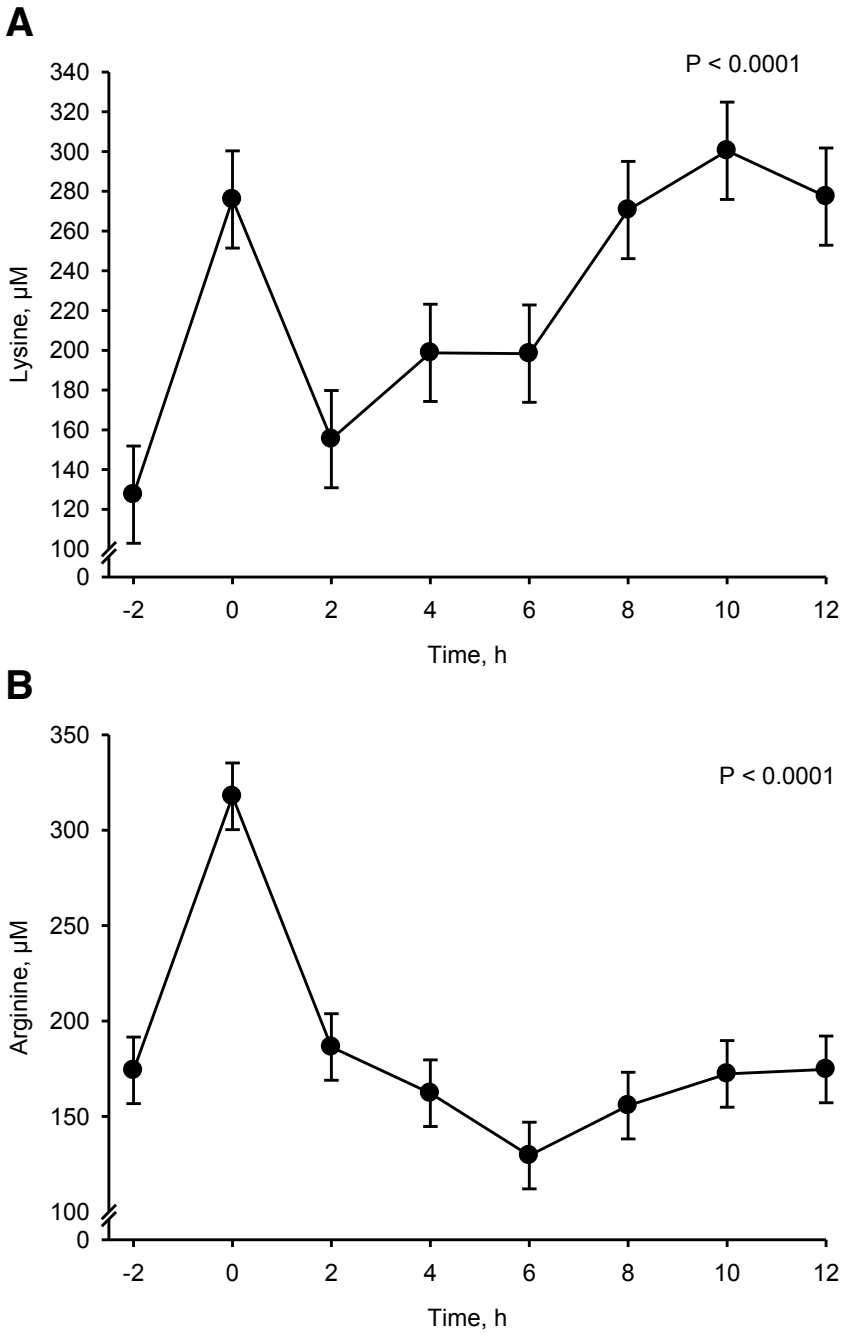

Figure 3.10. Changes in plasma lysine (A) and arginine (B) levels in lipopolysaccharide (LPS, 10 µg/kg BW) treated pigs. Pigs were food-deprived overnight, fed at t = -2 and treated with LPS at t = 0. Values are LSMEANS ± SEM (n = 9).

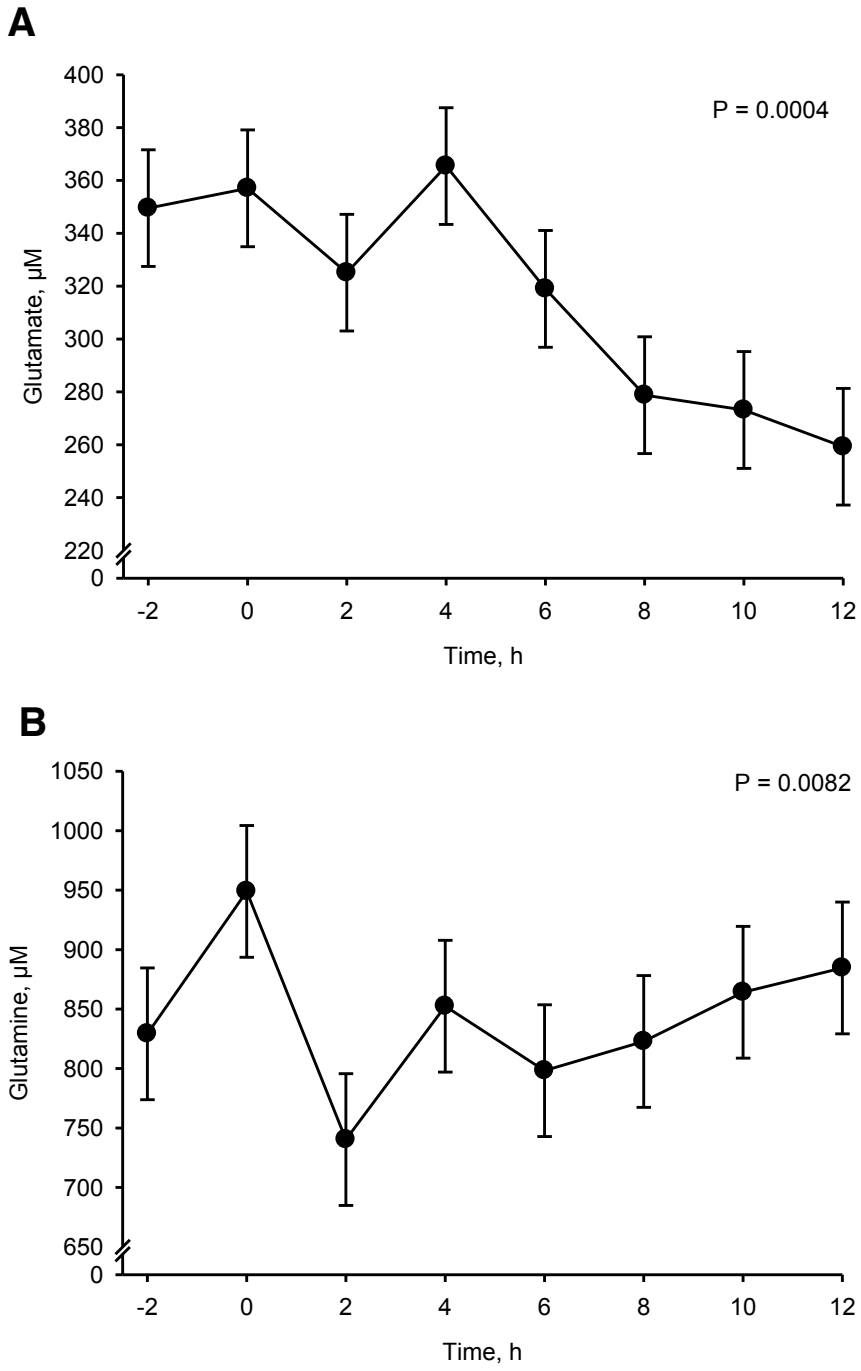

Figure 3.10. Changes in plasma glutamate (A) and glutamine (B) levels in lipopolysaccharide (LPS, 10 µg/kg BW) treated pigs. Pigs were food-deprived overnight, fed at t = -2 and treated with LPS at t = 0. Values are LSMEANS ± SEM (n = 9).

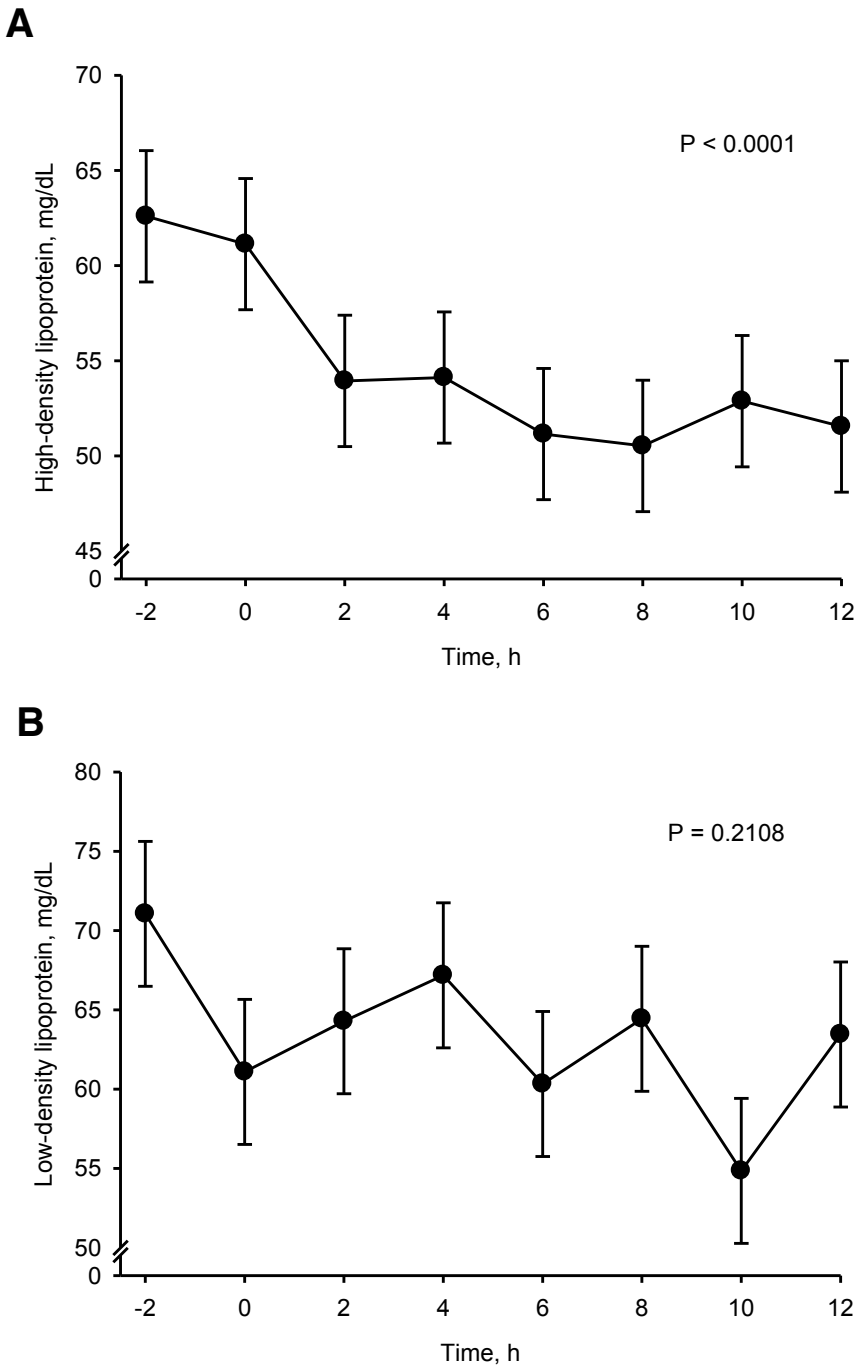

Figure 3.11. Changes in plasma high density lipoprotein (A) and low density lipoprotein (B) levels in lipopolysaccharide (LPS, 10 μg/kg BW) treated pigs. Pigs were food-deprived overnight, fed at t = -2 and treated with LPS at t = 0. Values are LSMEANS ± SEM (n = 9).

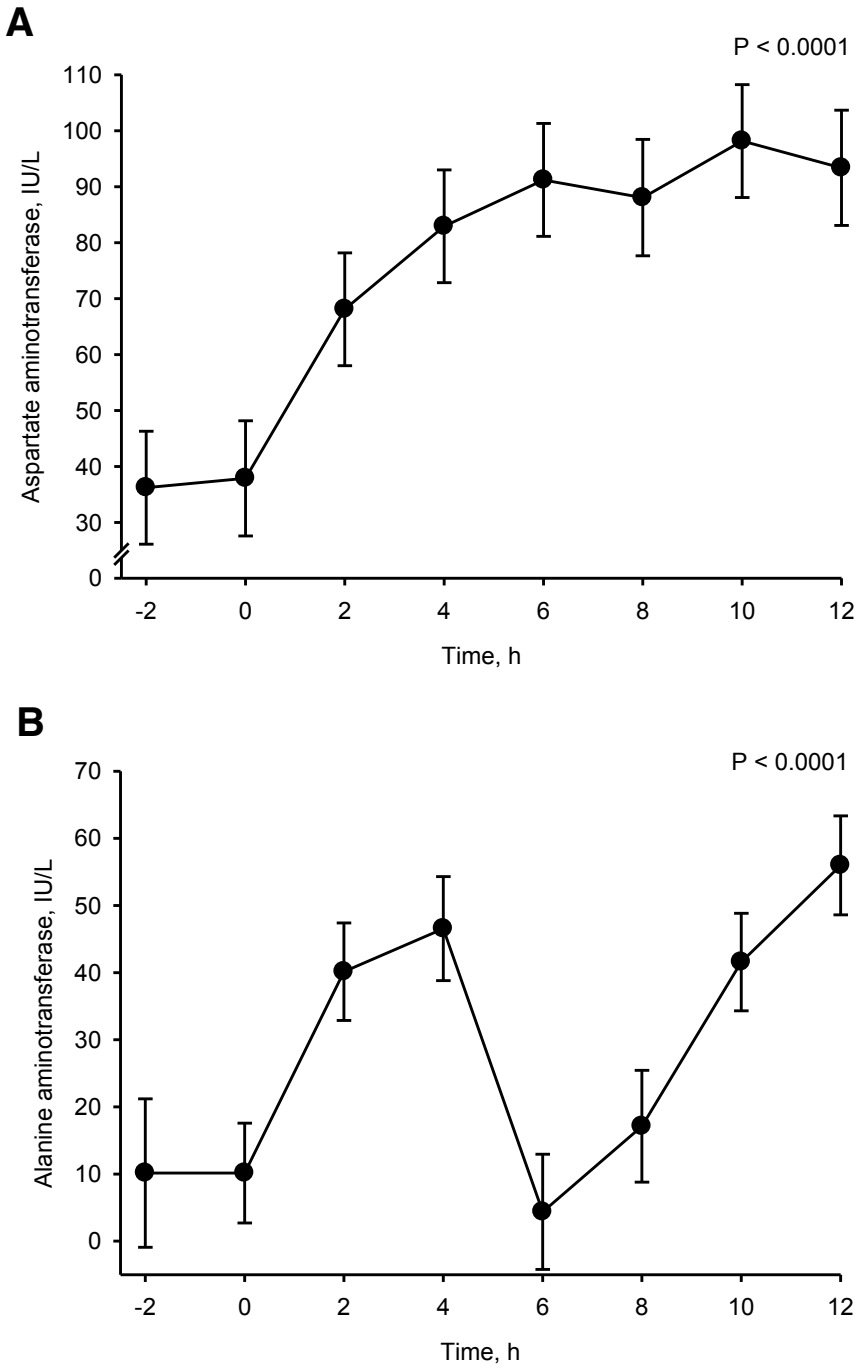

Figure 3.12. Changes in plasma asptartate aminotransferase (A) and alanine aminotransferase (B) levels in lipopolysaccharide (LPS, 10 μg/kg BW) treated pigs. Pigs were food-deprived overnight, fed at t = -2 and treated with LPS at t = 0. Values are LSMEANS ± SEM (n = 9).

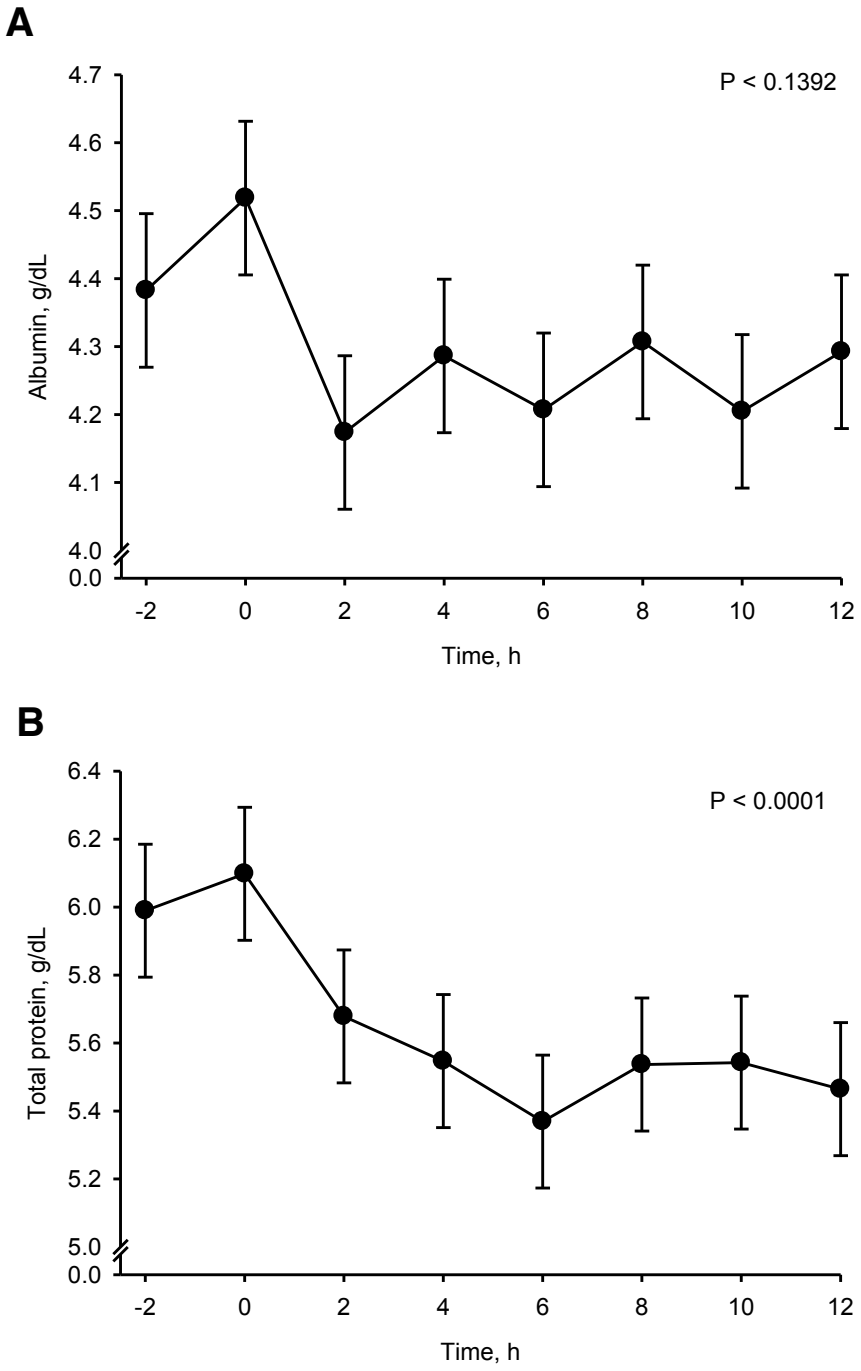

Figure 3.13. Changes in plasma albumin (A) and total protein (B) levels in lipopolysaccharide (LPS, 10 µg/kg BW) treated pigs. Pigs were food-deprived overnight, fed at t = -2 and treated with LPS at t = 0. Values are LSMEANS ± SEM (n = 9).

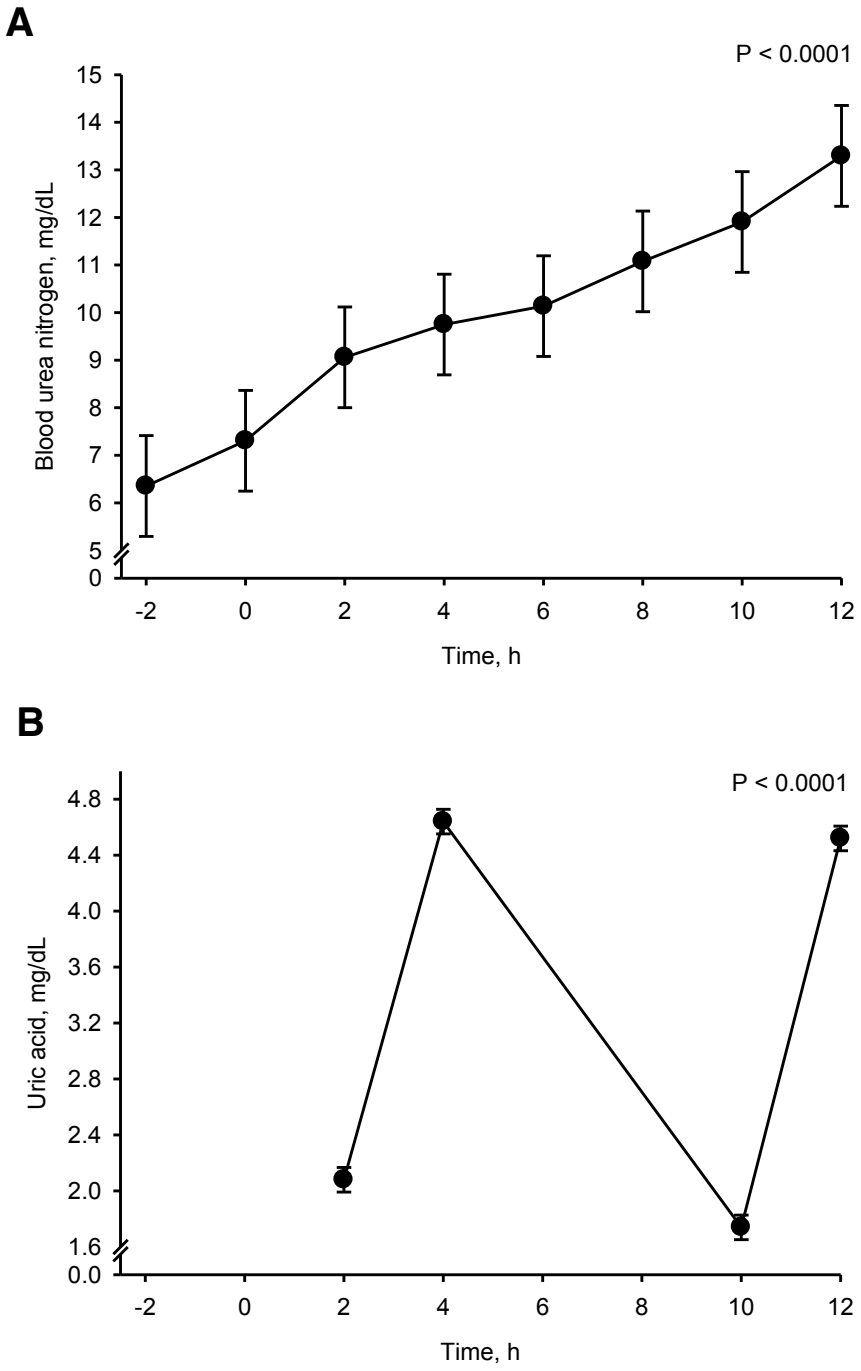

Figure 3.14. Changes in blood urea nitrogen (A) and plasma uric acid (B) levels in lipopolysaccharide (LPS, 10 µg/kg BW) treated pigs. Pigs were food-deprived overnight, fed at t = -2 and treated with LPS at t = 0. Values are LSMEANS ± SEM (n = 9).

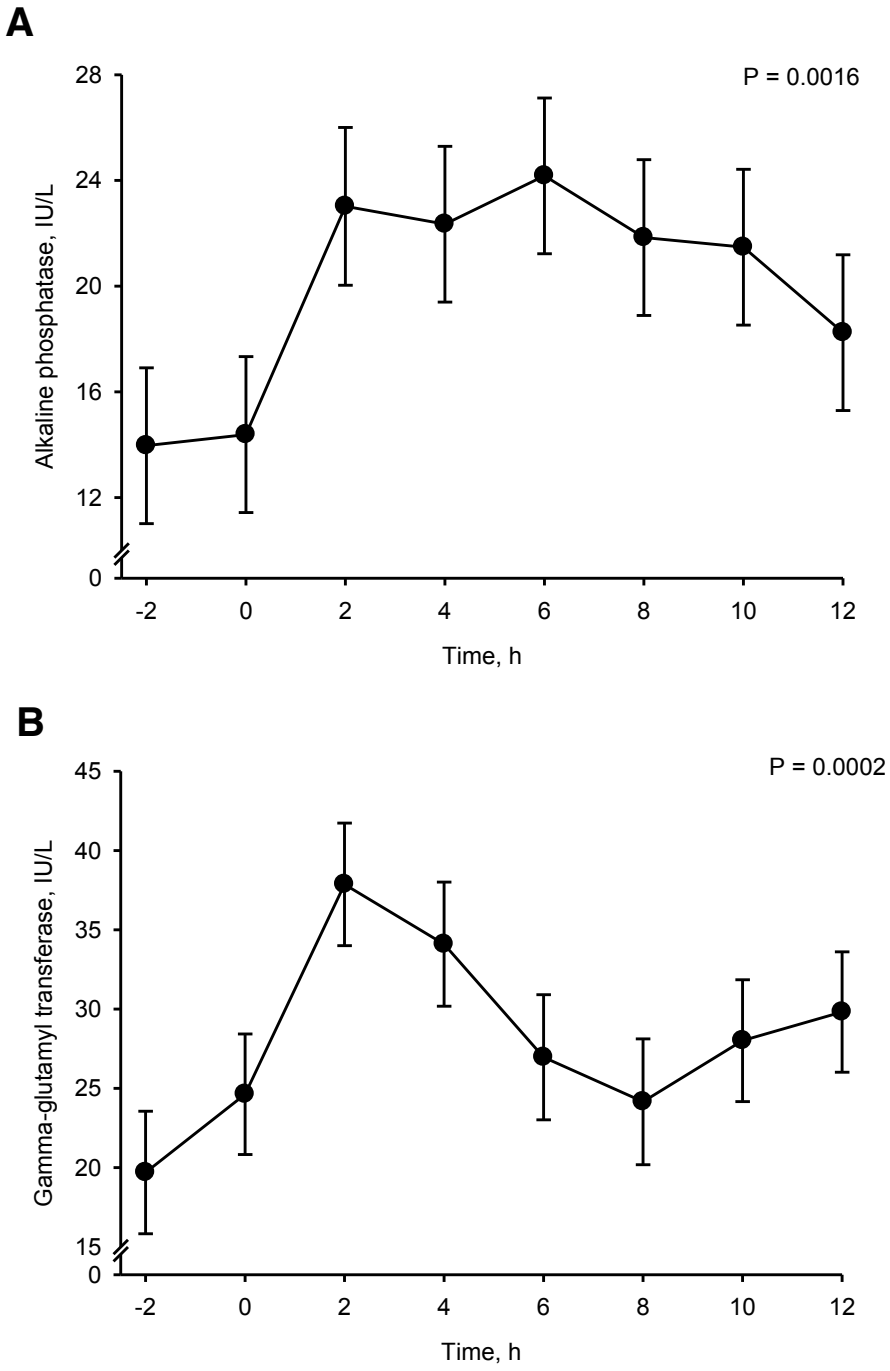

Figure 3.15. Changes in plasma alkaline phosphatase (A) and gamma-glutamyl tansferase (B) levels in lipopolysaccharide (LPS, 10 μg/kg BW) treated pigs. Pigs were food-deprived overnight, fed at t = -2 and treated with LPS at t = 0. Values are LSMEANS ± SEM (n = 9).

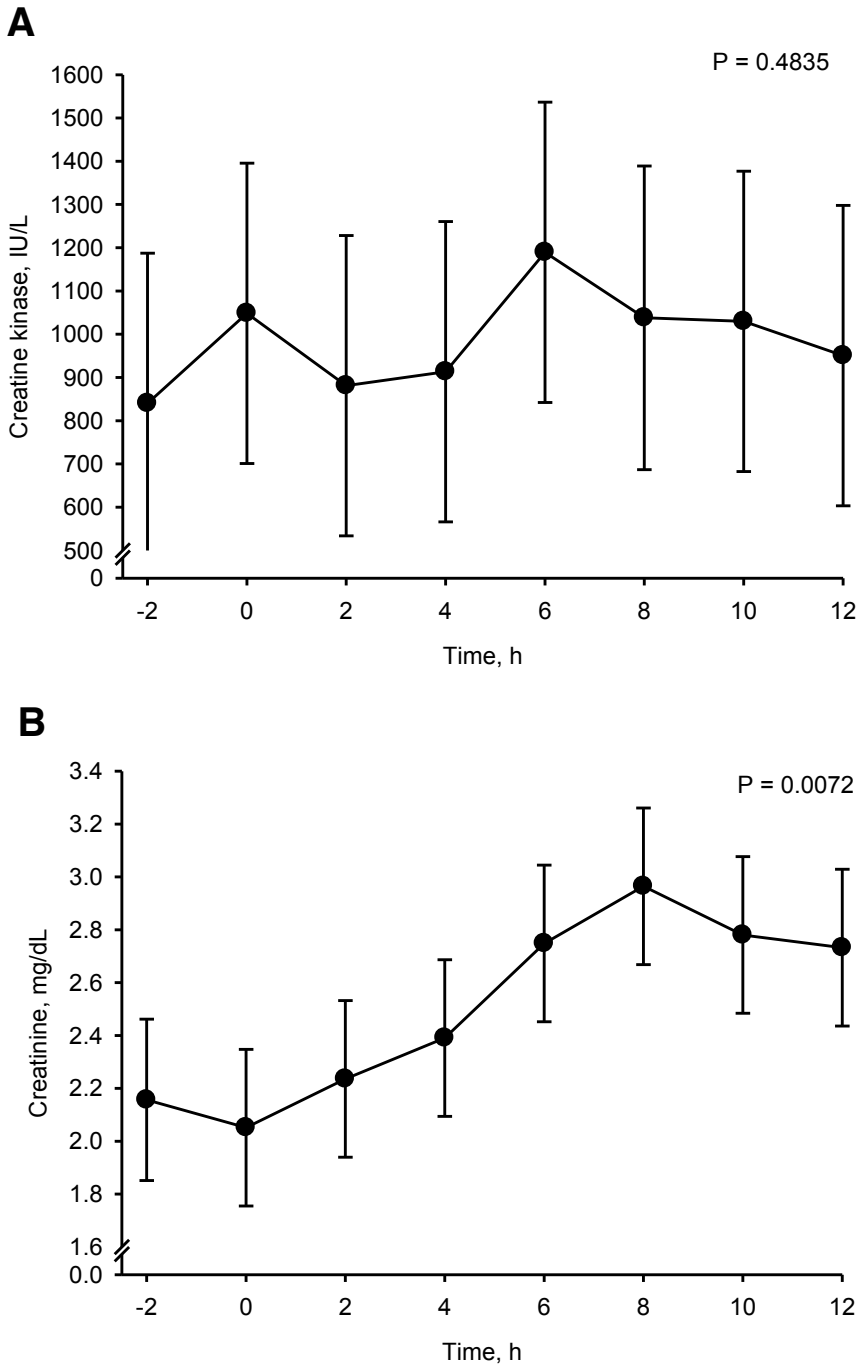

Figure 3.16. Changes in plasma creatine kinase (A) and creatinine (B) levels in lipopolysaccharide (LPS, 10 μg/kg BW) treated pigs. Pigs were food-deprived overnight, fed at t = -2 and treated with LPS at t = 0. Values are LSMEANS ± SEM (n = 9).

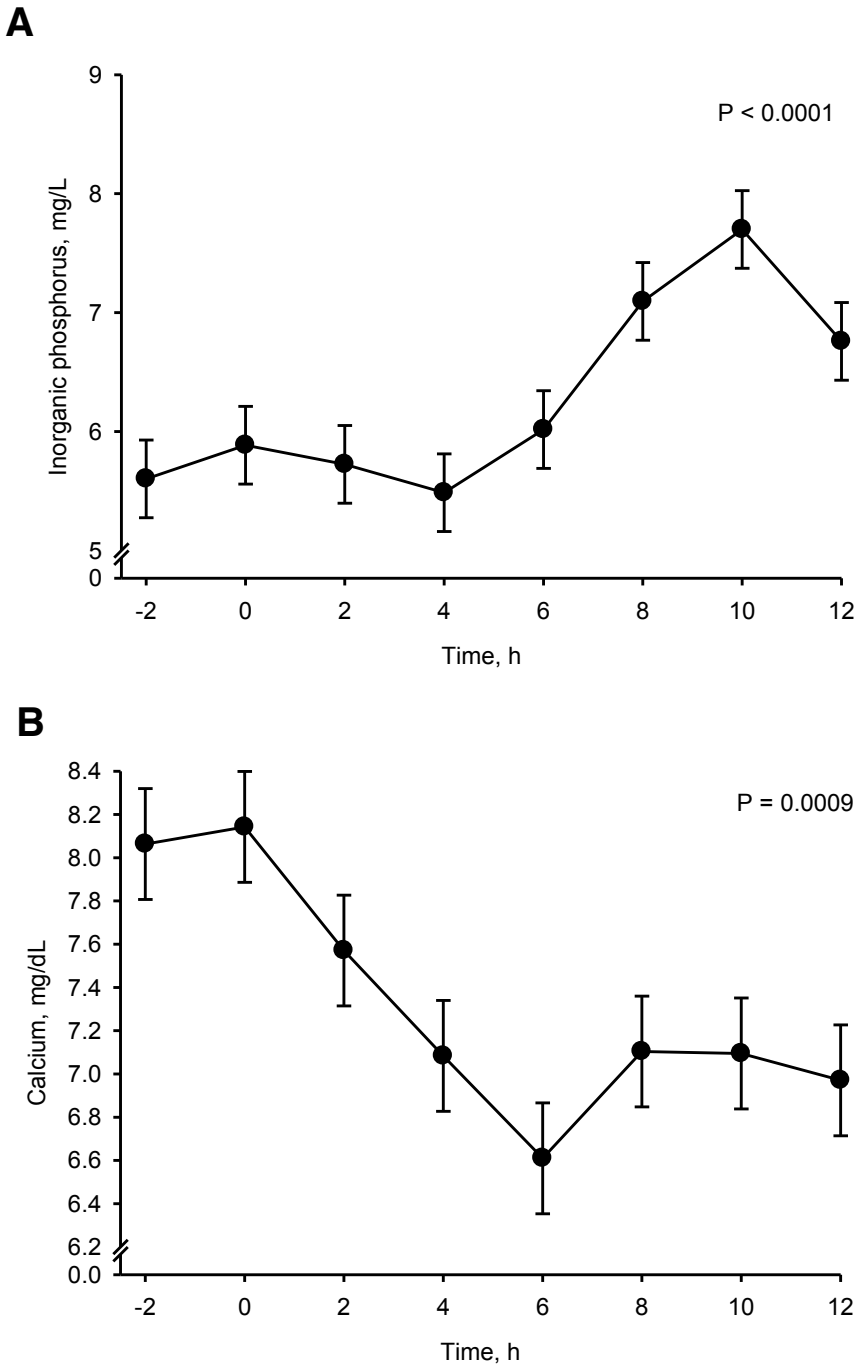

Figure 3.17. Changes in plasma inorganic phosphorus (A) and calcium (B) levels in lipopolysaccharide (LPS, 10 µg/kg BW) treated pigs. Pigs were food-deprived overnight, fed at t = -2 and treated with LPS at t = 0. Values are LSMEANS ± SEM (n = 9).

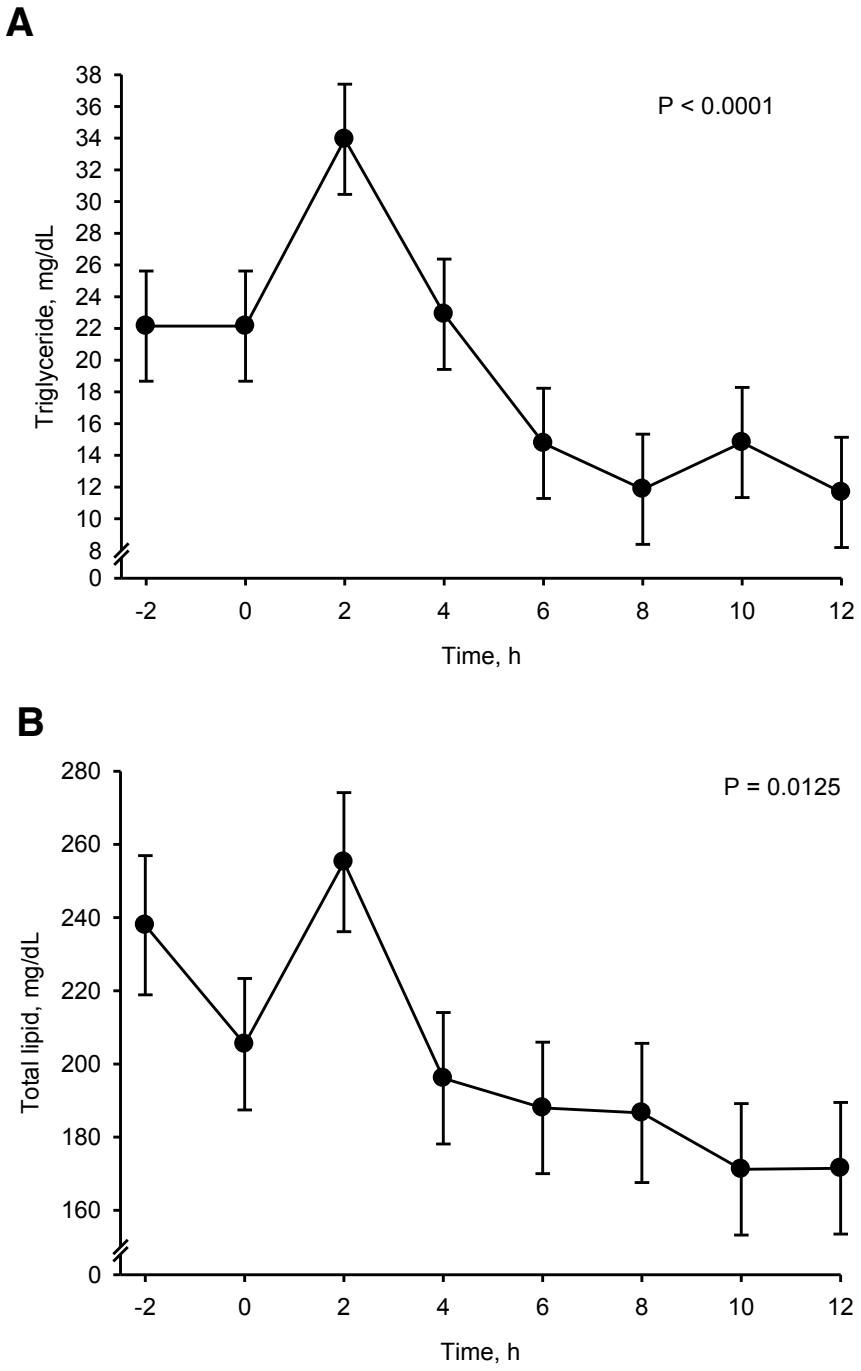

Figure 3.18. Changes in plasma triglyceride (A) and total lipid (B) levels in lipopolysaccharide (LPS, 10 µg/kg BW) treated pigs. Pigs were food-deprived overnight, fed at t = -2 and treated with LPS at t = 0. Values are LSMEANS ± SEM (n = 9).

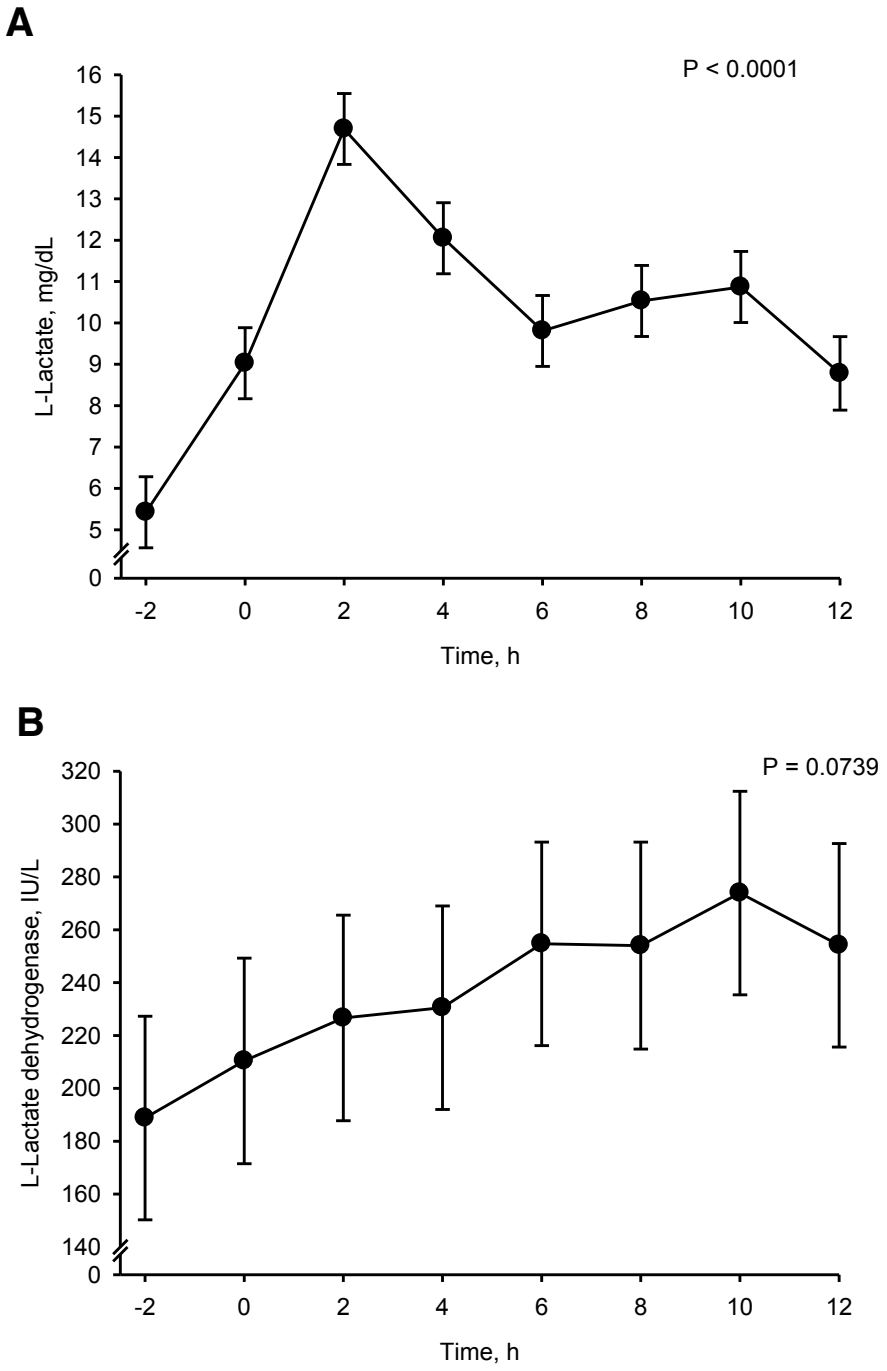

Figure 3.19. Changes in plasma L-lactate (A) and L-lactate dehydrogenase (B) levels in lipopolysaccharide (LPS, 10 µg/kg BW) treated pigs. Pigs were food-deprived overnight, fed at t = -2 and treated with LPS at t = 0. Values are LSMEANS ± SEM (n = 9).

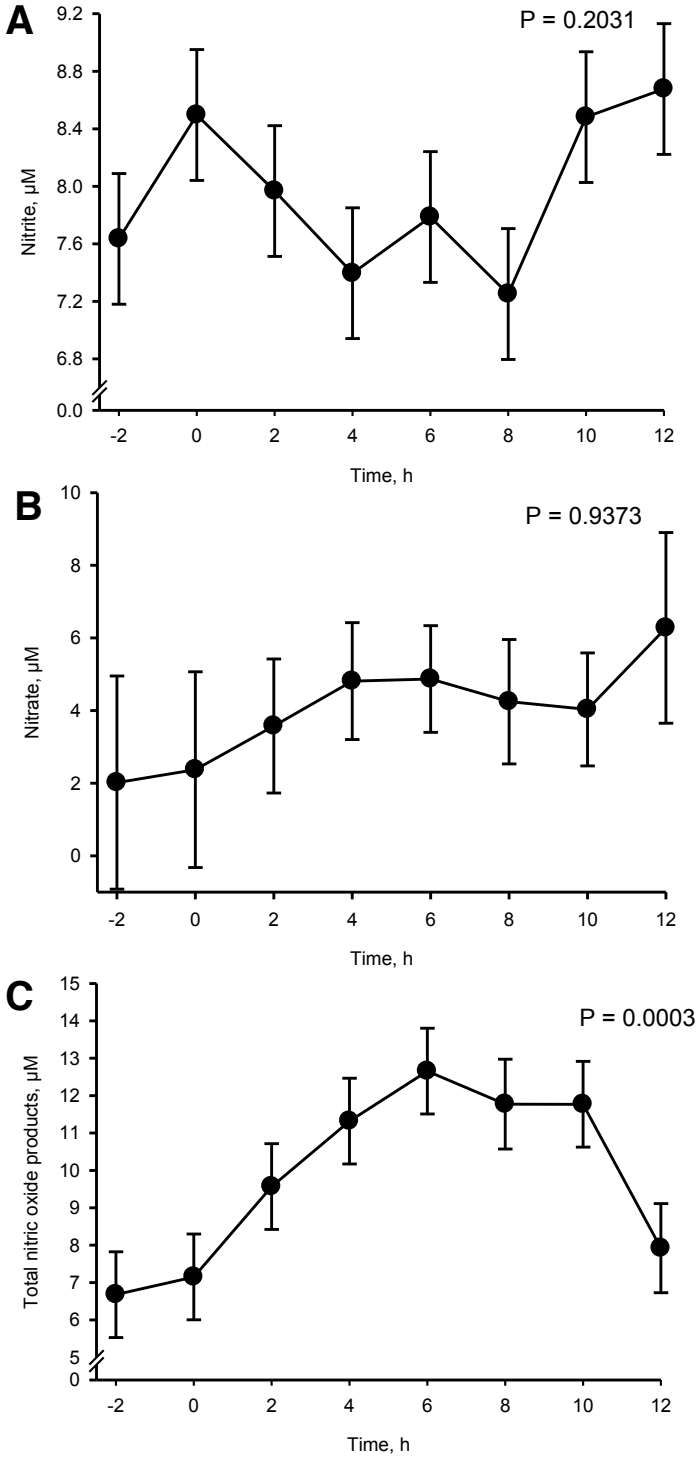

Figure 3.20. Changes in plasma nitrite (A), nitrate (B), and total nitric oxide products (C) levels in lipopolysaccharide (LPS, 10 µg/kg BW) treated pigs. Pigs were food-deprived overnight, fed at t = -2 and treated with LPS at t = 0. Values are LSMEANS ± SEM (n = 9).

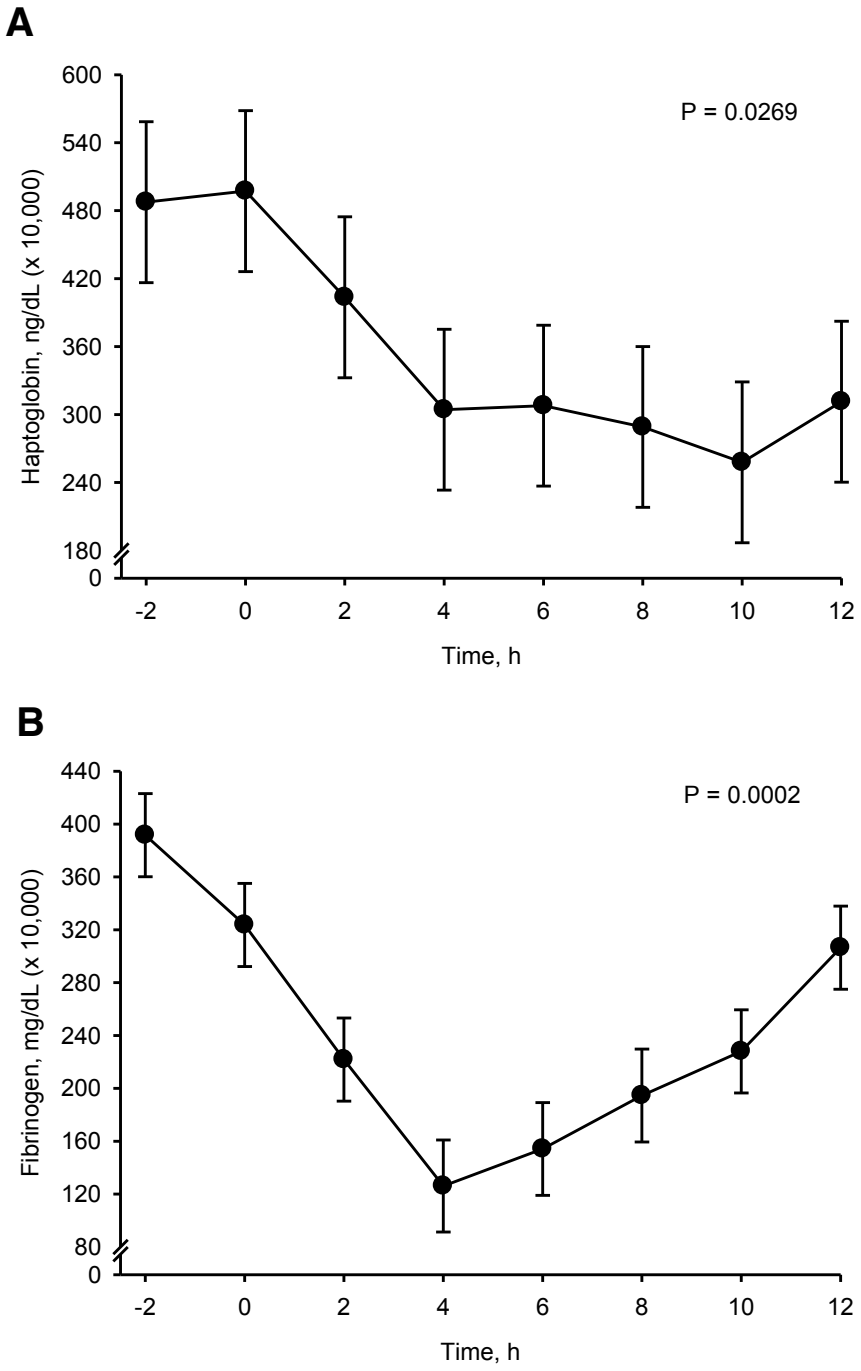

Figure 3.21. Changes in plasma haptoglobin (A) and fibrinogen (B) levels in lipopolysaccharide (LPS, 10 µg/kg BW) treated pigs. Pigs were food-deprived overnight, fed at t = -2 and treated with LPS at t = 0. Values are LSMEANS ± SEM (n = 9).

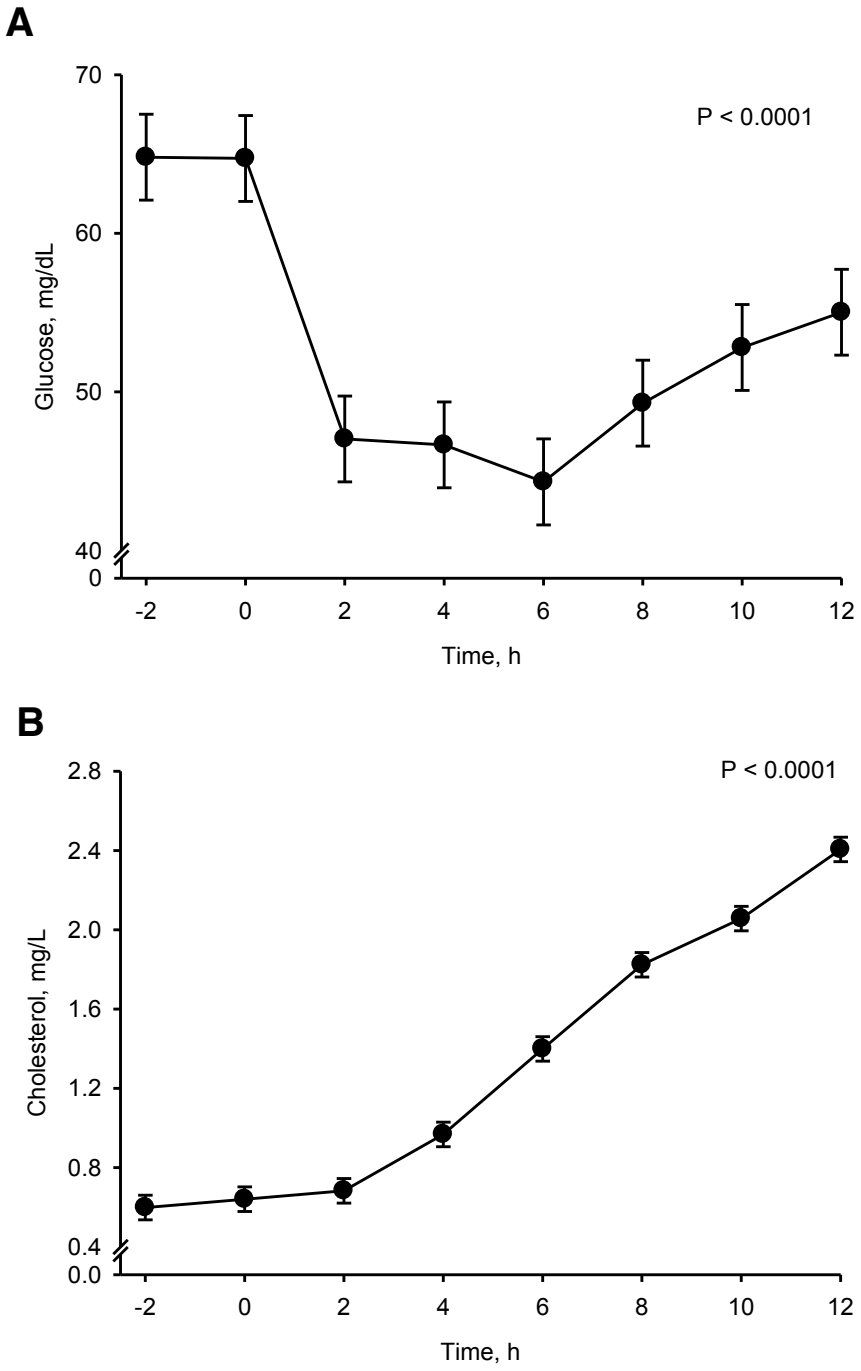

Figure 3.22. Changes in plasma glucose (A) and cholesterol (B) levels in lipopolysaccharide (LPS, 10 µg/kg BW) treated pigs. Pigs were food-deprived overnight, fed at t = -2 and treated with LPS at t = 0. Values are LSMEANS ± SEM (n = 9).

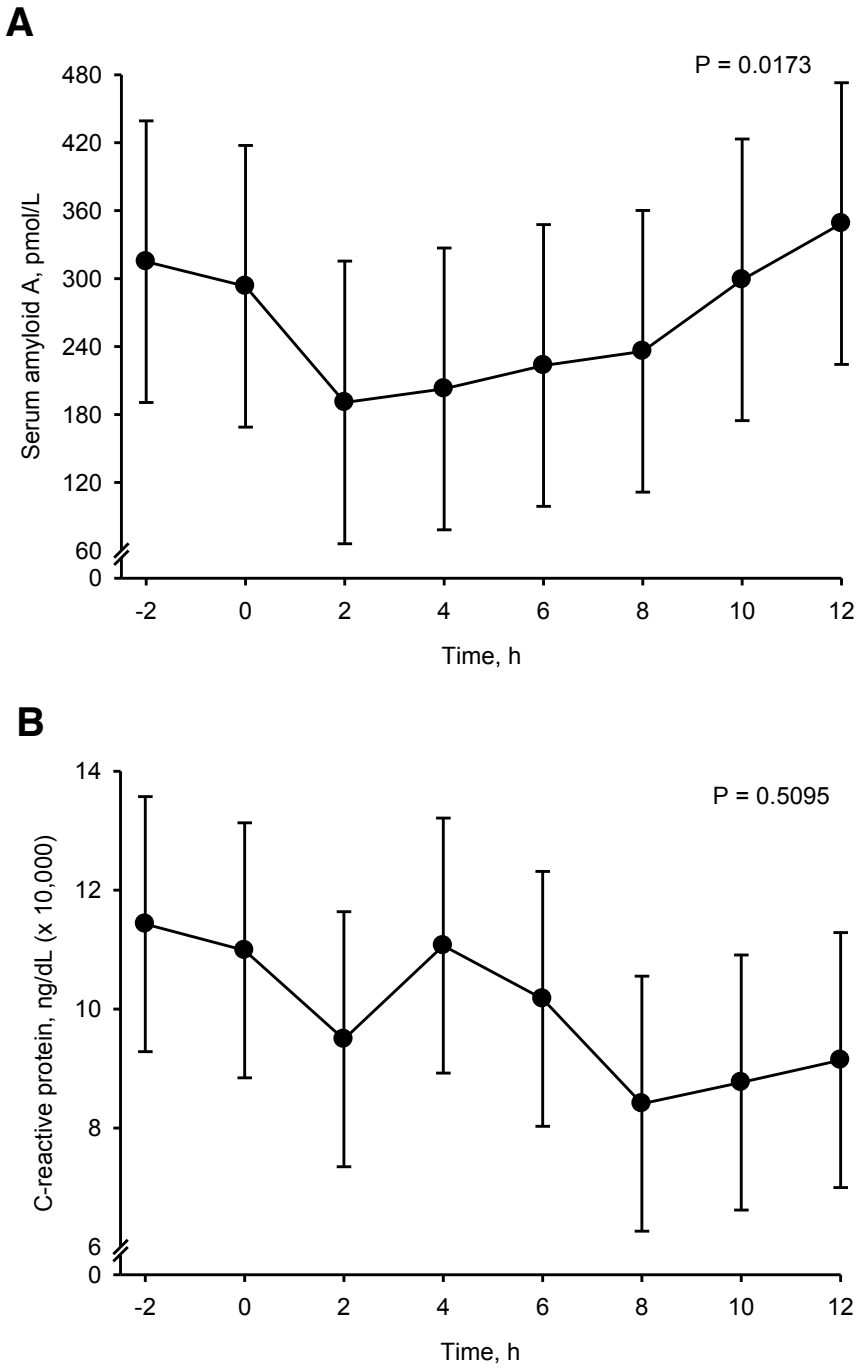

Figure 3.23. Changes in plasma serum amyloid A (A) and c-reactive protein (B) levels in lipopolysaccharide (LPS, 10 µg/kg BW) treated pigs. Pigs were food-deprived overnight, fed at t = -2 and treated with LPS at t = 0. Values are LSMEANS ± SEM (n = 9).

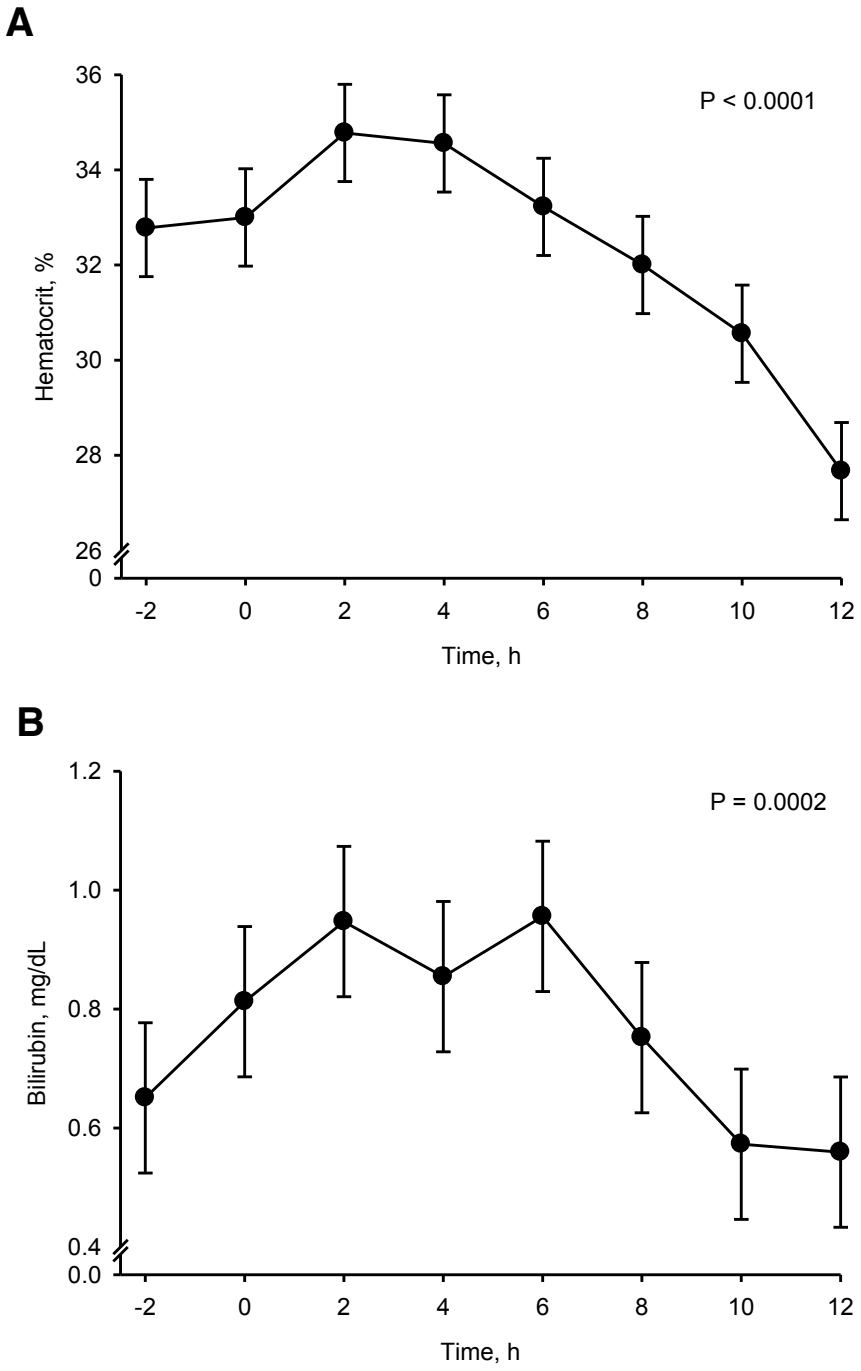

Figure 3.24. Changes in plasma hematocrit (A) and bilirubin (B) levels in lipopolysaccharide (LPS, 10 µg/kg BW) treated pigs. Pigs were food-deprived overnight, fed at t = -2 and treated with LPS at t = 0. Values are LSMEANS ± SEM (n = 9).

3.8 Literature Cited

Agwunobi, A. O., C. Reid, P. Maycock, R. A. Little, and G. L. Carlson. 2000. Insulin resistance and substrate utilization in human endotoxemia. J. Clin. Endocrinol. Metab. 85:3770-3778.

Argiles, J. M., and F. J. Lopez-Soriano. 1990. The effects of tumor necrosis factor-α (cachectin) and tumor growth on hepatic amino acid utilization in the rat. Biochem. J. 226:123-126.

Cohen, S. A., M. Meys, and T. L. Tarvin. 1989. The Pico-Tag Method: A manual of advanced Techniques for amino acid analysis. [WM02, Rev. 1]. Milford, MA, Waters Division of Millipore.

Escobar, J., J. W. Frank, A. Suryawan, H. V. Nguyen, S. R. Kimball, L. S. Jefferson, T. A. Davis. 2006. Regulation of cardiac and skeletal muscle protein synthesis by individual branched-chain amino acids in neonatal pigs. Am. J. Physiol. Endocrinol. Metab. 290:E612-E621.

Johnson, R. W. and J. Esocbar. 2005 Cytokine regulation of protein accretion in growing animals In. *Biology of metabolism in growing animals*, vol. 3. D. G. Burrin and H. J. Mersman, Eds. Elsevier. Pgs: 83-106.

Kitchenham, B., S. MacDonell, L. Pickard, M. Shepperd. 1999. Assessing prediction systems: The Information Science Discussion Paper Series. 99:1-23.

Klasing, K. C. and R. E. Austic. 1984. Changes in protein synthesis due to an inflammatory challenge. Proc. Soc. Exp. Bio. Med. 176:285-291.

Lambalgen, A. A. van, M. T. E. Rasker, G. C. van den Bos, and L. G. Thus. 1988. Effects of endotoxemia on systemic plasma loss and hematocrit in rats. Microvascular Res. 36:291-304.

Lang, C. H., G. J. Bagby, C. Dobrescu, S. Nelson, and J. J. Spitzer. 1992. Modulation of glucose metabolic response to endotoxin by granulocyte colony-stimulating factor. Am. J. Physiol. 263:R1122-R1129.

Le Floc'h, N. D. Melchior, and C. Obled. 2004. Modifications of protein and amino acid metabolism during inflammation and immune system activation. Livestock Prod. Sci. 87:37-45.

Mori, M. 2007. Regulation of nitric oxide synthesis and apoptosis by arginase and arginine recycling. J. Nutr. 137:1616S-1620S.

Orellana, R. A., P. M. J. O'Connoer, H. V. Nguyen, J. A. Bush, A. Suryawan, M. C. Thivierge, M. L. Fiorotto, and T. A. Davis. 2002. Endotoxemia reduces skeletal muscle protein synthesis in neonates. Am. J. Physio. Endocrinol. Metab. 283:E909-E916.

Reeds, P. J., C. R. Fjeld, F. Jahoor. 1994. Do the differences between the amino acid compositions of acute-phase and muscle proteins have a bearing on nitrogen loss in traumatic states? J. Nutr. 124:906-910.

Reeds, P. J. and F. Jahoor. 2001. The amino acid requirements of disease. Clin Nutr. Supp. 1:15-22.

Saedeleer, V. De, E. Wechsung, and A. Houvenaghel. 1991. Endotoxin in the conscious piglet: Its effect on some general and gastrointestinal myoelectrical parameters. Vet. Res. Comm. 15:227-238.

Stipanuk, M. H. and M. Watford. 2000. Amino acid metabolism. In: *Biochemical and physiological aspects of human nutrition*. M. H. Stipanuk, ed. W.B. Saunders Co, Pgs:233-286.

Webel, D. M., B. N. Finck, D. H. Baker, and R. W. Jonhson. 1997. Time course of increased plasma cytokines, cortisol, and urea nitrogen in pigs following intraperitoneal injection of lipopolysaccharide. J. Anim. Sci. 75:1514-1520.

Wu, G. 1998. Intestinal mucosal amino acid catabolism. J. Nutri. 128:1249-1252.

Chapter 4

Validation of 12-hour prediction equations

4.1 Abstract

The nutritional requirements of sick animals or humans have not been well outlined. During an acute or chronic illness blood metabolites are routinely measured; however, amino acid (AA) levels are not. Amino acids are important for mounting a strong immune response, and being able to predict their level using blood metabolites can possibly improve the recovery of acute and chronically ill patients. Nutritional management with AA could possibly aid in the recovery of sick patients. The aim of this study was to validate prediction equations generated during a lipopolysaccharide (LPS) study where blood metabolites and AA were measured for 12 h after a single LPS dose (Chapter 3). Pigs (19.1 ± 0.37 kg) were surgically fitted with an indwelling jugular catheter, allowed to recover, food-deprived overnight, fed (t = -2), and treated with either sterile saline (n = 16) or 10 μg/kg BW of LPS (n = 15) at t = 0. Blood samples were collected at t = -2, 0, 0.5, 1, 1.5, 2, 3, 4, 5, 6, 8, 10, 12, 14, 16, 18, 20, 22, and 24 h after LPS treatment to quantify plasma AA and metabolites. Area under the curve (AUC) was calculated for a select group of AA to further investigate their AA balance. Compared to saline-treated pigs, AUC calculations indicate that all AA analyzed were initially under a negative balance and only arginine, lysine, methionine, and phenylalanine eventually switched to a positive balance while isoleucine, leucine, threonine, tryptophan, and tyrosine remain negative for the entire 24-h study. As expected, rectal temperature and blood urea nitrogen values were greater in LPS treated pigs. Using equations created with data from a 12-h study, predicted and residual values were generated for each pig at each time point. Observed and predicted values were analyzed for

the ability of the equations to predict plasma AA concentrations. Results indicate that equations generated using the 12-h data poorly predicted changes in amino acid levels in pigs treated with LPS and blood samples collected for 24-h after LPS.

4.2 Introduction

Foodborne pathogens like *Salmonella* impact human and animal health. *Salmonella* infections are responsible for 27% of all bacterial infections in humans each year (Mead et al., 1999) and cause an estimated $2.4 billion loss to the livestock industry each year (ERS/USDA, 2003). Gram-negative bacteria (i.e. *Salmonella*) have a lipopolysaccharide (LPS) layer that is responsible for causing a large pro-inflammatory response and septic shock like symptoms. Lipopolysaccharide is commonly used to induce a disease like state in animals. Administering LPS or inducing a *Salmonella* infection, in humans or pigs, results in increased body temperature, anorexia, and possibly diarrhea (Dritz et al., 1996; Webel et al., 1997; Merck, 2003). Additionally, LPS and *Salmonella* induce the release of pro-inflammatory cytokines (e.g., IL-1β, IL-6, and TNF-α), which have been shown to decrease skeletal muscle protein synthesis yet increase skeletal muscle proteolysis and liver protein synthesis (Orellana et al., 2002). The increase in skeletal muscle proteolysis is meant to liberate amino acids (AA) to be used by the liver or immune cells for production of acute phase proteins (APP) and cytokines, respectively (Orellana et al., 2002). Reeds et al. (1994), showed that aromatic AA derived from mixed muscle proteins are potentially rate limiting for the synthesis of hepatic APP. A reduction in aromatic AA could hinder APP production; thereby, decreasing the ability of the host to mount a strong immune response. Metabolic changes occurring in sick animals and humans alter nutritional requirements and we are currently unsure how to best feed them.

The goals of this study were to validate prediction equations generated in a previous study using blood metabolites (e.g., glucose and LDL) to estimate plasma AA. In addition, we aimed to quantify plasma AA balance between healthy and immune-stimulated pigs over a 24-h period.

To accomplish the second goal, we calculated the area under the curve (AUC) for individual AA as is commonly done in glucose tolerance test studies. There are 3 main methods to calculate AUC: (1) incremental area method, which subtracts baseline measurements from all other measurements; (2) positive incremental area method, where values greater than the baseline are used; and (3) total AUC. Total AUC is a better method compared to using incremental area or positive incremental area because it accounts for all variations in the data. Incremental and positive incremental, and total AUC will yield similar results if all data points are above baseline values (Potteiger et al., 2002). We elected to use total AUC because it is likely that some plasma AA levels will be lower than the baseline measurement after prolonged LPS treatment. Total AUC was used in this study to analyze individual differences in plasma AA of saline and LPS treated pigs.

4.3 Materials and Methods

The Virginia Tech Institutional Animal Care and Use Committee approved all procedures.

4.3.1 Animals, housing, diets, and experimental protocol

A total of 30 crossbred pigs (19.1 ± 0.37 kg BW) were individually housed in pens located inside an environmentally controlled room. Rooms were individually ventilated with 100% clean air (i.e., no recirculation), and were under negative pressure at all times, and an

automated system controlled the temperature and lighting (18 h light: 6 h dark with lights on at 0600) of each individual room. Each pen contained a plastic coated expanded metal floor, a nipple waterer, and self-feeder. All pigs were fed a common corn-soybean meal diet at 90% of their free-choice average daily feed to insure complete consumption of each meal bout. The diet was formulated to meet or exceed nutritional requirements of pigs this size (NRC, 1998). Pigs were fed 3 times each d and had free access to water. After an adjustment period of 4 d, indwelling jugular vein catheters were surgically implanted for serial blood collection as previously described (Escobar et al., 2006). All pigs were treated for 3 d post-surgery with i.v. flunixin meglumine (4 mg/kg BW, twice each d for pain management, Flunixijet, Butler Animal Health, Dublin, OH) and i.m. ceftiofur-HCl (5mg/kg BW, once each d as a bacterial prophylaxis, Excenel-RTU, Pfizer, New York, NY). Blood was collected 2-h prior to LPS exposure from pigs that had been food-deprived overnight. A venous blood sample was collected and pigs were fed one third of their normal morning feed intake every 20 minutes for the next 1-h. At time = 0, half of the pigs (n = 16) were intravenously infused with sterile 0.9% saline and the remaining pigs (n = 15) were dosed with 10 μg/kg of BW of lipopolysaccharide (LPS) from *E. coli* (055:B5, Sigma-Aldrich, St. Louis, MO) suspended in 0.9% sterile saline (i.e. 1 ml/10 kg BW, 1.96 ± 0.51 ml). Blood samples were collected from pigs for 24 h post LPS treatment at t = -2, 0, 0.5, 1, 2, 3, 4, 5, 6, 8, 10, 12, 14, 16, 18, 20, 22, and 24 h after LPS administration. Blood samples were collected in Li-heparinized tubes and centrifuged at 3,000×g for 5 min at 4°C and the resulting plasma was collected, transferred to 2-mL microcentrifuge tubes (Eppendorf, Hamburg, Germany), and stored at -80ºC until analyzed for AA and various metabolites.

4.3.2 Analyses of blood metabolites

Various clinical-grade commercial kits (Table 4.1) were purchased to determine the concentration of plasma metabolites according to manufacturer's instructions. Direct low density lipoprotein cholesterol, triglyceride-glycerophosphate oxidase, creatinine, amylase, urea nitrogen, aspartate aminotransferase, direct high density lipoprotein cholesterol, total bilirubin, calcium, γ-glutamyl transferase, lactate dehydrogenase, inorganic phosphorus, total lipid, alanine aminotransferase, alkaline phosphatase, albumin, creatine kinase, and total protein assay kits were purchased from Teco Diagnostics (Anaheim, CA).

4.3.3 Plasma amino acids

Plasma samples (500 μL) were combined with an equal volume of 0.4 mM norleucine (Sigma Aldrich, CAS 327-57-1) as the internal standard, filtered at 10,000×g for 10 min at 4°C using 10k MW cutoff filters (Pall Corp., Port Washington, NY). An aliquot (25 μL) was transferred to a glass Kimble tube, vacuum dried, derivatized with phenyl isothiocyanate (Acros Organics, Geel, Belgium, CAS 103-72-0), and separated using a 2695 Alliance HPLC equipped with a 30-cm Pico-Tag column, 2487 UV/Vis detector, and Empower software (all from Waters Corp., Milford, MA) using previously described conditions (Cohen et al., 1989). All AA concentrations are expressed in μmol/L.

4.3.4 Area under the curve

Total area under the curve in μM×h (AUC) for control (AUC_C) and LPS (AUC_L) treated pigs were determined using SAS (SAS Institute, Cary, NC) for phenylalanine, tyrosine, arginine,

methionine, leucine, isoleucine, lysine, tryptophan, and threonine (Shiang, 2008). The correction factor of 0.075 L plasma/kg BW (Talbot and Swenson, 1970) was used to convert AUC to μmole•kg BW^{-1}•h^{-1} as a unit of AA metabolism. When applicable, two AUC were calculated for each AA and treatment to better calculate AA anabolism and catabolism. Each AUC was corrected for time based on the intersecting time between LPS and control treatments. If the treatments never crossed, then the time was 24-h. Thus, AA metabolization was calculated using the following equation:

$$\text{AA metabolism} = (AUC_L - AUC_C) \times \frac{0.075\ \text{L}}{\text{g BW}} \times \frac{1}{h^2}$$

4.3.5 Statistical analyses and prediction equations

Data was checked for normality and strong outliers were removed using the PROC UNIVARIATE procedure of SAS. The PROC MIXED procedure of SAS (Tukey adjustment) was used to examine effects of treatment on amino acid and metabolite concentrations. Means are presented as least square means (LSMEANS) ± pooled SE. Means were considered different with a $P < 0.05$. Plasma AA levels were predicted using equations generated from a 12-h LPS study (Chapter 3). We used equations with 1, 5, 10, 15, or 20 terms in the equation to predict the AA concentration. In addition, plasma AA were measured to generate observed versus predicted (i.e., observed – predicted) plots as a measurement of prediction accuracy in pigs for 24 h after treatment with LPS. Data were split into 2 groups: t = -2 through 12 h were in subset 1 (i.e., induction phase) and t = 14 through 24 h were in subset 2 (i.e., recovery phase) to determine the ability of the equations to accurately predict AA concentrations. The PROC REG procedure of SAS was used to determine the slope and, for each model tested, with a BY statement to separate the effects of the 2 groups. GPLOT in SAS was used to generate scatterplots of the residuals

versus predicted values. The 95% confidence interval and regression equation is displayed on each GPLOT graph. Only GPLOT for lysine is shown as an example of the statistics generated for each AA tested. Additionally, lysine was used as a test AA to examine the ability of the prediction equations to predict AA concentrations using the data generated from the 12-h study as a way to test that the equations worked properly. Slope bias, mean bias, root mean square prediction (RMSE), and variation (RMSPE/actual mean × 100) were evaluated for each AA examined. The slope of each residual versus predicted plot was determined via PROC REG by setting residuals equal to predicted. To calculate RMSE the residuals were squared, summed, divided by the number of observations and finally the square root of that value was calculated. The PROC MIXED procedure of SAS was used to determine the LSMEANS and standard error (SE) for each equation, for each time point, so we could graph predicted against observed values. All statistics for AA analyzed (Lys, Met, Phe, Ile, Leu, Arg, Trp, Tyr, and Thr) were examined when 1, 5, 10, 15, or 20 terms were included in the model.

4.4 Results and Discussion

4.4.1 Plasma amino acids and blood metabolites

As expected, LPS treatment resulted in elevated ($P < 0.002$) rectal temperatures (Figure 4.1) and blood urea nitrogen (BUN, Figure 4.16A) compared to control pigs. As seen in the 12-h study, AA concentrations increased after consumption of a meal and LPS treatment resulted in a decrease ($P = 0.0002$) in the majority of AA. A reduction in motility along the gastrointestinal tract is commonly observed in response to LPS possibly contributing episodes of diarrhea or death of the animal (Saedeleer et al.,1991) thus decreasing the digestion and absorption of nutrients along the gastrointestinal tract. The relationship between phenylalanine (Phe) and

tyrosine (Tyr) was altered during the immunological insult with LPS. In healthy animals, Phe can be readily converted to Tyr and as plasma Phe levels increase plasma Tyr levels should increase; however, in LPS treated pigs this did not occur. Plasma Phe began increasing 2 h after LPS while Tyr levels continued to decrease (Figure 4.2). This example strongly implies that AA metabolism is changed during endotoxemia.

In rats challenged with LPS, plasma concentrations of Leu, Ile, and Val decreased over time (Wannemacher, 1977). In our study, plasma levels of Leu (Figure 4.8A), Val (Figure 4.10B), and Ile (Figure 4.8B) markedly decreased below baseline levels during the first 2 h after LPS treatment of fed pigs while plasma concentrations of the AA in saline controls remained elevated over baseline values. Furthermore, plasma Leu, Val, and Ile levels returned to baseline between 8 to 14 h after LPS treatment. Most importantly, plasma Leu, Val, and Ile in LPS treated pigs never exceeded time-matched levels of saline treated pigs. Leucine is a known potent stimulator of skeletal muscle protein synthesis in healthy animals (Escobar et al., 2004). In sick animals, however, skeletal muscle protein synthesis is severely decreased (Orellana et al., 2002). Release of branched chain AA (BCAA) from skeletal muscle during sepsis or disease is purportedly lower compared to the liberation of other AA, especially the aromatic Phe, Tyr, and Trp (Reeds et al., 1994). Once released from skeletal muscle, BCAA are catabolized in muscle to their corresponding keto-acids, which can travel to liver to be used as energy sources. Thus, during disease, sepsis, anorexia, or starvation skeletal muscle can breakdown protein, generating BCAA that can serve as an important energy source in an attempt to reduce skeletal muscle proteolysis (Wannamacher, 1977).

The carbon skeleton and ammonia generated during BCAA catabolism may also be used to produce alanine (Ala) and glutamine (Gln), which are released in large quantities in humans

and rats from skeletal muscle (Wannamacher, 1977). Alanine is an important AA for hepatic gluconeogenesis. It also contributes in the nitrogen shuttling to liver for urea and pyruvate, with the latter also being involved in shuttling energy between muscle and liver via the Cori cycle (Wannamacher, 1977; Stipanuk and Watford, 2000). The fact that Ala is one of the main AA liberated by skeletal muscle could explain the marked rise in circulating Ala after LPS treatment in the current study (Figure 4.12A). However, based on its roles in nitrogen and energy shuttling, plasma values are expected to be low. Increased plasma Ala and alanine aminotransferase (Figure 4.14B) levels may be interpreted as impairment in the Glucose-Alanine cycle or hepatic inability to deaminate Ala.

Blood urea nitrogen is a classic indicator of skeletal muscle proteolysis that is normally elevated during immunological activation (Webel et a., 1997). In the control-saline treated pigs, BUN levels were never different ($P > 0.99$) from the baseline (pre-fed) levels. In a previous 12-h blood sampling study (Chapter 3), BUN levels increased linearly after LPS treatment and that same linear increase was observed in the current 24-h study (Figure 4.16A). Blood urea nitrogen levels did not become different from baseline or control treated pigs until 8 h post-LPS and remained elevated ($P < 0.04$), and by the conclusion of the trial (24 h post-LPS) BUN levels had returned to baseline (P 0.9957). Blood urea nitrogen levels peaked and began decreasing at 12 h after LPS treatment. Therefore, short-term BUN mathematical behavior is a linear increase but when measured over a longer period of time. In the present study, however, BUN levels had not returned to baseline levels after 24 h.

Arginine (Arg, Figure 4.3B) catabolism can lead to the production of citrulline (Cit, Figure 4.3A) and nitric oxide or to the production of ornithine (Orn, Figure 4.3B) and urea depending on the availability of nitric oxide synthase or arginase, respectively. During a

bacterial infection the production of nitric oxide is important for mounting a robust immune response; however, after LPS treatment, arginase activity has been shown to be increased in mice thus increasing urea production (Nelin et al., 2007). In the current study, Arg levels were decreased ($P < 0.059$) in LPS treated animals during the first 6 h post-LPS and were not different ($P > 0.079$) from saline treated control pigs for the remainder of the 24-h sampling period, except at 10 ($P = 0.05$) and 18 h ($P = 0.03$) post-LPS where Arg levels were different between the 2 groups. Thus Arg appears to be in high demand during the induction of disease for the removal of nitrogen and as animals recover, BUN and Arg levels normalize.

Creatine is also liberated from muscle during the production of urea, travels to the liver, and is converted to creatinine (Crtn) or phosphoryl-creatine. Creatinine is filtered by the kidneys for excretion from the body in urine making it a possible indirect marker of skeletal muscle proteolysis. Creatine kinase (CK) is responsible for the reversible conversion between phosphoryl-creatine (which can be converted to Crtn or to phosphoryl-creatinine and then to Crtn) and creatine and is found mainly in skeletal muscle. There is debate on the validity of using Crtn as a marker of muscle activity and muscle mass in humans or animals because phosphoryl-creatinine is an intermediate that could potentially impact the ability to accurately monitor muscle mass simply using Crtn. Additionally, in rabbits, research has shown that Crtn can be converted to other compounds (e.g., arginine, creatine, etc.) that could also lead to a false measurement of muscle mass (Wyss and Kaddurah-Daouk, 2000). In the current study, in the control-saline treated pigs, creatine kinase (Figure 4.18A, $P > 0.23$) and creatinine (Figure 4.18B, $P > 0.10$) levels were no different ($P > 0.23$) from baseline (pre-fed) levels for the entire 24 h trial. However, in LPS treated animals both CK and Crtn appear to have an almost cyclic response, where both metabolites initially increase, decline, rise again, and then slowly return to

baseline levels. Even with the cyclic response, CK levels were elevated ($P < 0.05$) after LPS treatment over the control-saline treated animals for the entire 24 h study, thus another indication of skeletal muscle. Creatinine levels were elevated ($P < 0.025$) over the Crtn levels in control treated pigs in response to LPS except at t = 0.5, 2, 6, 8, 16, and 18 h post-LPS and at 24-h post-LPS Crtn levels were no different between the 2 groups.

Yet another, indicator of skeletal muscle activity is the enzyme aspartate aminotransferase (AST). Aspartate aminotransferase (Figure 4.14A) levels were elevated ($P < 0.03$) over control treated animals after LPS treatment (with the exception of t = 1.5, 3 and 12 h post-LPS, where the levels were no different ($P > 0.07$) between the control and LPS groups). Aspartate aminotransferase levels had returned to the level of the control treated animals by the conclusion of the study ($P = 0.17$ at t = 24 h).

As was seen in the 12-h trial (Chapter 3), hematocrit (HCT) levels were elevated in response to LPS. In the 12-h trial saline was infused into the animal during sampling, possibly confounding the HCT results; however, during the current (24-h) trial, saline was not infused into the animals in an attempt to reduce any effect on HCT due to something other than LPS. Hematocrit levels were greater ($P < 0.01$) than control animals for the first 8 h of the trial (except at t = 2, $P = 0.10$) with them peaking at t = 5 (39.67 ± 0.95) and were numerically lower than the HCT levels of the control treated animals from t = 10 through t = 24 h. At the conclusion of the study (t = 24 h), HCT levels were still lower ($P = 0.03$) than the control-saline animals. Initially, it appears that there is a loss of plasma water resulting in an increase in HCT and then a recovery is observed where HCT levels decrease and in some instances levels can fall below baseline values. Hematocrit values under baseline could indicate a reduction in the number of circulating

blood cells (Lambalgen et al., 1988), possibly due to increased blood coagulation (Saedeleer et al., 1991).

4.4.2 Area under the curve

Results indicate that Ile, Leu, Thr, Trp, and Tyr were in a negative balance during the entire 24-h study compared to controls (Table 4.2). Arg, Lys, Met, and Phe were initially in a negative balance but changed to a positive balance within the first 12- h after LPS treatment (Table 4.2). These results can be interpreted to suggest a high and prolonged demand for Ile, Leu, Thr, Trp, and Tyr during sickness induction and recovery whereas Arg, Lys, Met, and Phe are needed at high levels only during the induction phase. Because plasma Lys, Met, and Phe exceed baseline and approach postprandial levels, it can be interpreted to suggest that these AA are freed from muscle in excess of bodily needs during the recovery phase and their likely fate is deamination and excretion from the body. In LPS treated pigs, plasma behavior of taurine closely follows that of Met and can be used as an indirect measurement of sulfur AA catabolism, which could potentially indicate lower requirements for these AA during disease.

4.4.3 Accuracy of predicted plasma amino acids during 24-h LPS study

A series of prediction equations were generated using data from the 12-h LPS study (Chapter 3). When examining the ability of a model to predict a value the model should be tested for mean and slope bias. There is a slope or mean bias if the slope is positive or negative or if the sum of the residuals mean is different from zero (St. Pierre, 2003). The mean of

predicted values, mean of residual values, slope, and R^2 of the model for the 24-h values using the 12-h prediction equations are presented in Table 4.4. These data are further split to look at the statistics presented for either the induction (t = -2 to 12-h) or recovery (t = 14 to 24 h) phases during LPS treatment. Regardless of phase (i.e., induction or recovery), there was a strong slope bias for predicted AA indicating a linear negative trend (Tables 4.4A and B, Figures 4.23 - 4.27). Overall, a mean bias was also evident and strong because the mean of the squared residuals was not zero (Table 4.4A and B). Sum of squared residuals varied greatly in predicting 24-h AA concentration levels with the closest and furthest values from zero were at -1.60 and 322.34, respectively, indicating biased means.

Plots of observed versus predicted values indicate the ability of the equations to predict 24-h AA concentrations using 1, 5, 10, 15, or 20 terms in the model (Figures 4.13 - 4.21). One term model was not able to follow the flux in AA and is a relatively straight line; however, the more terms added to the equation seems to cause drastic changes in AA possibly due to over-parameterization of the model. Thus meaning there could be 1 or more terms strongly influencing the predicted AA level. Therefore, prediction equations generated during the 12-h study should be revisited to remove strong biasing terms and re-tested against the independent 24-h study.

4.4.4 Accuracy of predicted plasma amino acids during 12-h LPS study

To ensure that equations were indeed capable of accurate predictions we examined the same statistics from the original 12-h data set (Chapter 3) and results for each AA are shown in Tables 4.5A and B. Observed versus predicted (Figure 4.22) and residual versus predicted

plots (Figures 4.28 to 4.30) are only shown for Lys. As expected, the mean bias was considerably reduced when equations were applied to the 12-h study since these were the data used to generate the equations. In addition, the sum of the squared residuals ranged from -0.003 to -36.64, and represents about a 10-fold improvement over the aforementioned 24-h study. Furthermore, when 20 terms were included in the model the slope was practically zero and residuals were evenly distributed around zero indicating no slope bias and proper functioning of predicting equations.

The number of terms needed in a model cannot be accurately determined using the 24-h predicted values due to the inability of the equations to perform. As seen with the 24-h AA predicted values, when predicting AA values from the 12-h dataset the inclusion of just 1 term in the model yields a fairly linear line (Figure 4.22A). Indicating 1 term in the model cannot accurately predict changes in AA levels. Examining the predicted versus observed plots (Figure 4.22 A and B), including 5 terms in the model leads to an under-estimation of the AA concentration (i.e., residual greater than mean) while including 10, 15, or 20 terms in the model leads to an over-estimation of AA concentration (i.e., residual less than mean). Looking at mean or slope bias, including 20 terms in the model yields the least amount of bias yet this is not practical in clinical sets (Table 4.5A and B). After 20 terms in the model, including 5 terms in the model yields the next lowest slope and offers the 3rd lowest sum of squared residuals. Ideally, creating prediction equations with 4 to 10 terms could be beneficial at predicting AA levels in sick patients. Determining when animals or humans are in a negative AA balance can result in individualized nutritional care of patients and could possibly aid in their recovery.

4.5 Implications

Predicting AA levels using blood metabolites is possible; however, the use of non-linear terms (e.g., quadratic, cubic, log, etc.) should be evaluated. Additionally, a greater data set including varying lengths, agents, and severity of disease may be needed to reduce mean and slope biases. Using LPS to induce an immune response and metabolic alterations should be used as a proof of technique and actual pathogenic agents (e.g., *E. coli*, *Salmonella*) should be used to develop equations for clinical applications. Area under the curve is a useful calculation to indirectly determine AA balance during disease and provides an initial estimate of AA needs.

4.6 Tables

Table 4.1. List of all metabolites analyzed

Acronym	Description	Assay	Units	Provider
ALT	Alanine aminotransferase	Colorimetric	IU/L	Teco Diagnostics, A526-120
ALB	Albumin	Colorimetric	g/dL	Teco Diagnostics, A502-480
ALK	Alkaline phosphatase	Colorimetric	IU/L	Teco Diagnostics, A506-120
AMY	Amylase	Enzymatic, kinetic	IU/L	Teco Diagnostics, A533-60
AST	Aspartate aminotransferase	Colorimetric	IU/L	Teco Diagnostics, A561-120
BIL	Bilirubin	Colorimetric	mg/dL	Teco Diagnostics, B576-480
BUN	Blood urea nitrogen	Enzymatic, endpoint	mg/dL	Teco Diagnostics, B551-132
CA	Calcium	Colorimetric	mg/dL	Teco Diagnostics, C503-480
CHOL	Cholesterol	Enzymatic, endpoint	mg/L	Teco Diagnostics, C509-400
CK	Creatine kinase	Enzymatic, kinetic	IU/L	Teco Diagnostics, C512-240
CRTN	Creatinine	Colorimetric	mg/dL	Teco Diagnostics, C513-480
GGT	Gamma-glutamyl transferase	Enzymatic, kinetic	IU/L	Teco Diagnostics, G571-150
HAPT	Haptoglobin	ELISA	ng/dL	Immunology Consultants Lab., e-5hpt
HCT	Hematocrit	Centrifugation	%	In-house
HDL	High-density lipoprotein	Colorimetric	mg/dL	Teco Diagnostics, H513-100
iP	Inorganic phosphorus	Colorimetric	mg/L	Teco Diagnostics, I515-480
LDH	L-Lactate dehydrogenase	Enzymatic, kinetic	IU/L	Teco Diagnostics, L535-240
LDL	Low-density lipoprotein	Colorimetric	mg/dL	Teco Diagnostics, L530-100
TL	Total lipid	Colorimetric	mg/dL	Teco Diagnostics, T526-480
TP	Total protein	Biuret	g/dL	Teco Diagnostics, T528-480
TG	Triglyceride	Enzymatic, endpoint	mg/dL	Teco Diagnostics, T531-400
UA	Uric acid	Enzymatic, end-point	mg/dL	Teco Diagnostics, U580-240

Table 4.2. Calculated individual amino acid balance in fed pigs treated with lipopolysaccharide[1].

	Negative				Positive			
Amino Acid	Time[2]	Balance[3]	Std Err	P-value[4]	Time[2]	Balance[3]	Std Err	P-value[4]
Ala	---	---	---	---	24	0.736	0.118	<0.0001
Arg	12	-0.368	0.050	0.0005	12	0.103	0.035	0.1325
Cit	20	-0.009	0.004	0.1100	4	0.680	0.345	0.2201
Gln	24	-0.236	0.028	<0.0001	---	---	---	---
Glu[5]	16	-0.294	0.088	0.0125	8	0.057	0.481	0.9145
His	6	-0.253	0.028	<0.0001	18	0.032	0.011	0.0701
Ile	24	-0.098	0.015	<0.0001	---	---	---	---
Leu	24	-0.114	0.023	0.0007	---	---	---	---
Lys	5	-1.345	0.317	0.0018	19	0.136	0.029	0.0101
Met	6	-0.172	0.017	<0.0001	18	0.056	0.009	<0.0001
Orn	24	-0.056	0.014	0.0376	---	---	---	
Phe	6	-0.298	0.025	<0.0001	18	0.176	0.016	<0.0001
Tau	---	---	---	---	24	0.176	0.036	0.0001
Thr	12	-0.482	0.042	<0.0001	12	0.104	0.059	0.2133
Trp	24	-0.039	0.008	<0.0001	---	---	---	---
Tyr	24	-0.057	0.005	<0.0001	---	---	---	---
Val	24	-0.166	0.054	0.0305	---	---	---	---

[1] Control pigs (n = 16) were treated, i.v., with sterile saline and LPS pigs (n = 15) treated, i.v., with 10 μg/kg BW of *E. coli*-LPS
[2] Time interval used in amino acid balance calculation
[3] Balance calculated from total area under the curve, units= μmole•kg BW^{-1}•h^{-1}
[4] *P*-value calculated from area under the curve
[5] Glu was the only AA to initially be positive and then negative

Table 4.3. Actual (observed) value of selected AA for both trials[1,2,3,4]

	12-h Trial	24-h Trial	
AA	Group 1	Group 1	Group 2
Phe	152.01 ± 4.87	92.01 ± 2.49	116.74 ± 2.56
Lys	225.49 ± 10.90	164.74 ± 7.53	163.25 ± 4.88
Trp	68.23 ± 2.74	26.26 ± 1.00	28.31 ± 1.50
Met	63.30 ± 2.04	29.19 ± 1.09	41.26 ± 1.47
Leu	240.95 ± 77.73	154.47 ± 3.84	164.24 ± 4.24
Ile	117.14 ± 5.57	72.54 ± 2.29	95.81 ± 2.65
Arg	184.09 ± 8.6	130.56 ± 4.95	130.11 ± 3.74
Tyr	127.31 ± 5.05	199.00 ± 6.95	157.95 ± 6.28
Thr	200.88 ± 49.92	73.43 ± 1.59	55.22 ± 1.26

[1]Means of observed AA concentrations, μM, from 12 and 24-h LPS trial

[2]Trial 1, 12-h data only has 1 group as trial was only 12 h

[3]Trial 2, 24-h data was split into 2 groups, Group 1 (t = -2 to 12 h) and Group 2 (t = 14 to 24 h)

[34]Values presented as means ± std err

Table 4.4A. Statistics using prediction equations created from 12-h LPS trial to predict AA levels of 24-h LPS trial[1,2]

	Terms in model	Mean of Predicted		RMSPE[3]		CV[4]		Mean of Residuals		Slope[5,*]		Std err of slope[5]	
		Grp 1	Grp 2	Grp 1	Grp 2	Grp 1	Grp 2	Grp 1	Grp 2	Grp 1	Grp 2	Grp 1	Grp 2
Phe	1	129.61	146.06	55.96	48.36	60.82	41.43	-37.49	-28.67	-0.809	-1.112	0.075	0.092
	5	74.44	120.43	85.97	87.76	93.44	75.18	17.81	-1.81	-0.927	-1.118	0.031	0.033
	10	4.55	36.58	127.32	120.07	138.38	102.85	88.69	83.21	-0.934	-1.134	0.031	0.036
	15	13.21	61.15	119.93	94.98	130.34	81.36	78.77	56.96	-0.878	-1.112	0.027	0.044
	20	6.28	43.74	122.7	103.41	133.36	88.58	85.59	74.22	-0.892	-1.159	0.032	0.054
Lys	1	254.4	268.12	129.4	116.27	78.55	71.22	-90.6	-104.85	0.707	-2.804	0.343	0.47
	5	144.08	179.92	152.98	91.6	92.86	56.11	20.83	-16.36	-0.943	-1.166	0.071	0.071
	10	4.25	149.97	297.18	176.05	180.39	107.84	162.78	16.52	-0.902	-0.961	0.033	0.033
	15	-119.81	26.27	424.73	293.15	257.82	179.57	281.06	139.3	-0.907	-0.968	0.023	0.022
	20	-167.59	-58.67	431.55	322.3	261.96	197.43	322.34	224.18	-0.905	-0.96	0.028	0.029
Trp	1	35.96	27.22	19.58	16.01	74.56	56.55	-9.67	1.06	-0.955	-1.581	0.087	0.29
	5	-83.2	-100.56	127.67	131.63	486.18	464.96	109.69	128.7	-0.957	-0.813	0.015	0.049
	10	-59.79	-58.67	110.54	93.14	420.94	329.00	86.87	87.03	-0.947	-0.814	0.015	0.044
	15	-57.77	-30.42	108.85	67.92	414.51	239.92	84.55	58.21	-0.952	-0.809	0.016	0.04
	20	-52.68	-29.44	104.76	66.86	398.93	236.17	79.03	58.54	-0.947	-0.796	0.017	0.046
Met	1	59.1	63.04	33.4	26.56	114.42	64.37	-29.93	-21.63	-0.646	-1.057	0.136	0.222
	5	49.21	65.26	36.23	34.17	124.12	82.82	-20.21	-23.67	-0.841	-0.822	0.033	0.058
	10	7.58	35.19	65.51	46.15	224.43	111.85	21.16	4.66	-0.908	-0.87	0.016	0.03
	15	15.66	49.17	61.31	43.49	210.04	105.40	12.34	-10.44	-0.906	-0.869	0.016	0.038
	20	14.03	56.4	63.63	45.81	217.99	111.03	13.61	-17.53	-0.905	-0.864	0.017	0.039

[1]Prediction equations generated with PROC REG, described in previous chapter and were tested on the data generated in the 24-h LPS trial

[2]Trial 24 data split into 2 groups, Group 1 (t = -2 to 12 h) and Group 2 (t = 14 to 24 h)

[3]RMSPE = root mean square prediction error

[4]CV = (RMSPE/actual mean) × 100

[5]Slope and standard error of the slope were generated by regressing residual = predicted in PROC REG.

* Slope $P < 0.0001$ for all

Table 4.4B. Statistics using prediction equations created from 12-h LPS trial to predict AA levels of 24-h LPS trial[1,2]

	Terms in model	Mean of Predicted		RMSPE[3]		CV[4]		Mean of Residuals		Slope[5,*]		Std err of slope[5]	
		Grp 1	Grp 2	Grp 1	Grp 2	Grp 1	Grp 2	Grp 1	Grp 2	Grp 1	Grp 2	Grp 1	Grp 2
Leu	1	285	292.65	140.63	136.29	91.04	82.98	-131.18	-128.68	-0.57	-1.24	0.153	0.255
	5	125.72	165.78	127.31	92.5	82.42	56.32	28.78	-1.6	-0.908	-0.901	0.031	0.048
	10	47.86	139.2	256.33	150.49	165.94	91.63	105.04	24.83	-0.933	-0.863	0.016	0.026
	15	4.68	62.21	250.23	174.35	161.99	106.16	145.87	105.7	-0.916	-0.857	0.018	0.031
	20	3.65	51.01	249.86	185.47	161.75	112.93	146.8	117.9	-0.925	-0.864	0.018	0.031
Ile	1	147.36	152.9	81.82	100.01	112.79	104.38	-75.08	-57.12	-0.778	-0.763	0.128	0.22
	5	78.51	102.95	67.97	78.58	93.70	82.02	-5.24	-6.02	-0.914	-0.849	0.035	0.042
	10	15.08	45.07	110.94	75.21	152.94	78.50	58.37	51.74	-0.889	-0.805	0.023	0.038
	15	-1.11	33.62	125.59	105.54	173.13	110.16	73.59	64.31	-0.892	-0.851	0.021	0.034
	20	4.72	38.67	122.52	103.1	168.90	107.61	66.42	60.39	-0.897	-0.85	0.021	0.043
Arg	1	236.95	247.06	128.32	124.33	98.28	95.56	-107.37	-116.39	-0.909	-1.202	0.151	0.168
	5	93.96	123.85	151.64	105.9	116.15	81.39	37.65	10.92	-0.995	-0.965	0.04	0.038
	10	103.73	182.79	179.95	139.8	137.83	107.45	25.17	-50.02	-0.961	-0.951	0.03	0.031
	15	-27.15	73.5	291.25	204.4	223.08	157.10	157.33	57.71	-0.941	-0.947	0.022	0.02
	20	-52.72	28.13	299.56	214.78	229.44	165.08	178.76	102.54	-0.931	-0.946	0.022	0.023
Thr	1	180.82	172.09	97.41	59.29	132.66	107.37	19.46	-14.21	-2.466	0.526	0.404	0.708
	5	120.38	89.79	132.67	85.42	180.68	154.69	80.2	66.03	-1.238	-0.388	0.151	0.146
	10	65.33	75.09	189.09	120.07	257.51	217.44	136.1	78.56	-0.901	-0.691	0.069	0.045
	15	31.35	47.29	224.97	135.51	306.37	245.40	171.47	107.69	-0.959	-0.64	0.067	0.052
	20	25.48	41.88	230.4	137.36	313.77	248.75	177.94	113.13	-0.959	-0.601	0.067	0.058
Tyr	1	149.06	154.23	80.51	100.01	40.46	63.32	-75.94	-98.79	-1.016	-0.9	0.096	0.112
	5	113.13	103.67	72.91	78.58	36.64	49.75	-39.02	-46.86	-0.961	-1.022	0.029	0.024
	10	41.67	54.99	119.5	75.21	60.05	47.62	31.55	0.18	-0.978	-1.002	0.015	0.02
	15	-3.75	-7.92	134.03	105.54	67.35	66.82	76.68	62.7	-0.971	-0.997	0.016	0.018
	20	-2.02	-7.84	129.92	103.1	65.29	65.27	74.36	63.68	-0.978	-0.994	0.017	0.02

[1]Prediction equations generated with PROC REG, described in previous chapter and were tested on the data generated in the 24-h LPS trial

[2]Trial 24 data split into 2 groups, Group 1 (t = -2 to 12 h) and Group 2 (t = 14 to 24 h)

[3]RMSPE = root mean square prediction error

[4]CV = (RMSPE/actual mean) × 100

[5]Slope and standard error of the slope were generated by regressing residual = predicted in PROC REG.

* Slope $P < 0.0001$ for all

Table 4.5A. Statistics using prediction equations created from 12-h LPS trial to predict AA levels of 12-h LPS trial[1]

	Terms in model	Mean of Pred values	RMSPE[2]	CV[3]	Mean of residuals	Slope[4]	Std err of slope[4]	P-value[4]
Phe	1	162.221	40.718	26.79	-10.151	-0.357	0.242	0.1446
	5	161.677	32.119	21.13	-7.618	-0.132	0.115	0.2578
	10	155.598	24.129	15.87	1.37	-0.141	0.083	0.099
	15	157.082	26.06	17.14	2.265	-0.211	0.082	0.0142
	20	161.855	16.535	10.88	0.005	-1.2E-05	0.07	0.9999
Lys	1	250.334	95.641	42.41	-25.715	-0.496	0.383	0.1996
	5	244.611	91.723	40.68	-18.107	-0.495	0.12	0.0001
	10	268.083	116.009	51.45	-36.644	-0.591	0.087	<0.0001
	15	247.622	100.176	44.43	-16.182	-0.518	0.079	<0.0001
	20	249.888	44.474	19.72	0.005	-7.5E-06	0.091	0.9999
Trp	1	67.443	23.038	33.77	0.787	-0.486	0.273	0.0796
	5	62.827	32.028	46.94	3.907	-0.694	0.076	<0.0001
	10	64.66	29.209	42.81	2.02	-0.592	0.081	<0.0001
	15	63.682	27.487	40.29	2.956	-0.545	0.083	<0.0001
	20	87.449	23.074	33.82	-19.526	-0.063	0.079	<0.0001
Met	1	66.921	17.994	28.43	-3.617	-0.872	0.446	0.0546
	5	67.91	18.212	28.77	-5.28	-0.524	0.162	0.002
	10	66.992	19.238	30.39	-2.769	-0.546	0.115	<0.0001
	15	65.378	16.555	26.15	-0.428	-0.415	0.129	<0.0001
	20	66.904	10.633	16.80	-0.003	-9.1E-05	0.132	0.9999

[1]Prediction equations generated with PROC REG, described in previous chapter and were tested on the data generated in the 12-h LPS trial

[2]RMSPE = root mean square prediction error

[3]CV = (RMSPE/actual mean) × 100

[4]Slope, standard error of the slope, and p-value associated with the slope were generated by regressing residual = predicted in PROC REG.

Table 4.5B. Statistics using prediction equations created from 12-h LPS trial to predict AA levels of 12-h LPS trial[1]

	Terms in model	Mean of Pred values	RMSPE[2]	CV[3]	Mean of residuals	Slope[4]	Std err of slope[4]	P-value[4]
Leu	1	260.116	80.668	33.48	-19.406	-0.534	0.247	0.0337
	5	264.05	85.39	35.44	-23.625	-0.577	0.11	<0.0001
	10	269.611	95.935	39.82	-20.921	-0.672	0.099	<0.0001
	15	258.212	46.52	19.31	2.999	-0.078	0.104	0.4597
	20	265.387	45.565	18.91	0.02	0.000006	0.114	1.000
Ile	1	129.302	48.782	41.64	-12.201	-0.496	0.203	0.0173
	5	125.697	43.58	37.20	-8.763	-0.407	0.1	0.0001
	10	123.867	51.505	43.97	-3.959	-0.549	0.094	<0.0001
	15	127.761	48.597	41.49	-1.357	-0.495	0.1	<0.0001
	20	135.292	29.09	24.83	-2.151	-0.00073	0.116	0.995
Arg	1	204.013	74.5	40.47	-19.636	-0.467	0.168	0.0069
	5	209.279	76.11	41.34	-26.158	-0.48	0.101	<0.0001
	10	206.318	71.14	38.64	-18.519	-0.425	0.092	<0.0001
	15	220.903	89.204	48.46	-31.56	-0.562	0.096	<0.0001
	20	213.497	42.584	23.13	-2.575	0.0074	0.098	0.9407
Thr	1	205.209	41.562	20.69	-8.036	-0.047	0.204	0.8205
	5	200.75	43.007	21.41	-4.297	-0.388	0.127	0.0033
	10	201.429	45.152	22.48	-1.496	-0.41	0.123	0.0016
	15	203.391	34.641	17.24	-0.613	-0.181	0.123	0.1489
	20	204.968	29.104	14.49	0.004	-5E-06	0.12	1.000
Tyr	1	132.238	45.285	35.57	-5.057	-0.655	0.202	0.0018
	5	133.01	34.19	26.86	-2.798	-0.271	0.107	0.014
	10	134.728	43.351	34.05	-4.037	-0.493	0.092	<0.0001
	15	128.783	41.598	32.67	2.086	-0.458	0.086	<0.0001
	20	135.806	20.496	16.10	0.008	8.3E-06	0.077	<0.0001

[1]Prediction equations generated with PROC REG, described in previous chapter and were tested on the data generated in the 12-h LPS trial

[2]RMSPE = root mean square prediction error

[3]CV = (RMSPE/actual mean) × 100

[4]Slope, standard error of the slope, and p-value associated with the slope were generated by regressing residual = predicted in PROC REG.

4.7. Figures

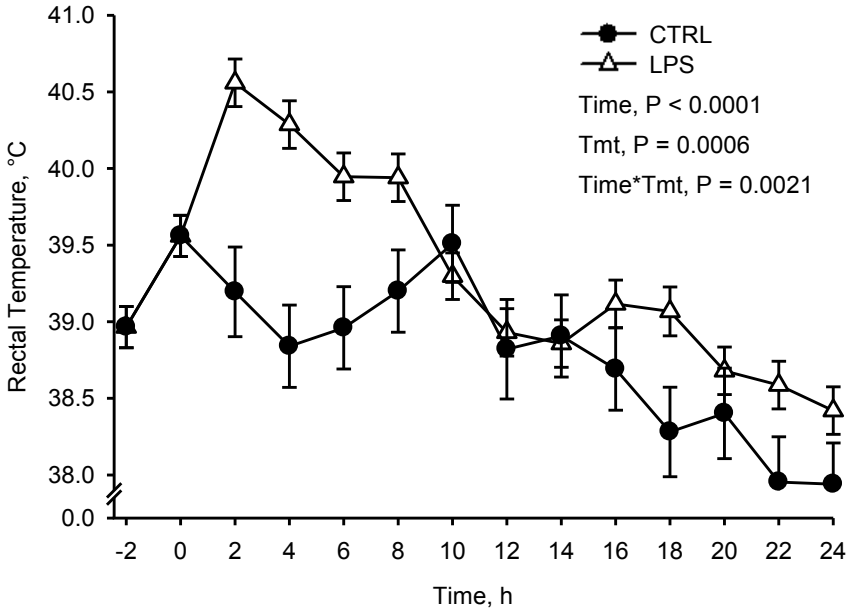

Figure 4.1. Changes in rectal temperature in sterile saline (n = 16) or *E. coli* lipopolysaccharide (LPS, 10 µg/kg BW) treated pigs (n = 15). Pigs were food-deprived overnight and fed at t = -2, and treated with saline or LPS at t = 0. Values are LSMEANS ± SEM.

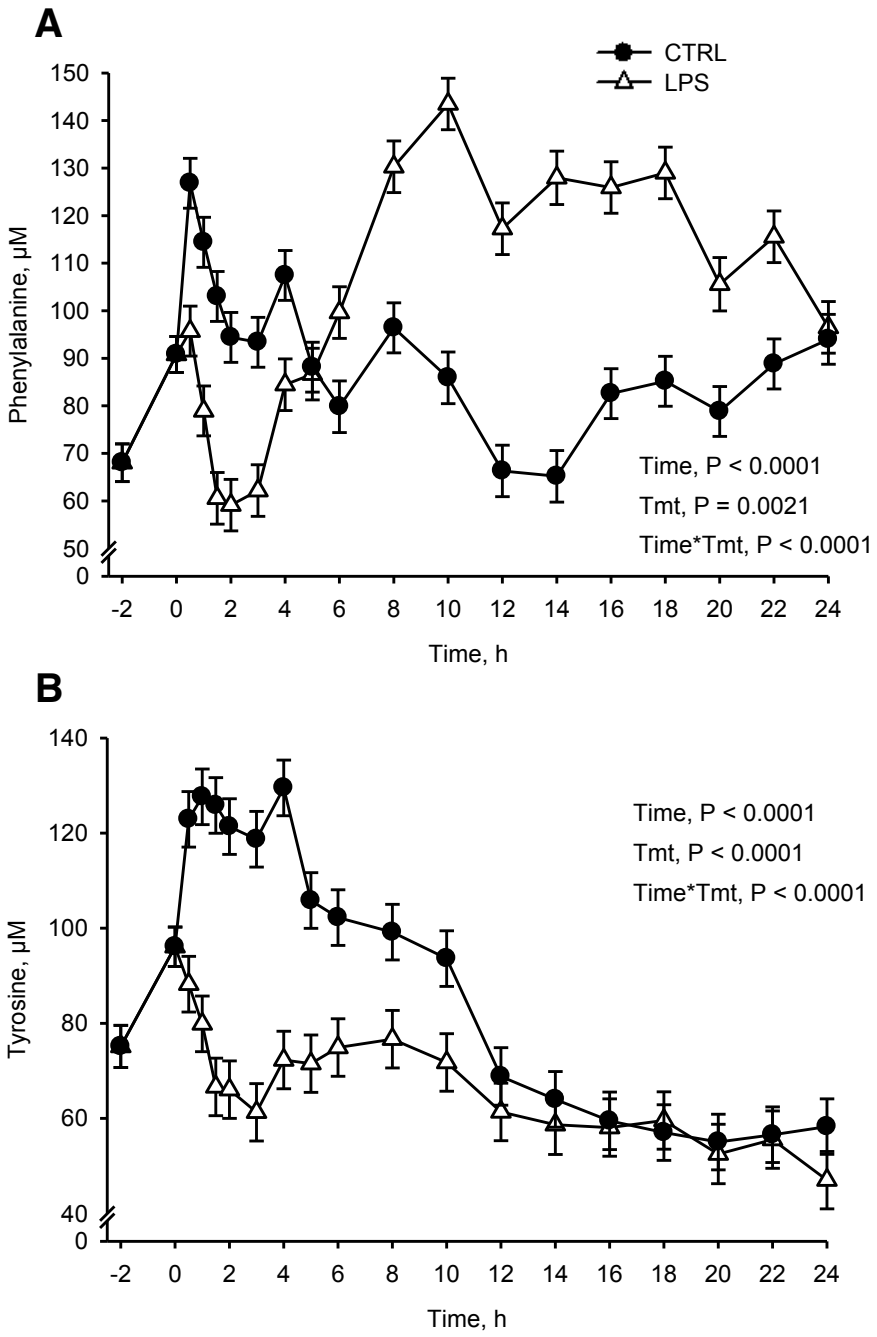

Figure 4.2. Changes in plasma phenylalanine (A) and tyrosine (B) levels in sterile saline (n = 16) or *E. coli* lipopolysaccharide (LPS, 10 µg/kg BW) treated pigs (n = 15). Pigs were food-deprived overnight and fed at t = -2, and treated with saline or LPS at t = 0. Values are LSMEANS ± SEM.

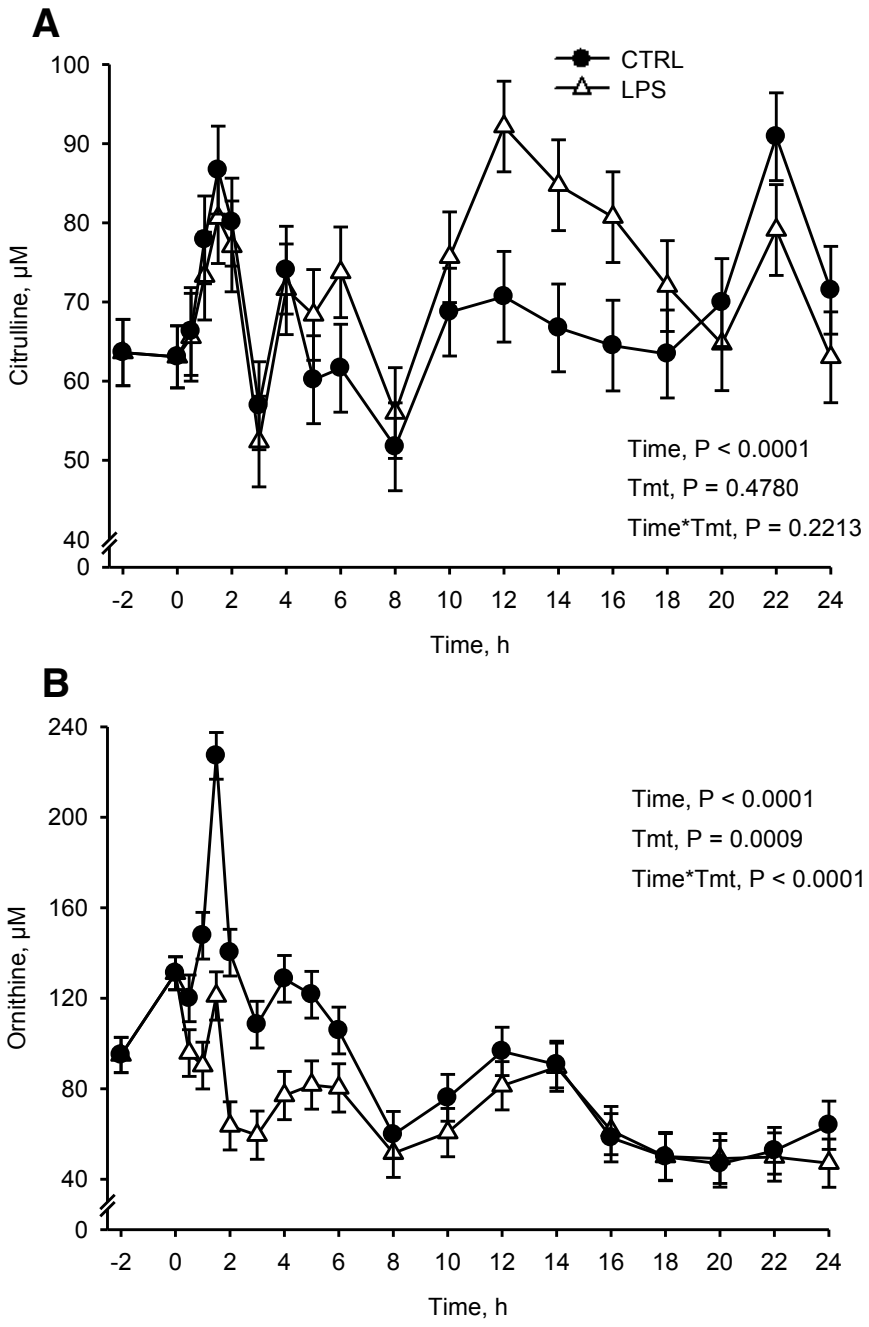

Figure 4.3. Changes in plasma citrulline (A) and ornithine (B) levels in sterile saline (n = 16) or *E. coli* lipopolysaccharide (LPS, 10 μg/kg BW) treated pigs (n = 15). Pigs were food-deprived overnight and fed at t = -2, and treated with saline or LPS at t = 0. Values are LSMEANS ± SEM.

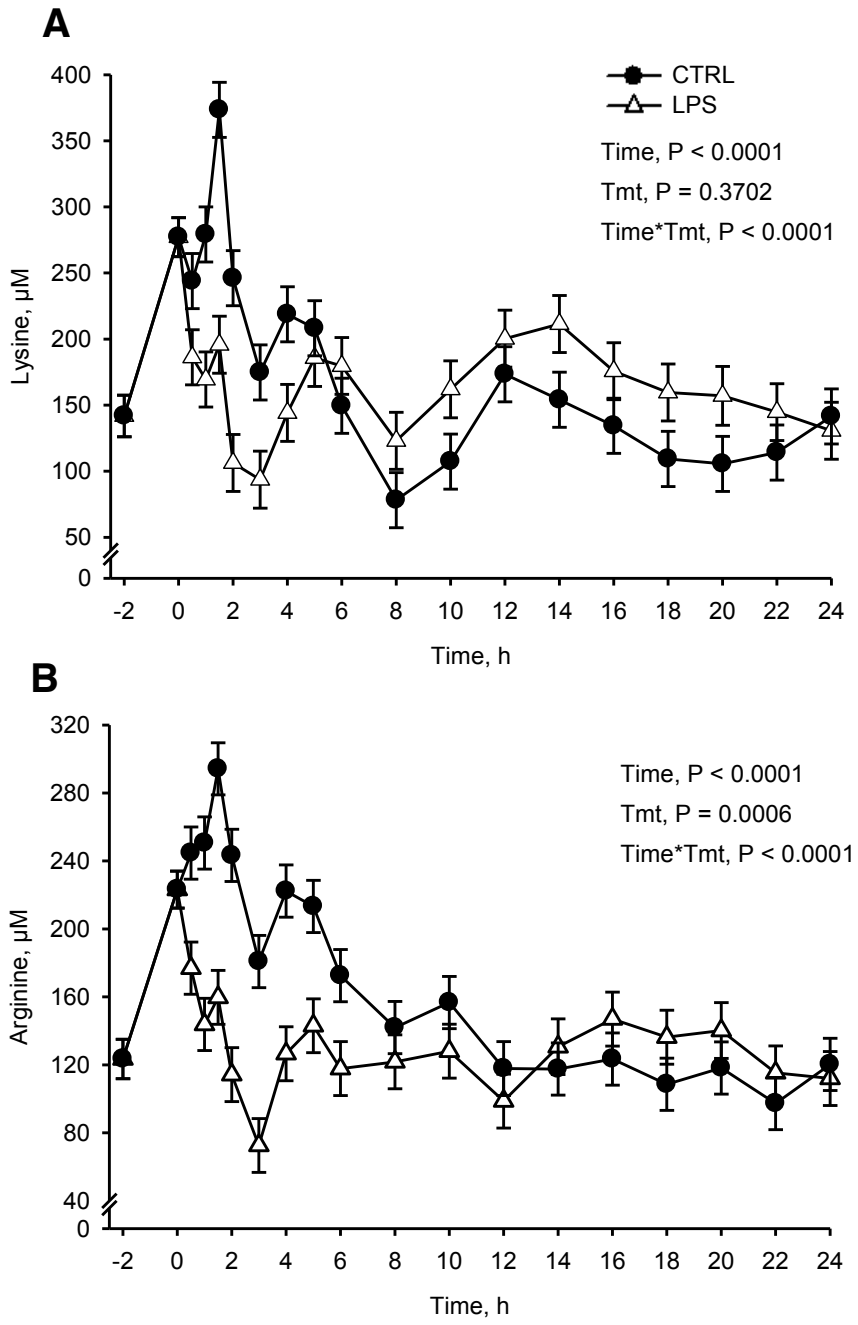

Figure 4.4. Changes in plasma lysine (A) and arginine (B) levels in sterile saline (n = 16) or *E. coli* lipopolysaccharide (LPS, 10 µg/kg BW) treated pigs (n = 15). Pigs were food-deprived overnight and fed at t = -2, and treated with saline or LPS at t = 0. Values are LSMEANS ± SEM.

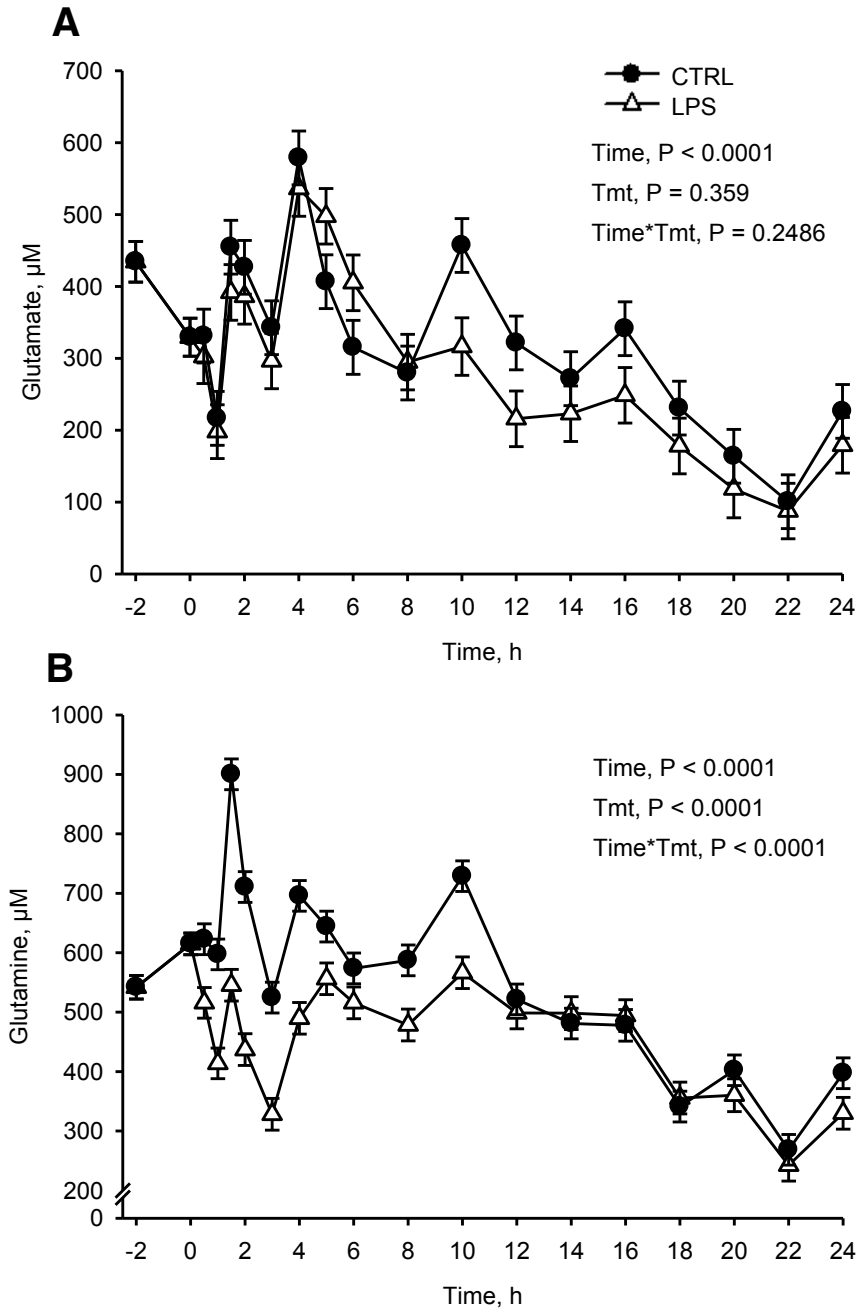

Figure 4.5. Changes in plasma glutamate (A) and glutamine (B) levels in sterile saline (n = 16) or *E. coli* lipopolysaccharide (LPS, 10 µg/kg BW) treated pigs (n = 15). Pigs were food-deprived overnight and fed at t = -2, and treated with saline or LPS at t = 0. Values are LSMEANS ± SEM.

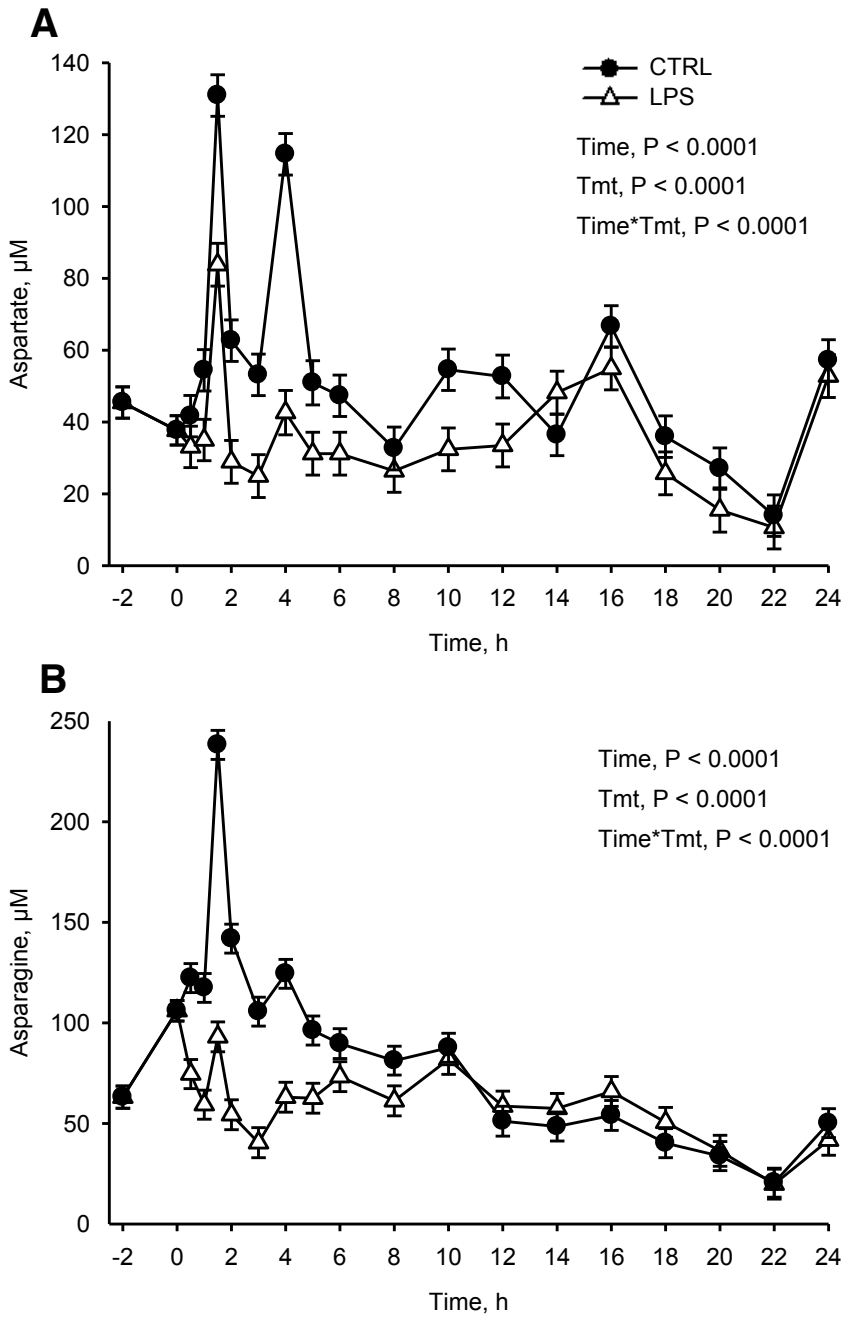

Figure 4.6. Changes in plasma aspartate (A) and asparagine (B) levels in sterile saline (n = 16) or *E. coli* lipopolysaccharide (LPS, 10 µg/kg BW) treated pigs (n = 15). Pigs were food-deprived overnight and fed at t = -2, and treated with saline or LPS at t = 0. Values are LSMEANS ± SEM.

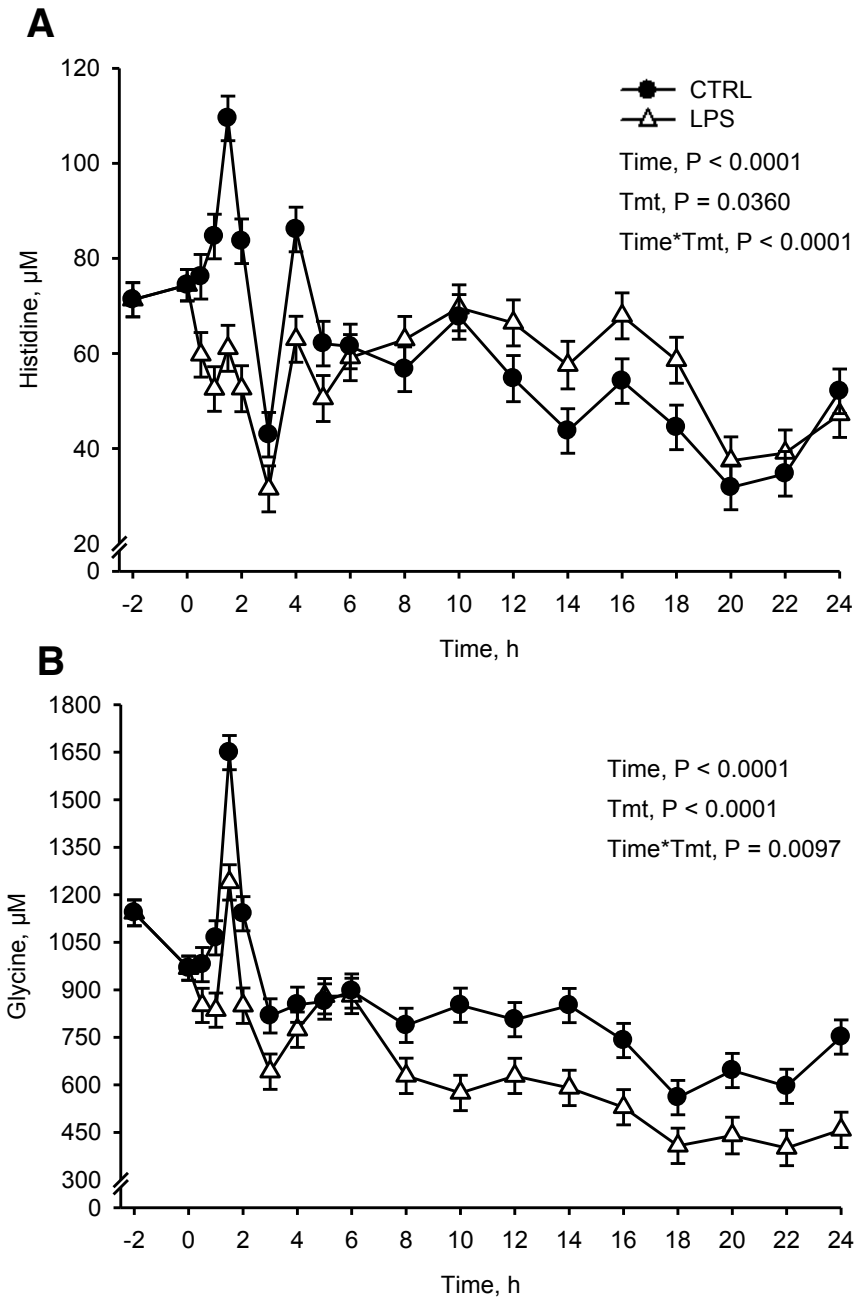

Figure 4.7. Changes in plasma histidine (A) and glycine (B) levels in sterile saline (n = 16) or *E. coli* lipopolysaccharide (LPS, 10 µg/kg BW) treated pigs (n = 15). Pigs were food-deprived overnight and fed at t = -2, and treated with saline or LPS at t = 0. Values are LSMEANS ± SEM.

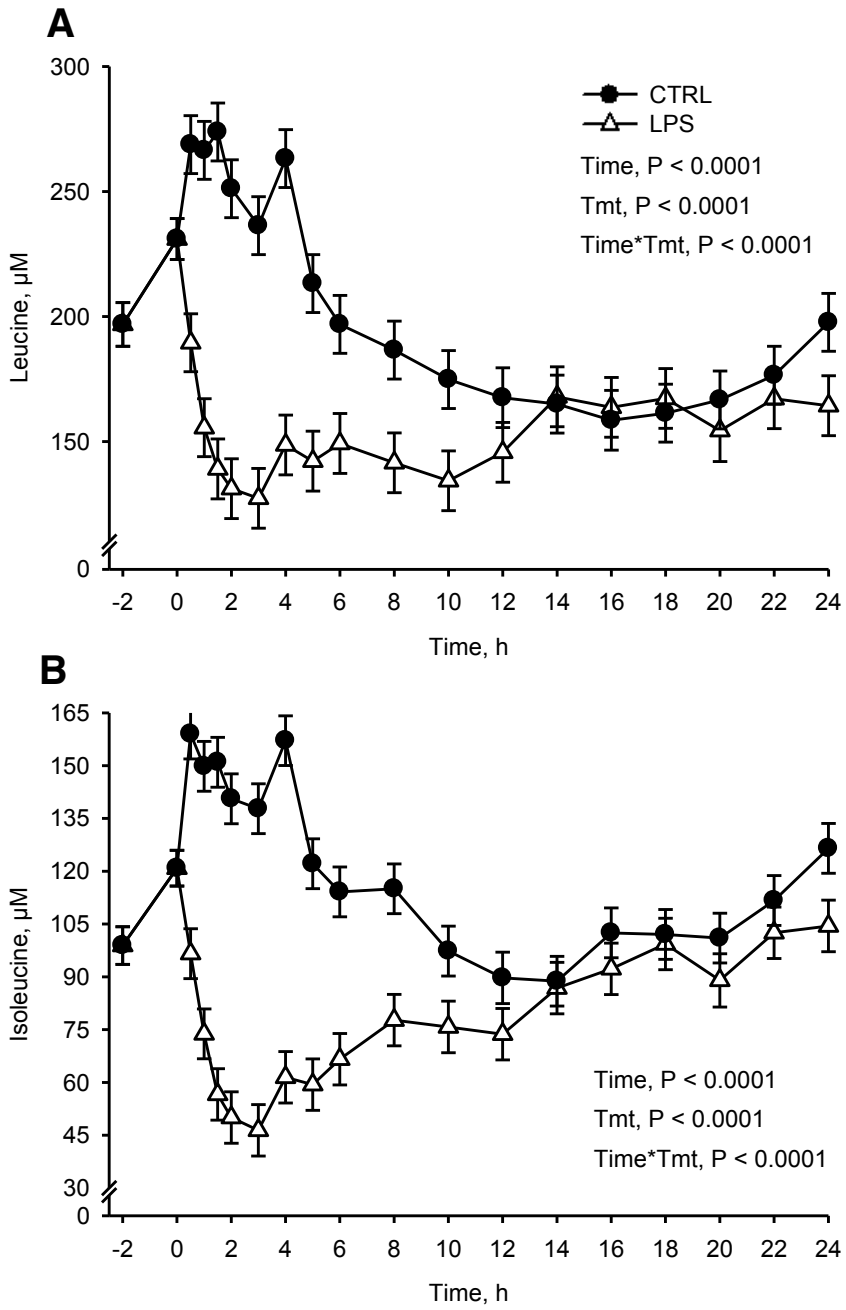

Figure 4.8. Changes in plasma leucine (A) and isoleucine (B) levels in sterile saline (n = 16) or *E. coli* lipopolysaccharide (LPS, 10 µg/kg BW) treated pigs (n = 15). Pigs were food-deprived overnight and fed at t = -2, and treated with saline or LPS at t = 0. Values are LSMEANS ± SEM.

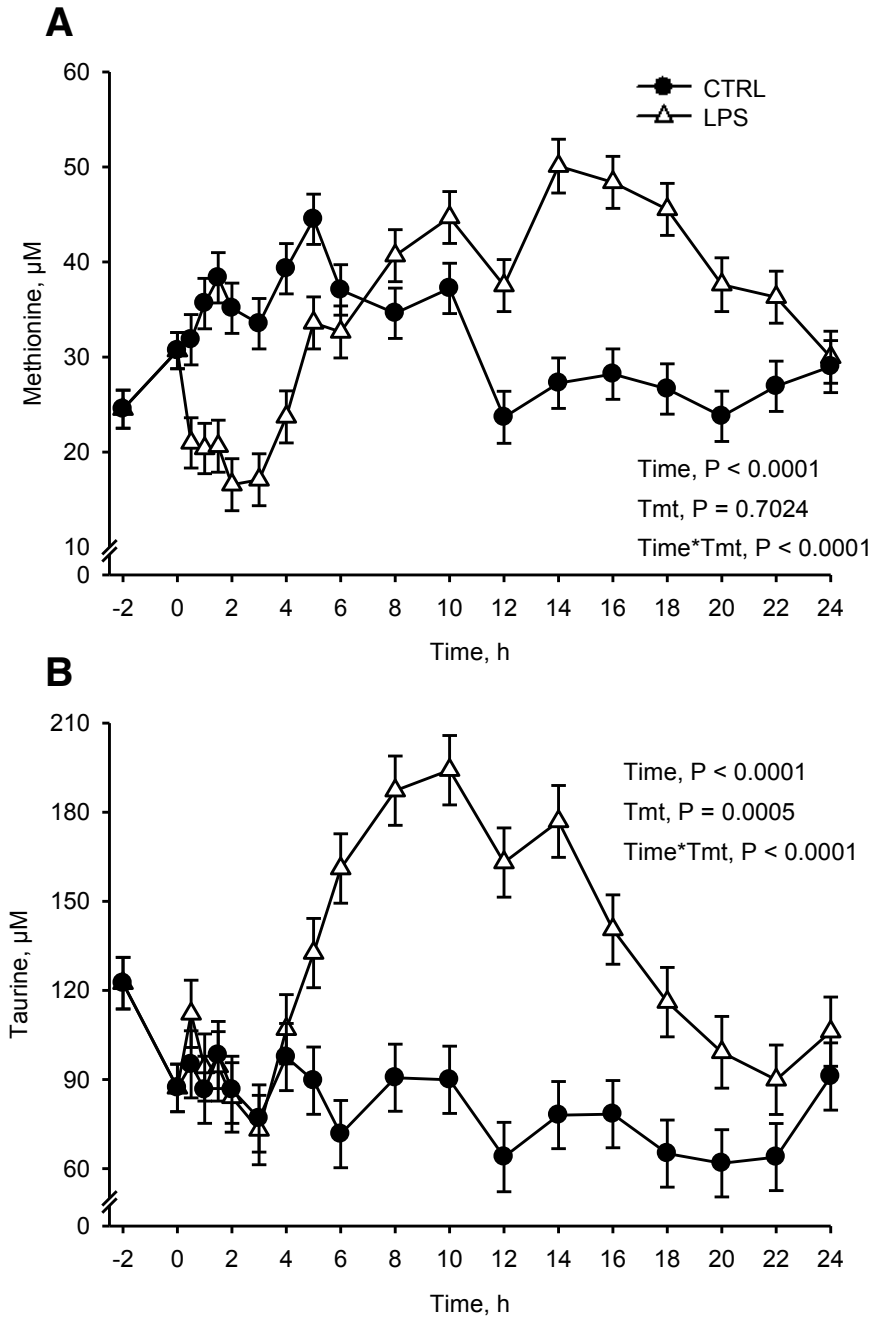

Figure 4.9. Changes in plasma methionine (A) and taurine (B) levels in sterile saline (n = 16) or *E. coli* lipopolysaccharide (LPS, 10 µg/kg BW) treated pigs (n = 15). Pigs were food-deprived overnight and fed at t = -2, and treated with saline or LPS at t = 0. Values are LSMEANS ± SEM.

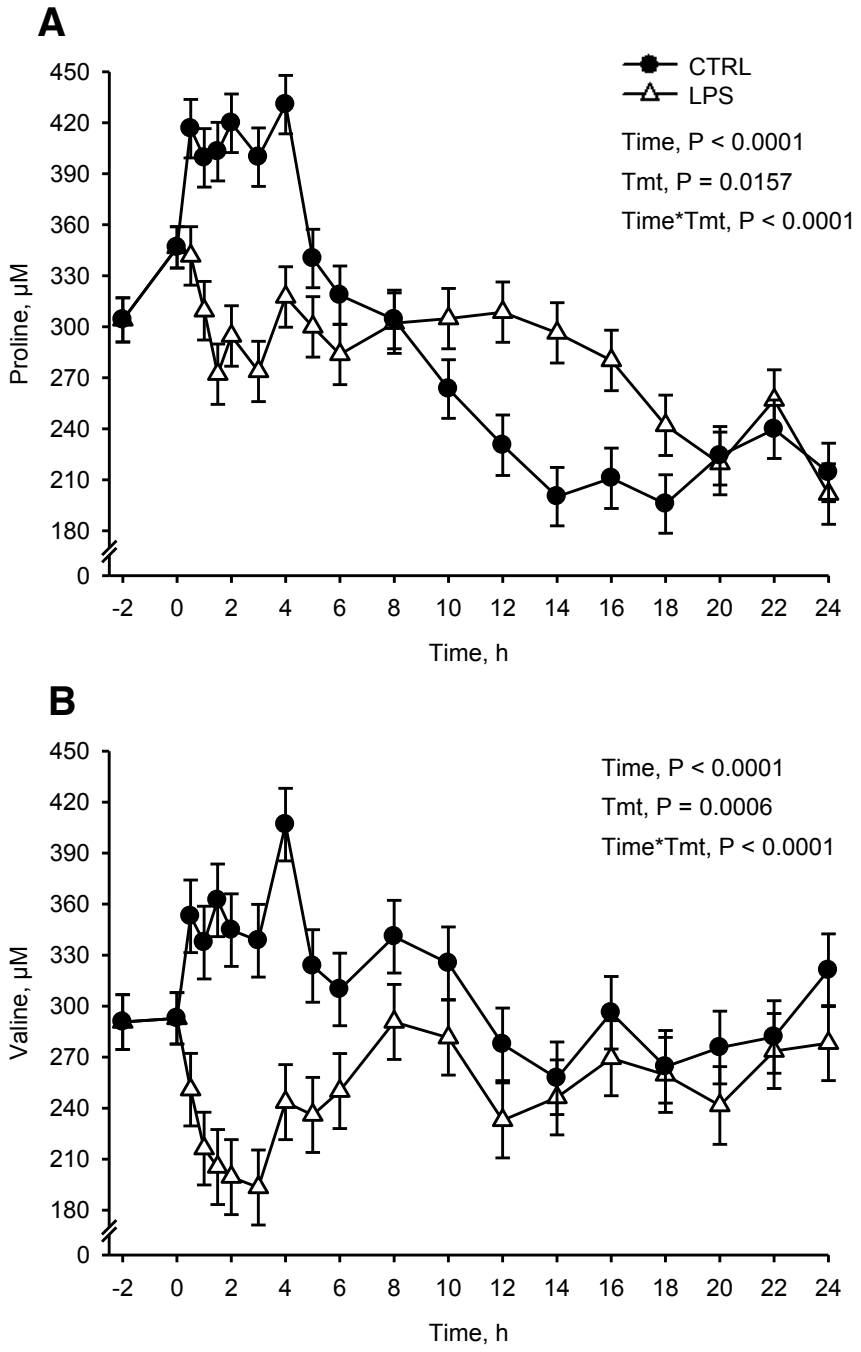

Figure 4.10. Changes in plasma proline (A) and valine (B) levels in sterile saline (n = 16) or *E. coli* lipopolysaccharide (LPS, 10 µg/kg BW) treated pigs (n = 15). Pigs were food-deprived overnight and fed at t = -2, and treated with saline or LPS at t = 0. Values are LSMEANS ± SEM.

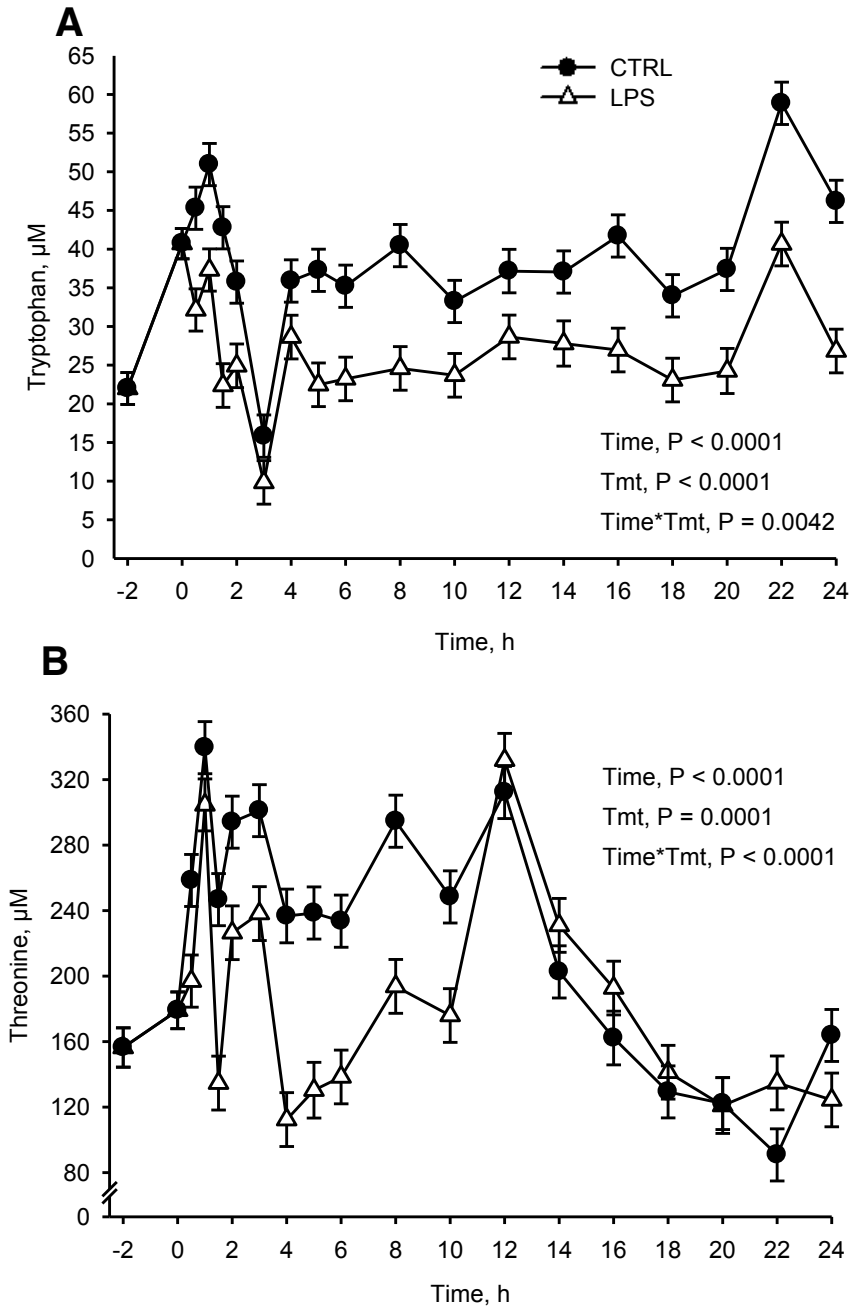

Figure 4.11. Changes in plasma tryptophan (A) and threonine (B) levels in sterile saline (n = 16) or *E. coli* lipopolysaccharide (LPS, 10 µg/kg BW) treated pigs (n = 15). Pigs were food-deprived overnight and fed at t = -2, and treated with saline or LPS at t = 0. Values are LSMEANS ± SEM.

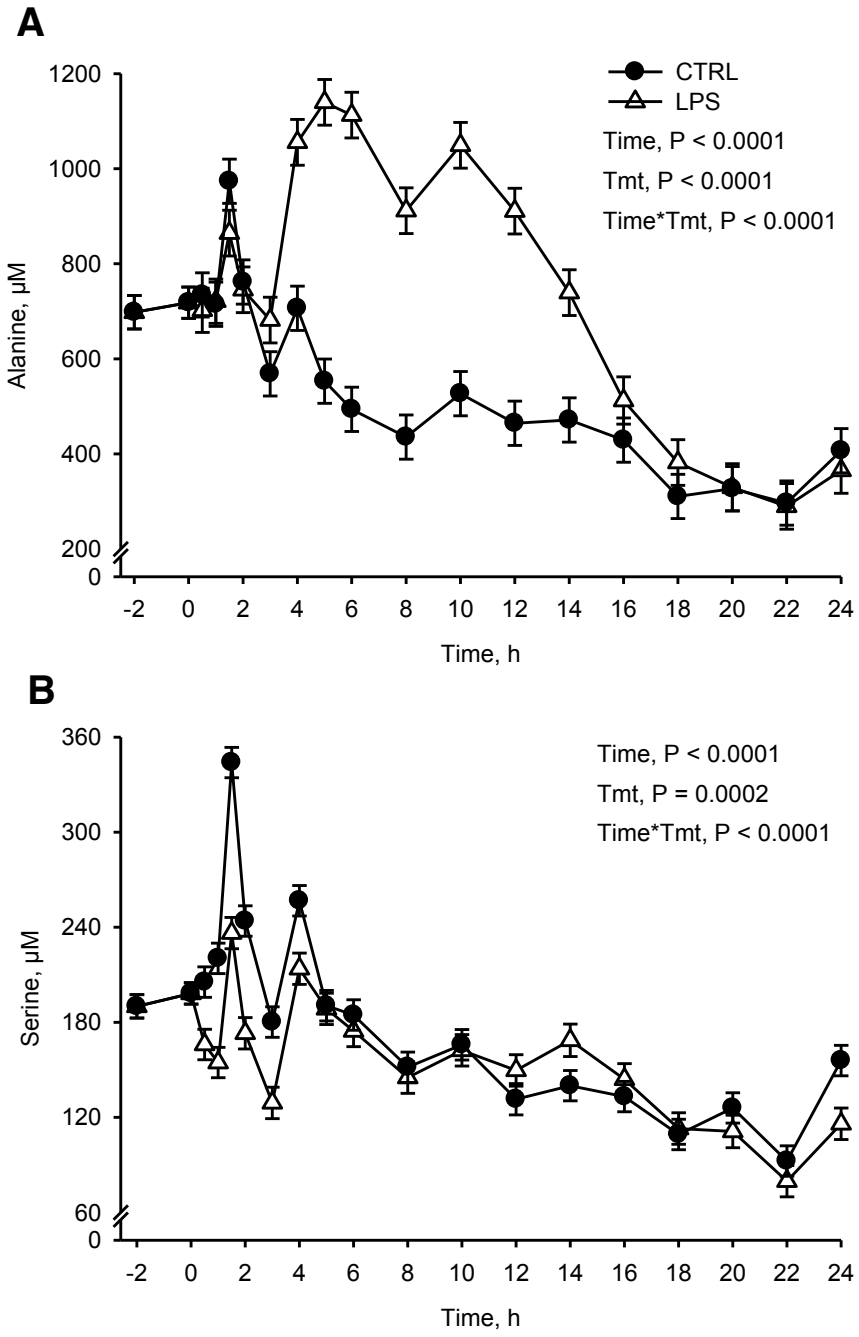

Figure 4.12. Changes in plasma alanine (A) and serine (B) levels in sterile saline (n = 16) or *E. coli* lipopolysaccharide (LPS, 10 µg/kg BW) treated pigs (n = 15). Pigs were food-deprived overnight and fed at t = -2, and treated with saline or LPS at t = 0. Values are LSMEANS ± SEM.

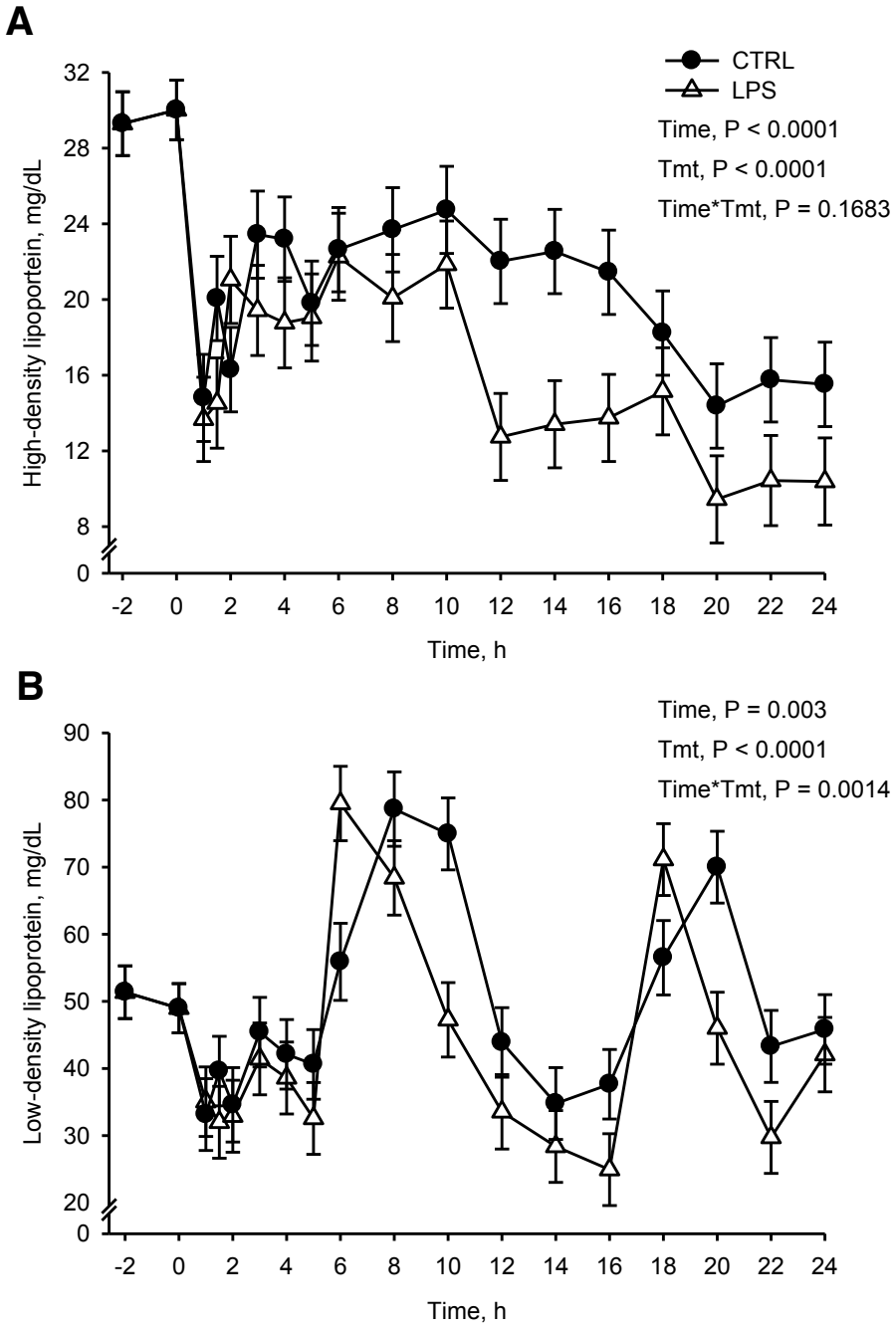

Figure 4.13. Changes in plasma high-density lipoprotein (A) and low-density lipoprotein (B) levels in sterile saline (n = 16) or *E. coli* lipopolysaccharide (LPS, 10 µg/kg BW) treated pigs (n = 15). Pigs were food-deprived overnight and fed at t = -2, and treated with saline or LPS at t = 0. Values are LSMEANS ± SEM.

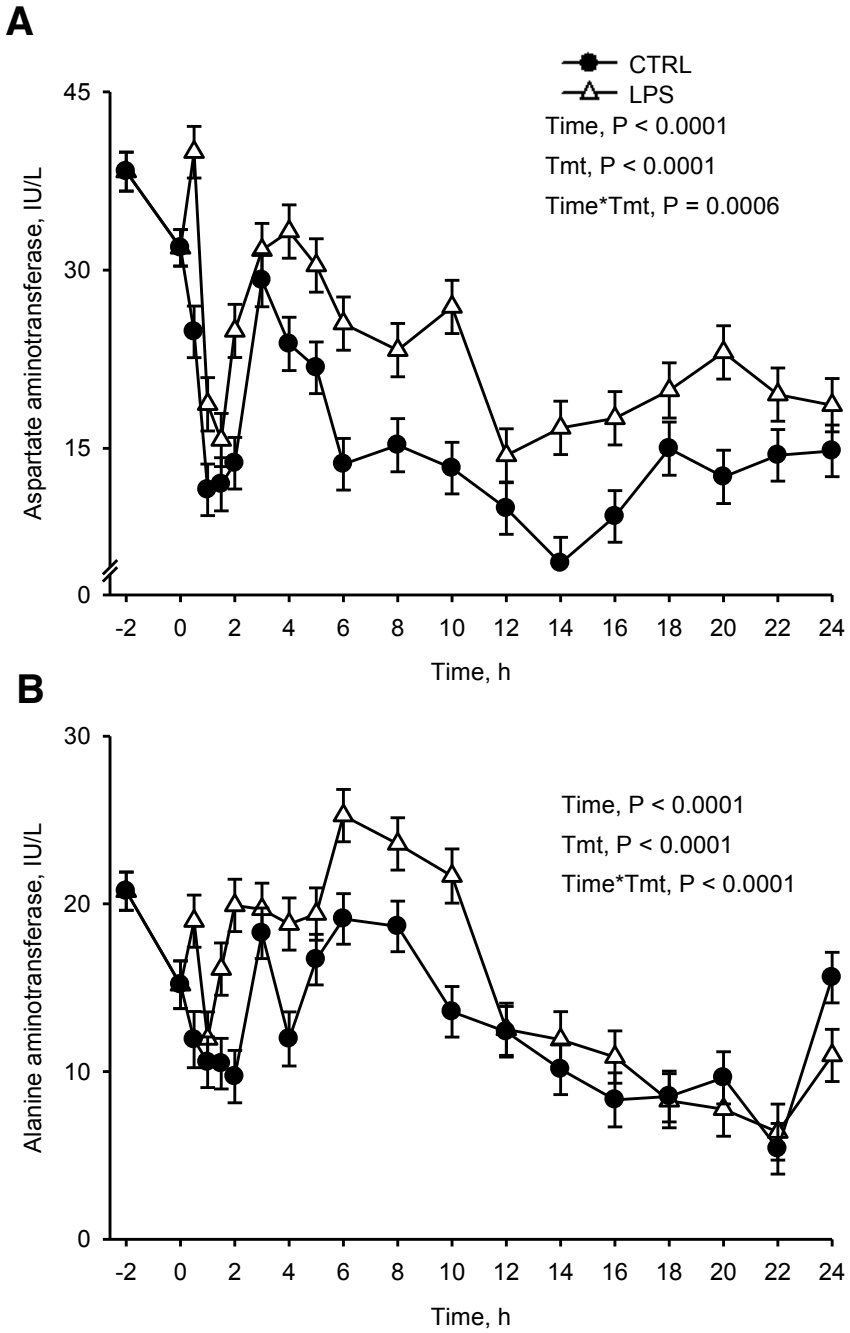

Figure 4.14. Changes in plasma aspartate aminotransferase (A) and alanine aminotransferase (B) levels in sterile saline (n = 16) or *E. coli* lipopolysaccharide (LPS, 10 µg/kg BW) treated pigs (n = 15). Pigs were food-deprived overnight and fed at t = -2, and treated with saline or LPS at t = 0. Values are LSMEANS ± SEM.

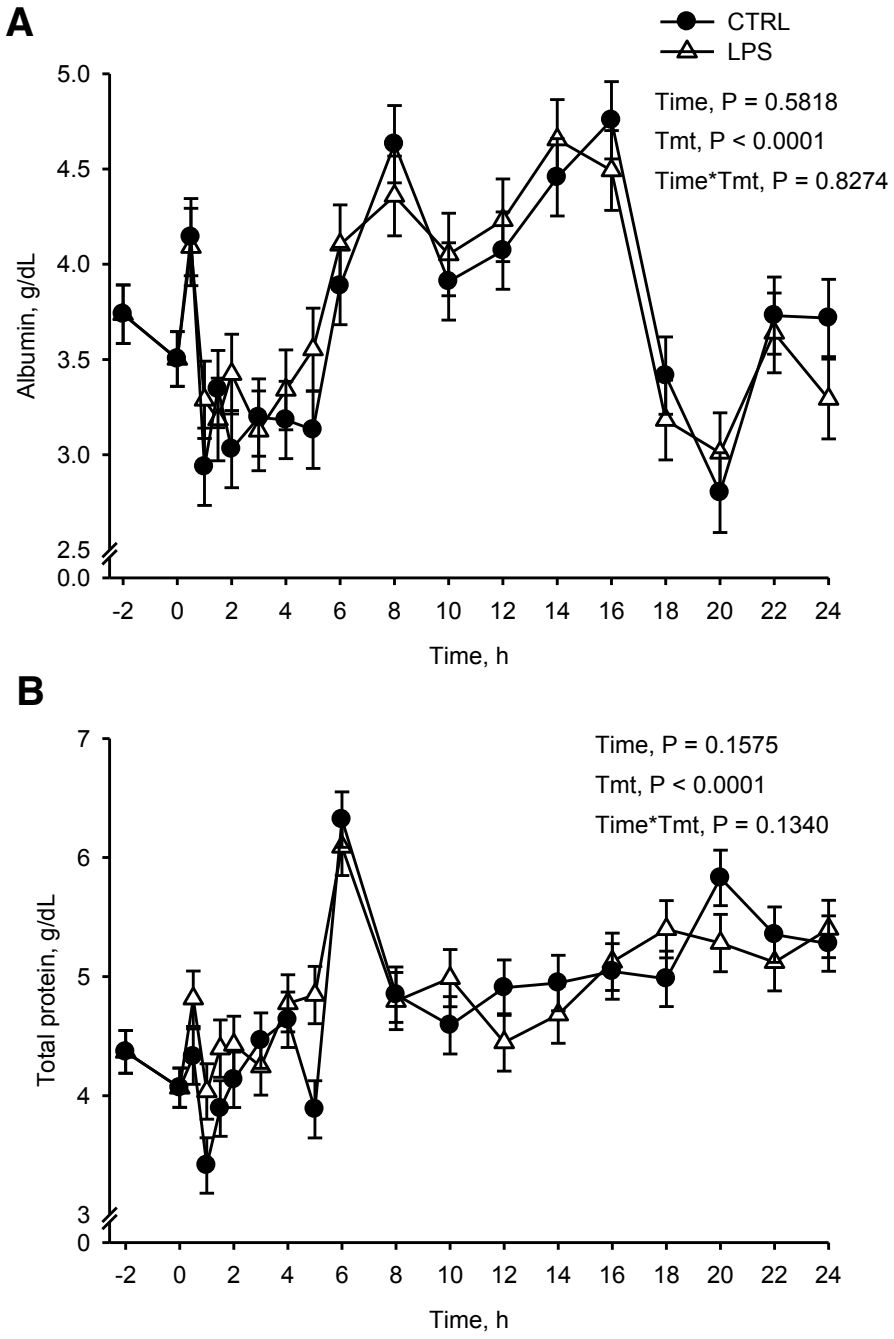

Figure 4.15. Changes in plasma albumin (A) and total protein (B) levels in sterile saline (n = 16) or *E. coli* lipopolysaccharide (LPS, 10 µg/kg BW) treated pigs (n = 15). Pigs were food-deprived overnight and fed at t = -2, and treated with saline or LPS at t = 0. Values are LSMEANS ± SEM.

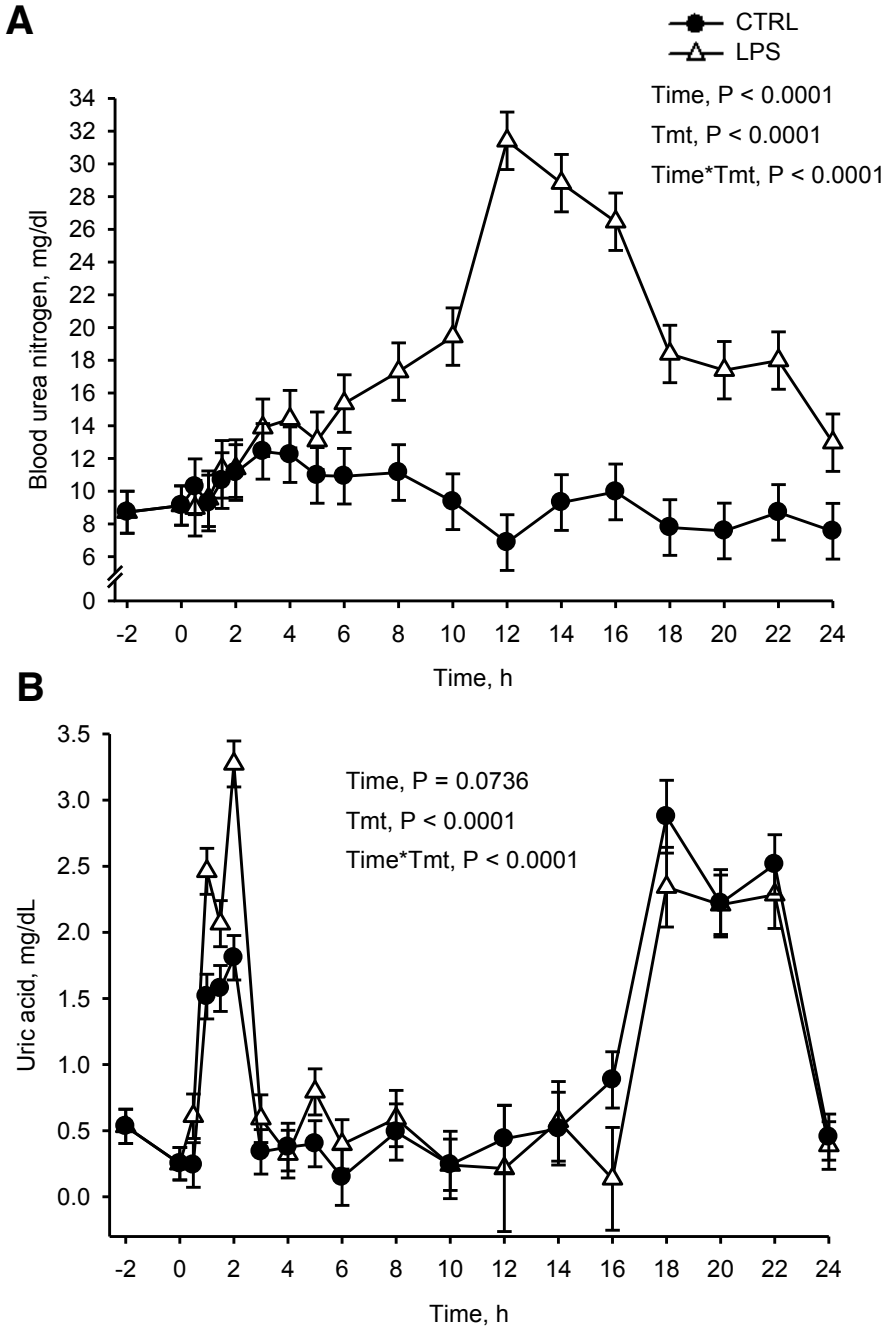

Figure 4.16. Changes in plasma blood urea nitrogen (A) and uric acid (B) levels in sterile saline (n = 16) or *E. coli* lipopolysaccharide (LPS, 10 µg/kg BW) treated pigs (n = 15). Pigs were food-deprived overnight and fed at t = -2, and treated with saline or LPS at t = 0. Values are LSMEANS ± SEM.

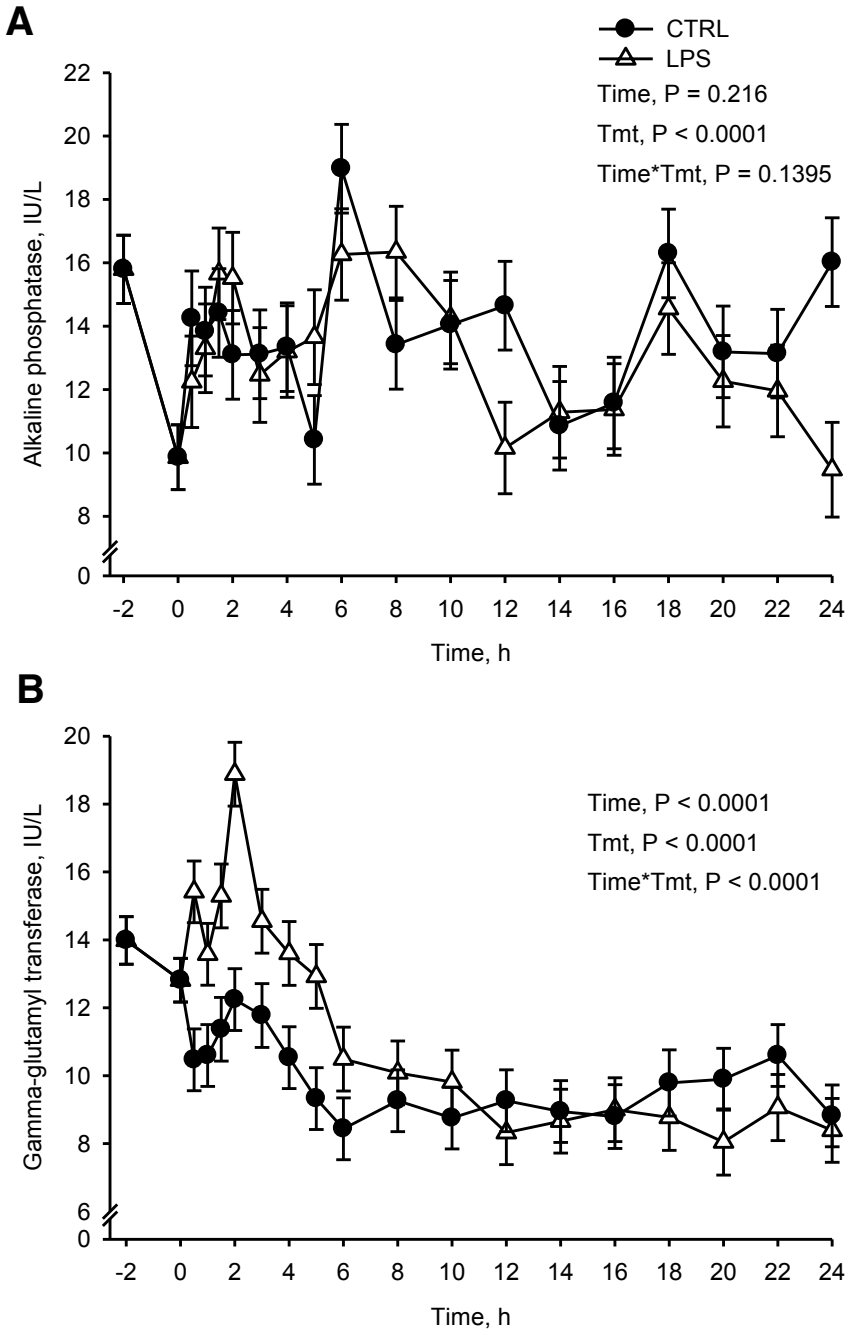

Figure 4.17. Changes in plasma alkaline phosphatase (A) and gamma-glutamyl transferase (B) levels in sterile saline (n = 16) or *E. coli* lipopolysaccharide (LPS, 10 µg/kg BW) treated pigs (n = 15). Pigs were food-deprived overnight and fed at t = -2, and treated with saline or LPS at t = 0. Values are LSMEANS ± SEM.

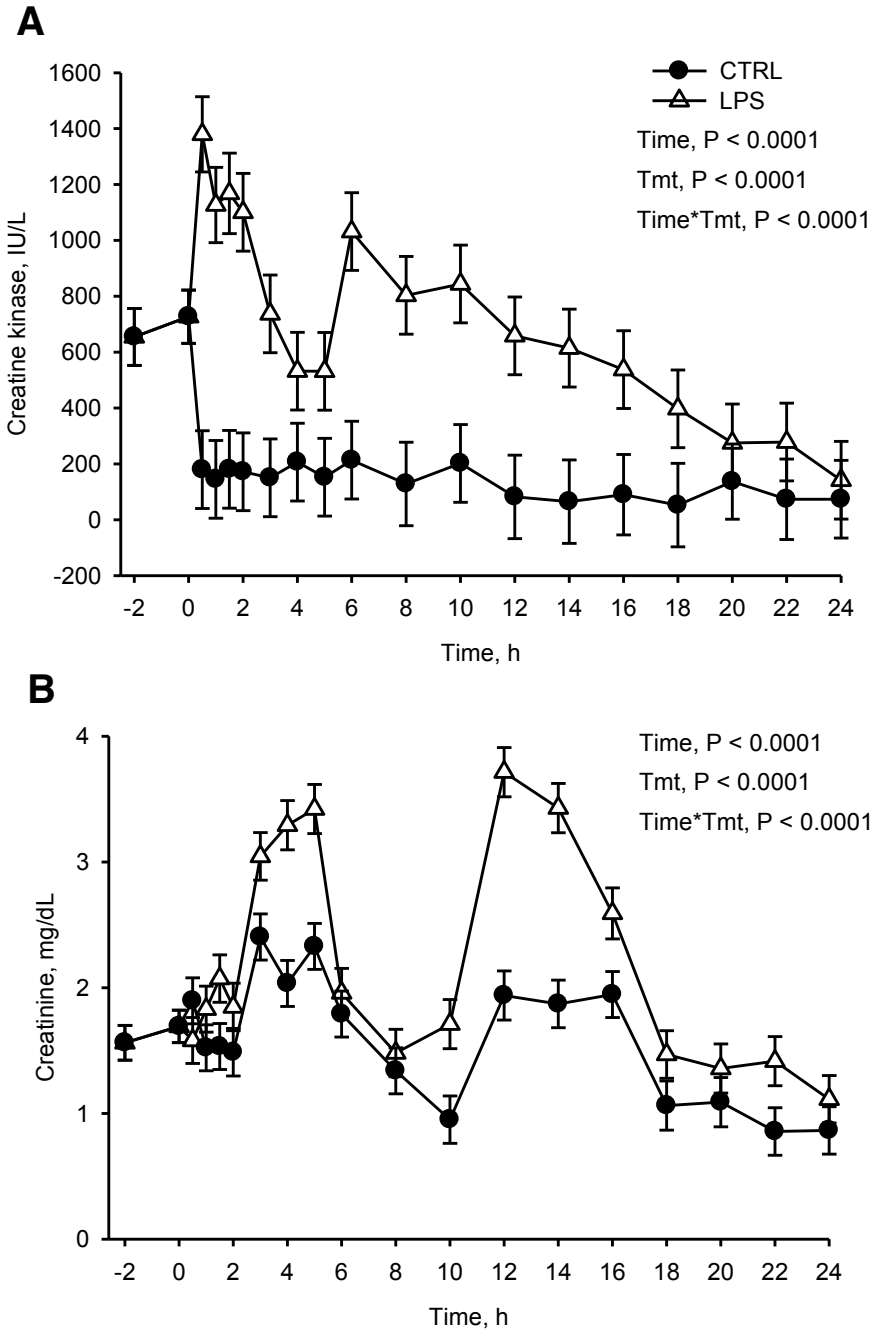

Figure 4.18. Changes in plasma creatine kinase (A) and creatinine (B) levels in sterile saline (n = 16) or *E. coli* lipopolysaccharide (LPS, 10 µg/kg BW) treated pigs (n = 15). Pigs were food-deprived overnight and fed at t = -2, and treated with saline or LPS at t = 0. Values are LSMEANS ± SEM.

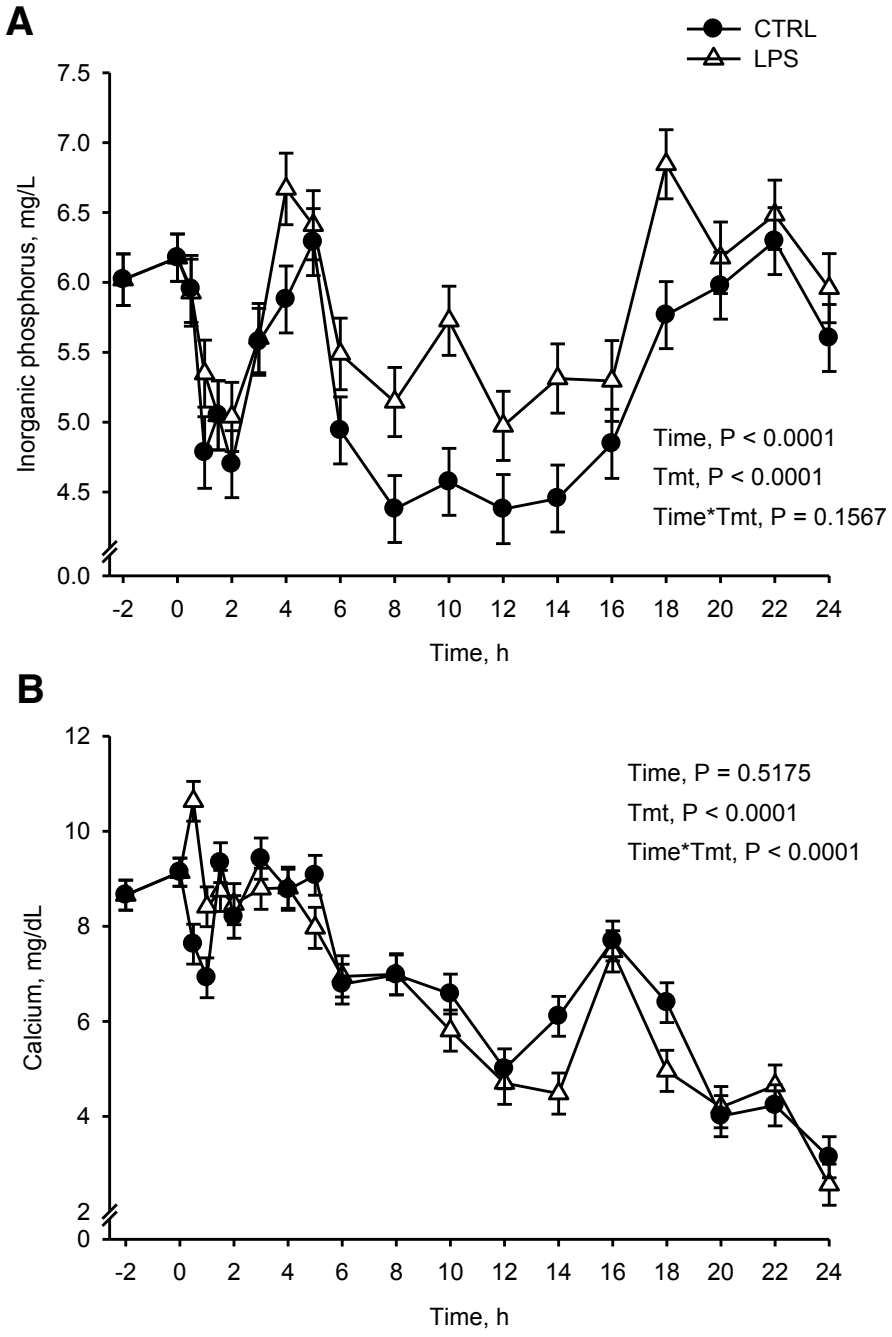

Figure 4.19. Changes in plasma inorganic phosphorus (A) and calcium (B) levels in sterile saline (n = 16) or *E. coli* lipopolysaccharide (LPS, 10 μg/kg BW) treated pigs (n = 15). Pigs were food-deprived overnight and fed at t = -2, and treated with saline or LPS at t = 0. Values are LSMEANS ± SEM.

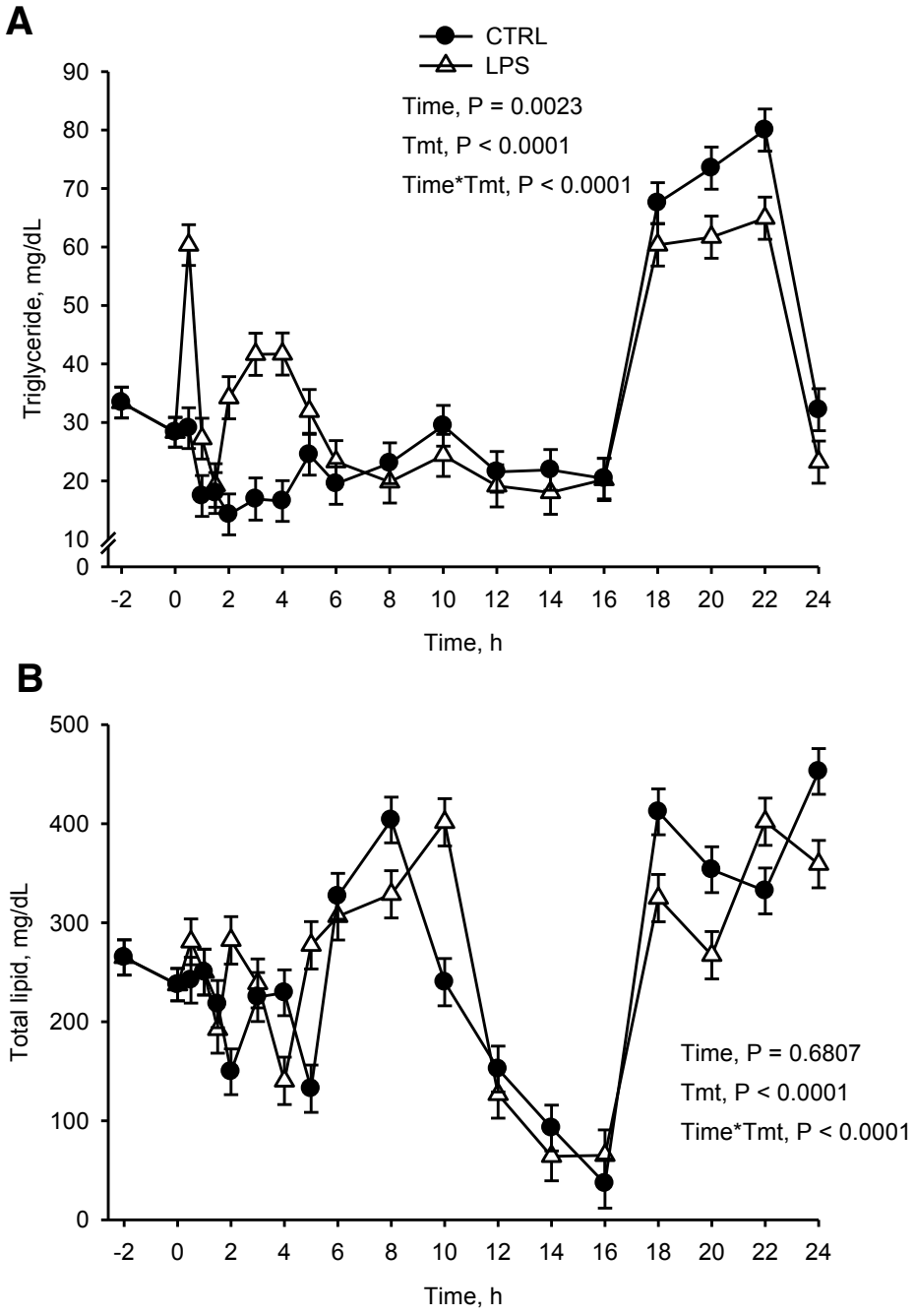

Figure 4.20. Changes in plasma triglyceride (A) and total lipid (B) levels in sterile saline (n = 16) or *E. coli* lipopolysaccharide (LPS, 10 µg/kg BW) treated pigs (n = 15). Pigs were food-deprived overnight and fed at t = -2, and treated with saline or LPS at t = 0. Values are LSMEANS ± SEM.

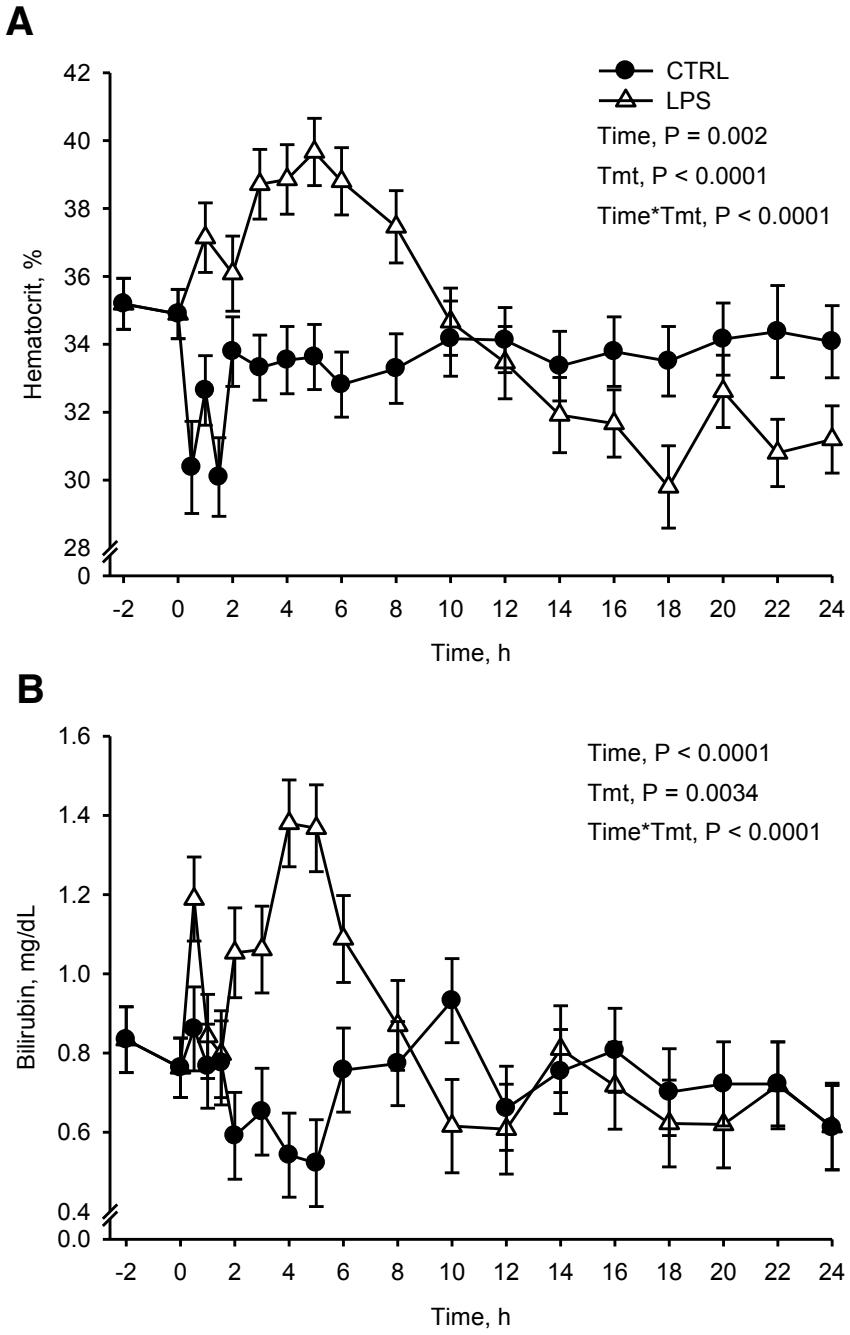

Figure 4.21. Changes in hematocrit (A) and plasma bilirubin (B) levels in sterile saline (n = 16) or *E. coli* lipopolysaccharide (LPS, 10 µg/kg BW) treated pigs (n = 15). Pigs were food-deprived overnight and fed at t = -2, and treated with saline or LPS at t = 0. Values are LSMEANS ± SEM.

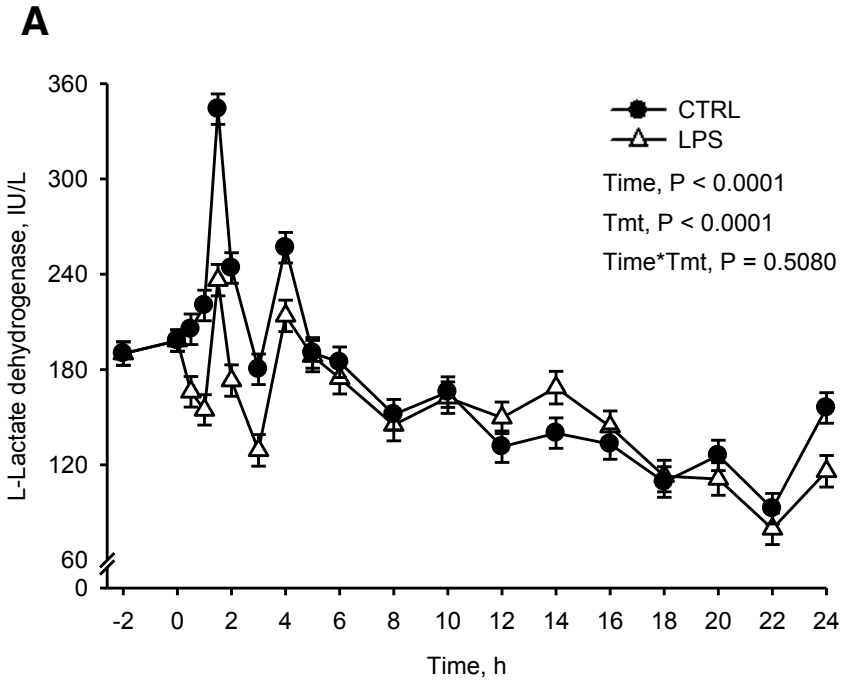

Figure 4.22. Changes in plasma lactate dehydrogenase levels in sterile saline (n = 16) or *E. coli* lipopolysaccharide (LPS, 10 µg/kg BW) treated pigs (n = 15). Pigs were food-deprived overnight and fed at t = -2, and treated with saline or LPS at t = 0. Values are LSMEANS ± SEM.

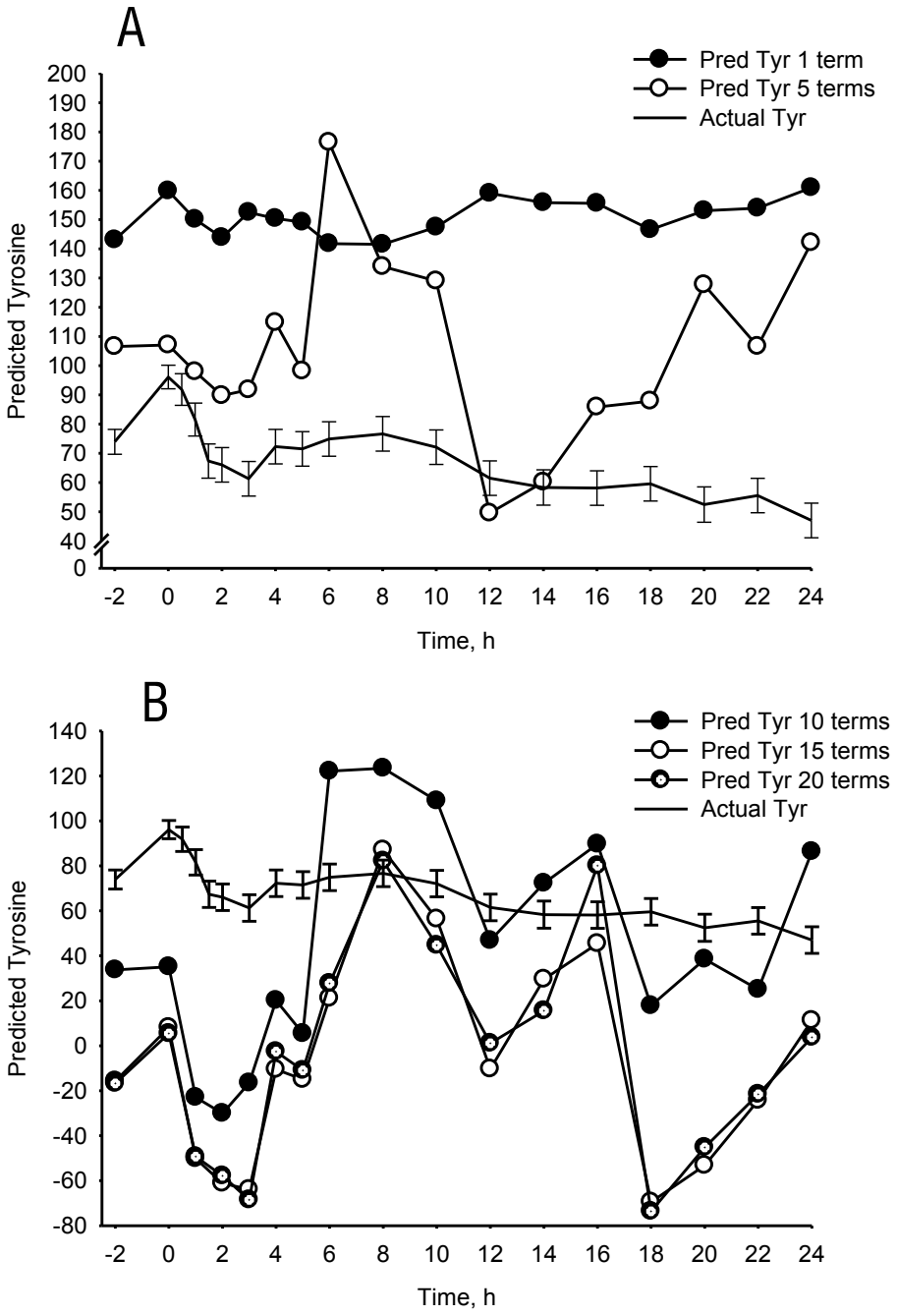

Figure 4.23. Observed versus Predicted plot using 1, 5, 10, 15, or 20 terms in the model to predict plasma tyrosine levels in *E. coli* lipopolysaccharide (LPS, 10 µg/kg BW) treated pigs. Prediction equations were generated using PROC REG from data from the 12-h trial and the equations were used to predict AA changes in pigs monitored post-LPS for 24 h.

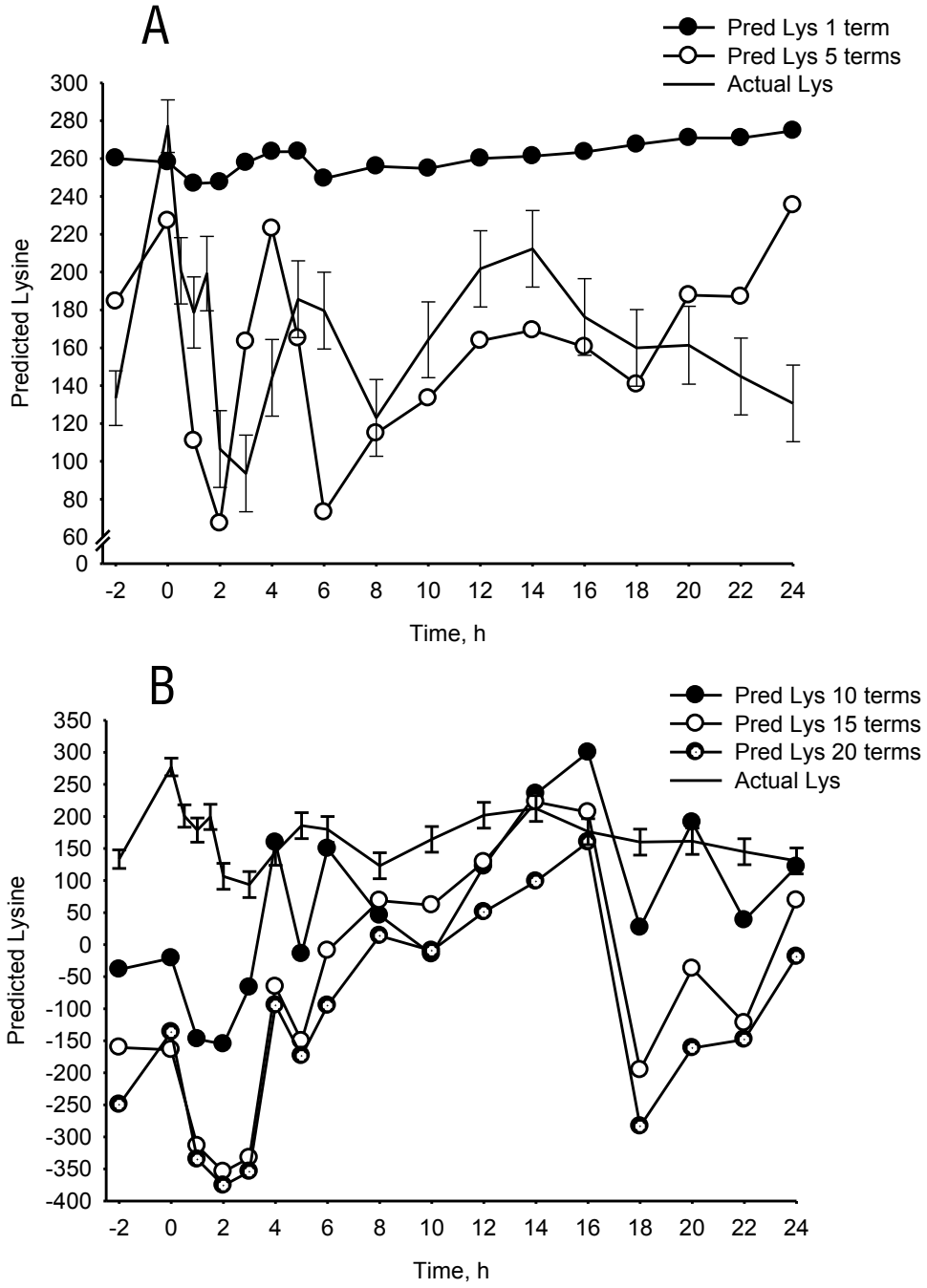

Figure 4.24. Observed versus Predicted plot using 1, 5, 10, 15, or 20 terms in the model to predict plasma lysine levels in *E. coli* lipopolysaccharide (LPS, 10 µg/kg BW) treated pigs. Prediction equations were generated using PROC REG from data from the 12-h trial and the equations were used to predict AA changes in pigs monitored post-LPS for 24 h.

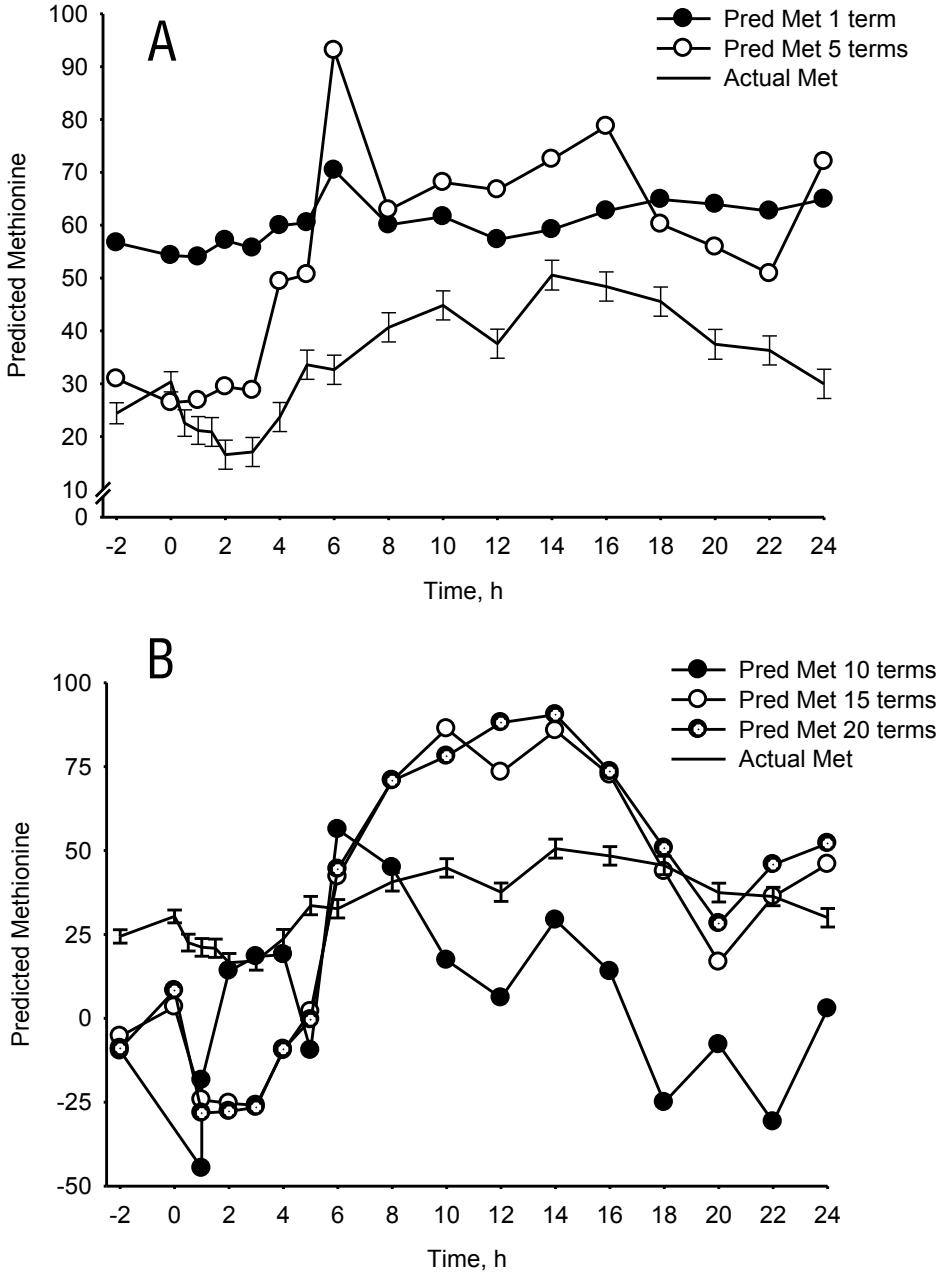

Figure 4.25. Observed versus Predicted plot using 1, 5, 10, 15, or 20 terms in the model to predict plasma methionine levels in *E. coli* lipopolysaccharide (LPS, 10 µg/kg BW) treated pigs. Prediction equations were generated using PROC REG from data from the 12-h trial and the equations were used to predict AA changes in pigs monitored post-LPS for 24 h.

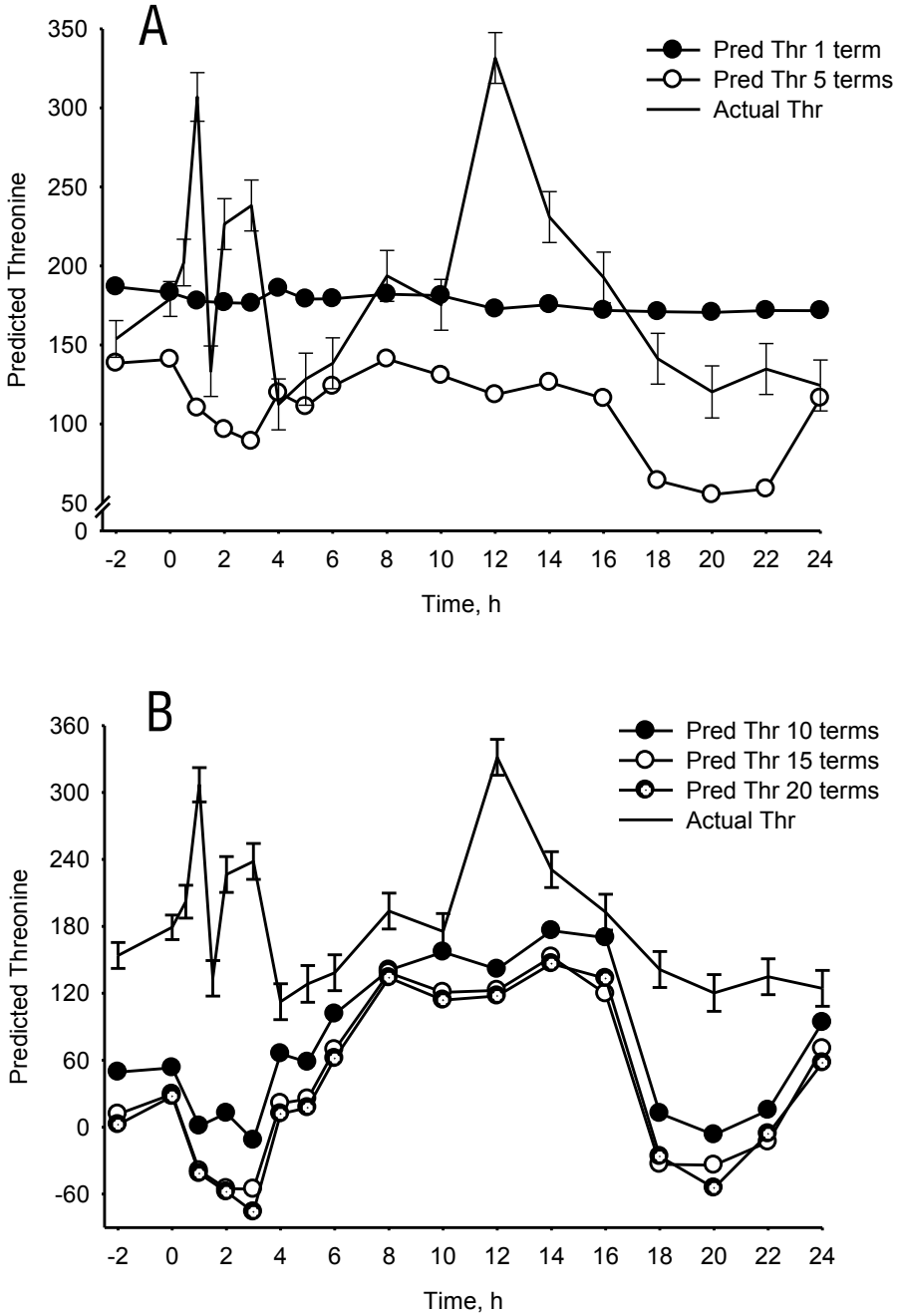

Figure 4.26. Observed versus Predicted plot using 1, 5, 10, 15, or 20 terms in the model to predict plasma threonine levels in *E. coli* lipopolysaccharide (LPS, 10 µg/kg BW) treated pigs. Prediction equations were generated using PROC REG from data from the 12-h trial and the equations were used to predict AA changes in pigs monitored post-LPS for 24 h.

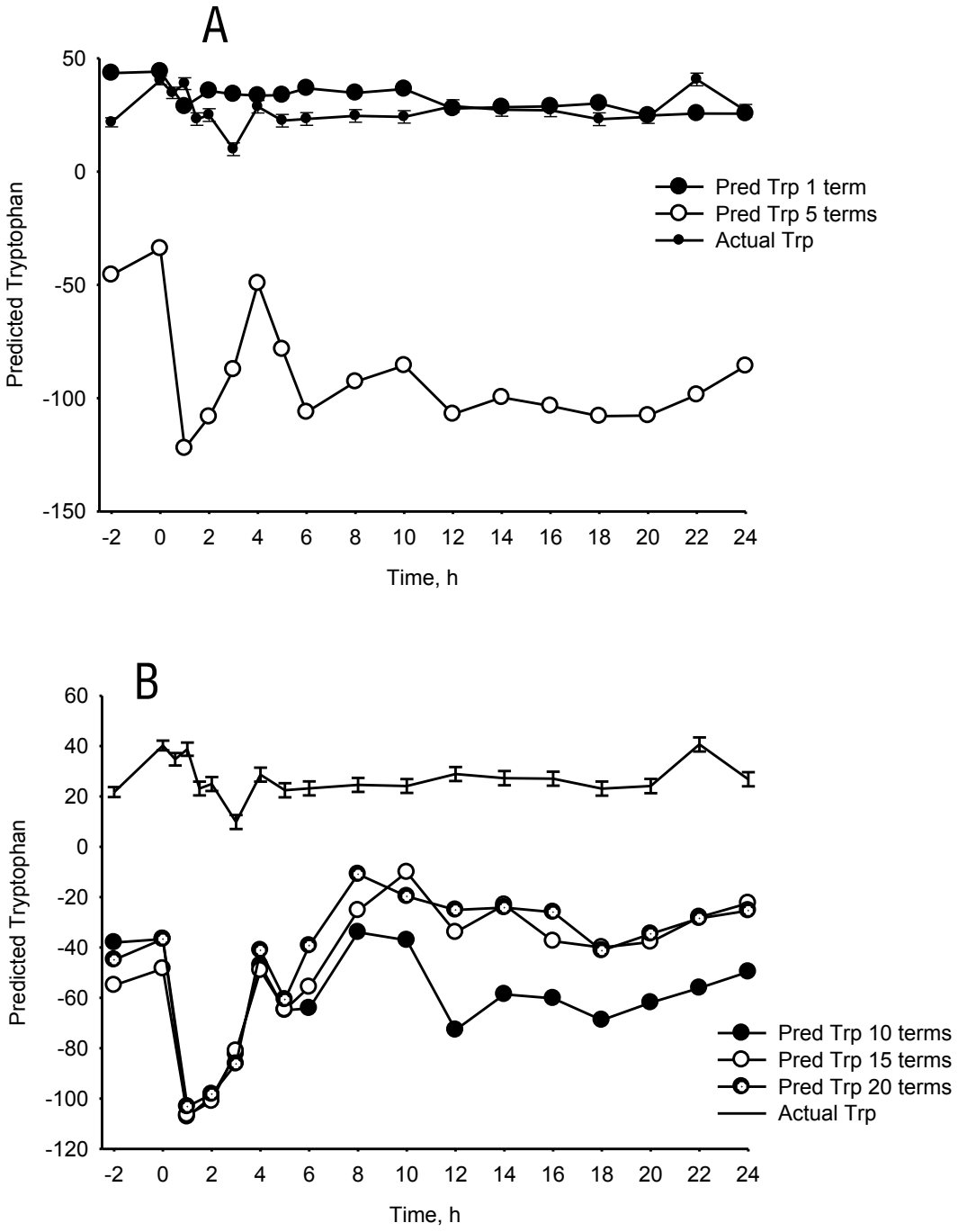

Figure 4.27. Observed versus Predicted plot using 1, 5, 10, 15, or 20 terms in the model to predict plasma tryptophan levels in *E. coli* lipopolysaccharide (LPS, 10 µg/kg BW) treated pigs. Prediction equations were generated using PROC REG from data from the 12-h trial and the equations were used to predict AA changes in pigs monitored post-LPS for 24 h.

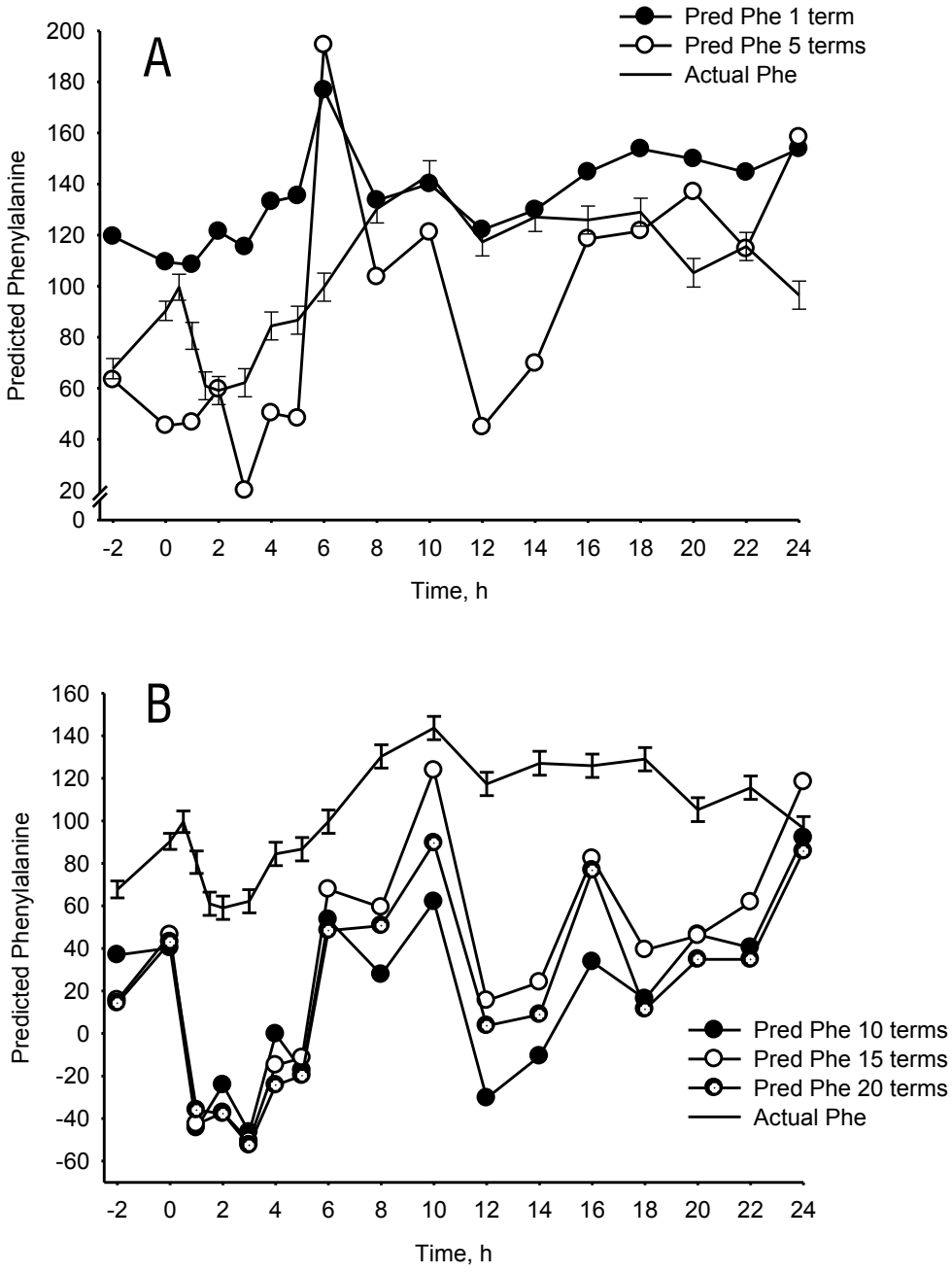

Figure 4.28. Observed versus Predicted plot using 1, 5, 10, 15, or 20 terms in the model to predict plasma phenylalanine levels in *E. coli* lipopolysaccharide (LPS, 10 µg/kg BW) treated pigs. Prediction equations were generated using PROC REG from data from the 12-h trial and the equations were used to predict AA changes in pigs monitored post-LPS for 24 h.

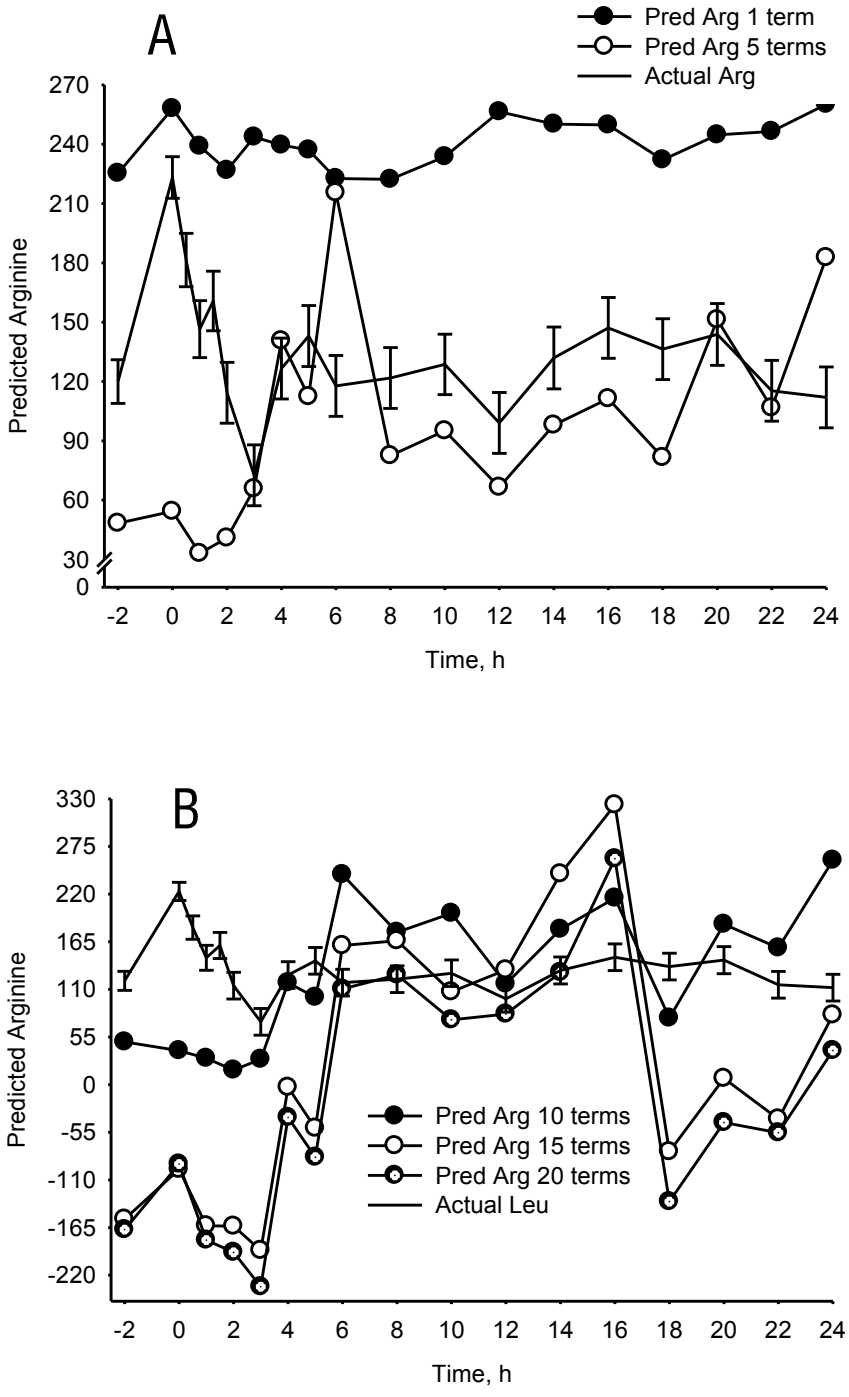

Figure 4.29. Observed versus Predicted plot using 1, 5, 10, 15, or 20 terms in the model to predict plasma arginine levels in *E. coli* lipopolysaccharide (LPS, 10 µg/kg BW) treated pigs. Prediction equations were generated using PROC REG from data from the 12-h trial and the equations were used to predict AA changes in pigs monitored post-LPS for 24 h.

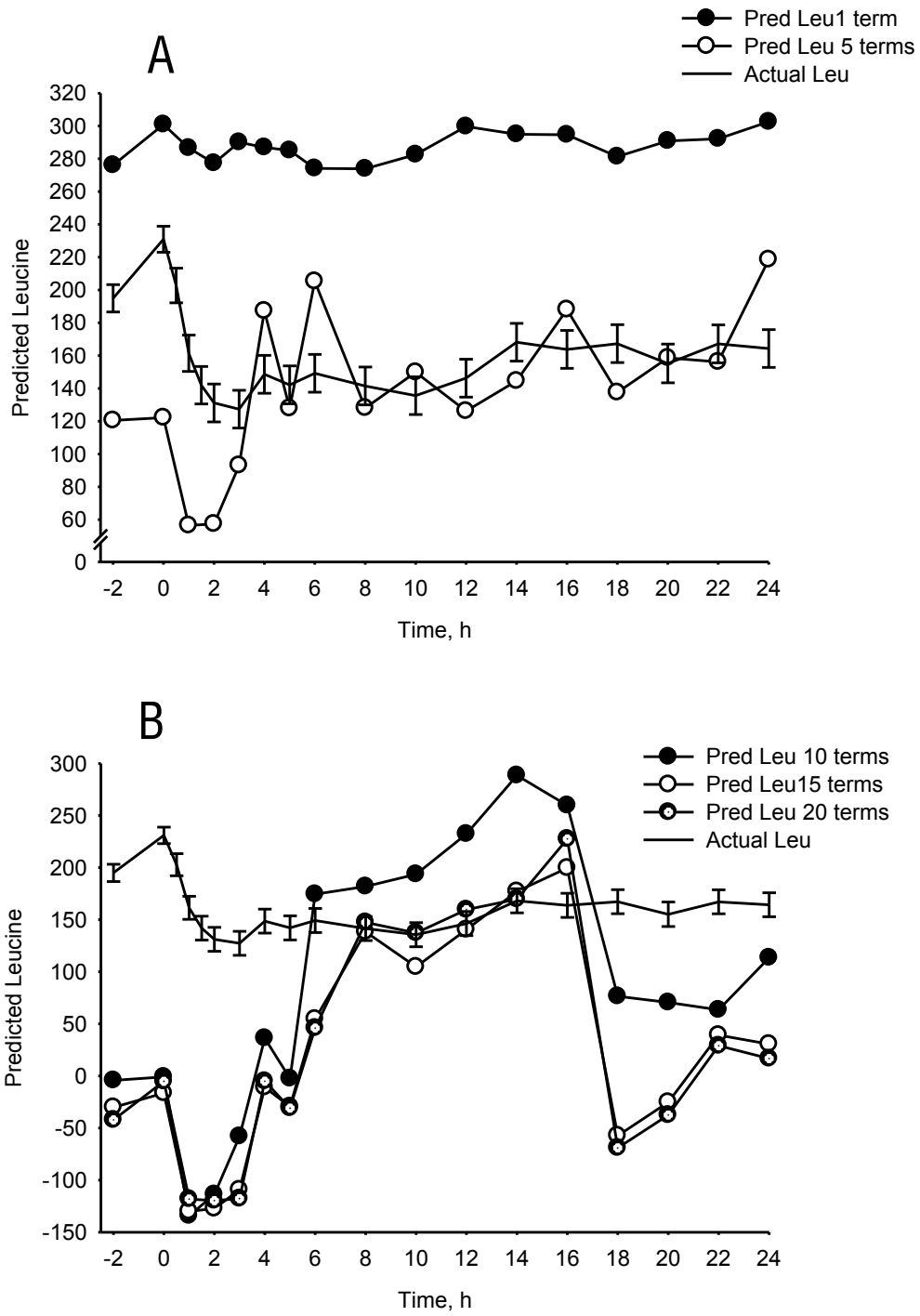

Figure 4.30. Observed versus Predicted plot using 1, 5, 10, 15, or 20 terms in the model to predict plasma leucine levels in *E. coli* lipopolysaccharide (LPS, 10 µg/kg BW) treated pigs. Prediction equations were generated using PROC REG from data from the 12-h trial and the equations were used to predict AA changes in pigs monitored post-LPS for 24 h.

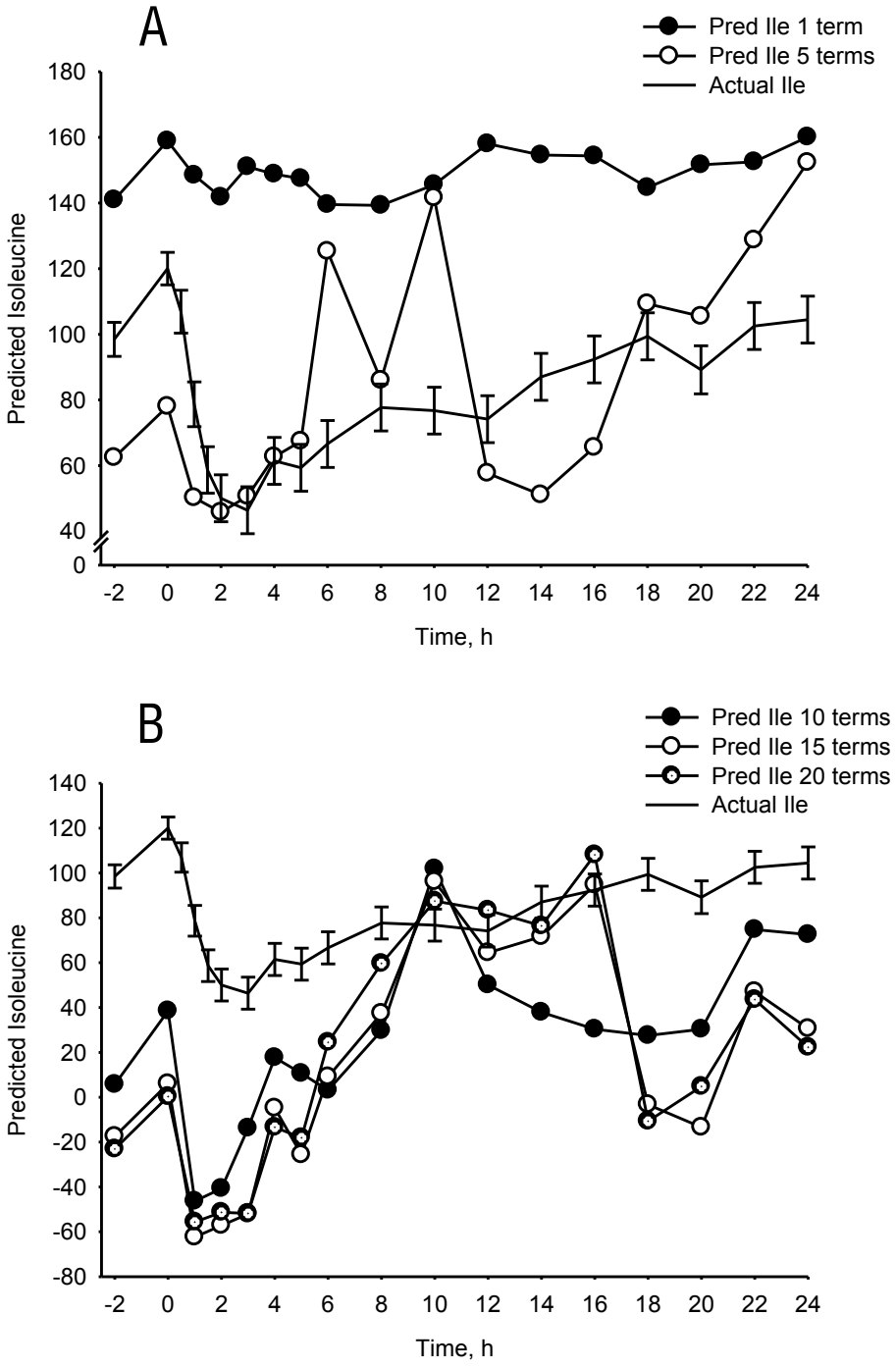

Figure 4.31. Observed versus Predicted plot using 1, 5, 10, 15, or 20 terms in the model to predict plasma isoleucine levels in *E. coli* lipopolysaccharide (LPS, 10 µg/kg BW) treated pigs. Prediction equations were generated using PROC REG from data from the 12-h trial and the equations were used to predict AA changes in pigs monitored post-LPS for 24 h.

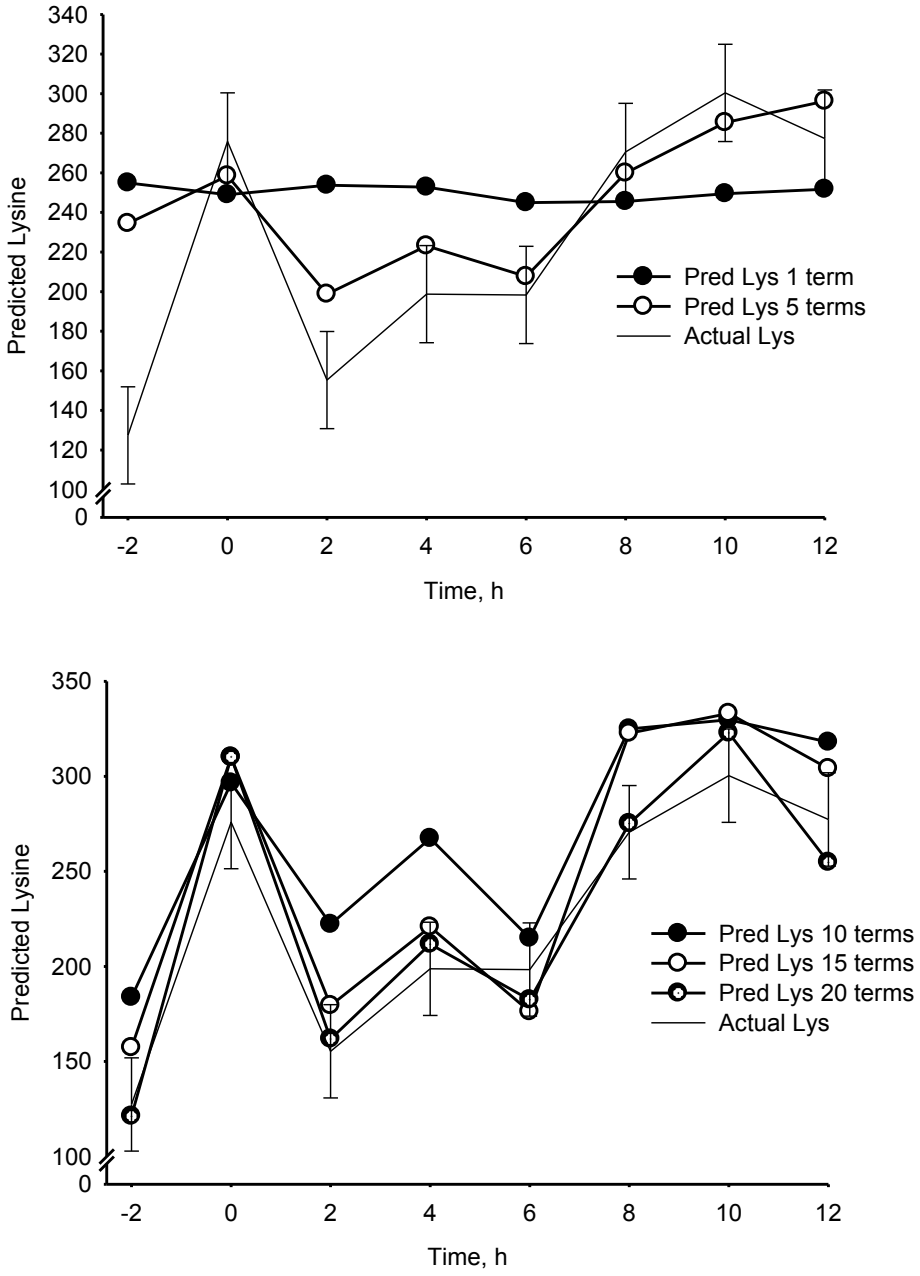

Figure 4.32. Observed versus Predicted plot using 1, 5, 10, 15, or 20 terms in the model to predict plasma lysine levels in *E. coli* lipopolysaccharide (LPS, 10 µg/kg BW) treated pigs. Prediction equations were generated using PROC REG from data from the 12-h trial and the equations were used to predict AA changes in pigs monitored post-LPS for 12 h.

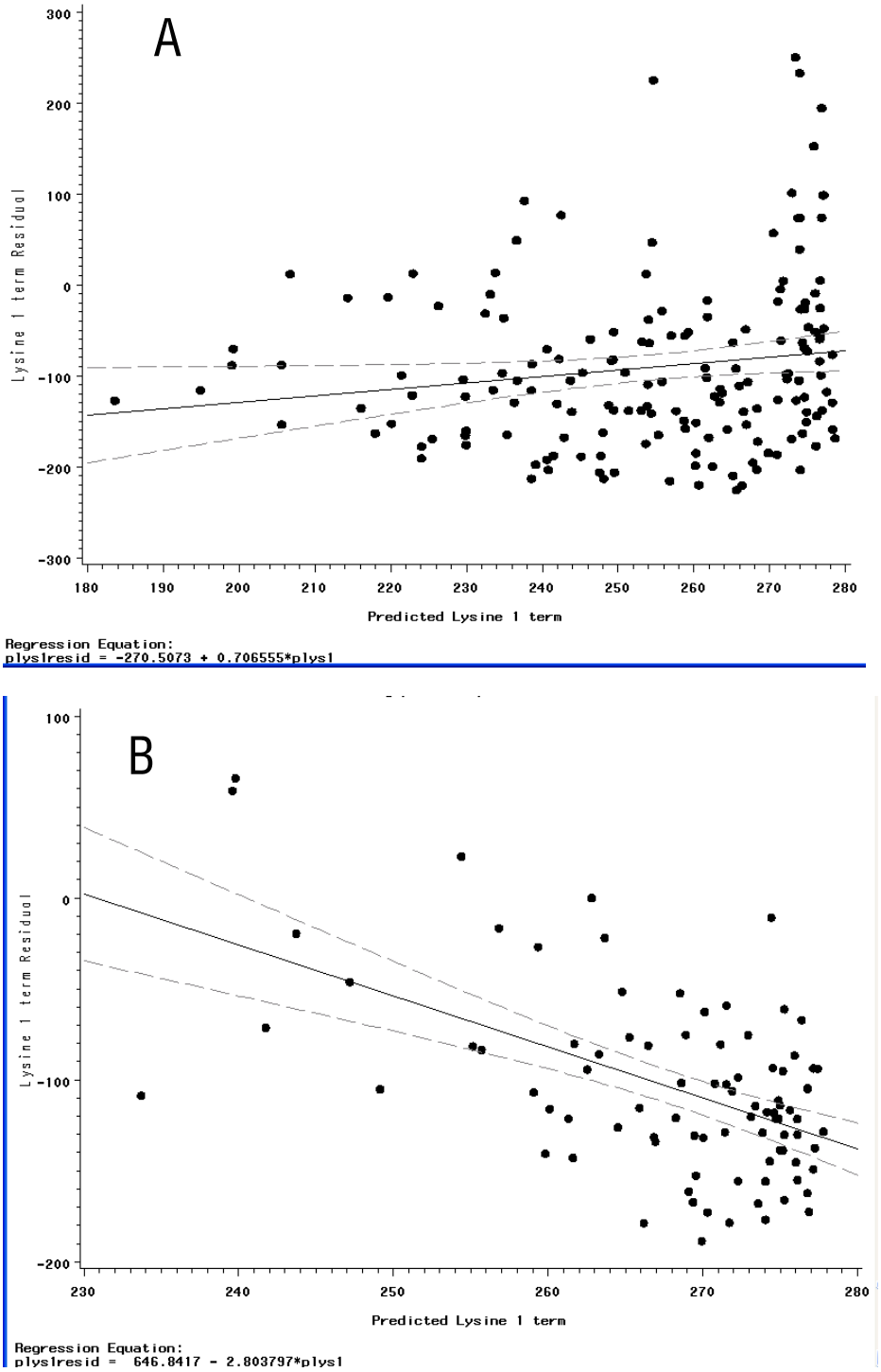

Figure 4.33. SAS generated GPLOT showing residual versus predicted for lysine when 1 term was included in the model for (A) group 1 (t = -2 to 12) or (B) group 2 (t = 14 to 24). Prediction equations were generated using PROC REG from data from the 12-h trial and the equations were used to predict AA changes in pigs monitored post-LPS for 24 h. 95% confidence interval shown on plot and regression equation shown in bottom left hand corner of graph.

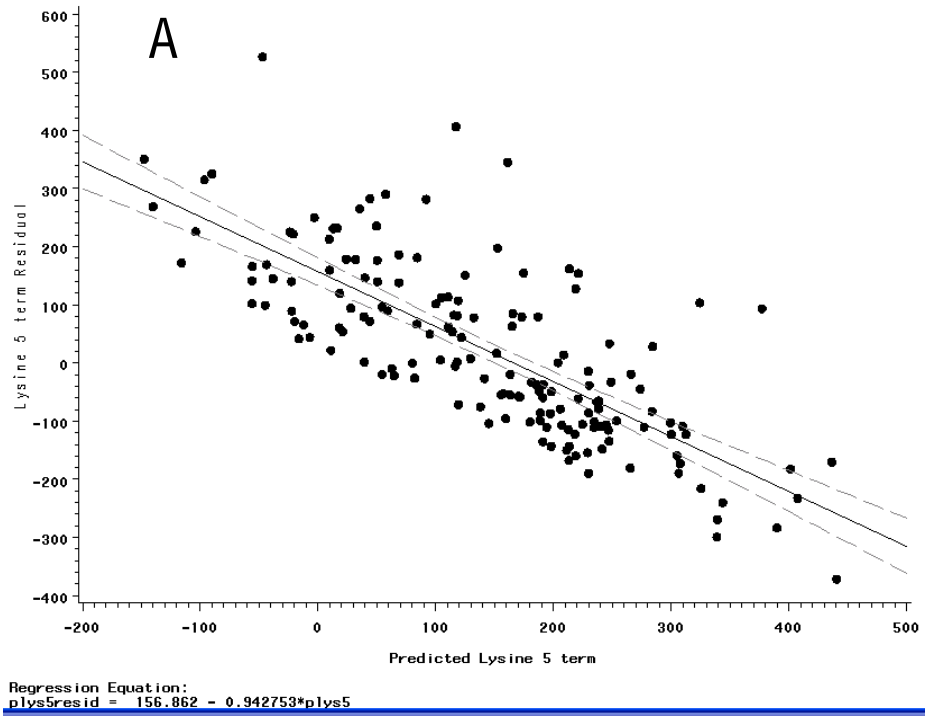

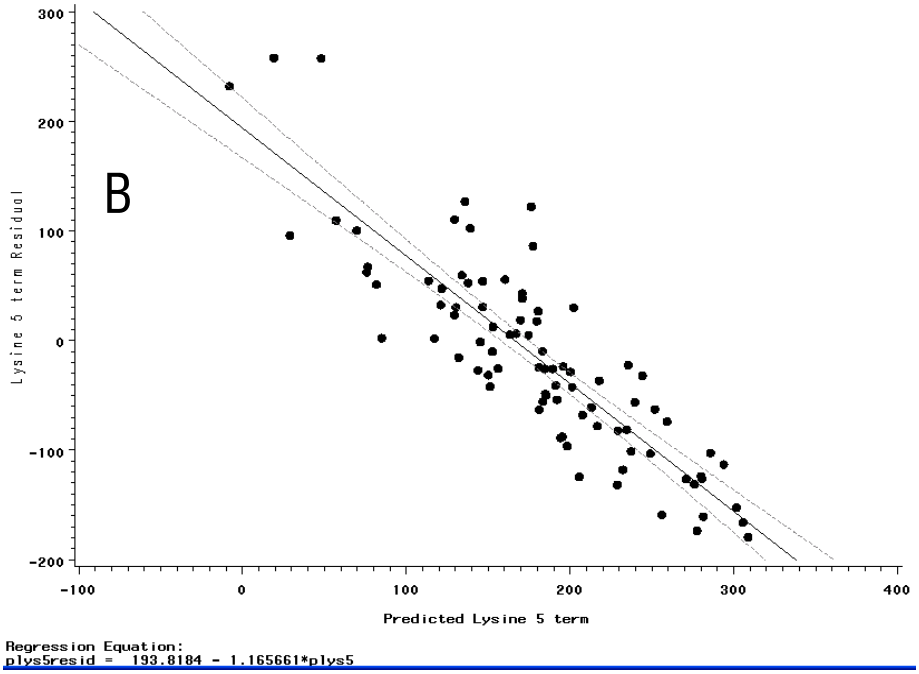

Figure 4.34. SAS generated GPLOT showing residual versus predicted for lysine when 5 terms were included in the model for (A) group 1 (t = -2 to 12) or (B) group 2 (t = 14 to 24). Prediction equations were generated using PROC REG from data from the 12-h trial and the equations were used to predict AA changes in pigs monitored post-LPS for 24 h. 95% confidence interval shown on plot and regression equation shown in bottom left hand corner of graph.

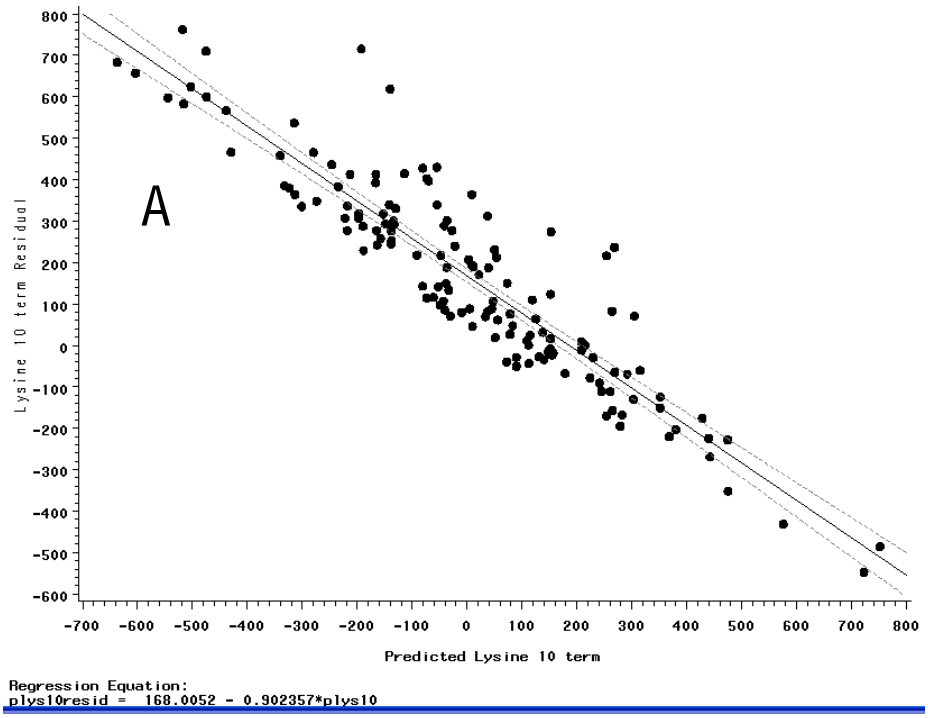

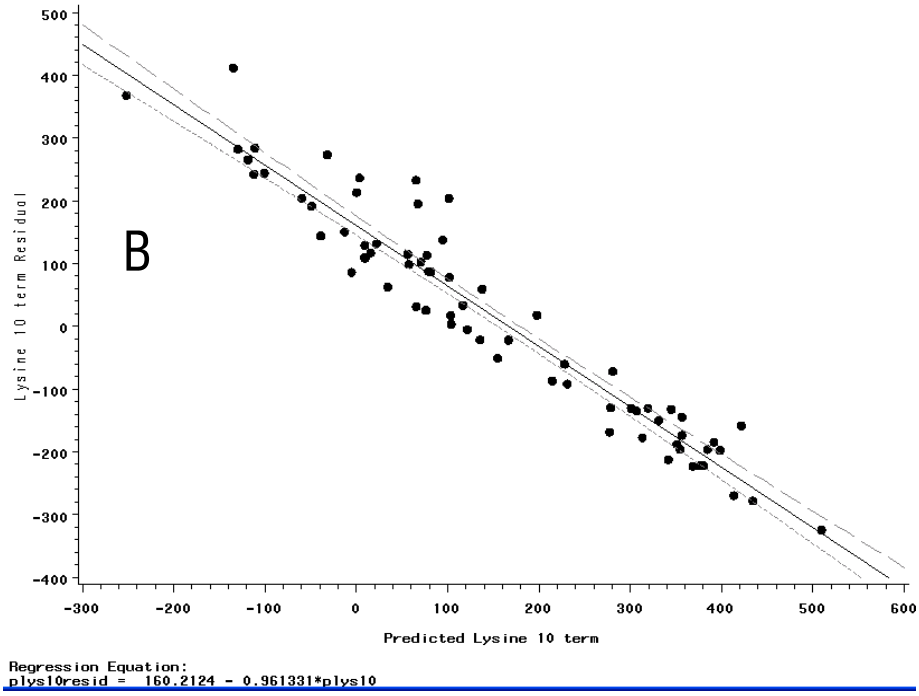

Figure 4.35. SAS generated GPLOT showing residual versus predicted for lysine when 10 terms were included in the model for (A) group 1 (t = -2 to 12) or (B) group 2 (t = 14 to 24). Prediction equations were generated using PROC REG from data from the 12-h trial and the equations were used to predict AA changes in pigs monitored post-LPS for 24 h. 95% confidence interval shown on plot and regression equation shown in bottom left hand corner of graph.

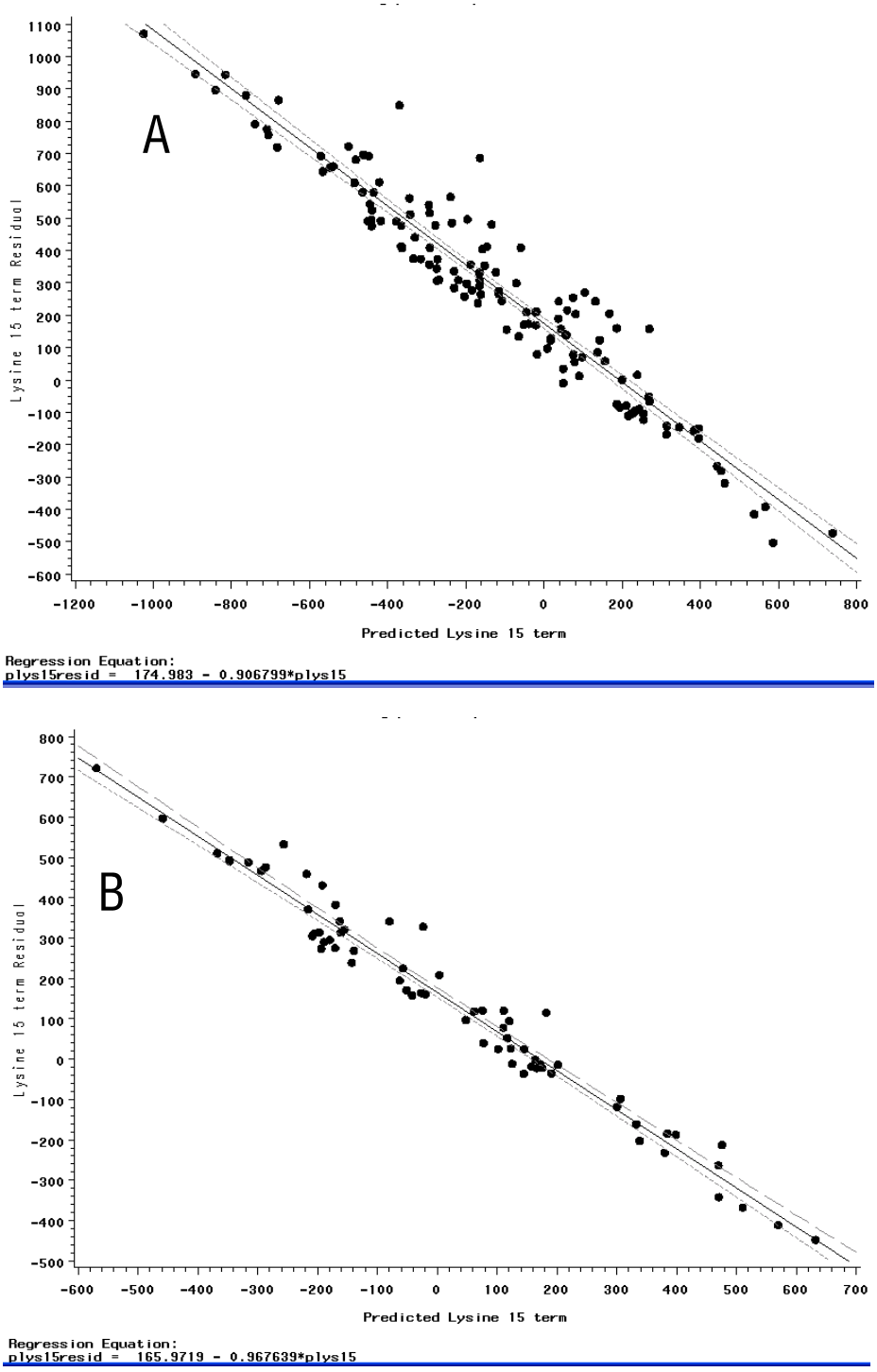

Figure 4.36. SAS generated GPLOT showing residual versus predicted for lysine when 15 terms were included in the model for (A) group 1 (t = -2 to 12) or (B) group 2 (t = 14 to 24). Prediction equations were generated using PROC REG from data from the 12-h trial and the equations were used to predict AA changes in pigs monitored post-LPS for 24 h. 95% confidence interval shown on plot and regression equation shown in bottom left hand corner of graph.

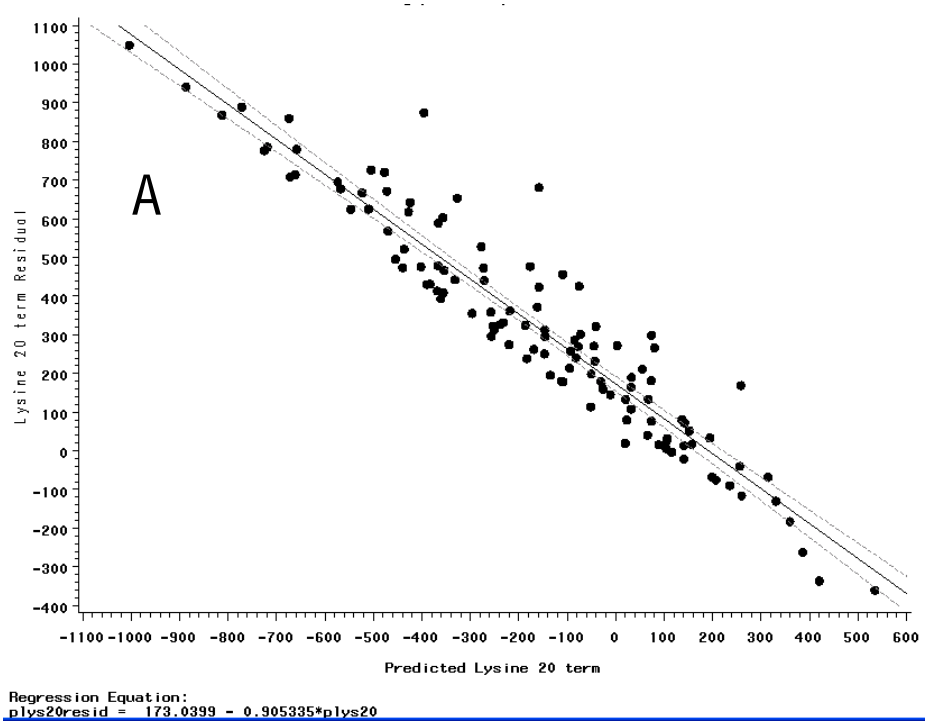

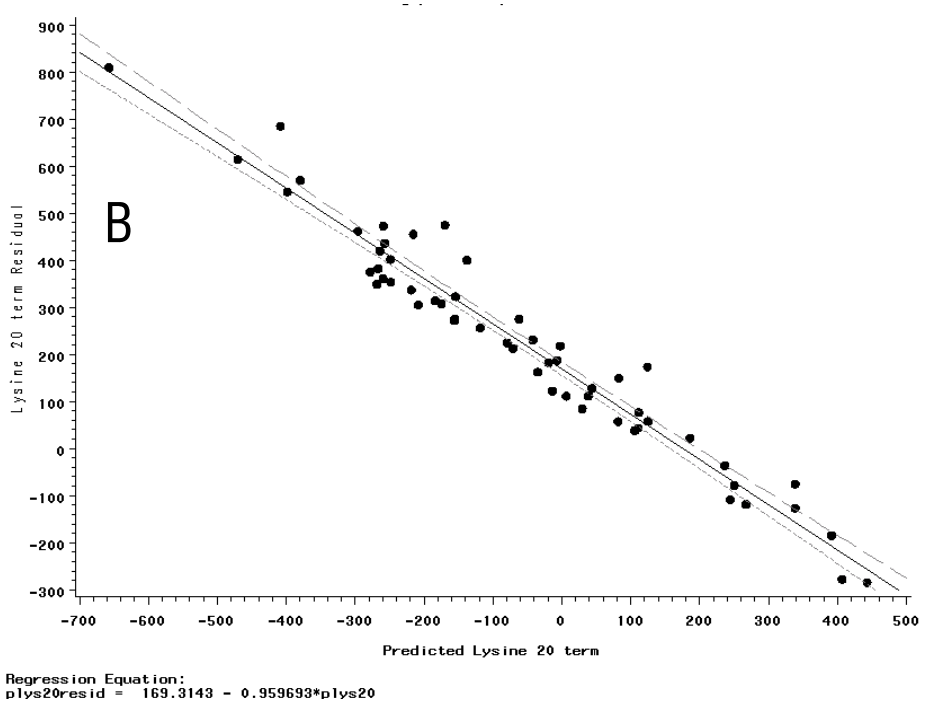

Figure 4.37. SAS generated GPLOT showing residual versus predicted for lysine when 20 terms were included in the model for (A) group 1 (t = -2 to 12) or (B) group 2 (t = 14 to 24). Prediction equations were generated using PROC REG from data from the 12-h trial and the equations were used to predict AA changes in pigs monitored post-LPS for 24 h. 95% confidence interval shown on plot and regression equation shown in bottom left hand corner of graph.

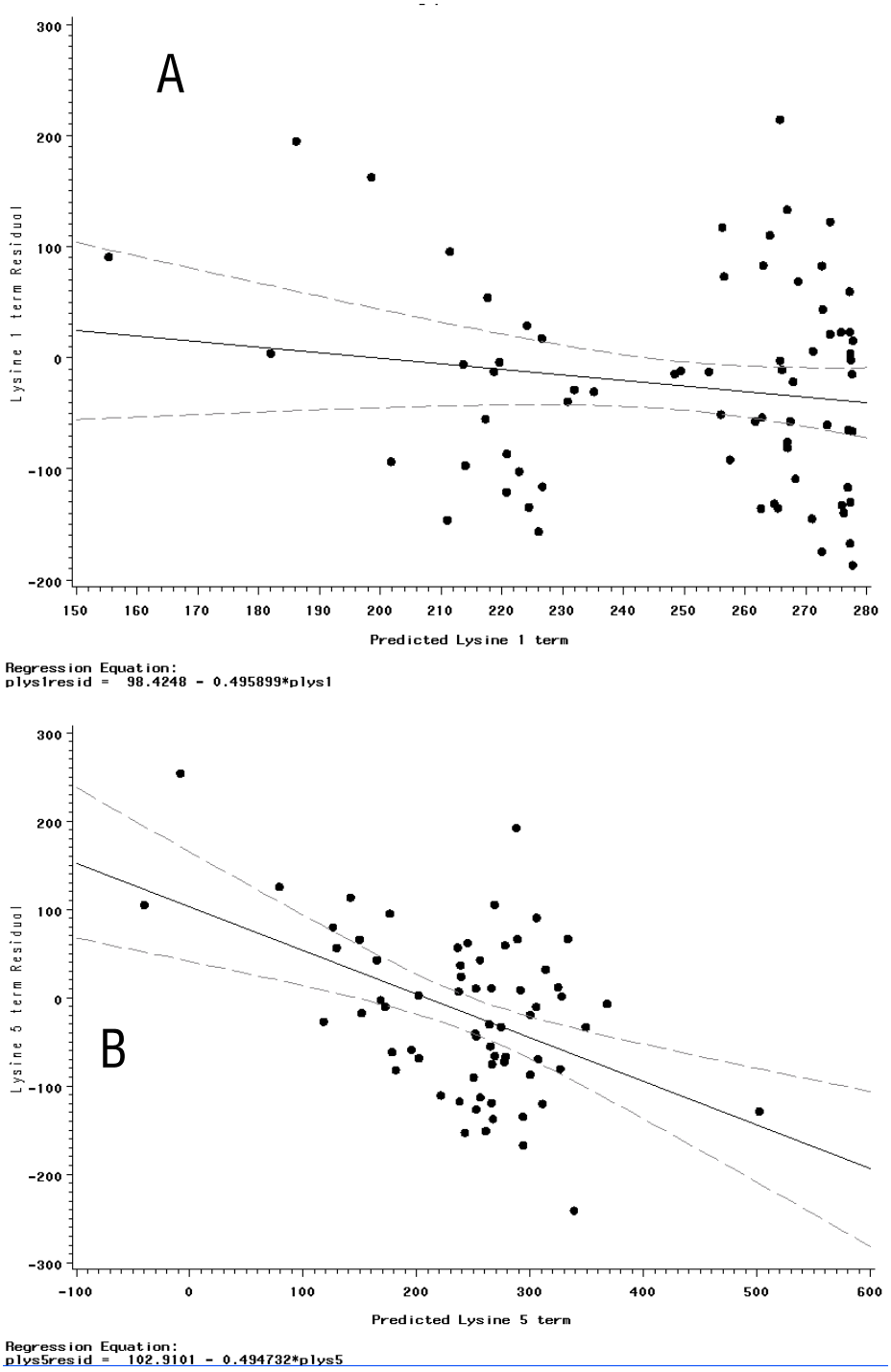

Figure 4.38. SAS generated GPLOT showing residual versus predicted for lysine when (A) 1 or (B) 5 terms were included in the model for group 1 (t = -2 to 12). Prediction equations were generated using PROC REG from data from the 12-h trial and the equations were used to predict AA changes in pigs monitored post-LPS for 12 h. 95% confidence interval shown on plot and regression equation shown in bottom left hand corner of graph.

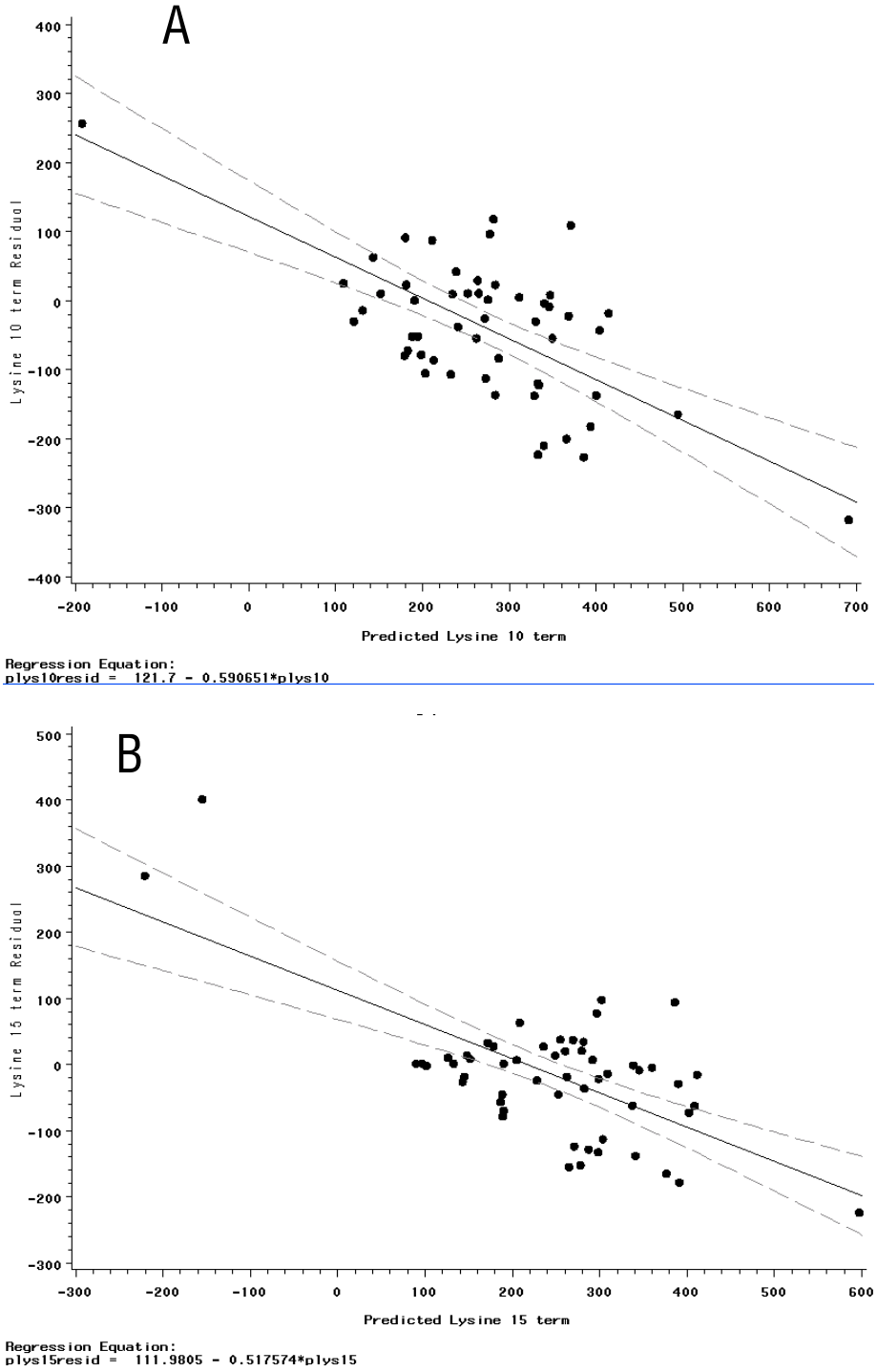

Figure 4.39. SAS generated GPLOT showing residual versus predicted for lysine when (A) 10 or (B) 15 terms were included in the model for group 1 (t = -2 to 12). Prediction equations were generated using PROC REG from data from the 12-h trial and the equations were used to predict AA changes in pigs monitored post-LPS for 12 h. 95% confidence interval shown on plot and regression equation shown in bottom left hand corner of graph.

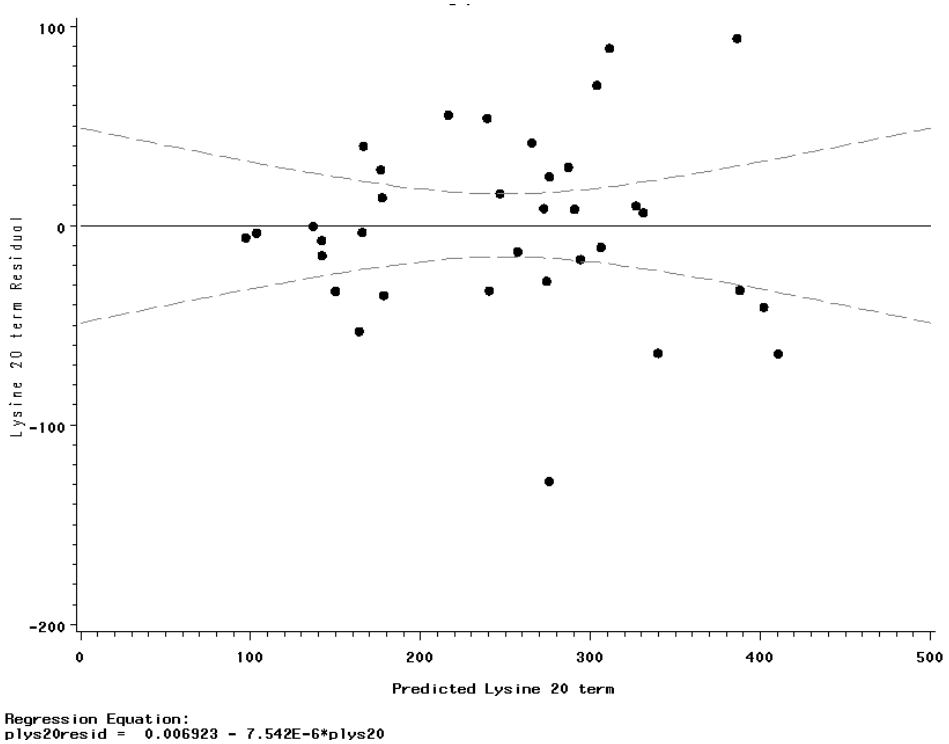

Figure 4.40. SAS generated GPLOT showing residual versus predicted for lysine when 20 terms were included in the model for group 1 (t = -2 to 12). Prediction equations were generated using PROC REG from data from the 12-h trial and the equations were used to predict AA changes in pigs monitored post-LPS for 12 h. 95% confidence interval shown on plot and regression equation shown in bottom left hand corner of graph.

4.8 Literature cited

Cohen, S. A., M. Meys, and T. L. Tarvin. 1989. The Pico-Tag Method: A manual of advanced Techniques for amino acid analysis. [WM02, Rev. 1]. Milford, MA, Waters Division of Millipore.

Dritz, S. S., K. Q. Owen, R. D. Goodband, J. L. Nelssen, M. D. Tokach, M. M. Chengappa, and F. Blecha. 1996. Influence of lipopolysaccharide-induced immune challenge and diet complexity on growth performance and acute-phase protein production in segregated early-weaned pigs. J. Anim. Sci. 74:1620-1628.

ERS/USDA. 2003. Calculating the cost of Foodborne Illness: A New Tool to Value Food Safety Risks. Economic Research Service. United States Department of Agriculture. http://www.ers.usda.gov. Accessed June 20, 2008.

Escobar, J. J. W. Frank, A. Suryawan, H. V. Nguyen, S. R. Kimball, L. S. Jefferson, and T. A. Davis. 2004. Physiological rise in plasma leucine stimulates muscle protein synthesis in neonatal pigs by enhancing translation initiation factor activation. Endocrinology and Metab. 288:E914-E921.

Escobar, J., J. W. Frank, A. Suryawan, H. V. Nguyen, S. R. Kimball, L. S. Jefferson, T. A. Davis. 2006. Regulation of cardiac and skeletal muscle protein synthesis by individual branched-chain amino acids in neonatal pigs. Am. J. Physiol. Endocrinol. Metab. 290:E612-E621.

Lambalgen, A. A. van, M. T. E. Rasker, G. C. van den Bos, and L. G. Thijs. 1988. Effects of endotoxemia on systemic plasma loss and hematocrit in rats. Microvascular Res. 36:291-304.

Mead, P.S., L. Slutsker, V. Dietz, L. F. McCraig, J. S. Bresee, C. Shapiro, P. M. Griffin, and R. V. Tauxe. 1999. Food-related illness and death in the United States. Emerg. Infect. Dis. 5:607-625.

Merck & Co., Inc. 2003. Infections: Bacterial *Salmonella* infections. Merck, Whitehouse Station, NJ. http://www.merck.com/mmhe/sec17/ch190/ch190p.html. Accessed August 27, 2008.

NRC. 1998. Nutrient Requirements of Swine. 10th ed. Natl. Acad. Press, Washington, DC.

Nelin, L. D., X. Wang, Q. Zhao, L. G. Chicoine, T. L. Young, D. M. Hatach, B. K. English, and Y. Liu. 2007. MKP-1 switches arginine metabolism from nitric oxide synthase to arginase following endotoxin challenge. Am. J. Physiol. Cell. Physiol. 293:C632-C640.

Orellana, R. A., P. M. J. O'Connoer, H. V. Nguyen, J. A. Bush, A. Suryawan, M. C. Thivierge, M. L. Fiorotto, and T. A. Davis. 2002. Endotoxemia reduces skeletal muscle protein synthesis in neonates. Am. J. Physio. Endocrinol. Metab. 283:E909-E916.

Potteiger, J. A., D. J. Jacobsen, and J. E. Donnelly. 2002. A comparison of methods for analyzing glucose and insulin areas under the curve following nine months of exercise in overweight adults. International J. Obesity. 26:87-89.

Reeds, P. J., C. R. Fjeld, and F. Jahoor. 1994. Do the differences between the amino acid compositions of acute-phase and muscle proteins have a bearing on nitrogen loss in traumatic stress. J. Nutr. 124:906-910.

Saedeleer, V. De, E. Wechsung, and A. Houvenaghel. 1991. Endotoxin in the conscious piglet: Its effect on some general and gastrointestinal myoelectrical parameters. Vet. Res. Comm. 15:227-238.

Shiang, Keh-Dong. 2008. The SAS calculations of areas under the curve (AUC) for multiple metabolic readings. http://www.lexjansen.com/wuss/2004/posters/c_post_the_sas_calculations_.pdf. Accessed Oct. 27, 2011.

Stipanuk, M. H. and M. Watford. 2000. Amino acid metabolism. In: *Biochemical and physiological aspects of human nutrition*. M. H. Stipanuk, ed. W.B. Saunders Co, Pgs:233-286.

Talbot, R. B. and M. J. Swenson. 1970. Blood volume of pigs from birth through 6 weeks of age. Am. J. Physio. 218:1141-1144.

Wannemacher, R. W. 1977. Key role of various individual amino acids in host response to infection. Am. J. Clin. Nutr. 30:1269-1280.

Webel, D. M., B. N. Finck, D. H. Baker, and R. W. Jonhson. 1997. Time course of increased plasma cytokines, cortisol, and urea nitrogen in pigs following intraperitoneal injection of lipopolysaccharide. J. Anim. Sci. 75:1514-1520.

Wyss, M. and R. Kaddurah-Daouk. 2000. Creatine and creatinine metabolism. Physiol. Rev. 80:1107-1213.

CHAPTER 5

Development of a porcine *Salmonella* infection model

5.1 Abstract

Salmonellosis results in a major economic loss to the animal industry as well as being the source of about 27% of all human bacterial infections each year. Therefore, the objective of this study was to develop a porcine *Salmonella* model to study the impact of a bacterial infection on the nutritional status of nonruminant mammals. Pigs (n = 20) were weaned at 21 d of age, blocked by BW and assigned to an experimental (sterile broth or *Salmonella*) group. Pigs were fed a conventional 3-phase nursery diets (0-7 d, 7-21 d, and 21-35 d) with ad libitum access to water and feed. On d 14, pigs were orally inoculated with 10^9 CFU of *Salmonella enterica* serovar Typhimurium DT104 or sterile broth. During d 17-20, all pigs were treated with 5 mg/kg BW i.m. ceftiofur-HCl. Growth performance was measured during pre-inoculation (PRE; 0-14 d), sick (SICK; 14-21 d), and post-inoculation (POST; 21-35 d). Body weight and ADG were measured weekly. Rectal temperature (RT) was measured weekly during PRE and POST, and every 12 h during SICK. Pigs inoculated with *Salmonella* had decreased ADG and BW, and elevated RT during SICK ($P < 0.001$). Furthermore, fecal *Salmonella* CFU ($\log_{10}$) was modestly correlated ($P < 0.002$) with BW (r = -0.22), ADFI (r = -0.27), ADG (r = -0.36), G:F ratio (r = -0.18), and RT (r = 0.52) during SICK. Following antibiotic administration all *Salmonella*-infected pigs stopped shedding *Salmonella* and their RT returned to baseline. The inoculating dose of 10^9 CFU of *Salmonella* Typhimurium successfully resulted in an active bacterial infection that behaved and responded comparably to field cases.

5.2 Introduction

Salmonella is one of the most commonly reported human bacterial infections in the US each year (FSIS/USDA, 2006). Human cases of salmonellosis usually result from improper handling of food and/or poor hygiene. Persons afflicted with salmonellosis experience increased body temperatures and gastrointestinal upsets. Most *Salmonella* cases are self-limiting, however, a small percentage of cases become life threatening. In such cases, it is attributed to bacterial translocation into the bloodstream and other organs, or because the patient is severely dehydrated. Salmonellosis also occurs in food animals leading to a possible risk of human exposure through food derived from these animals. *Salmonella* cases in animal agriculture result in an economic impact to the producers with an estimated $2.4 billion loss annually (ERS/USDA, 2003).

Of the more than 2,500 different serotypes of *Salmonella*, *Salmonella* Enteriditis and Typhimurium are the most common *Salmonella* related causes of disease in animals and humans (CDC, 2005). Rodents inoculated with *Salmonella* Typhimurium exhibit symptoms similar to that of a human infected with *Salmonella* Typhi. While this animal model serves as an important model of Typhoid Fever, it does not reflect an animal model for studying human gastroenteritis (Sharan et al., 2011). Therefore, our objective was to develop a salmonellosis animal model in weaned pigs. Pigs are a reasonable choice for a human animal model because they have similar digestive systems and have similarly sized organs unlike rodents (Lunney, 2007). In addition, *Salmonella* infections are prevalent in nursery pigs and this model could be used to evaluate intervention strategies for the swine industry.

5.3 Materials and Methods

All procedures were approved by both Virginia Tech Institutional Animal Care and Use Committee and Biosafety Committee and conducted in a Biosafety Level (BSL)-2 facility. In addition, all analytical procedures and bacterial analyses were conducted in approved BSL-2 laboratories.

5.3.1 Bacterial strain and culture

Feed ingredients, mixed diets, and initial fecal samples were enriched in Gram-negative Hajna broth at 37°C for 24 h (BD Bioscience, Franklin Lake, NJ) before plating onto Brilliant Green Agar (BGA, BD Bioscience) plates for qualitative determination of *Salmonella spp.* *Salmonella enterica* subspecies *enterica* serovar Typhimurium DT104 was obtained from the American Type Culture Collection (ATCC, BAA-185, Manassas, VA). This strain was isolated from a pig in Denmark and was resuscitated in 10 mL of tryptic soy broth (TSB) at 37°C for 24 h and plated onto tryptic soy agar (TSA, BD Bioscience). A single colony was rendered resistant to the antibiotics nalidixic acid (Acros Organics, Morris Plains, NJ; CAS 389-08-2) and novobiocin (BD Bioscience; CAS 1476-53-5) through sequential transfer onto TSA plates of increasing concentrations until achieving a final resistance to 20 μg/mL and 25 μg/mL, respectively (i.e., *S.* Typhimurium $Nal^{R}Nov^{R}$). The choice of a nalidixic acid and novobiocin resistant strain was to reduce the possibility of detecting *Salmonella* that were not introduced in this experiment. The final strain was tested for susceptibility to 5 mg/kg ceftiofur-HCl (Pfizer Animal Health, New York, NY) to insure antibiotic efficacy of pig treatments. *Salmonella* Typhimurium $Nal^{R}Nov^{R}$ was cultured overnight at 37°C in TSB medium on an orbital shaker (New Brunswick Scientific, Edison, NJ) at 150 rpm and bacterial populations were estimated by

spectrophotometry at 600 nm. For inocula preparation, *S.* Typhimurium $Nal^{R}Nov^{R}$ were harvested at 7,500 × g for 10 min at 4°C, and resuspended in sterile TSB.

5.3.2 Animals, housing, diets, and experimental protocol

Pigs (Smithfiled Premium Genetics 1020, Waverly, VA) obtained from a commercial swine farm (Waverly, VA) were weaned at 21 d of age (7.02 ± 0.27 kg) and transported to a BSL-2 facility. Twenty pigs in each of 2 replicate trials were used, for a total of 40 pigs (20 pigs per treatment). Pigs were blocked by BW, and randomly assigned to treatments within block. Treatments were inoculation with sterile broth or *Salmonella*. Individual rectal swabs were collected at arrival to the BSL-2 facility to initially screen for the presence of *Salmonella*. All samples were incubated at 37°C for 24 h in Gram-negative Hajna broth for enrichment, followed by plating onto BGA to screen for *Salmonella* indicative colonies

Pigs were housed in individual pens and segregated in 2 identical rooms according to their assigned inocula (sterile broth or *Salmonella*) to minimize the potential for cross-contamination. Inocula conditions were tested in both rooms during the 2 replicate trials of the study. Rooms were discretely ventilated with 100% clean air (i.e., no recirculation), and were under negative pressure at all times, and automated systems controlled the temperature and lighting (18 h light:6 h dark with lights on at 0600) of each individual room. Each pen contained a plastic coated expanded metal floor, a nipple waterer, and self-feeder. Pigs were fed a 3-phase corn-soybean meal nursery diet (Table 1; phase 1, 0-7 d; phase 2, 7-21 d; phase 3, 21-35 d post weaning) formulated to meet or exceed NRC recommendations for nutrients and contained no antibiotics (NRC, 1998). Prior to feeding, all feed ingredients and mixed diets were screened for the presence of *Salmonella* and were negative.

The experimental protocol was designed to simulate an enteric disease outbreak and antibiotic treatment in a nursery facility after weaning. Thus, pigs were weaned, inoculated, allowed to develop clinical signs of disease, treated with antibiotic, and allowed to recover. The experiment consisted of 3 periods: pre-inoculation (PRE; 0-14 d), sick (SICK; 14-21 d), and post-inoculation (POST; 21-35 d). Pigs and feeders were weighed every 7 d to determine ADG, ADFI, and G:F ratio. Rectal temperatures (RT) were measured weekly during PRE and POST, and every 12 h during SICK. On d 14, conscious pigs were administered 5 mL of TSB containing 10^9 colony-forming units (CFU) of *S.* Typhimurium $Nal^R Nov^R$ or 5 mL of sterile TSB orally.

Daily rectal swabs were collected after inoculation (d 14-21) to determine fecal shedding of *S.* Typhimurium $Nal^R Nov^R$. From d 17, all pigs were treated daily with 5 mg/kg BW i.m. ceftiofur-HCl for 4 d. On d 35, pigs were euthanized with a lethal dose of 120 mg/kg BW of sodium pentobarbital i.v. (Beuthanasia-D, Schering-Plough, Union, NJ). Carcasses were disposed as regulated medical waste in accordance to university, local, state, and federal regulations.

5.3.3 Enumeration of *S. Typhimurium* $Nal^R Nov^R$

During the morning chore (0800), about 10 g of feces was collected from each pig daily during d 14-21 using a sterile fecal loop, contents were placed in a sterile filter bag, and immediately processed with 90 mL of buffered peptone water (BPW, BD Biosciences) in a stomacher for 2 min to create a fecal slurry. The fecal slurry was then serially diluted and plated, in duplicate, onto BGA plates containing 20 μg/mL of nalidixic acid and 25 μg/mL of novobiocin. The plates were allowed to air dry and then incubated at 37°C for 24 h. Plates were

then inspected for white colonies with red-pink halos, indicative of *Salmonella*. Initial presumptive positive plates were confirmed on xylose lysine tergitol 4 (XLT-4) agar, the presence of black round colonies was indicative of *S.* Typhimurium $Nal^{R}Nov^{R}$. The total number of *Salmonell*a colonies on each plate was quantified to determine daily shedding rates for each pig.

5.3.4 Intestinal morphology

Upon euthanasia intestinal samples were collected for morphology. A sample from the duodenum, jejunum, and ileum (2-3 cm in length) was placed in 15-ml plastic conical tubes containing 10 ml of phosphate-buffered formalin (Fisher Scientific, Fairlawn, NJ). Tissue sections of duodenum (about 20 cm caudal of gastroduodenal junction), jejunum (about 50% of intestinal length), and ileum (about 20 cm proximal of ileocecal junction) were sent to a commercial histology laboratory (HISTO-Scientific Research Laboratories, Mt. Jackson, VA) for microscope slide preparation and staining (Zhao et al., 2007). Three random cuts (5 μm each) from each tissue section (duodenum, jejunum, and ileum) were mounted on microscope slides and stained with Alcian blue and Periodic acid-Schiff to identify goblet cells (Dunsford et al., 1990). One evaluator per intestinal section was used to obtain morphological data. Evaluators randomly reviewed slides without knowledge of treatments. A total of twelve representative measurements were read for each tissue section. The following endpoints were measured: villus height (μm), villus width (μm), crypt depth (μm), number of goblet cells in the villus perimeter, and number of goblet cells in each crypt. Villus perimeter (VP) was calculated as follows: $VP = h \times 2 + w$, where h is villus height and w is villus width. A modified cylinder area equation was used to calculate villus area (VA) as follows: $VA = [\pi \times (w \div 2)^2] + (\pi \times w) \times h$; where, w is

width of villus and h is height of villus. Data from the three tissue cuts per tissue section were averaged to create a single value for each of the described endpoints.

5.3.5 Statistical analysis

Growth performance and RT data were analyzed with the PROC MIXED procedure of SAS (SAS Inst. Inc., Cary, NC), replicate was used as a random effect (Kaps and Lamberson, 2004). The model included ADG, ADFI, BW, and RT across the 3 periods (PRE, SICK, and POST). Fecal analysis of *Salmonella* shedding was also determined with PROC MIXED with replicate as a random effect and using pig as repeated measures. Least squares means were obtained using Tukey adjustment. Significance was declared at $P \leq 0.05$ and tendency at $P < 0.10$.

5.4 Results

5.4.1 Rectal temperature and *Salmonella* shedding

All pigs were initially fecal negative for *Salmonella* before inoculation. Furthermore, pigs that received sterile broth never shed *Salmonella* or developed a febrile response. These results clearly indicate that non-infected pigs indeed were disease free during the study. Experimental infection with *Salmonella* resulted in a marked increase ($P < 0.001$) in RT during SICK (Figure 5.1). This febrile response is a clear indication that pigs were clinically sick and had developed a systemic immune response. A linear reduction in RT of *Salmonella*-infected pigs was observed from d 17 (start of i.m. ceftiofur-HCl) to the end of antibiotic treatment on d 21. Inoculated pigs shed *Salmonella* for 5 d with the most bacteria being shed for the first 3 d after inoculation (Figure 5.2).

5.4.2 Growth performance

Inoculation with *Salmonella* drastically reduced ($P < 0.005$) ADG, ADFI, and BW of pigs compared to non-inoculated pigs (Table 5.1). Growth performance was negatively correlated ($P < 0.002$) with fecal shedding of *Salmonella* during SICK: BW (r = -0.22), ADFI (r = -0.27), ADG (r = -0.36), and G:F ratio (r = -0.18). These negative correlations suggest that increased fecal shedding of *Salmonella* is partially associated with poorer growth performance.

5.4.3 Intestinal morphology

These measurements were taken 2 wk after pigs stopped shedding *Salmonella* in feces and had clinically recovered from the experimental infection. Pigs receiving the *Salmonella* inoculation had a reduced ($P = 0.04$) number of goblet cells present in the duodenal crypt (Table 5.2). Additionally, ileal villus width was reduced ($P = 0.01$) in *Salmonella* challenged animals.

5.5 Discussion

In humans, *Salmonella* infection results in a febrile response, gastrointestinal upset and reduced appetite. The results of this study show that similar results were obtained in weaned pigs experimentally inoculated with 10^9 CFU of *Salmonella enterica* serovar Typhimurium. In both the elderly and young, *Salmonella* can be life threatening. Treatment in serious cases of *Salmonella* includes hospitalization and fluid replacement therapy and in septic cases antibiotics are prescribed (Merck, 2003). This model could be used to investigate the nutritional and immunological impacts of *Salmonella* on pig health and possibly find additional treatment options to help the recovery of infected patients.

Enhanced intestinal morphology has been associated with greater weight gain in healthy and sick pigs (Pluske et al., 1996; Zijlstra et al., 1997). Changes in bacterial populations and intestinal morphology could be acting concomitantly to enhance the recovery of pigs experimentally infected with *Salmonella*. Pigs infected with *Salmonella* in the present study were febrile for 5.5 d after inoculation (i.e., 2.5 d after i.m. treatment ceftiofur-HCl) compared to 1-3 d in a comparable study (Burkey et al., 2004). This comparison suggests that the strain of *Salmonella* Typhimurium used in the present study appears to be more pathogenic to pigs. This observation is important to consider because pigs did not recover naturally from the disease and instead received treatment with an antibiotic to which *Salmonella* was specifically tested to be sensitive. Yet, it took 2.5 d of i.m. antibiotic treatment to return RT to PRE levels and 3 d to eliminate *Salmonella* shedding in feces.

5.6 Implications

We conclude that we were able to successfully create a porcine model of salmonellosis. This is important because it may be used as a dual model for both pig and human nutritional and immunological studies.

5.7 Tables

Table 5.1. Least square means for growth performance in pigs orally gavaged with sterile broth or *Salmonella*[1].

	Broth	*Salmonella*[1]	SEM	P-value Inoc.[2]
Pre-inoculation[3]				
ADG, kg	0.042	- - -	0.021	- - -
ADFI, kg	0.046	- - -	0.004	- - -
G:F ratio	0.705	- - -	0.456	- - -
BW, kg	7.16	- - -	0.128	- - -
Rectal temperature, °C	39.40	- - -	0.062	- - -
Sick[4]				
ADG, kg	0.441	0.312	0.034	0.007
ADFI, kg	0.922	0.637	0.029	< 0.0001
G:F ratio	0.460	0.503	0.093	0.7441
BW, kg	10.01	8.95	0.138	< 0.0001
Rectal temperature, °C	39.54	40.09	0.028	< 0.0001
Post-sick[5]				
ADG, kg	0.570	0.534	0.019	0.179
ADFI, kg	1.177	1.072	0.046	0.111
G:F ratio	0.499	0.515	0.018	0.5236
BW, kg	17.84	15.96	0.487	0.0078
Rectal temperature, °C	39.95	39.86	0.063	0.3051
Overall				
ADG, kg	0.430	0.326	0.026	0.0053
ADFI, kg	0.888	0.663	0.029	< 0.0001
G:F ratio	0.506	0.509	0.081	0.9788
BW, kg	10.84	9.82	0.236	0.0025
Rectal temperature, °C	39.56	40.01	0.025	< 0.0001

[1] *Salmonella* Typhimurium resistant to the antibiotics nalidixic acid (Nal^R) and novobiocin (Nov^R).
[2] Inoc., inoculation with either sterile broth (Broth) or *S.* Typhimurium Nal^RNov^R.
[3] From weaning to before pigs were orally gavage with sterile broth or 10^9 CFU *S.* Typhimurium Nal^RNov^R on d 14 post-weaning.
[4] Day 14 to 21 post-weaning. All pigs were treated with 5 mg/kg BW i.m. ceftiofur-HCl on d 17-20.
[5] Day 21 to 35 post-weaning.

Table 5.2. Least square means for small intestinal morphology of pigs after an oral gavage of sterile broth or *Salmonella*[1].

	Broth	*Salmonella*[1]	SEM	P-value Inoc.[2]
Duodenum				
Villus height, μm	575.78	576.20	18.246	0.987
Crypt depth, μm	365.80	363.10	10.568	0.856
Villus/Crypt ratio	1.61	1.66	0.074	0.660
Villus width, μm	144.51	137.05	3.163	0.104
No. goblet cell/villus	27.08	23.58	1.704	0.155
Villus goblet, No./μm	0.02	0.02	0.001	0.081
No. goblet cell/crypt	20.46	18.02	0.810	0.040
Crypt goblet, No./μm	0.06	0.05	0.002	0.062
Villus area, mm^2	0.27	0.27	0.011	0.652
Jejunum				
Villus height, μm	469.00	486.08	11.701	0.309
Crypt depth, μm	302.92	308.77	7.461	0.583
Villus/Crypt ratio	1.59	1.59	0.056	0.985
Villus width, μm	133.59	128.91	2.050	0.115
No. goblet cell/villus	20.87	20.37	1.525	0.816
Villus goblet, No./μm	0.019	0.02	0.001	0.284
No. goblet cell/crypt	22.44	23.72	0.965	0.342
Crypt goblet, No./μm	0.076	0.072	0.003	0.335
Villus area, mm^2	0.211	0.212	0.007	0.881
Ileum				
Villus height, μm	421.43	446.28	18.688	0.161
Crypt depth, μm	292.11	290.91	6.911	0.903
Villus/Crypt ratio	1.49	1.52	0.051	0.632
Villus width, μm	138.71	130.83	2.067	0.011
No. goblet cell/villus	23.49	23.94	1.417	0.823
Villus goblet, No./μm	0.024	0.02	0.001	0.682
No. goblet cell/crypt	21.60	21.90	0.996	0.833
Crypt goblet, No./μm	0.07	0.08	0.003	0.542
Villus area, mm^2	0.20	0.20	0.006	0.983

[1] *Salmonella* Typhimurium resistant to the antibiotics nalidixic acid (Nal^R) and novobiocin (Nov^R).
[2] Inoc., inoculation with either sterile broth (Broth) or *S.* Typhimurium $Nal^R Nov^R$

5.8 Figures

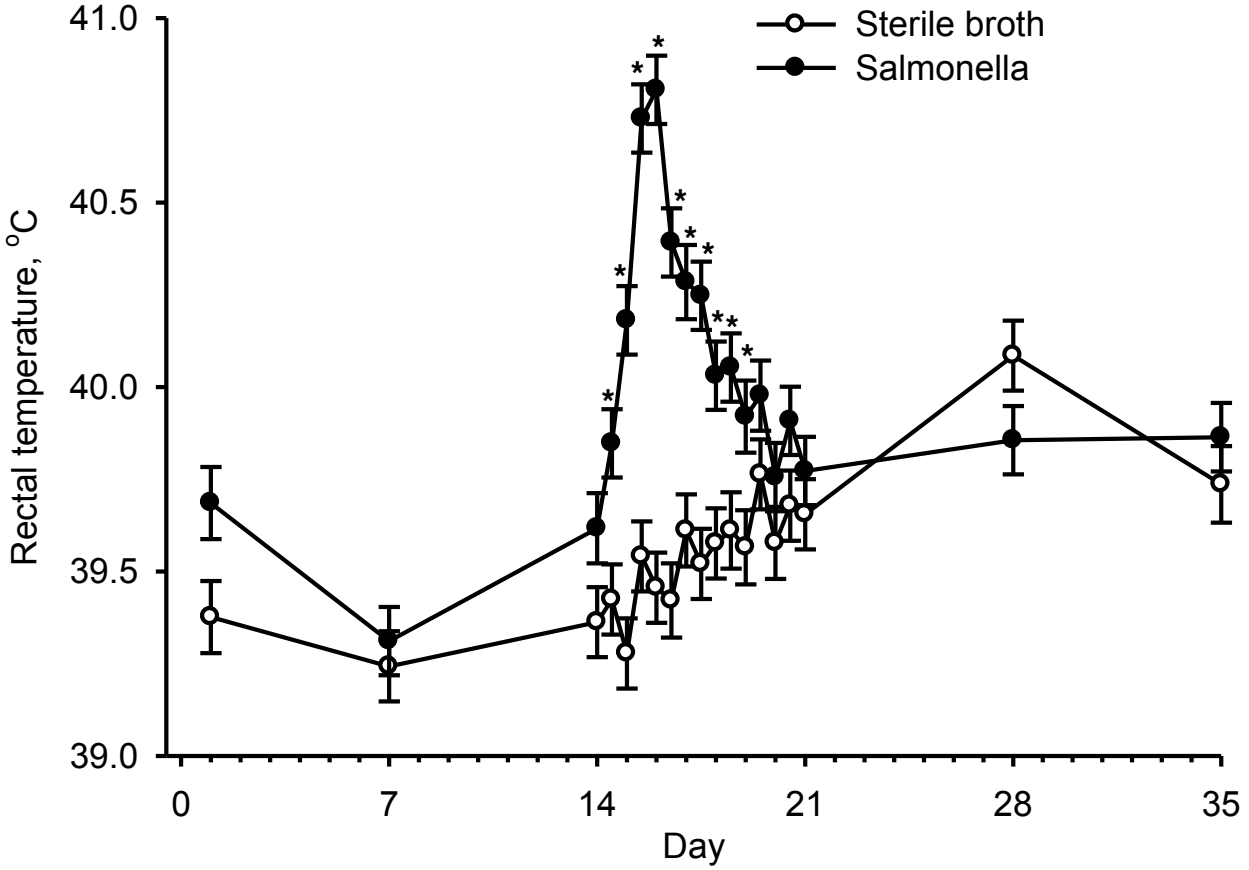

Figure 5.1. Effect of infection with *Salmonella* on rectal temperature. From weaning (d = 1) pigs had ad libitum access to a nursery diet. Pigs were inoculated with 5 mL containing 10^9 CFU *Salmonella* Typhimurium resistant to the antibiotics nalidixic acid and novobiocin (*Salmonella*) on d 14 after weaning or received 5 mL of sterile broth (Broth). Pigs were treated with 5 mg/kg BW i.m. ceftiofur-HCl on d 17-20. Inoculation with *Salmonella* increased rectal temperature ($P < 0.01$) on d 14.5 through 19 compared to non-infected controls. Values are means ± SEM (n = 20). * Mean differ from Broth within day, $P < 0.01$.

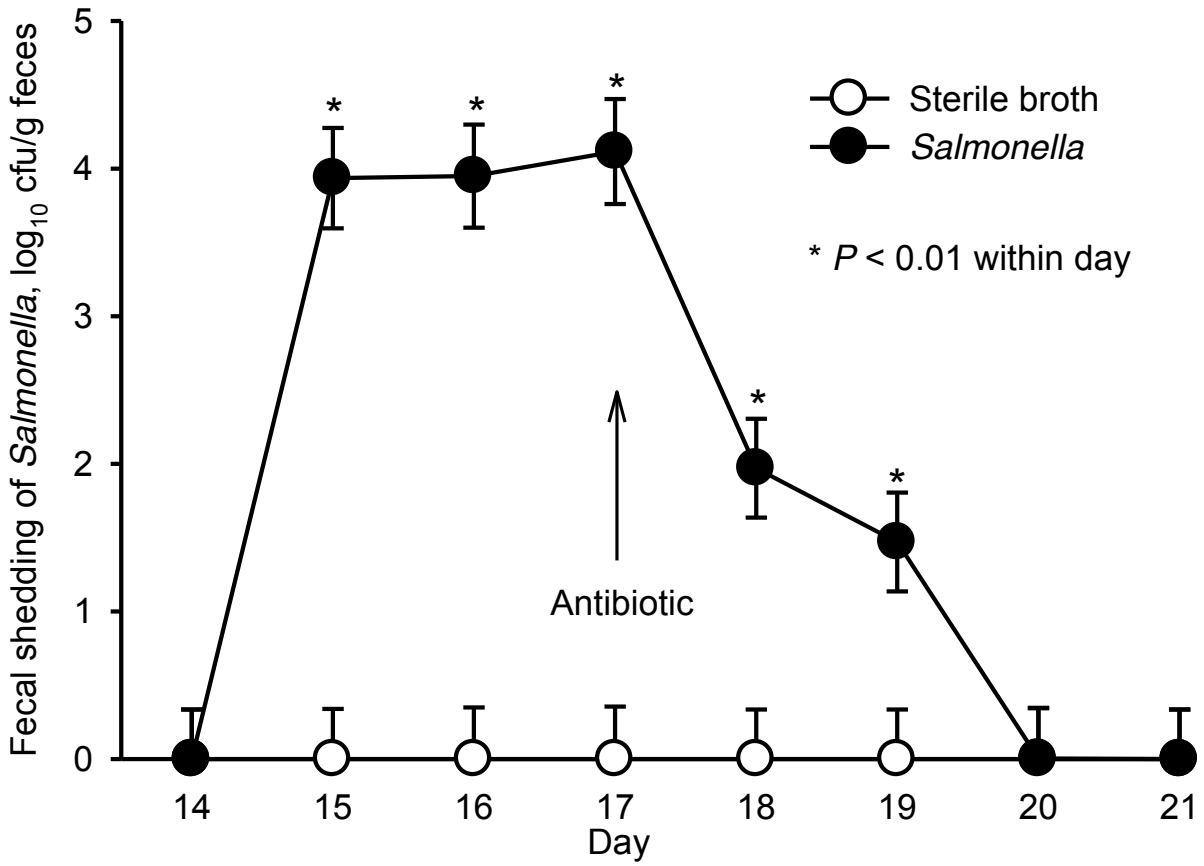

Figure 5.2. Effect of infection with *Salmonella* on fecal shedding of *Salmonella*. From weaning (d = 1) pigs had ad libitum access to a nursery diet. Pigs were inoculated with 5 mL containing 10^9 CFU *Salmonella* Typhimurium resistant to the antibiotics nalidixic acid and novobiocin (*Salmonella*) on d 14 after weaning or received 5 mL of sterile broth (Broth). Pigs were treated with 5 mg/kg BW i.m. ceftiofur-HCl on d 17-20. Values are means ± SEM (n = 20). * Means without a common letter within day differ, $P < 0.05$.

5.9 Literature Cited

Burkey, T. E., S. S. Dritz, J. C. Nietfeld, B. J. Johnson, and J. E. Minton. 2004. Effect of dietary mannanoligosaccharide and sodium chlorate on the growth performance, acute-phase response, and bacterial shedding of weaned pigs challenged with *Salmonella enterica* serotype Typhimurium. J. Anim. Sci. 82:397-404.

CDC. 2005. Bacterial Foorborne and Diarrheal Disease National Case Surveillance. Annual Report, 2005. Centers for Disease Control and Prevention. Division of Foodborne, Bacterial, and Mycotic Diseases.

Dunsford, B. R., W. E. Haensly, and D. A. Knabe. 1990. Neutral and acidic goblet cell concentrations in the small intestine of the unweaned pig. Biol. Neonate 57:194-199.

ERS/USDA. 2003. Calculating the cost of Foodborne Illness: A New Tool to Value Food Safety Risks. Economic Research Service. United States Department of Agriculture. http://www.ers.usda.gov. Accessed June 20, 2008.

FSIS/USDA. 2006. Foodborne Illness and Disease: *Salmonella* Questions and Answers. Food Safety and Inspection Service. United States Department of Agriculture. http://www.fsis.usda.gov. Accessed June 20, 2008.

Kaps, M. and W. R. Lamberson. 2004. Biostatistics for Animal Science. CABI Publishing, Cambridge, MA.

Lunney, J. K. 2007. Advances in swine biomedical model genomics. Intl. J. Bio. Sci. 3:179-184.

Merck & Co., Inc. 2003. Infections: Bacterial *Salmonella* infections. Merck, Whitehouse Station, NJ. http://www.merck.com/mmhe/sec17/ch190/ch190p.html. Accessed August 27, 2008.

NRC. 1998. Nutrient Requirements of Swine. 10th ed. Natl. Acad. Press, Washington, DC.

Pluske, J. R., M. J. Thompson, C. S. Atwood, P. H. Bird, I. H. Williams, and P. E. Hartmann. 1996. Maintenance of villus height and crypt depth, and enhancement of disaccharide digestion and monosaccharide absorption, in piglets fed on cows' whole milk after weaning. Br. J. Nutr. 76:409-422.

Sharan, R., S. Chhibber, and R. H. Reed. 2011. A murine model to study antibacterial effect of copper in infectivity of *Salmonella enterica* serovar Typhimurium. Int. J. Environ. Res. Public Health. 8:21-36.

Zhao, J., A. F. Harper, M. J. Estienne, K. E. Webb, Jr., A. P. McElroy, and D. M. Denbow. 2007. Growth performance and intestinal morphology responses in early weaned pigs to supplementation of antibiotic-free diets with an organic copper complex and spray-dried plasma protein in sanitary and nonsanitary environments. J. Anim Sci. 85:1302-1310.

Zijlstra, R. T., S. M. Donovan, J. Odle, H. B. Gelberg, B. W. Petschow, and H. R. Gaskins. 1997. Protein-energy malnutrition delays small-intestinal recovery in neonatal pigs infected with rotavirus. J. Nutr. 127:1118-1127.

CHAPTER 6

Quantification of N-τ-methyl-L-histidine in pig plasma

6.1 Abstract

Nτ-methyl-L-histidine (NτMH) is a post-translationally modified amino acid mainly present in muscle protein. It has been used as an indirect marker of muscle proteolysis because once released it cannot be reincorporated into protein, and hence, it is destined for excretion. However, NτMH is likely acetylated (Ac-NτMH) in the liver, which interferes with derivatization procedures needed for its quantification. Our objectives were to optimize procedures to hydrolyze and to quantify changes in NτMH after lipopolysaccharide (LPS) treatment. Blood was collected from 8 random growing pigs into Li-heparinized tubes to obtain plasma. First, we evaluated 2 hydrolysis procedures (6 M HCl and 70% perchloric acid, PCA) to remove the acetylation. Results indicate that plasma hydrolysis with HCl for 24 h at 110°C yielded higher ($P < 0.01$) NτMH levels compared to PCA. Results also indicate that about 15% of NτMH in pig plasma is found in the free form and the rest is Ac-NτMH. Pigs (N = 9, 33.4 ± 1.1 kg) fitted with indwelling jugular catheters were treated with 10 μg/kg BW of *E. coli*-derived LPS i.v. Blood samples were collected 12 h later for NτMH and plasma urea nitrogen (PUN) quantification. Only plasma Ac-NτMH levels changed in response to LPS treatment. Furthermore, PUN and Ac-NτMH were both elevated 12 h after LPS challenge, which collectively suggests muscle proteolysis. In conclusion, pig plasma must be acid hydrolyzed in order to accurately monitor and report changes in NτMH when used as an indirect marker of muscle protein breakdown.

6.2 Introduction

Exogenous (e.g., environmental conditions and pathogens) and endogenous (e.g., hormones and cytokines) factors can greatly influence skeletal muscle protein accretion, the net balance between synthesis and degradation. In agricultural animals and humans, skeletal muscle makes up the largest tissue in the body. Disease, starvation, and injury are known to cause rapid increases in muscle proteolysis, which can be measured using isotopic techniques (e.g., tracer-to-tracee ratio) that require specialized analytical equipment and training, blood vessel catheterization for serial blood collection. Hence, these procedures can be expensive and time consuming.

Measuring urinary Nτ-methyl-L-histidine (NτMH) has been used and validated as an indicator of muscle protein degradation in humans (Elia et al., 1981; Long et al., 1975; Young and Munro, 1978), rats (Young et al., 1972), cattle (Harris and Milne, 1981b), rabbits (Harris et al., 1977), and chickens (Hillgartner et al., 1981) but not in sheep (Harris and Milne, 1980) and pigs (Harris and Milne, 1981a). Released NτMH from skeletal muscle during proteolysis cannot be reused for protein synthesis, and it is therefore excreted from the body in urine as NτMH and its N-acetyl derivative (Ac-NτMH, Young et al., 1972). The gut contribution to the NτMH pool has been reported at less than 15% of the daily excretion in adult rats (Brenner et al., 1987). As with any other urinary excretion compound, it must travel in plasma to reach the kidneys to be eliminated from the body. In humans, NτMH exists mainly in the free, non-acetylated, form in plasma and urine (Young and Munro, 1978); however, this may not be the case in other animal species. For example, significant differences in urinary excretion of NτMH and Ac-NτMH, according to changes in BW, have been reported in rats (Young et al., 1972).

Derivatization with various compounds (e.g., phenylisothiocyanate, PITC; ninhydrin; fluorescamine; orthophthalaldehyde, etc.) followed by liquid chromatography is the most common procedure to quantify free amino acids. To quantify protein-bound amino acids, samples are subjected to anoxic acid hydrolysis. Acetylation of NτMH apparently interferes with derivatization procedures. Further, acid hydrolysis has been used to remove the acetylation of NτMH, thus making it possible to quantify total NτMH by conventional amino acid analysis (Kuhl et al., 1996). For this study, we derivatized NτMH with PITC, which has been concluded to be a sensitive method for the quantification of NτMH and other amino acids (Cohen et al., 1989; Forsberg and Liu, 1989).

Since first proposed as an adequate indirect marker for muscle proteolysis to date, there has been a change in compound nomenclature. The current synonyms for NτMH are 1-methyl-L-histidine (1MH) and archaic 3-methyl-L-histidine (3MH); and for π-methyl-L-histidine (πMH) are 3MH and archaic 1MH. This change in nomenclature and inconsistent use of 1MH and 3MH in the literature can lead to confusion and even to obtain incorrect standards from chemical suppliers. Accurate quantification of plasma NτMH is a minimally invasive procedure that will facilitate the use of this compound to monitor muscle protein breakdown compared to urine collection, which can be cumbersome in single- and group-housed agricultural animals. Thus, the objectives of this study were to determine the best procedure for quantifying total NτMH, the major form of plasma NτMH in pigs, and the effect of endotoxemia on pig plasma NτMH levels.

6.3 Materials and methods

All animal procedures were approved by the Virginia Tech Institutional Animal Care and Use Committee. Pure NτMH (CAS 332-80-9), πMH (CAS 368-16-1), and other amino acid

standards were purchased from Sigma-Aldrich (St. Louis, MO), all other chemicals were obtained from Fisher Scientific (Suwanee, GA) or VWR (West Chester, PA). Acid solutions of 6M HCl and 70% perchloric acid (w/v) were prepared in distilled water.

6.3.1 NτMH hydrolysis and analyses

Blood samples were collected in Li-heparinized Vacutainers (BD, Franklin Lakes, NJ) and plasma was obtained after centrifugation at 3,000×g for 5 min at 4°C, and stored at -80°C until analyses. Plasma samples (500 μL) were filtered at 10,000×g for 10 min at 4°C using 10k MW cutoff filters (Pall Corp., Port Washington, NY). Filtered plasma (25 μL) was subjected to vaporized anoxic acid hydrolysis with HCl or PCA at 110°C for 0 (i.e., no acid hydrolysis), 2, 4, 8, 12, or 24 h as previously described (Cohen et al., 1989). After acid hydrolysis, samples were vacuum dried, derivatized with PITC, separated, and analyzed with norleucine as an internal standard using a 2695 Alliance HPLC with a 30-cm Pico-Tag column, 2487 UV/Vis detector, and Empower software (all from Waters Corp., Milford, MA) using previously described conditions (Cohen et al., 1989). An amino acid standard containing NτMH and πMH was used for identification and quantification of plasma amino acids. Total NτMH was quantified from acid hydrolyzed plasma, free NτMH was quantified from non-hydrolyzed plasma, and Ac-NτMH was calculated as: total - free. Amino acid concentrations are expressed in μmol/L.

6.3.2 Effect of LPS on plasma NτMH in pigs

Pigs (33.4 ± 1.1 kg, N = 9) were housed in an environmentally controlled facility as previously described (Price et al., 2010) and acclimated for 10 d before surgery. Pigs were fitted with one indwelling jugular catheter as previously described (Escobar et al., 2006). For 3 d post-

surgery, pigs received 4 mg/kg BW of i.v. flunixin (Butler Animal Health, Dublin, OH) twice a d for analgesia and 5 mg/kg BW of i.m. ceftiofur-HCl (Pfizer, New York, NY) once a d as bacterial prophylaxis. Pigs were fed, 3 times each d, a corn-soybean meal based diet (free of animal products) that met or exceeded nutrient recommendations (NRC, 1998) at about 90% of estimated ad libitum consumption to insure complete consumption of each meal; water access was ad libitum. Four d after surgery, pigs were feed-deprived overnight and venous blood samples were collected 2 h and immediately before (i.e., t = 0) sterile i.v. injection of *E. coli* 055:B5 (Sigma-Aldrich) lipopolysaccharide (LPS, 10 μg/kg BW) in 0.9% sterile saline. Rectal temperature and blood samples were collected at 1- and 2-h intervals, respectively. Plasma was obtained, stored, and analyzed as indicated before. Plasma samples from 0 and 12 h were acid hydrolyzed, or not, to quantify free NτMH, total NτMH, and πMH. Plasma urea nitrogen (PUN, Teco Diagnostics, Anaheim, CA) was quantified at 2-h interval after LPS injection.

6.3.3 Statistical Analysis

Pig was considered the experimental unit. Data normality was tested using the univariate procedure of SAS (SAS Institute, Cary, NC) and all data were normally distributed. The mixed procedure of SAS with repeated measures using time as fixed effect for a complete randomized design was used to test the effect of LPS on plasma NτMH, PUN, and rectal temperature. Least square means were compared using a *t*-test and Tukey adjustment in SAS. Data are presented as least squared means ± pooled SE.

6.4 Results

A positive correlation (r = 0.97, $P < 0.001$), was obtained between theoretical and analyzed concentrations of NτMH ranging from 0.06 to 600 μM (data not shown). Incubation time of pure NτMH with either HCl or PCA had no effect ($P = 0.36$ and 0.46, respectively) on quantitative recoverability compared to non-hydrolyzed standard (data not shown). Hydrolysis with HCl increased ($P = 0.002$) plasma levels of total NτMH by 2 h of incubation and levels remained elevated compared to baseline, non-hydrolyzed, control plasma (Figure 6.1). To the contrary, none of the evaluated incubation times with PCA was different from baseline ($P = 0.95$ to 0.99, Figure 6.1). After 24 h of acid hydrolysis, plasma NτMH concentrations were higher with HCl compared to PCA ($P < 0.01$). Furthermore, our findings demonstrate that about 15% of NτMH in healthy pig plasma was found as free form and the majority was Ac-NτMH (Figure 6.2).

To experimentally increase skeletal muscle proteolysis, pigs were treated i.v. with LPS, which increased ($P < 0.02$) rectal temperature and PUN compared to baseline values (Figure 6.3). Plasma concentrations of free NτMH did not change after LPS treatment ($P = 0.99$, Figure 6.4). Administration of LPS increased ($P = 0.003$) total NτMH in plasma by 55% compared to t = 0 (control, pre-LPS samples). Thus, calculated plasma concentrations of Ac-NτMH were also increased ($P = 0.002$). Finally, meaningful concentrations of πMH (current 3MH, archaic 1MH) where not found in the plasma of healthy pigs and in those treated with an i.v. bolus of LPS either before or after acid hydrolysis.

6.5 Discussion

In both biomedical and agricultural research the use of simple, affordable, and minimally invasive techniques are highly desirable. Our results clearly demonstrate that in healthy and LPS-challenged pigs the majority of NτMH found in plasma is acetylated. More importantly, Ac-NτMH was the only fraction that increased after LPS treatment. These results can be interpreted to suggest that pigs have a high degree of acetylation, presumably in liver (Young et al., 1972). Low recovery of administered labeled NτMH (about 66% of dose) has been previously reported (Cowgill and Freeburg, 1957) in rat urine. However, the authors' recovered 32% of labeled NτMH as an acid-labile compound, which was later suggested to be Ac-NτMH (Young et al., 1972). Our results indicate that about 15% of NτMH was found in the free form in pig plasma, which is near to the 21% reported previously in pig urine (Harris and Milne, 1981a). Therefore, it is plausible that previous unsuccessful attempts to validate NτMH as a marker for muscle degradation in pigs (Harris and Milne, 1981a), and perhaps other species (Harris and Milne, 1980), could have been confounded by not accounting for Ac-NτMH. Muscle release of NτMH, under various conditions, has been quantified from rats (Brenner et al., 1987; Cowgill and Freeburg, 1957; Forsberg and Liu, 1989; Kuhl et al., 1996; Young et al., 1972), rabbits (Harris et al., 1977), cattle (Harris and Milne, 1981b), humans (Bilmazes et al., 1978; Elia et al., 1981; Long et al., 1975), chickens (Cowgill and Freeburg, 1957; Hillgartner et al., 1981), and frogs (Cowgill and Freeburg, 1957). Collectively, results from this wide range of animal species in addition to our results, indicate that plasma NτMH can be used as an acceptable indicator of muscle protein degradation. Because of nomenclature changes and confusion when consulting past, current, and future reports on this subject, care must be exercised due to the possibility that researchers may have, inadvertently, used an incorrect standard and hence were quantifying the

erroneous methylhistidine compound of interest. Finally, it would be advisable to quantify free, acetylated, and total NτMH in other agriculturally important species to determine which fraction should be quantified in response to well-characterized procedures and/or compounds known to increase muscle proteolysis.

6.6 Figures

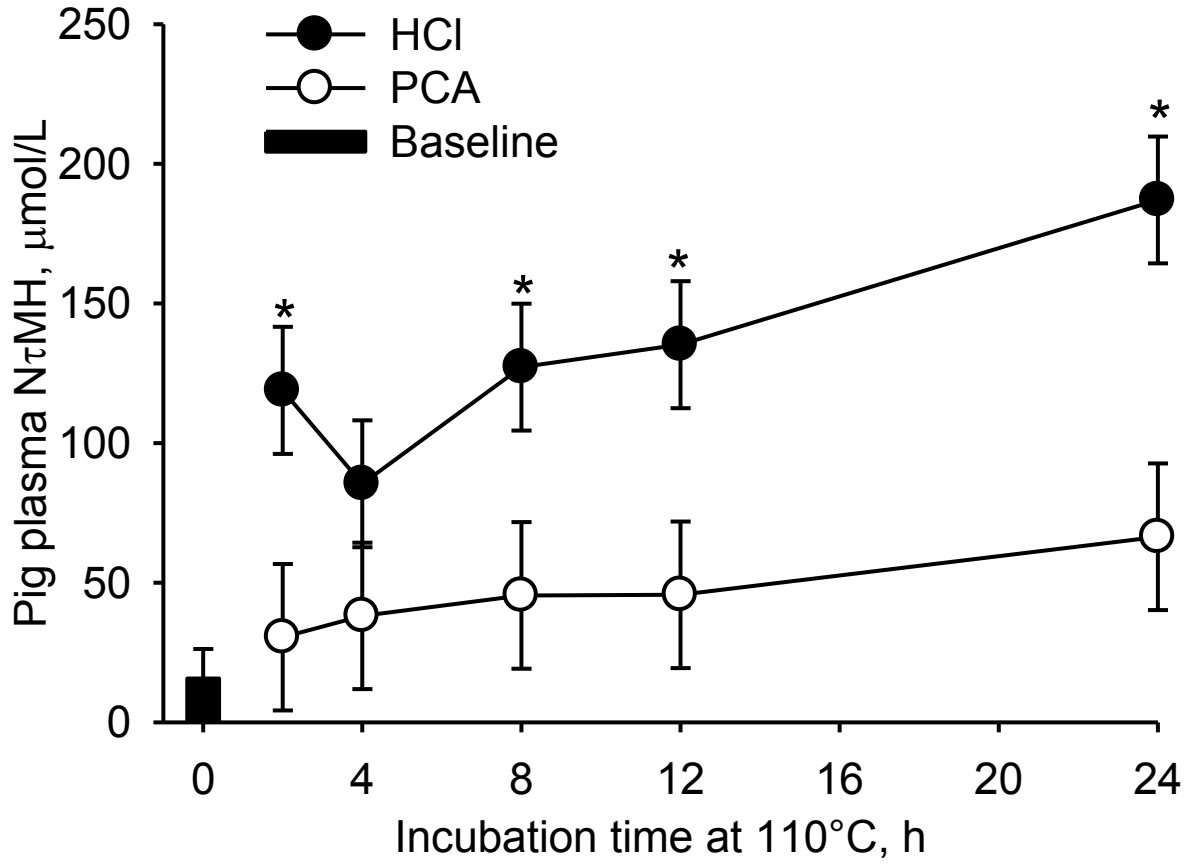

Figure 6.1. Effect of incubation time with either 6 M HCl or 70% perchloric acid (PCA) on total Nτ-methyl-L-histidine (NτMH) concentration in pig plasma. Values are means ± SEM (n = 8). *Means differ from baseline at $P < 0.01$.

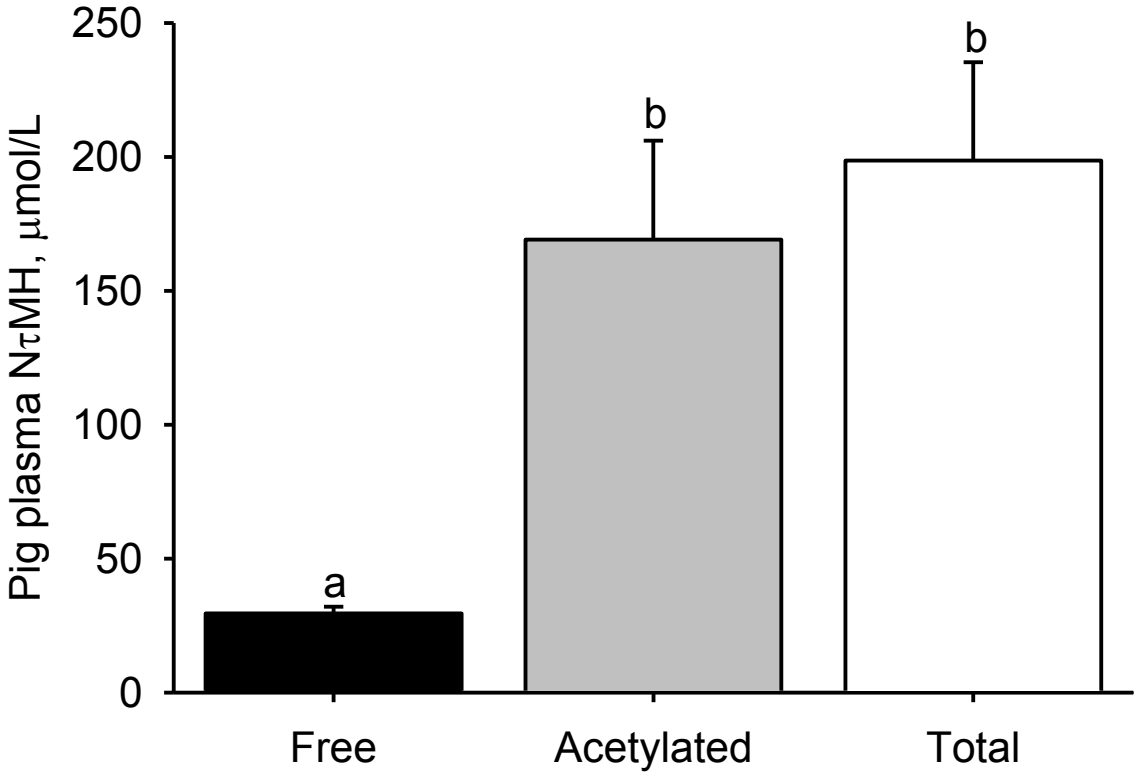

Figure 6.2. Distribution of free, acetylated, and total Nτ-methyl-L-histidine (NτMH) in plasma of healthy growing pigs. Plasma samples were acid hydrolyzed with 6 M HCl for 24 h at 110°C. Values are means ± SEM (n = 22). [a,b] Means without a common letter differ, $P < 0.005$.

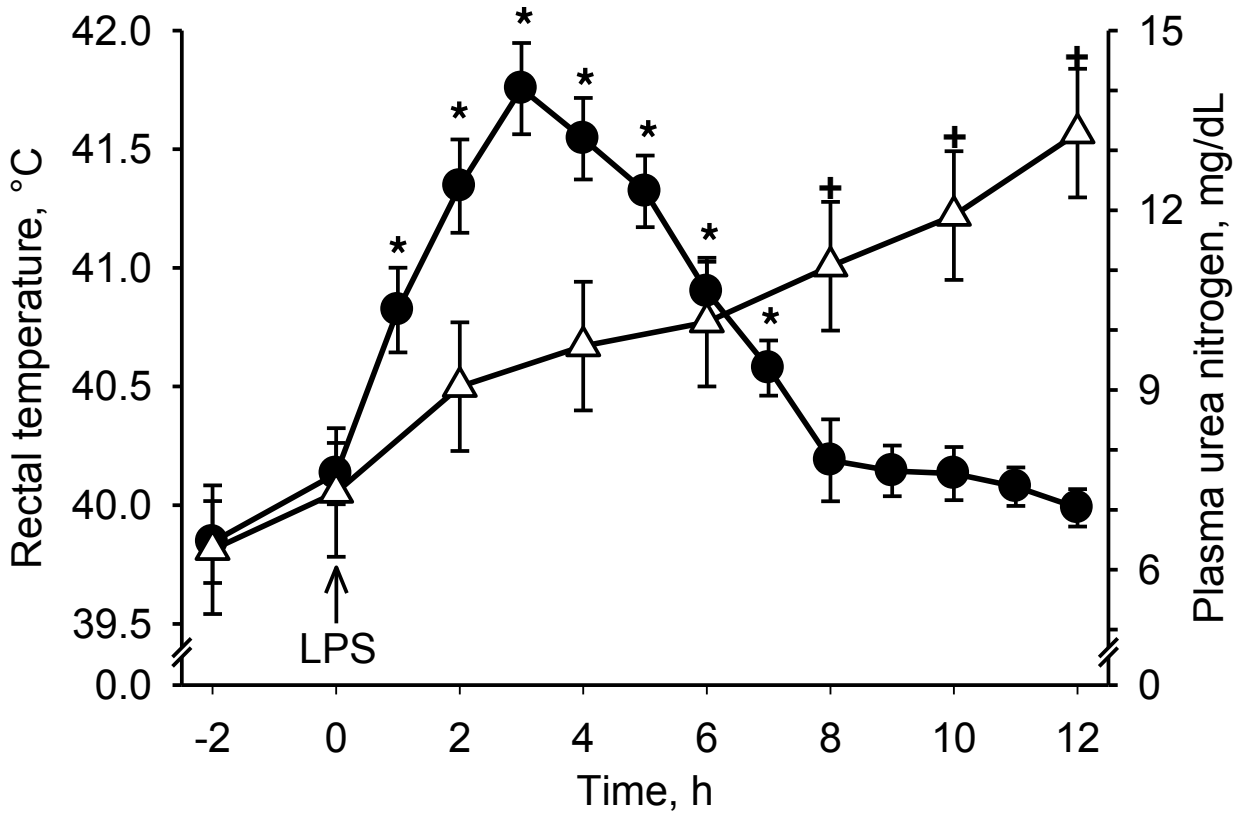

Figure 6.3. Changes in rectal temperature (●) and plasma urea nitrogen (△) in pigs treated i.v. with 10 μg/kg BW of *E. coli* 055:B5 lipopolysaccharide (LPS) in 0.9% sterile saline. Values are means ± SEM (n = 9). Means with superscript differ from t = -2 at $P < 0.02$ for rectal temperature (*) and plasma urea nitrogen (+).

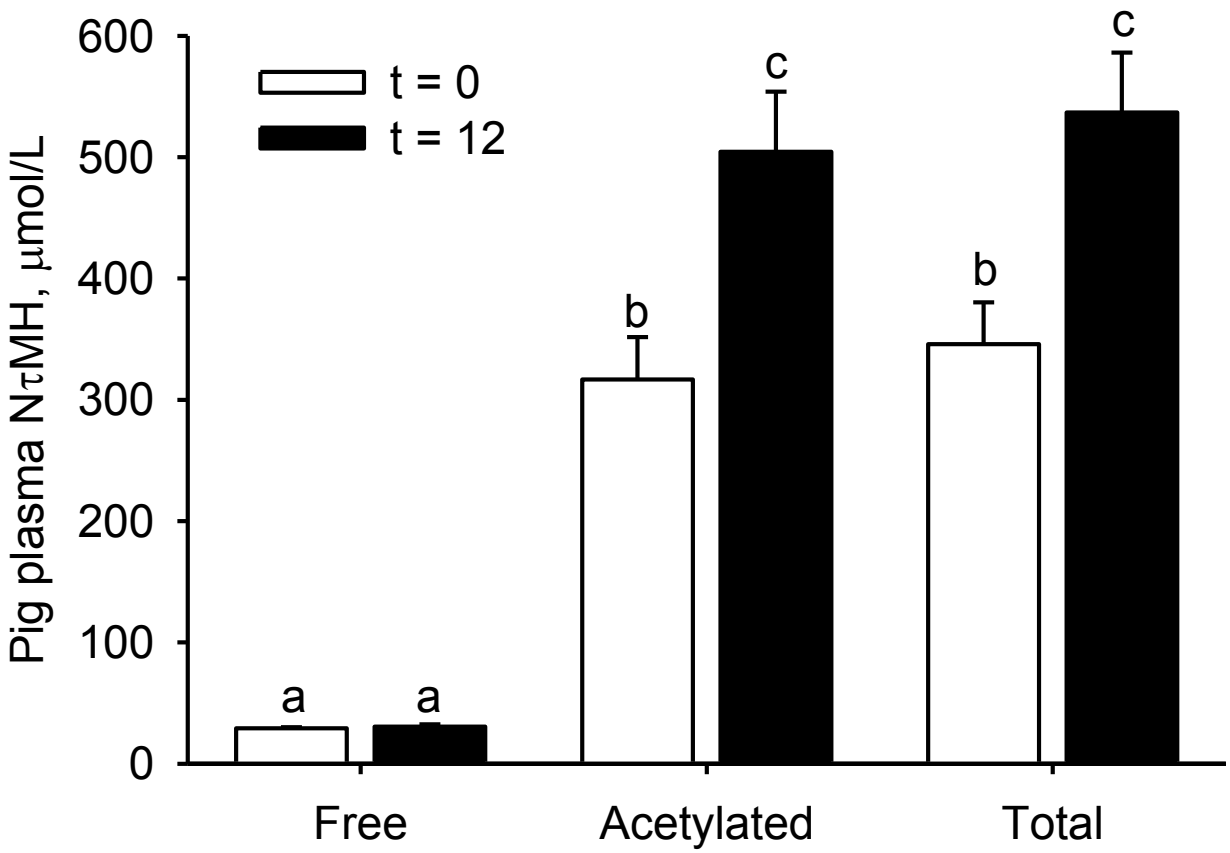

Figure 6.4. Changes in plasma Nτ-methyl-L-histidine (NτMH) levels before (t = 0) and 12 h (t = 12) after i.v. treatment with 10 μg/kg BW of *E. coli* 055:B5 lipopolysaccharide (LPS) in 0.9% sterile saline. Values are means ± SEM (n = 9). [a,b,c] Means without a common letter differ, $P <$ 0.003.

6.7 Literature Cited

Bilmazes, C., R. Uauy, L. N. Haverberg, H. N. Munro, and V. R. Young. 1978. Muscle protein breakdown rates in humans based on Nτ-methylhistidine (3-methylhistidine) content of mixed proteins in skeletal muscle and urinary output of Nτ-methylhistidine. Metabolism 27:525-530.

Brenner, U., L. Herbertz, P. Thul, M. Walter, M. Meibert, J. M. Muller, and H. Reinauer. 1987. The contribution of small gut to the 3-methylhistidine metabolism in the adult rat. Metabolism 36:416-418.

Cohen, S. A., M. Meys, and T. L. Tarvin. The Pico-Tag Method: A manual of advanced techniques for amino acid analysis. [WM02, Rev. 1]. 1989. Milford, MA, Waters Division of Millipore.

Cowgill, R. W. and B. Freeburg. 1957. The metabolism of methylhistidine compounds in animals. Arch. Biochem. Biophys. 71:466-472.

Elia, M., A. Carter, S. Bacon, C. G. Winearls, and R. Smith. 1981. Clinical usefulness of urinary 3-methylhistidine excretion in indicating muscle protein breakdown. Br. Med. J. (Clin. Res. Ed.) 282:351-354.

Escobar, J., J. W. Frank, A. Suryawan, H. V. Nguyen, S. R. Kimball, L. S. Jefferson, and T. A. Davis. 2006. Regulation of cardiac and skeletal muscle protein synthesis by individual branched-chain amino acids in neonatal pigs. Am. J. Physiol. Endocrinol. Metab. 290:E612-E621.

Forsberg, N. E. and C. C. Liu. 1989. Phenylisothiocyanate derivatization of Nτ-methylhistidine: A method of assessing myofibrillar protein-degradation. Nutr. Res. 9:1269-1276.

Harris, C. I. and G. Milne. 1980. The urinary excretion of Nτ-methyl histidine in sheep: an invalid index of muscle protein breakdown. Br. J. Nutr. 44:129-140.

Harris, C. I. and G. Milne. 1981a. The inadequacy of urinary Nτ-methyl histidine excretion in the pig as a measure of muscle protein breakdown. Br. J. Nutr. 45:423-429.

Harris, C. I. and G. Milne. 1981b. The urinary excretion of Nτ-methyl histidine by cattle: validation as an index of muscle protein breakdown. Br. J. Nutr. 45:411-422.

Harris, C. I., G. Milne, G. E. Lobley, and G. A. Nicholas. 1977. 3-Methylhistidine as a measure of skeletal-muscle protein catabolism in the adult New Zealand white rabbit. Biochem. Soc. Trans. 5:706-708.

Hillgartner, F. B., A. S. Williams, J. A. Flanders, D. Morin, and R. J. Hansen. 1981. Myofibrillar protein degradation in the chicken: 3-Methylhistidine release *in vivo* and *in vitro* in normal and genetically muscular-dystrophic chickens. Biochem. J. 196:591-601.

Kuhl, D. A., J. T. Methvin, and R. N. Dickerson. 1996. Standardization of acid hydrolysis procedure for urinary 3-methylhistidine determination by high-performance liquid chromatography. J. Chromatogr. B Biomed. Appl. 681:390-394.

Long, C. L., L. N. Haverberg, V. R. Young, J. M. Kinney, H. N. Munro, and J. W. Geiger. 1975. Metabolism of 3-methylhistidine in man. Metabolism 24:929-935.

NRC. 1998. Nutrient Requirements of Swine. 10th ed. Natl. Acad. Press, Washington, DC.

Price, K. L., H. R. Totty, H. B. Lee, M. D. Utt, G. E. Fitzner, I. Yoon, M. A. Ponder, and J. Escobar. 2010. Use of *Saccharomyces cerevisiae* fermentation product on growth performance and microbiota of weaned pigs during *Salmonella* infection. J. Anim. Sci. 88:3896-3908.

Young, V. R., S. D. Alexis, B. S. Baliga, H. N. Munro, and W. Muecke. 1972. Metabolism of administered 3-methylhistidine. Lack of muscle transfer ribonucleic acid charging and quantitative excretion as 3-methylhistidine and its N-acetyl derivative. J. Biol. Chem. 247:3592-3600.

Young, V. R. and H. N. Munro. 1978. Nτ-methylhistidine (3-methylhistidine) and muscle protein turnover: An overview. Fed. Proc. 37:2291-2300.

Chapter 7

Overall conclusions and implications

7.1 Conclusions

The goal of this dissertation was to establish principles for nutritional intervention of sick animals and humans. Two lipopolysaccharide (LPS) trials were conducted to determine changes in plasma amino acids (AA) and metabolites during an acute immune challenge, and to better quantify in pigs a known marker of skeletal muscle degradation in humans and rodents. Results indicate an initial marked decrease in plasma AA after LPS treatment, which is interpreted as a profound and rapid catabolism of several AA. Eight to 12 h after LPS administration, some AA returned to baseline values and some exceeded to reach postprandial levels. These results are interpreted as a recovery from the immunological insult and normalization of metabolic processes. The increase over baseline values can be attributed to excess of specific AA compared to bodily and metabolic needs and they are presumably derived from skeletal muscle proteolysis. We refine analytical procedures to determine N-τ-methyl-histidine (NτMH), which has been validated as an indirect marker of skeletal muscle proteolysis. However, NτMH exist in free and acetylated forms, and the main form in pig plasma was unknown. Plasma levels of free NτMH were not changed after LPS administrations whereas acetylated NτMH values drastically increase. Our combined results indicate high levels of muscle proteolysis. Catabolism of essential AA was enhanced after LPS treatment and with marked dynamic changes during the induction and recovery phases of the sickness model. Changes in plasma AA were further quantified to estimate individual rates of AA anabolism and catabolism during immune activation. We also developed several prediction equations (containing 1 to 10 terms in

the model) in a hope to serve as a potential base for individualized nutritional intervention of sick patients. However, continued work on the models is required to improve the models. Finally, we developed an infectious disease model in young pigs with *Salmonella enterica* serovar Typhimurium that closely resembles human salmonellosis. This model will be useful to determine nutritional changes of patients afflicted with enteric bacterial diseases.

7.2 Implications

Lipopolysaccharide has been proven to be a good model of acute endotoxemia. Changes to AA and blood metabolite metabolism in response to LPS treatment impact nutrient requirements. Area under the curve (AUC) proved to be a good indicator of AA balance in plasma. The many prediction equations that were created do have the ability to predict changes in AA; however, future work with the equations is required. While, LPS is an excellent acute model of disease, a chronic model of disease (i.e., *Salmonella* infection) is required to fine tune the prediction equations. NτMH was proven to be another marker of skeletal muscle proteolysis available to swine scientist. Eventually, determining the major fraction in other species, such as poultry, cows, sheep, and horses, is necessary as it is easily determined in labs already set-up to measure AA.